

Doctorate Program in Molecular Oncology
and Endocrinology
Doctorate School in Molecular Medicine

XX cycle - 2004–2007
Coordinator: Prof. Giancarlo Vecchio

**“BRAF and MEK inhibitors in the
treatment of aggressive thyroid carcinomas”**

Paolo Salerno

University of Naples Federico II
Dipartimento di Biologia e Patologia Cellulare e Molecolare
“L. Califano”

Administrative Location

Dipartimento di Biologia e Patologia Cellulare e Molecolare “L. Califano”
Università degli Studi di Napoli Federico II

Partner Institutions

Italian Institutions

Università di Napoli “Federico II”, Naples, Italy
Istituto di Endocrinologia ed Oncologia Sperimentale “G. Salvatore”, CNR, Naples, Italy
Seconda Università di Napoli, Naples, Italy
Università del Sannio, Benevento, Italy
Università di Genova, Genoa, Italy
Università di Padova, Padua, Italy

Foreign Institutions

Johns Hopkins School of Medicine, Baltimore, MD, USA
Johns Hopkins Krieger School of Arts and Sciences, Baltimore, MD, USA
National Institutes of Health, Bethesda, MD, USA
Ohio State University, Columbus, OH, USA
Université Paris Sud XI, Paris, France
Universidad Autonoma de Madrid, Spain
Centro de Investigaciones Oncologicas (CNIO), Spain
Universidade Federal de Sao Paulo, Brazil
Albert Einstein College of Medicine of Yeshiwa University, USA

Supporting Institutions

Università di Napoli “Federico II”, Naples, Italy
Ministero dell’Istruzione, dell’Università e della Ricerca
Istituto Superiore di Oncologia (ISO)
Terry Fox Foundation, Canada
Istituto di Endocrinologia ed Oncologia Sperimentale “G. Salvatore”, CNR, Naples, Italy
Centro Regionale di Competenza in Genomica (GEAR)

Faculty

Italian Faculty

Giancarlo Vecchio, MD, Co-ordinator
Salvatore Maria Aloj, MD
Francesco Beguinot, MD
Maria Teresa Berlingieri, PhD
Angelo Raffaele Bianco, MD
Bernadette Biondi, MD
Francesca Carlomagno, MD
Gabriella Castoria, MD
Angela Celetti, MD
Annamaria Cirafici, PhD
Mario Chiariello, MD
Vincenzo Ciminale, MD
Annamaria Colao, MD
Alma Contegiacomo, MD
Sabino De Placido, MD
Monica Fedele, PhD
Pietro Formisano, MD
Alfredo Fusco, MD
Massimo Imbriaco, MD
Paolo Laccetti, MD
Antonio Leonardi, MD
Barbara Majello, PhD
Rosa Marina Melillo, MD
Claudia Miele, PhD
Francesco Oriente, MD
Roberto Pacelli, MD
Giuseppe Palumbo, PhD
Silvio Parodi, MD
Giuseppe Portella, MD
Giorgio Punzo, MD
Antonio Rosato, MD
Massimo Santoro, MD
Giampaolo Tortora, MD
Donatella Tramontano, PhD
Giancarlo Troncone, MD
Bianca Maria Veneziani, MD
Giuseppe Viglietto, MD
Roberta Visconti, MD

Foreign Faculty

National Institutes of Health (USA)

Michael M. Gottesman, MD
Silvio Gutkind, PhD
Stephen Marx, MD
Ira Pastan, MD
Phil Gorden, MD

Johns Hopkins School of Medicine (USA)

Vincenzo Casolaro, MD
Pierre Coulombe, PhD
James G. Herman MD
Robert Schleimer, PhD

Johns Hopkins Krieger School of Arts and Sciences (USA)

Eaton E. Lattman, MD

Ohio State University, Columbus (USA)

Carlo M. Croce, MD

Albert Einstein College of Medicine of Yeshiva University (USA)

Luciano D' Adamio, MD
Nancy Carrasco

Université Paris Sud XI (France)

Martin Schlumberger, MD

Universidad Autonoma de Madrid (Spain)

Juan Bernal, MD, PhD
Pilar Santisteban

Centro de Investigaciones Oncologicas (Spain)

Mariano Barbacid, MD

Universidade Federal de Sao Paulo (Brazil)

Janete Maria Cerutti
Rui Maciel

PAOLO SALERNO

**“BRAF and MEK inhibitors in
the treatment of aggressive
thyroid carcinomas”**

Doctoral dissertation

TABLE OF CONTENTS

<i>LIST OF PUBLICATIONS</i>	4
<i>ABBREVIATIONS</i>	5
<i>ABSTRACT</i>	6
1. INTRODUCTION	7
1.1 Thyroid gland	7
1.2 Thyroid Carcinoma	7
1.2.1 PTC	8
1.2.2 FTC	9
1.2.3 ATC	10
1.2.4 MTC	10
1.3 Dominant oncogenes involved in thyroid carcinoma	11
1.3.1 MAPK pathway	12
1.3.2 PI3K/AKT	25
1.4 Molecularly targeted cancer therapy	26
1.4.1 ERK pathway inhibitors	27
1.4.2 Novel molecular therapy strategies for undifferentiated thyroid carcinoma	30
2 AIMS OF THE STUDY	32
3. MATERIALS AND METHODS	33
3.1 Compounds	33
3.2 Cell cultures	33
3.3 Cell proliferation assays	34
3.4 FACS analysis	35
3.5 RNA silencing (attached manuscript#1)	35
3.6 Protein studies	36
3.7 Antibodies	36
3.8 BRAF kinase assay (attached manuscript #1)	36
3.9 Reverse transcription and quantitative PCR (attached manuscript #5)	37
3.10 Tumorigenicity in nude mice (attached manuscript #1)	38
3.11 Statistical Analysis	38
4 RESULTS	39
4.1 Effects of genetic BRAF knock-down in BRAF mutant thyroid carcinoma cells (attached manuscript #1).	39
4.2 Biochemical effects of BAY 43-9006 in BRAF mutant thyroid carcinoma cells (attached manuscript #1).	40

4.3	Biological effects of BAY 43-9006 in BRAF mutant thyroid carcinoma cells (attached manuscript #1).	42
4.3	PD0325901 inhibits the proliferation of BRAF mutant thyroid carcinoma cells (attached manuscript #5)	45
4.4	PD0325901 inhibits the ERK pathway in BRAF mutant thyroid carcinoma cells (attached manuscript #5)	49
4.5	Transient nature of ERK inhibition in thyroid carcinoma cells (attached manuscript #5)	51
4.6	Regulatory circuits elicited by MEK inhibition in thyroid carcinoma cells (attached manuscript #5)	53
5	<i>DISCUSSION</i>	62
7	<i>ACKNOWLEDGEMENTS</i>	70
8	<i>REFERENCES</i>	71

LIST OF PUBLICATIONS

This dissertation is based upon the following publications:

1. Salvatore G, De Falco V, **Salerno P**, Nappi TC, Pepe S, Troncone G, Carlomagno F, Melillo RM, Wilhelm SM, Santoro M. BRAF is a therapeutic target in aggressive thyroid carcinoma. *Clin Cancer Res* 2006;12(5):1623-9.
2. Salvatore G, Nappi TC, **Salerno P**, Jiang Y, Garbi C, Ugolini C, Miccoli P, Basolo F, Castellone MD, Cirafici AM, Melillo RM, Fusco A, Bittner ML, Santoro M. A cell proliferation and chromosomal instability signature in anaplastic thyroid carcinoma. *Cancer Res* 2007;67:10148-10158.
3. De Falco V, Guarino V, Avilla E, Castellone MD, **Salerno P**, Salvatore G, Faviana P, Basolo F, Santoro M, Melillo RM. Biological role and potential therapeutic targeting of the chemokine receptor CXCR4 in undifferentiated thyroid cancer. *Cancer Res* 2007;67 (in press).
4. Nappi TC, **Salerno P**, *et al.* Identification of polo-like kinase 1 as a potential therapeutic target in anaplastic thyroid carcinoma. Manuscript in preparation.
5. **Salerno P**, Nappi TC, *et al.* Multiple regulatory circuits affect ERK inhibition upon MEK targeting in thyroid carcinoma cells. Manuscript in preparation

ABBREVIATIONS

ATC	anaplastic thyroid carcinoma
BRAF	B-type RAF
CML	chronic myelogenous leukemia
CV-PTC	classic variant of papillary thyroid carcinoma
DMEM	Dulbecco's modified Eagle's medium
DMSO	dimethyl sulfoxide
DUSP	dual specificity phosphatase
EGFR	epidermal growth factor receptor
ERK	extracellular signal-regulated kinase
FBS	fetal bovine serum
FDA	food and drug administration
FMTC	familial medullary thyroid carcinoma
FTC	follicular thyroid carcinoma
FV-PTC	follicular variant of papillary thyroid carcinoma
GDNF	glial-derived neurotrophic factor
GIST	gastrointestinal stromal tumors
IC ₅₀	half maximal inhibitory concentration
MAPK	mitogen-activated protein kinase
MEK	MAP kinase kinase or ERK kinase
MEN2	multiple endocrine neoplasia type 2
MTC	medullary thyroid carcinoma
NSCLC	non small cell lung cancer
PDC	poorly differentiated carcinoma
PI3K	phosphatidylinositol-3 kinase
PTC	papillary thyroid carcinoma
RCC	renal cell carcinoma
RET	rearranged during transfection
siRNA	small interference RNA
TCV-PTC	tall cell variant of papillary thyroid carcinoma
WDTC	well differentiated thyroid carcinoma
WT	wild type

ABSTRACT

The RAS-RAF-MEK-ERK or “ERK” (extracellular signal regulated kinase) cascade is a highly conserved signaling module in eukaryotes, that is often targeted by oncogenic mutations. Thyroid carcinoma is the most common endocrine malignancy and is often associated to oncogenic conversion of proteins acting in the ERK cascade. Activation of BRAF (B-type RAF) occurs in about 44% of papillary and 25% of undifferentiated thyroid carcinoma. Moreover, BRAF mutation is associated with adverse thyroid carcinoma clinical features, like extracapsular invasion, metastases and clinical recurrence. Genetic alterations targeting components of the ERK cascade other than BRAF, such as RAS and RET mutations, are also associated with thyroid carcinoma. While well differentiated thyroid cancer is treated by surgery and adjuvant radioiodine treatment, there is only modest therapeutic option for patients that fail radioiodine ablation. Thus, the ERK pathway might be a promising target for molecular therapy of thyroid carcinoma. In this dissertation, we have studied, at the biological and molecular level, the effects of BRAF/ERK targeting in thyroid carcinoma cell lines. To this aim, we applied RNA interference and small molecule inhibitors of BRAF and MEK kinases. Some of these compounds are in clinical development. Our data demonstrate that BRAF and MEK inhibition is a promising approach to reduce proliferation of BRAF mutant thyroid carcinoma cells. However, multiple regulatory circuits, that are targeted by BRAF/MEK inhibitors, need to be taken into consideration to further increase their efficacy.

1. INTRODUCTION

1.1 Thyroid gland

The thyroid gland is formed by two cell populations: follicular and parafollicular (C-cells) cells; most of the thyroid follicular cells are derived from the endodermal diverticulum, whereas a minority of them derives from the ultimobranchial body. The parafollicular cells are neural-crest derived; they originate from the ultimobranchial body and are interspersed in small groups among the follicles in the intermediate part of the thyroid lobes (Pearse and Carneiro 1967, Reynolds et al. 2001). Follicular cells concentrate inorganic iodide from the bloodstream to produce the hormones thyroxine (T₄) and its bioactive derivative triiodothyronine (T₃) from thyroglobulin. The parafollicular C-cells secrete calcitonin, which is involved in bone formation. Calcitonin secretion is stimulated by elevated calcium concentration in the serum (Lin et al. 1991).

1.2 Thyroid Carcinoma

Malignant thyroid tumors comprise a heterogeneous group of neoplasms with distinctive clinical and pathological features (Kondo et al. 2006). Table 1 summarizes the principal clinico-pathological features of thyroid carcinoma. More than 90% of thyroid carcinomas are derived from follicular cells while the remainder originates from the C-cells or from other cell types. The vast majority of follicular cell malignancies are well-differentiated (WDTC) carcinomas and include papillary (PTC) and follicular (FTC) carcinomas. WDTC is in general characterized by indolent behavior and very good therapeutic response (Schlumberger 1998, De Lellis 2006, Durante et al 2006).

Undifferentiated, or anaplastic, carcinoma (ATC) is very rare and ranks among the most lethal human malignancies, with a median survival from diagnosis of less than 1-year (Are et al. 2006, Pasięka 2003). Poorly differentiated thyroid carcinoma (PDC) lies, both morphologically and behaviorally, between WDTC and ATC, with an average 5-year survival rate of about 50% (Volante et al 2007, Pulcrano et al 2007). Medullary thyroid carcinoma (MTC), which originates from C-cells, comprises approximately 5% of primary thyroid carcinoma and has a 5-year survival rate of approximately 80% (Leboulleux et al. 2004).

Table 1: Clinico-pathological features of thyroid cancer (modified from Kondo et al. 2006)

Tumor Type	Prevalence	Age	Lymph-node metastasis	Distant metastasis	Survival (5 year)
PTC	80-90%	20-50	<50%	5-7%	>90%
FTC	5-10%	40-60	<5%	20%	>90%
PDC	~5%	50-60	30-80%	30-80%	50%
ATC	~2%	60-80	40%	20-50%	1-17%
MTC	~5%	30-60	50%	15%	80%

1.2.1 PTC

PTC is defined as a malignant epithelial tumor that shows evidence of follicular cell differentiation and presents characteristic nuclear features (Kondo et al. 2006). PTC represents the most common thyroid malignancy (Table 1) and also the most common pediatric thyroid malignancy. Numerous variants of PTC are recognized (classic, follicular, tall-cell, solid, diffuse sclerosing). One of the most common and diagnostically challenging ones is the follicular variant (FV-PTC). These tumors may be encapsulated or not and are composed almost exclusively of follicles having the characteristic nuclear features of PTC. Lymph-node metastases are rare in FV-PTC (De Lellis 2006, Kondo et al. 2006). Some PTC variants are recognized as more aggressive with

respect to classic PTC (CV-PTC); however, tumor stage or grade may be more important to assess prognosis than the histological subtype (Leboulleux et al. 2005). The solid variant comprises approximately 8% of sporadic PTC and is relatively common in children following radiation exposure. This variant is associated with a higher frequency of distant metastases and a less favorable outcome than CV-PTC (Nikiforov et al. 2001). The diffuse sclerosing variant is more common in children than adults and has a higher frequency of pulmonary metastases than CV-PTC. Tall-cell (TCV-PTC) and columnar-cell variants are also thought to have a worse prognosis than CV-PTC (Asklen and LiVolsi 2000); importantly, as described below, TCV-PTC has a very high prevalence of BRAF mutations. The term papillary “microcarcinoma” is referred to those tumors measuring less than 1 cm in diameter. Clinical management of PTC is based on total thyroidectomy, followed by adjuvant radioiodine therapy and thyroid hormone replacement to suppress TSH (Schlumberger 1998, Schlumberger 2007). Recently, guidelines for WDTC treatment have been set-up by american and european taskforces (Pacini et al. 2006, Cooper et al. 2006).

1.2.2 FTC

The WHO defines FTC as a malignant epithelial tumor with evidence of follicular cell differentiation but lacking the diagnostic nuclear features of PTC (Sobrinho-Simoes et al. 2004). FTC comprises less than 10% of thyroid malignancies and it occurs in the 5th decade of life (Table 1). FTC is rare in children. In general, FTC is encapsulated and composed of follicles or follicular cells arranged in follicular, solid or trabecular patterns. FTC is classified, according to the level of invasion, in: FTC with limited vascular invasion (minimally invasive FTC) and FTC with evidence of widespread

vascular invasion (widely invasive FTC). Tumors of the last category are associated with significant morbidity and mortality (De Lellis 2006).

1.2.3 ATC

ATC is the most aggressive thyroid tumor, and ranks among the most lethal human malignancies, with a median survival from diagnosis of ~4-12 months (McIver et al. 2001, Are et al. 2006, Pasieka 2003). Despite accounting for only 2-5% of all thyroid tumors, ATC is responsible for more than half of the deaths attributed to thyroid cancer (Table 1). Clinically, these tumors usually present during the 6th to 7th decade of life as a rapidly enlarging neck mass that extends locally, compressing the adjacent structures and tends to disseminate both to regional nodes and to distant sites, including lung, pleura, bone and brain. Worse prognosis associated with large tumor mass, distant metastases, and acute obstructive symptoms (Pierie et al. 2002, McIver et al. 2001). Current treatment of ATC has often only palliative purposes, particularly relief of airway compression, having little impact on patient's survival (De Crevoisier et al. 2004).

1.2.4 MTC

MTC derives from the neuroendocrine C-cells of the thyroid. Sporadic disease accounts for 80% of cases; the remainder 20% of patients inherit MTC in the context of autosomal dominant multiple endocrine neoplasia type 2 syndromes (MEN2A, MEN2B and FMTC). Sporadic MTC usually presents with palpable thyroid nodules in the 3rd-6th decades of life (Table 1). Total thyroidectomy is recommended for MTC patients. Clinical recurrence in the neck or

mediastinum is a common problem for MTC patients (Leboulleux et al. 2004, Cote and Gagel 2004).

1.3 Dominant oncogenes involved in thyroid carcinoma

A significant increase in our understanding of thyroid tumorigenesis at the molecular level has been obtained in the past three decades. Recent review articles (see for instance Kondo et al. 2006) summarize this knowledge. Briefly, WDTC is typically associated to the oncogenic conversion of proto-oncogenes coding for proteins acting in growth factor signal transduction cascade (the ERK and the PI3K cascades). A subgroup of FTC is characterized by the PAX8-PPAR γ rearrangement. Finally, undifferentiated or poorly-differentiated thyroid carcinoma (ATC and PDC), but not WDTC, features loss-of-function of the p53 tumor suppressor. Table 2 summarizes these genetic alterations. In this dissertation, we will refer in particular to signal transduction cascades (mainly the ERK one) with a view of using this information to hypothesize possible novel therapeutic strategies.

Table 2: Genetic alterations in thyroid cancer (modified from Kondo et al. 2006)

Genetic alteration	PTC	FTC	ATC	sporadic MTC
RET rearrangement	13-43%	—	—	—
RET mutation	—	—	—	30-50%
NTRK1 rearrangement	5-13%	—	—	—
BRAF mutation	44%	—	25%	—
RAS mutation	0-21%	40-53%	20-60%	—
PPAR γ rearrangement	—	25-63%	—	—
P53 mutation	—	—	67-88%	—
PIK3CA amplification or mutation	1-14%	13-29%	15-39%	—

1.3.1 MAPK pathway

The mitogen-activated protein kinase (MAPK) pathways are evolutionarily conserved kinase modules that play fundamental roles in several cell functions. Aberrant regulation of MAPK cascades contributes to cancer and other human diseases. MAPK cascades function downstream of cell surface receptors and other cytoplasmic signaling proteins (Sebolt-Leopold and Herrera 2004, Roberts and Der 2007). Mammalian cells possess four well characterized MAPK modules. They share a common architecture with three protein kinases that act sequentially: a MAPK kinase kinase (MAPKKK), a MAPK kinase (MAPKK) and a MAPK. The terminal kinases (MAPK) are the ERK1/2, the c-Jun amino-terminal kinases (JNK), p38 kinases (p38) and ERK5 (Roberts and Der 2007). The ERK pathway is activated by growth factor-stimulated cell surface receptors, whereas the JNK, p38 and ERK5 pathways are activated by stress and growth factors. In this dissertation we will refer in particular to the ERK pathway (**Figure 1**).

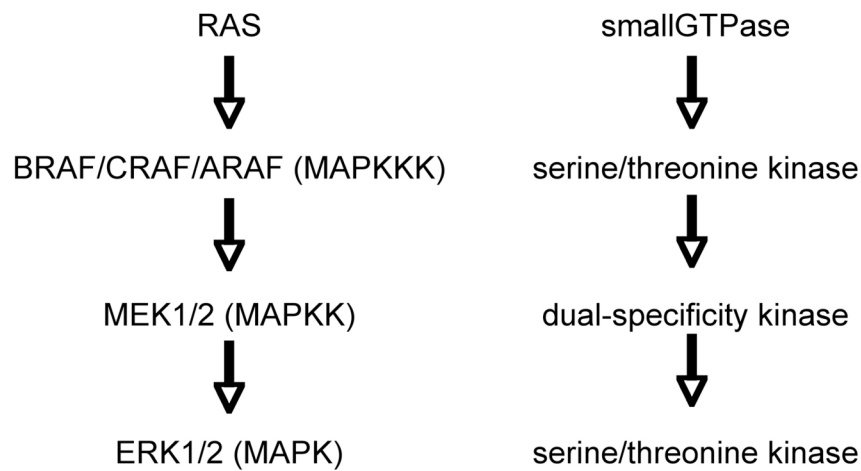


Fig 1: Schematic representation of the ERK signaling module.

When growth factors bind to their cognate receptors, conformational changes are induced in the receptor, leading to receptor dimerization, kinase activation, autophosphorylation and activation of proteins, such as the RAS small GTPase, at the inner surface of the cell membrane. The activated RAS, in turn, activates RAF family (CRAF, BRAF, ARAF) serine/threonine kinases. RAFs activate MEK1/2 dual-specificity kinases through phosphorylation on Ser217/Ser221 in their activation loop. Finally, MEK1/2 activate the ERK (p44 and p42 ERKs) subgroup of MAPKs by dual-phosphorylation on Thr202/Tyr204 within the Thr-Glu-Tyr motif in the activation loop (Sebolt-Leopold and Herrera 2004, Roberts and Der 2007). ERK integrates responses to extracellular signals by regulating gene expression, cytoskeletal rearrangements, and metabolism, as well as cell proliferation, differentiation, and apoptosis (MacCorkle and Tan 2005, Torii et al. 2004). MEK and ERK activation is transient and is followed by the initiation of negative feedback mechanisms that terminate the signal (Amit et al. 2007). These include up-regulated expression of dual-specificity

phosphatases (DUSPs, also referred to as MAPK phosphatases -MKP), which are able to dephosphorylate ERKs, thereby controlling intensity and duration of ERKs stimulation (Jeffrey et al. 2007). A schematic representation of the growth factor signaling to ERK is provided in **Figure 2**.

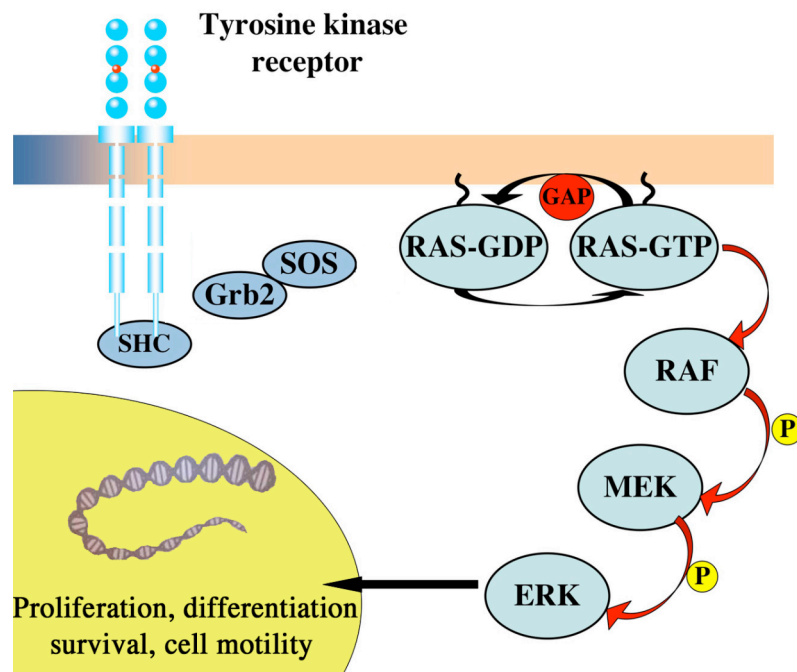


Fig. 2: Schematic representation of growth factor receptors signaling to ERK. Tyrosine-phosphorylated receptors recruit intracellular docking proteins/adapters such as Shc and Grb2 which in turn bring SOS, a RAS exchange factor (GEF), in close proximity to RAS. GTP loading on RAS fires the cascade. Phosphorylated p44 and p42 ERKs translocate to the nucleus, where they phosphorylate and regulate various transcription factors.

Importantly, oncogenic conversion of proteins in the ERK cascade is very frequently observed in human cancer. Prominent examples include mutations in growth factor receptors (like EGFR in lung cancer and RET in thyroid cancer), RAS mutations (in pancreatic, lung colon and thyroid carcinoma), and BRAF mutations in melanomas and thyroid carcinoma (Mercer and Pritchard 2003, Rodriguez-Viciano et al. 2005). Hereafter, oncogene mutations occurring in thyroid cancer are described, with a particular view to those intercepting the ERK cascade. A summary of the major genetic alterations found in thyroid cancer is reported in Table 2.

1.3.1.1 RET

The RET (REarranged during Transfection) proto-oncogene codes for a single-pass transmembrane receptor tyrosine kinase (Manie' et al. 2001). RET protein contains three functional domains: an extracellular ligand-binding domain, a hydrophobic transmembrane domain and an intracellular tyrosine kinase (TK) domain (**Figure 3**). The ligands of the RET receptor are growth factors belonging to the glial cell-line derived neurotrophic factor (GDNF) family (Manie' et al. 2001). Binding of the ligand causes receptor dimerization, autophosphorylation, and activation of the signaling cascade (Manie' et al. 2001). RET is normally expressed in neural crest and urogenital precursor cells. In the thyroid gland, RET is normally expressed in parafollicular C-cells but not in follicular cells. In a fraction (about 20%) of PTC, RET is oncogenically activated by chromosomal aberrations, resulting in the *in-frame* fusion of the 3'-portion of the RET gene (encoding the intracellular domain) to the 5'-portion of several unrelated gene partners, forming the chimeric RET/PTC oncogenes (Fusco et al. 1987, Grieco et al. 1990) (**Figure 3**). Virtually all breakpoints in RET occur within intron 11, leaving intact the intracellular and the TK domain of the receptor (**Figure 3**). Several RET/PTC variants have been reported, differing for the RET fusion partner (Santoro et

al. 2004). The RET partners share some common features: i) they are expressed in thyroid follicular cells, and therefore provide an active promoter for the expression of rearranged RET TK domain; ii) they contain protein-protein dimerization motifs and therefore mediate ligand-independent dimerization and activation of the truncated RET protein (Tong et al. 1997). The two most common RET/PTC variants are RET/PTC1 and RET/PTC3. RET/PTC1 is the RET fusion with the H4/CCDC6 gene (Grieco et al. 1990) while RET/PTC3 is the NCOA4-RET fusion (Santoro et al. 1994, Bongarzone et al. 1994). RET/PTC oncogenes transform thyroid cells in culture (Santoro et al. 1993) and initiate thyroid carcinomas in transgenic mice (Jhiang et al. 1996, Santoro et al. 1996, Powell et al. 1998). Several pieces of evidence indicate that RET/PTC transforming effects require signaling along the ERK pathway (Castellone et al. 2003, Knauf et al. 2003, Melillo et al. 2005). However, the wild-type receptor and truncated RET/PTC forms are also known to activate a number of other pathways, particularly the phosphatidylinositol-3 kinase (PI3K)/AKT pathway (Segouffin-Cariou et al. 2000, Miyagi et al. 2004, Jung et al. 2005, De Falco et al. 2005, Freche et al. 2005).

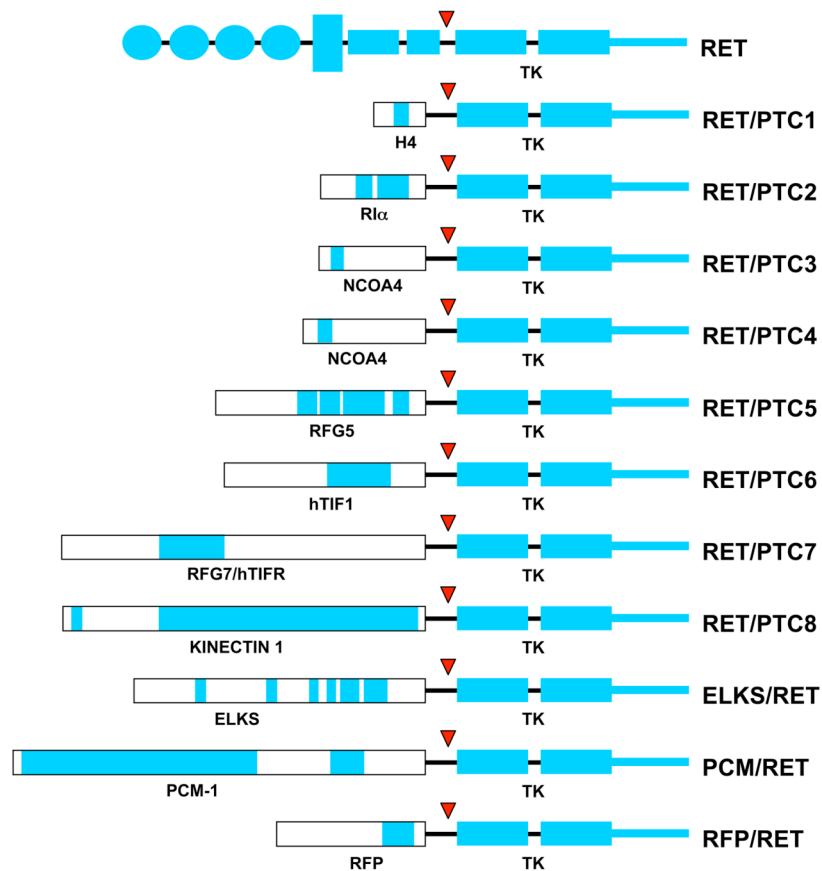


Fig. 3: Schematic representation of RET/PTC rearrangements

The prevalence of RET/PTC rearrangements is high in PTC from patients with a history of radiation exposure and pediatric PTC (Nikiforov et al. 1997, Bongarzone et al. 1996, Fenton et al. 2000, Soares et al. 1998). Overall, RET/PTC-positive PTC typically presents lymph node metastases, classic histology (CV-PTC), and a favorable prognosis (Adeniran et al. 2006).

Besides PTC also MTC is associated to oncogenic conversion of RET. Germ-line point mutations in RET are responsible for familial MEN2-associated MTC and similar mutations, at the somatic level, are found in a fraction (30-50%) of sporadic MTC cases (Manie' et al. 2001, Cote and Gagel 2003, Santoro and Carlomagno 2006).

1.3.1.2 RAS

RAS genes are the most common targets for somatic gain-of-function mutations in human cancer (Schubbert et al. 2007, Ramjaun and Downward 2007). Three different RAS are present in mammalian genome: HRAS, KRAS and NRAS. The three RAS genes encode four highly homologous 21 kD (p21) proteins: HRAS, NRAS, KRAS4A and KRAS4B (the 2 KRAS proteins result from alternative splicing at the C-terminus). The N-terminal portion of the RAS proteins comprises a highly conserved GTPase domain; the C-terminal hypervariable region contains residues that specify post-translational protein modifications (Schubbert et al. 2007). RAS proteins are bound to the inner leaflet of the cell membrane where they exhibit guanosine triphosphatase activity (GTPase). When RAS is in the inactive form it binds guanosine diphosphate (GDP), in the active form, instead, it is bound to GTP (Schubbert et al. 2007) (**Figure 2**). Guanine-nucleotide exchange factors (GEF), like SOS, are involved in the RAS activation step, while GTPase-activating proteins (GAP) are involved in the inactivation of RAS. In normal cells, RAS conveys intracellularly signals originating from tyrosine kinase membrane receptors to the ERK and many additional signaling cascades, including the PI3K-AKT pathway (Schubbert et al. 2007, Ramjaun and Downward 2007). RAL and RAC smallGTPases are additional RAS effectors; RAL, in turn, triggers the activity of phospholipase D while RAC regulates cytoskeleton dynamics. However, among the various RAS effectors, the BRAF-MEK-ERK cascade plays a prominent role in cell proliferation.

Activating RAS mutations occur in approximately 30% of human cancers. Specific RAS genes are mutated in different malignancies: KRAS mutations are prevalent in pancreatic, colorectal, endometrial, biliary tract, lung and cervical cancers; KRAS and NRAS mutations are found in myeloid

malignancies; and NRAS and HRAS mutations predominate in melanoma and bladder cancer, respectively (Schubbert et al. 2007). These mutations introduce amino-acid substitutions at positions 12, 13 and 61, and constitutively activate RAS function by impairing the intrinsic GTPase activity.

Mutations of all three RAS oncogenes have been identified in tumors originating from follicular thyroid cells. Up to 50% of FTC harbour RAS mutations (Kondo et al. 2006). RAS mutations are also found in benign adenomas and thyroid nodules, suggesting they may be early events in thyroid tumorigenesis. The NRAS mutation in codon 61 is the most frequent RAS mutation in FTC and it is more frequent in malignant than in benign thyroid tumors (Basolo et al. 2000, Garcia-Rostan et al. 2003). PDC and ATC (up to 60% of the cases) are often RAS mutation positive. RAS mutations in PTC are restricted to FV-PTC (Zhu et al. 2003, Di Christofaro et al. 2006). Overall, these clinico-pathological correlations suggest that RAS mutation may mark a subset of thyroid tumors that is more likely to undergo de-differentiation and tumor progression. The phenotype of NRAS(Q61) transgenic mice generated by our group is consistent with this view (Vitagliano et al. 2006). Mitsutake et al. (2005), Saavedra et al. (2000) and Knauf et al. (2006) demonstrated that the expression of oncogenic RAS, as well as BRAF (see below), alleles bypassed G2/M and mitotic spindle checkpoints and induced signs of genomic instability in thyrocytes, an observation that may explain the high oncogenic activity of these oncoproteins.

1.3.1.3 BRAF

BRAF (B-type RAF) belongs to the RAF family of serine/threonine kinases. There are three RAF kinases in mammals: ARAF, BRAF, and CRAF (or RAF-1) (Marais and Marshall 1996). The RAF proteins display a common architecture, with two N-terminal regulatory domains (CR1 and CR2) and one

kinase C-terminal domain (CR3) (**Figure 4**). The three RAF members show differences in tissue distribution and activation modalities. Importantly, several residues must be phosphorylated in ARAF and CRAF for full activation, while some of them are constitutively phosphorylated or replaced with phosphomimetic residues in BRAF. This makes BRAF activation more rapid and efficient than that of CRAF or ARAF (**Figure 4**). Accordingly, BRAF has a strong basal kinase activity and is the most potent activator of MEK in many cell types; this may account for the high prevalence of mutations in BRAF, rather than other RAF family members, in human tumors (Marais et al. 1997, Garnett and Marais 2004, Emuss et al. 2005, Dhomen and Marais 2007). In fact, whereas BRAF can be activated by single amino acid substitutions, CRAF and ARAF require at least two mutations for oncogenic conversion (Dhomen and Marais 2007).

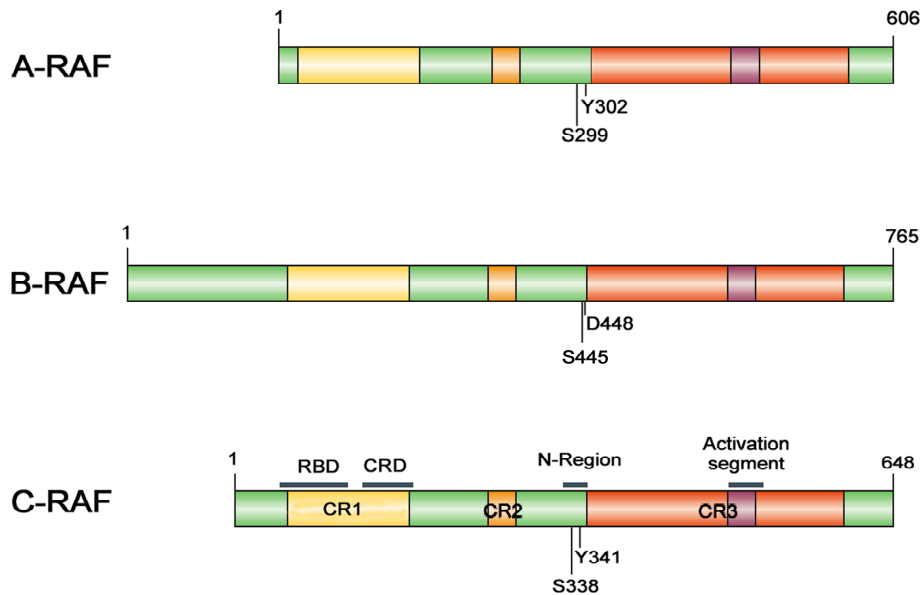


Fig. 4: Schematic representation of the RAF proteins. The three conserved regions: CR1 (yellow), CR2 (orange) and CR3 (red) are highlighted. The amino acids indicated below the individual isoforms refer to known regulatory phosphorylation sites. CR1 contains the RAS-

binding domain and CR3 contains the catalytic domain (the activation segment is highlighted in pink).

BRAF mutations were recently discovered to be a prime cause of aberrant activation of the ERK pathway in human cancer, particularly in melanoma, where approximately 70% of cases carry BRAF mutations (Dhomen and Marais 2007). Also ovarian, colon and thyroid (see below) carcinoma often harbours BRAF mutations.

The most common BRAF mutation (>90%), is a thymine to adenine transversion at nucleotide 1799 (T1799A) leading to a glutamic acid for valine substitution at position 600 (V600E). Other more rare mutations have been described (www.sanger.ac.uk/genetics/CGP/cosmic/). Importantly, most (but not all, see below) mutations have a gain-of-function effect. X-ray structural analysis has clarified that activating BRAF mutations invariably map in the activation loop of the kinase or the glycine-rich P loop (ATP-binding site). The inactive conformation of the BRAF kinase is maintained secondary to interactions between these two loops; therefore, the substitution of key residues within these domains disrupts the inactive conformation, switching the BRAF kinase into a catalytically competent conformation able to constitutively phosphorylate MEK (Wan et al. 2004). BRAFV600E kinase function is activated approximately 500-fold with respect to wild type protein. Moreover, it induces constitutive ERK signaling through hyperactivation of the MEK–ERK pathway, thereby stimulating proliferation, survival and transformation.

About 70 other oncogenic mutations in BRAF have been identified (www.sanger.ac.uk/genetics/CGP/cosmic/). Surprisingly, the activity of some BRAF mutants is actually impaired rather than potentiated. However, these impaired activity mutants can still activate MEK through CRAF (**Figure 5**). Indeed, BRAF can activate CRAF through a direct BRAF/CRAF protein-protein interaction, followed by allosteric activation and trans-phosphorylation of CRAF by BRAF (Garnett et al. 2005, Dhomen and Marais 2007).

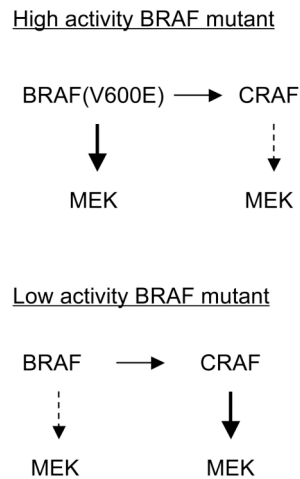


Fig. 5: Direct and indirect (via CRAF) BRAF signaling to MEK according to the potency of BRAF mutations (modified from Dhomen and Marais 2007).

BRAF mutation in thyroid carcinoma was initially reported about 5-years ago by three research groups and then confirmed by many other studies (Kimura et al. 2003, Soares et al. 2003, Cohen et al. 2003). The V600E accounts for the great majority of BRAF alterations in thyroid cancer (**Figure 6**); however, more rare mutations have also been described. In some cases, these rare changes are missense mutations, in others, they are small insertions/deletions. Virtually always, these mutations target residues close to the V600 amino acid in the activation loop of the kinase (Trovisco et al. 2004, Carta et al. 2006, Castro et al. 2006, Moretti et al. 2006, Hou et al. 2007, Koh et al. 2007, Lupi et al. 2007). The K601E mutation is prevalent in FV-PTC, a PTC variant that is, overall, rarely BRAF mutation positive (see also below) (Trovisco et al. 2004, Trovisco et al. 2005). Also the VKSR600-603del+T599I (Lupi et al. 2007) and the G474R (Castro et al. 2006) mutations have been so far found only in FV-PTC cases (Hou et al. 2007). Finally, another mechanism of BRAF activation

has been identified, involving an inversion of chromosome 7q that leads to the *in-frame* fusion between BRAF and the AKAP9 gene (Ciampi et al. 2005). The AKAP9-BRAF protein contains the BRAF kinase domain but it lacks the regulatory N-terminal region. This rearrangement is rare and found in PTC associated with radiation exposure (Fusco et al. 2005).

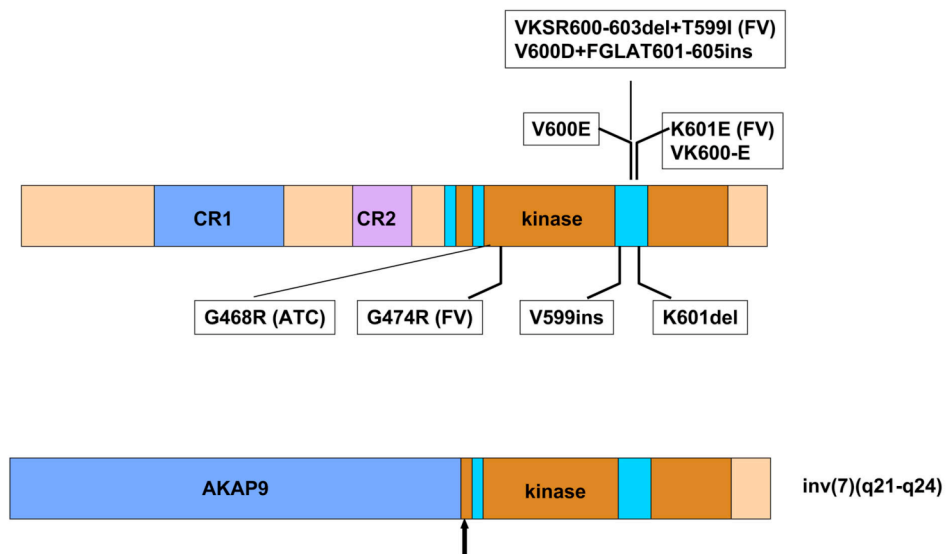


Fig. 6: BRAF mutations described in thyroid cancer

BRAF is the most common genetic event in PTC, occurring in approximately 44% of cases (Ciampi and Nikiforov 2005, Groussin and Fagin 2006, Xing 2007) (Table 2). FTC and benign thyroid tumors are invariably negative for BRAF mutations. Instead, BRAF mutations are found in ATC (about 25% of the cases) and PDC (Table 2). In ATC, BRAF mutations are typically present in those cases with morphological areas of PTC differentiation, and therefore probably derived from pre-existing PTC (Nikiforova et al. 2003). This suggests that BRAF mutation may play a role in promoting progression from differentiated to undifferentiated carcinomas. Consistently, a transgenic mouse

model demonstrated that thyroid targeting of BRAF initiates the formation of PTC than tends to progress to PDC (Knauf et al. 2005). These tumors frequently show invasion of blood vessels, thyroid capsule, and skeletal muscle (Knauf et al. 2005).

Interestingly, BRAF mutations and RET/PTC rearrangements are mutually exclusive, pointing to a key role played by the RET-BRAF-ERK cascade in PTC formation (Kimura et al. 2003). Several features differentiate PTC harbouring RET/PTC from those positive for BRAF mutation. Differently from RET/PTC, pediatric PTC (both sporadic and radiation-induced) have a low prevalence of BRAF mutations (Lima et al. 2004, Kumagai et al. 2004, Nikiforova et al. 2004). In general, BRAF mutation is associated with aggressive clinico-pathological characteristics. BRAF mutation occurs most commonly in TCV-PTC (~77%) than CV-PTC (~ 60%) and FV-PTC (~ 12%) (Xing 2007, Adeniran et al. 2006). Moreover, BRAF mutation correlates with advanced tumor stage, extrathyroid extension, advanced age, relapses and reduced disease-free survival (Xing 2007). In a large study conducted on 500 independent PTC samples, Lupi and colleagues found that BRAF mutation correlates with capsule infiltration (Lupi et al. 2007). Rodolico and colleagues (2007) recently demonstrated that metastatic PTC lesions in lymph nodes harboring BRAF mutation are larger in size than those harboring wild-type alleles. Systemic treatment of PTC is principally based on radioiodine therapy. However, thyroid cancer may lose radioiodine avidity, this being associated with increased morbidity and mortality (Schlumberger 1998, Schlumberger et al. 2007). BRAF mutation is typically associated to the loss of radioiodine avidity in PTC cells (Xing 2007).

It is still unclear why BRAF mutation is associated with increased aggressiveness and recurrence of PTC when compared with other genetic alterations that also intercept the ERK pathway. Plausible explanations may be the capability of BRAF oncogenes, similarly to RAS, of inducing genetic

instability (Mitsutake et al. 2005, Knauf et al. 2006), coupled with the preferential regulation exerted by BRAF of genes involved either in tumor invasion (like metalloproteases) or thyroid cell differentiation (like the NIS, sodium-iodine symporter) (Melillo et al. 2005, Mesa et al. 2006, Riesco-Eizaguirre et al. 2006, Xing 2007).

1.3.2 PI3K/AKT

Phosphatidylinositol 3-kinase (PI3K) is a heterodimer formed by p85 regulatory and p110 catalytic (PIK3CA) subunits. Ligand-mediated activation of tyrosine kinase receptors recruits p85-p110 complex on cell membrane where the p85 regulatory subunit can be phosphorylated; conformational changes relieve the inhibitory effect exerted by p85 on p110 activity (Vivanco and Sawyers 2002). Growth factor receptors can also activate PI3K indirectly through RAS, which can bind and activate the p110 subunit. Once activated, PIK3CA generates phosphatidylinositol-3-phosphate (PIP3), which functions as a second messenger to activate downstream effectors including the AKT/PKB protein kinase (Vivanco and Sawyers 2002). Termination of PI3K/AKT activity occurs through the lipid phosphatase activity of PTEN (Cantley and Neel 1999).

The PI3K/AKT pathway is involved in many cellular processes as cell survival, cell cycle progression, cell motility and invasion (Brazil et al. 2004). Genetic or epigenetic alterations causing gain-of-function of PI3K and AKT or loss-of-function of PTEN are associated to a wide spectrum of human cancers (Hay 2005). Reduced expression of PTEN is common in different types of thyroid tumors, particularly in more aggressive subtypes (Halachmi et al. 1998, Bruni et al. 2000, Frisk et al. 2002). FTC is characterized by increased expression of AKT1 and AKT2 (Ringel et al. 2001). Importantly, point

mutations and gene amplifications of PIK3CA have been found in a significant fraction of ATC and less frequently in WDTC (Garcia Rostan et al. 2005, Wang et al. 2007, Santarpia et al. 2007, Hou et al. 2007) (Table 2).

1.4 Molecularly targeted cancer therapy

“Targeted therapy” refers to measures that interfere with specific proteins involved in disease. This type of concept has been successfully applied to oncogenic protein kinases. The human genome contains 518 protein kinase genes (known as “kinome”). Recent highthroughput genomic sequencing efforts have demonstrated that the kinome is the favourite target of “driver” oncogenic mutations in human cancer (Bardelli et al. 2003, Sjöblom et al. 2006, Greenman et al. 2007). Importantly, protein kinases are “druggable” molecules and this has prompted scientists to search for new drugs able to intercept kinase function for cancer therapy (Sebolt-Leopold and English 2006, Baselga 2006, Sawyers 2007).

Kinase-directed small-molecule drugs and monoclonal antibodies are already used in the clinical setting. Most small-molecule compounds obstruct kinase activity by binding to the ATP pocket within the catalytic domain (ATP mimetics). These compounds were initially identified by random screening of libraries of natural products or synthetic compounds. Although the ATP binding pocket is highly conserved among the different kinases, there are significant differences in its primary sequence or tridimensional fold to warrant specificity of its targeting. Other compounds target regions outside the ATP-binding site of the enzyme (allosteric inhibitors); by binding to domains highly divergent among the various kinases, these compounds are believed to be more selective than the ATP mimetics (Sebolt-Leopold and English 2006, Baselga 2006).

The clinical efficacy of small molecule inhibitors of ABL, KIT and EGFR in different tumor types is witness to the power of this approach. To date, at least 10 different protein kinase inhibitors have received approval by the FDA (Food and Drug Administration). These include: the ABL and KIT inhibitor imatinib for the treatment of CML and GIST, the EGFR inhibitors erlotinib and gefitinib for NSCLC, and the multikinase inhibitors sunitinib and sorafenib (BAY 43-9006) for metastatic renal cancer (Baselga 2006).

The presence of activating mutations of a kinase may anticipate tumor responsiveness to its targeting in a given cancer patient. This is well illustrated by the case of EGFR inhibitors and NSCLC. Most tumors responsive to EGFR inhibitors had gain-of-function mutations in EGFR or an increased EGFR gene copy number. This could be explained by the fact that mutant EGFR variants were more efficiently inhibited than wild type protein by the EGFR targeting agents (gefitinib and erlotinib) but also by the observation that only EGFR-mutant NSCLC cells were addicted to EGFR signaling (Niculescu-Duvaz et al. 2007). In this context, the protein kinases of the ERK cascade appear to be excellent molecular targets for the treatment of thyroid cancer.

1.4.1 ERK pathway inhibitors

Two protein kinases in the ERK pathway have received attention as potential targets for pharmacological intervention: RAF and MEK. No ERK inhibitor, instead, is as yet available (Sebolt-Leopold and Herrera 2004, Kohno and Pouyssegur 2006, Roberts and Der 2007). RAS is a promising non-kinase target in the cascade. However, inhibitors directed at intercepting post-translational RAS protein modifications did not exerted sufficient specificity to prove that their clinical activity was indeed due to RAS inhibition (Roberts and Der 2007). Moreover, the RAS level of inhibition may prove not useful when the oncogenic mutation maps downstream, e.g. at the level of BRAF.

Several small-molecule RAF inhibitors have been developed (Table 3). One of them, sorafenib (BAY 43-9006), has been extensively studied in clinical trials and has been approved by the regulatory authorities for the treatment of metastatic renal cell carcinoma (RCC) (Wilhelm et al. 2006). BAY 43-9006 is a multitarget compound that inhibits besides RAF a range of other kinases, including many tyrosine kinases. Probably, BAY 43-9006 anti-angiogenic properties account for its clinical activity in RCC. In melanoma, instead, a tumor with high prevalence of BRAF mutations, BAY 43-9006 did not show significant clinical activity (Eisen et al. 2006). Other small molecule compounds are being developed against RAF kinases (Table 3).

Table 3. RAF/MEK inhibitors in clinical development (modified from Sebolt-Leopold and Herrera 2004, Roberts and Der 2007)

Agent	Company	Target	Clinical development
BAY 43-9006 (sorafenib)	Bayer	RAF, VEGFR, KIT, PDGFR, RET	Approved for advanced RCC
RAF265 (CHIR-265)	Novartis	ARAF, BRAF, CRAF	Phase I
PLX4032	Roche/Plexxi kon	BRAF(V600E)	Phase I
CI-1040 (PD184352)	Pfizer	MEK1/2	Clinical trials terminated
PD0325901	Pfizer	MEK1/2	Phase II: breast, colorectal ca., NSCLC, melanoma
AZD6244 (ARRY-142886)	AstraZeneca/ Array	MEK1/2	Phase II: NSCLC, melanoma, pancreatic ca.

Potent MEK inhibitors have been developed. These are selective, non ATP-competitive kinase inhibitors that bind to a pocket that is adjacent to, but distinct from the ATP-binding site. Binding of the inhibitor is thought to stabilize the inactive conformation of the kinase potentially inhibiting its function

(Sebolt-Leopold and Herrera 2004, Kohno and Pouyssegur 2006, Roberts and Der 2007, Messersmith et al. 2006). The development of pharmacological inhibitors of MEK was launched with the discovery of PD98059; this compound became a tool to explore the role of the ERK pathway but, because of its pharmaceutical limitations, it was not clinically developed. U0126 was subsequently reported as a dual MEK (MEK1/2) inhibitor more potent than PD98059 (half maximal inhibitory concentration $-IC_{50}$: 13 μ M). U0126 has also been widely used as a reagent for *in vitro* studies (Davies et al. 2000).

These initial anti-MEK compounds were followed by novel and more potent molecules that are being explored for clinical activity (Table 3 and **Figure 7**). The first MEK inhibitor reported to inhibit tumor growth *in vivo* was CI-1040 (PD184352). Its IC_{50} for MEK is 300nM and at doses as high as 10 μ M it did not inhibit other kinases (Davies et al. 2000). Although there was encouraging evidence of anti-tumour activity in the Phase I, similar results were not observed in Phase II (Rinehart et al. 2004, Lorusso et al. 2005, Wang et al. 2007). PD0325901, which is structurally highly similar to CI-1040, has been subsequently developed as a significantly more potent MEK inhibitor. PD0325901 has an IC_{50} of 1 nM against activated MEK1 and MEK2. This compound is also significantly more potent than CI-1040 *in vivo*. Anticancer activity of PD0325901 has been demonstrated for a broad spectrum of human tumor xenografts. Phase II trials with this agent are now in progress (Sebolt-Leopold and Herrera 2004, Massersmith et al. 2006, Brown et al. 2007). Finally, the benzimidazole AZD-6244 has also been reported to be a highly potent MEK inhibitor, with an IC_{50} of 12 nM against purified MEK (Yeh et al. 2007) and has recently entered clinical trials.

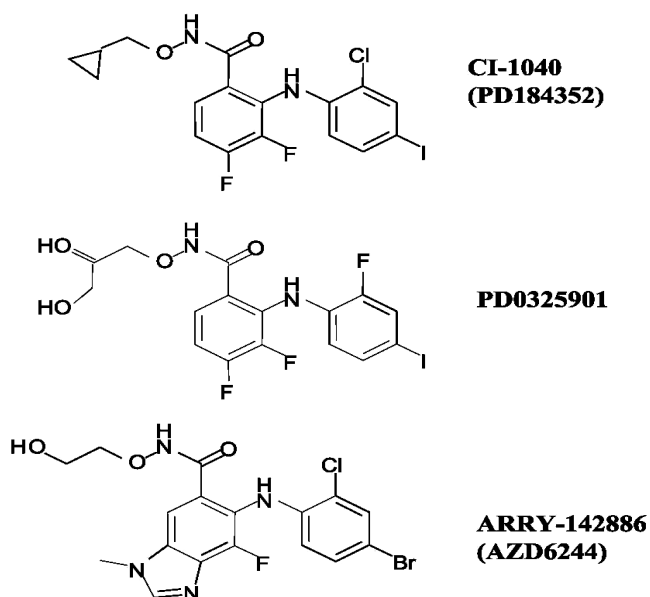


Fig. 7: Chemical structures of MEK inhibitors.

The X-ray structure of MEK1 in combination with a related molecule, PD318088, proved that the mode of binding of compounds of the “PD” series is non competitive with respect to ATP but rather involves an allosteric pocket mapping close to the ATP-binding one (Ohren et al. 2004).

1.4.2 Novel molecular therapy strategies for undifferentiated thyroid carcinoma

In recent years, an extensive program for the identification of potential therapeutic targets suitable to pharmacological intervention in ATC has been launched in our laboratory. Some of these studies are attached to this dissertation and lead to the identification of one serine/threonine kinase PLK1 (Polo-like kinase 1) (attached manuscripts #2 and 4) and one G-coupled transmembrane receptor (CXCR4) (attached manuscript #3) as overexpressed in ATC samples and cell lines and required for proliferation of ATC cells in culture. The results of these studies are briefly summarized below.

We have identified a gene expression signature associated with the high proliferative and aneuploid ATC phenotype (attached manuscript #2). Such expression profile featured the up-regulation of PLK1 that belongs to the *Polo* family of serine/threonine kinases. PLK1 plays a pivotal role in several G2 and M-phase related events, i.e., centrosome maturation, bipolar spindle formation, CDC2 (CDK1)-cyclin B activation, and anaphase-promoting complex/cyclosome (APC/C) activation. We could show that chemical and genetic (RNAi) blockade of PLK1 resulted in a potent cytotoxic effect in cultured ATC cells (attached manuscript #4).

CXCR4 is the receptor for the SDF-1/CXCL12 chemokine and we could show that ATC cell lines and ATC tumor samples overexpress CXCR4, both at the level of mRNA and protein. Treatment of ATC cells with SDF-1 induced proliferation and increased ERK phosphorylation. Importantly, these effects were blocked by the specific CXCR4 antagonist AMD3100 and by CXCR4 RNAi. Accordingly, AMD3100 effectively reduced ATC xenograft tumor growth in nude mice (attached manuscript #3).

The rest of this dissertation is based on the attached manuscripts #1 and 5, in which we have explored in detail the effects of BRAF-MEK blockade in thyroid carcinoma cells.

2 AIMS OF THE STUDY

The aim of this work was to evaluate the *in vitro* effects of ERK pathway blockade in cultured ATC cell lines. In particular:

- We analysed by cell growth and flow cytometry assays the activity of some classes of ERK pathway inhibitors, including the ATP-competitive BRAF inhibitor BAY-439006 and the non-ATP-competitive MEK inhibitor PD0325901.
- We analysed biochemically the capability of these compounds to hit their intended targets in thyroid carcinoma cells.
- We explored regulatory circuits elicited in thyroid carcinoma cells by these compounds and the possibility that such mechanisms may dampen the efficacy of the approach.

3. MATERIALS AND METHODS

The experimental procedures used in this study are described in detail in the attached publications. Only, a brief description is provided here.

3.1 Compounds

The chemical name of BAY 43-9006 (sorafenib) is: *N*- (3-trifluoromethyl-4-chlorophenyl)-*N'*-(4-(2-methylcarbamoyl pyridin-4-yl)oxyphenyl)urea. BAY 43-9006 was provided by Bayer HealthCare Pharmaceuticals (West Haven, CT, USA). For *in vitro* experiments, BAY 43-9006 was dissolved in dimethyl sulfoxide (DMSO). For *in vivo* experiments, it was dissolved in Cremophor EL/ethanol (50:50; Sigma Cremophor EL, 95% ethyl alcohol) at 4-fold (4X) the highest dose, foil-wrapped, and stored at room temperature (attached manuscript #1). The chemical name of PD0325901 is *N*-((*R*)-2,3-dihydroxy-propoxy)-3,4-difluoro-2-(2-fluoro-4-iodo-phenylamino)-benzamide.

PD0325901 was provided by Pfizer Inc, (New York, NY USA). PD0325901 was dissolved in DMSO at a concentration of 10 mM and stored at -80°C (attached manuscript #5). U0126, LY294004 and Wortmannin were purchased from Cell Signaling (Beverly, MA, USA). Orthovanadate was purchased from Sigma-Aldrich (St. Louis, MO, USA).

3.2 Cell cultures

The thyroid cell lines used in this study are described in Table 4. Cancer cells were grown in Dulbecco's modified Eagle's medium (DMEM) supplemented with 10% fetal bovine serum (FBS) (GIBCO, Paisley, PA), 2 mM L-glutamine and 100 units/ml penicillin-streptomycin (GIBCO). The P5 primary culture of normal human thyroid follicular cells was kindly donated by Francesco Curcio (Università di Udine). The rat-derived differentiated thyroid follicular cell lines

PCCI3 (hereafter named PC) and FRTL5 were grown in Coon's modified Ham F12 medium supplemented with 5% calf serum and a mixture of six hormones (6H), including thyrotropin (10mU/ml), hydrocortisone (10nM), insulin (10µg/ml), apo-transferrin (5µg/ml), somatostatin (10ng/ml), and glycyl-histidyl-lysine (10ng/ml) (Sigma-Aldrich, St. Louis, MO, USA) (Fusco et al. 1987).

Table 4: Cell lines used in this dissertation.

Name	Species	Primary/ Continuous	Tumor type	BRAF V600E status
FRO	Human	C	ATC	Homozygous
ARO	Human	C	ATC	Heterozygous
KAT4	Human	C	ATC	Heterozygous
FB1	Human	C	ATC	Heterozygous
SW1736	Human	C	ATC	Heterozygous
8505C	Human	C	ATC	Homozygous
BHT101	Human	C	ATC	Heterozygous
NPA	Human	C	PDC	Homozygous
BHP14.9	Human	C	PTC	Heterozygous
BCPAP	Human	C	PTC	Heterozygous
P5	Human	P	Normal	negative
PCCL3	Rat	C	Normal	negative
FRTL5	Rat	C	Normal	negative

3.3 Cell proliferation assays

5×10^4 cells were plated in 35-mm dishes in low serum ($\frac{1}{4}$ of normal serum concentration). The day after plating, the compounds or vehicle were added. The media was changed every 2 days and cells were counted in triplicate every day for four days (attached manuscripts #1 and 5)

3.4 FACS analysis

For cytofluorimetric analysis, cells were plated at 5×10^5 cells in 100-mm dishes in low serum. The following day, cells were incubated with fresh medium with or without the compound. Cells were collected every 12 hours after treatment and fixed in cold 70% ethanol in phosphate-buffered saline. Propidium iodide (25 $\mu\text{g/ml}$) was added in the dark, and samples were analyzed with a FACSscan flow cytometer (Becton Dickinson, San Jose, CA) interfaced with a Hewlett Packard computer (Palo Alto, CA).

3.5 RNA silencing (attached manuscript#1)

The small inhibitor duplex RNAs (siRNA) targeting human BRAF were chemically synthesized by PROLIGO (Boulder, CO). Sense strands for siRNA targeting were: BRAF: 5'-AGAAUUGGAUCUGGAUCAUTT-3'; and Lamin A/C: 5'-CUGGACUCCAGAAGAACATT-3'. As control, we used a non-specific siRNA duplex containing the same nucleotides but in irregular sequence (scrambled). For siRNA transfection, cells were grown under standard conditions. The day before transfection, 1×10^5 cells were plated in 35-mm dishes in DMEM supplemented with 10% FBS without antibiotics. Transfection was performed using 360 pmol of siRNA and 18 μl of oligofectamine reagent (Invitrogen, Groningen, The Netherlands), following the manufacturer's instruction. Cells were kept in 2.5% serum and counted 48 and 72 hours after transfection.

3.6 Protein studies

Immunoblotting experiments were performed according to standard procedures. Briefly, cells were harvested in lysis buffer (50 mM Hepes, pH 7.5, 150 mM NaCl, 10% glycerol, 1% Triton X-100, 1 mM EGTA, 1.5 mM MgCl₂, 10 mM NaF, 10 mM sodium pyrophosphate, 1 mM Na₃VO₄, 10 μg of aprotinin/ml, 10 μg of leupeptin/ml) and clarified by centrifugation at 10,000 g. For protein extraction, samples of mouse xenografts were snap-frozen and immediately homogenized in lysis buffer by using the Mixer Mill MM300 (Qiagen, Crawley, West Sussex, UK) (attached manuscript #1). Protein concentration was estimated with a modified Bradford assay (Bio-Rad, Munich, Germany). Antigens were revealed by an enhanced chemiluminescence detection kit (ECL, Amersham Pharmacia Biotech, Little Chalfort, UK). Signal intensity was evaluated and quantified with the Phosphorimager (Typhoon 8600, Amersham Pharmacia Biotech) interfaced with the ImageQuant software.

3.7 Antibodies

The antibodies used in this work are described in detail in the original articles (attached manuscripts #1 and 5).

3.8 BRAF kinase assay (attached manuscript #1)

Cells were cultured for 12 hours in serum-deprived medium. Thereafter, cells were treated with the indicated compounds for one hour; BRAF kinase was immunoprecipitated with the anti-BRAF antibody and resuspended in a kinase buffer containing 25 mM sodium pyrophosphate, 10 μCi ³²P ATP and 1 μg of recombinant GST-MEK (Upstate Biotechnology Inc., Lake Placid, NY). After 30 min incubation at 4°C, reactions were stopped by adding 2X Laemmli

buffer. Proteins were then subjected to 12% SDS gel electrophoresis. The radioactive signal was analyzed using a Phosphorimager (Molecular Dynamics).

3.9 Reverse transcription and quantitative PCR (attached manuscript #5)

Total RNA was isolated with the RNeasy Kit (Qiagen, Crawley, West Sussex, UK). One μg of total RNA from each sample was reverse-transcribed with the QuantiTect[®] Reverse Transcription (Qiagen) according to manufacturer's instructions. The effects of PD0325901 on the level expression of ERK phosphatases DUSP-5 and MKP-3 were measured by quantitative RT-PCR assay, using the Human ProbeLibray[™] system (Exiqon, Denmark). PCR reactions were performed in triplicate and fold changes were calculated with the formula: $2^{-(\text{sample 1 } \Delta\text{Ct} - \text{sample 2 } \Delta\text{Ct})}$, where ΔCt is the difference between the amplification fluorescent thresholds of the mRNA of interest and the mRNA of RNA polymerase 2 used as an internal reference. Primers sequences for targeted genes were:

MKP3 forward 5'-CGACTGGAACGAGAATACGG-3',

MKP3 reverse 5'-TTGGAACCTTACTGAAGCCACCT-3';

DUSP5 forward 5'-ACAAATGGATCCCTGTGGAA-3',

DUSP5 reverse 5'-CCTTTTCCCTGACACAGTCAA-3';

As control for normalization RNA polymerase 2 mRNA was amplified:
forward 5'-TGCGTGACATTAAGGAGAAG-3',

reverse 5'-GCTCGTAGCTCTTCTCCA-3'.

3.10 Tumorigenicity in nude mice (attached manuscript #1)

Animals were housed in barrier facilities at the Dipartimento di Biologia e Patologia Cellulare e Molecolare (University of Naples “Federico II”, Naples, Italy). The cells (1×10^6 ARO) were inoculated subcutaneously into the right flank of 4-week-old male BALB/c nu/nu mice (Jackson Laboratory, Bar Harbor, ME). When tumors reached approximately 100 mm^3 , the animals were treated with the compound or vehicle by oral gavages for five consecutive days/week for three weeks. Tumor diameters were measured with calipers. Tumor volumes (V) were calculated by the rotational ellipsoid formula: $V = A \times B^2/2$ (A = axial diameter; B = rotational diameter). Another group of animals (surrogate) was treated with vehicle or 60 mg/kg of BAY 43-9006 (5 animals per group) for 5 days starting when the tumors reached approximately 300 mm^3 . Tumors were excised three hours after the last dose and snap-frozen in liquid nitrogen and used for protein extraction. All animal manipulations were conducted in accordance with Italian regulations for experimentation on animals.

3.11 Statistical Analysis

Two-tailed unpaired Student's t test (normal distributions and equal variances) was used for statistical analysis. Differences were significant when $P < 0.05$. Statistical analysis was performed using the Graph Pad InStat software program (version 3.06.3, San Diego, CA, USA).

4 RESULTS

4.1 Effects of genetic BRAF knock-down in BRAF mutant thyroid carcinoma cells (attached manuscript #1).

We first studied the effect of BRAF expression knockdown by RNA interference (siRNA). We used two ATC cell lines: FRO that expresses only the mutated BRAFV600E allele and ARO carrying the same mutation at the heterozygous level (Table 4). We used siRNA against BRAF and, as control, a scrambled siRNA sequence or siRNA against the housekeeping lamin A/C mRNA. Results are described in the attached manuscript #1. Briefly, transfection with BRAF siRNA, but not with the control siRNA, reduced BRAF, but not CRAF, protein levels in ARO cells (**Figure 8A**).

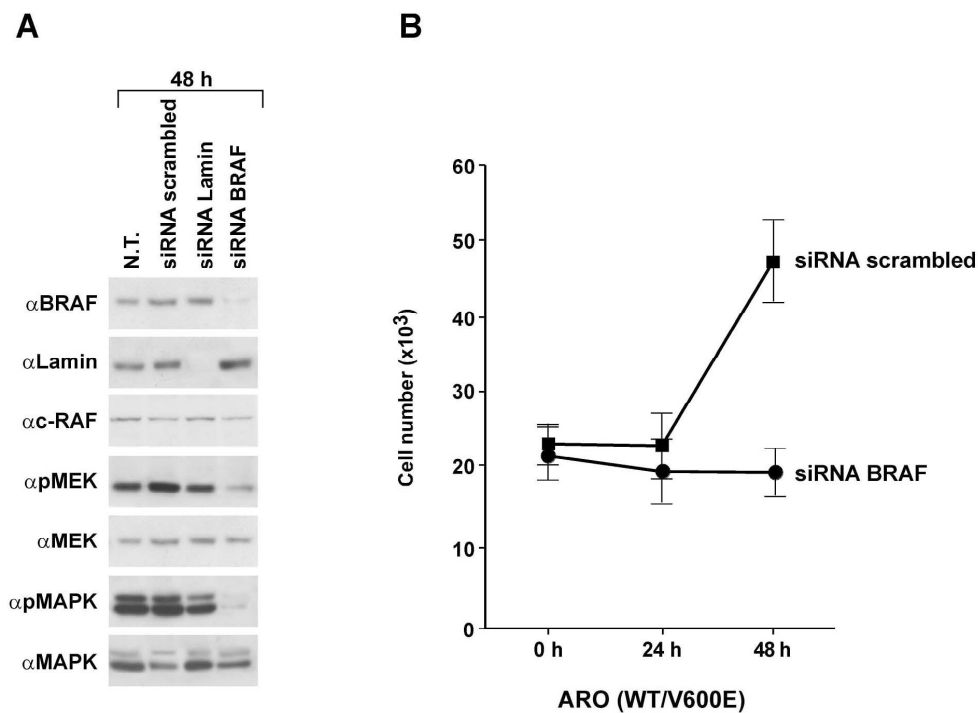


Fig. 8: Knockdown of BRAF by siRNA blocks ERK signaling pathway and growth of ARO cells (modified from attached manuscript #1, Fig.1).

BRAF silencing also resulted in a reduction of p44/42 ERK (MAPK) (~5 fold) and MEK1/2 (~3 fold) phosphorylation levels 48 hours after transfection (**Figure 8A**). Importantly, transient silencing of BRAF significantly inhibited the growth of ARO cells, whereas the negative control siRNA had virtually no effect (**Figure 8B**). Similar results were obtained in FRO cells (attached manuscript #1, Fig 1). Thus, BRAF mutant ARO and FRO cells depend on continuous BRAF expression to sustain ERK pathway stimulation and *in vitro* growth.

4.2 Biochemical effects of BAY 43-9006 in BRAF mutant thyroid carcinoma cells (attached manuscript #1).

We evaluated the effect of chemical BRAF inhibition in BRAF mutant thyroid carcinoma cells. To this aim, we used BAY 43-9006 (sorafenib) on the ATC cell lines ARO, KAT4 and FB1, carrying the BRAFV600E mutation at the heterozygous level, and 8505C, FRO and NPA, which carry only the mutated allele (Table 4). Cells were treated with different concentrations of BAY 43-9006 or vehicle (NT) and the phosphorylation of MEK1/2, p44/p42 ERK (MAPK) and p90RSK (a p44/p42 MAPK substrate) was monitored by immunoblot with phospho-specific antibodies. Antibodies recognizing the non-phosphorylated proteins were used for normalization. Experiments in representative cell lines are reported in **Figure 9**. Treatment with BAY 43-9006 reduced the phosphorylation of MEK1/2, p44/p42 MAPK and p90RSK with a half maximal inhibitory concentration (IC_{50}) of 1 μ M in ARO, KAT4 and NPA cells and of 500 nM in FB1, 8505C and FRO cells.

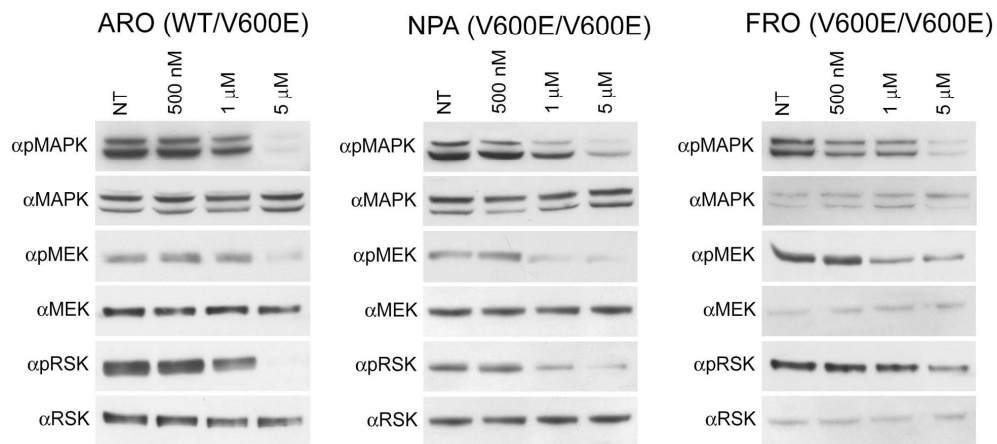


Fig. 9: *In vivo* inhibition of ERK cascade in BRAF mutant thyroid carcinoma cells by BAY 43-9006 (modified from attached manuscript #1, Fig. 2).

BAY 43-9006 is a multitarget agent. To verify whether the reduced phosphorylation of the ERK cascade was indeed mediated by BRAF inhibition, we performed an *in vitro* BRAF kinase assay. ARO and FRO cells were treated with different concentrations of compound or vehicle (NT); BRAF was immunoprecipitated and its kinase activity measured by the phosphorylation of recombinant GST-MEK protein. **Figure 10** shows that BAY 43-9006 readily inhibited BRAF enzymatic activity at the concentration of 1 μM.

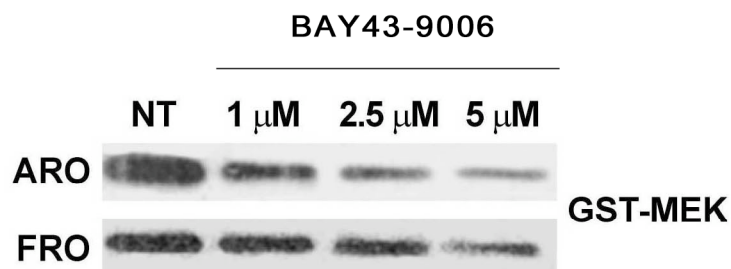


Fig. 10: *In vitro* inhibition of BRAF V600E kinase activity by BAY 43-9006 (modified from manuscript # 1, Fig. 3).

4.3 Biological effects of BAY 43-9006 in BRAF mutant thyroid carcinoma cells (attached manuscript #1).

We evaluated the effects exerted by BAY 43-9006 on ATC cell viability. To this aim, ATC cells were treated with different concentrations of BAY 43-9006 or vehicle and counted at different time points. **Figure 11** shows that the treatment readily reduced the growth of ATC cells but not of normal thyroid P5 cells. The average IC_{50} for the ATC cell lines tested was $\sim 1 \mu\text{M}$. At $5 \mu\text{M}$ BAY 43-9006, complete growth arrest was achieved ($P < 0.0001$).

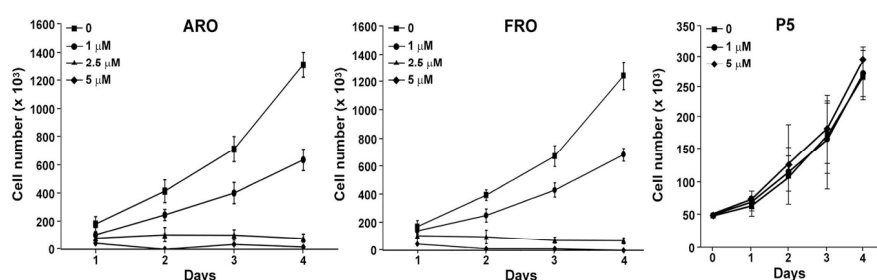


Fig. 11: BAY 43-9006 causes growth inhibition of BRAF mutant thyroid carcinoma cells (modified from manuscript # 1, Fig 4)

Finally, 1×10^6 ARO cells were injected subcutaneously in nude mice. When tumors reached $\sim 100 \text{ mm}^3$, animals (7 for each group) were randomized and treated *per os* 5 days/week with BAY 43-9006 (30 mg/kg or 60 mg/kg) or with vehicle. Tumor growth was monitored with calipers. After 22 days of treatment, mice treated with BAY 43-9006 at either 30 mg/kg or 60 mg/kg had significantly smaller tumors than control mice ($P < 0.0001$) (**Figure 12A**). A

group of mice (n=5) bearing tumors of approximately 300 mm³ were treated daily with 60 mg/kg of BAY 43-9006 or with vehicle for 5 days. Three hours after administration of the final dose, tumors were excised and used for protein extraction and immunoblot analysis. As shown in **Figure 12B**, tumor-growth inhibition was associated with a remarkable reduction of p44/42 MAPK, MEK1/2 and, at a lower extent, RSK *in vivo* phosphorylation levels. These findings suggest that, in the applied experimental conditions, BAY 43-9006 is able to hit the ERK pathway in tumor cells.

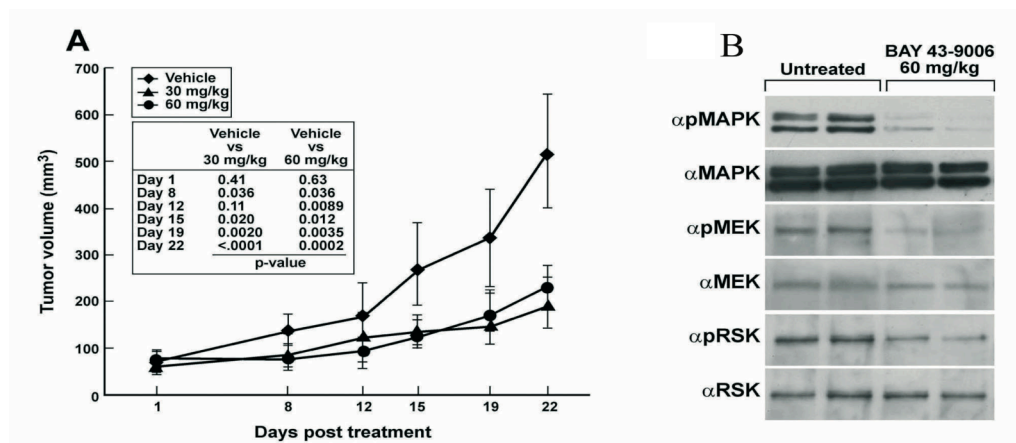


Fig. 12: (A) Anti-tumorigenic effects of BAY 43-9006 in ARO cell tumor xenografts. (B) Inhibition of ERK signaling cascade in ARO xenografts (modified from manuscript # I, Fig 5).

However, it is well-established that BAY 43-9006 is a multitarget agent and therefore it is feasible that its *in vivo* effects are also associated with inhibition of kinases other than BRAF (primarily VEGFR, thereby blocking tumor angiogenesis). Accordingly, prominent necrotic features were observed in treated xenografts suggesting that anti-angiogenic effects played a role in tumor shrinkage induced by BAY 43-9006 (**Figure 13**).

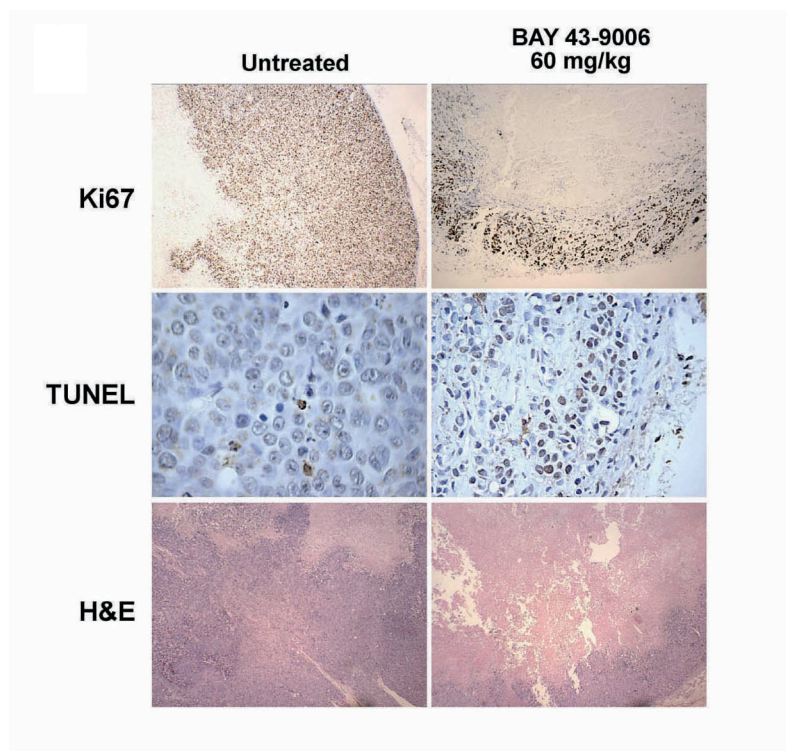


Fig. 13: ARO tumors (~300 mm³)-bearing animals were treated with vehicle or 60 mg/kg of BAY 43-9006 for 5 days. Tumors were excised and examined by conventional hematoxylin and eosin, and immunostaining with anti-Ki67/MIB-1. Apoptotic cell death rate was assessed by *in situ* labeling of DNA strand breaks (modified from manuscript # 1, Fig 5).

Overall, these experiments demonstrated that BAY 43-9006 exerts anti-tumor effects in an experimental model of ATC. Phase II clinical assessment of the compound is in progress in patients with metastatic or unresectable aggressive thyroid carcinomas (www.cancer.gov/clinicaltrials/). In melanomas, the clinical results with this compound used as a single agent have been disappointing (Eisen et al. 2006). The patients in the study were not stratified based on the presence of BRAF mutation: however, given the high prevalence of BRAF mutations in melanoma (> 70%) it is unlikely that the study was unsuccessful because of the lack of the genetic target in the enrolled patients. More likely, either the compound is *in vivo* not potent enough at intercepting BRAF or targeting BRAF alone in tumors as aggressive as advanced

melanomas is not sufficient. In any case, given its multitargeting activity, BAY 43-9006 does not appear to be a suitable agent to clarify whether BRAF targeting *in vivo* holds promise for the treatment of aggressive thyroid cancers. Other new BRAF-targeting compounds became available and we obtained promising preliminary results with those compounds of the PLX series (Table 4) (data not shown). Hereafter, in this dissertation, we report our findings relative to MEK targeting.

4.3 PD0325901 inhibits the proliferation of BRAF mutant thyroid carcinoma cells (attached manuscript #5)

Blocking MEK, the kinase immediately downstream BRAF in the ERK cascade (**Figure 1**), may be a suitable therapeutic alternative to direct BRAF targeting. Very potent and selective (non ATP-competitive) allosteric MEK kinase inhibitors are available. At least, given the high selectivity of these compounds, the approach should prove useful to define whether ERK pathway blockade holds promise for cancer treatment. Solit and colleagues have shown that cancer cells bearing an activating BRAF mutation are more sensitive to MEK kinase inhibitors than cells bearing different mutations (even in the same pathway, e.g. at the level of RAS) (Solit et al. 2006). Therefore, we selected again for the experiments thyroid carcinoma cell lines derived from aggressive tumor variants (ATC or PDC) and positive for oncogenic BRAF alleles. We used PD0325901 for these experiments. PD0325901 is a dual MEK inhibitor (equally potent on MEK1 and MEK2); its *in vitro* IC₅₀ is of 1 nM (Brown et al. 2007). The structurally related PD184352 compound did not inhibit kinases other than MEK up to 10 μM concentration (Davies et al. 2000).

We initially tested the effects of PD0325901 on the proliferation rate of ARO, BHT101, FRO and SW1736 ATC cell lines carrying homozygous or heterozygous BRAF V600E alleles (Table 4). Normal PC and FRTL5

thyrocytes served as control. Cells were treated with different concentrations of PD0325901 or vehicle (NT) and counted every day for four days. The average results of three independent determinations are reported in **Figure 14** and calculation of half maximal efficacy concentration (EC_{50}) is reported in **Figure 15**.

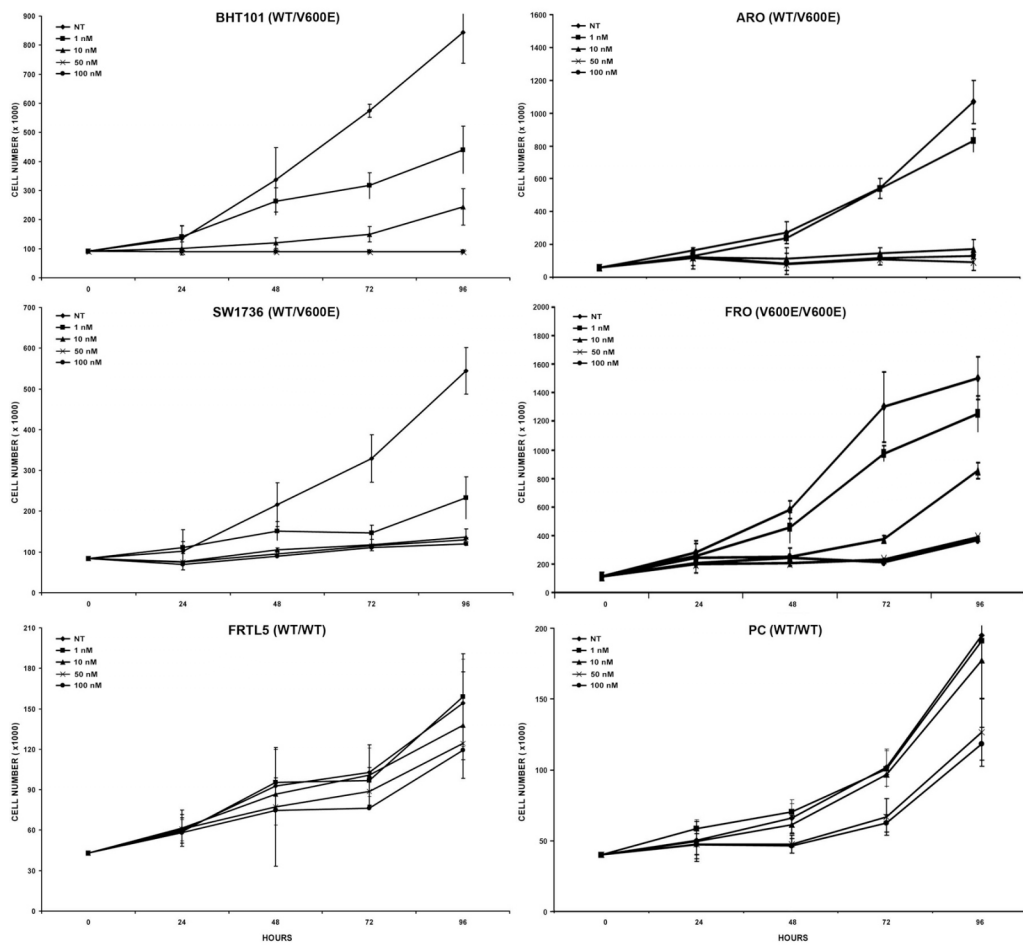


Fig. 14: PD0325901 treatment caused growth inhibition of BRAF mutant thyroid carcinoma cells but had no significant effect on normal thyrocytes (from attached manuscript #5).

Treatment with PD0325901 caused a dose-dependent growth inhibition of all carcinoma cell lines with a half maximal efficacy concentration (EC_{50}) ranging from 0.4 to 5 nM ($P < 0.0001$). Doses of 10 nM or higher had to be used to suppress ATC cell proliferation by 90%. Importantly, 50% growth inhibition was observed in normal thyrocytes only at concentrations ≥ 50 nM

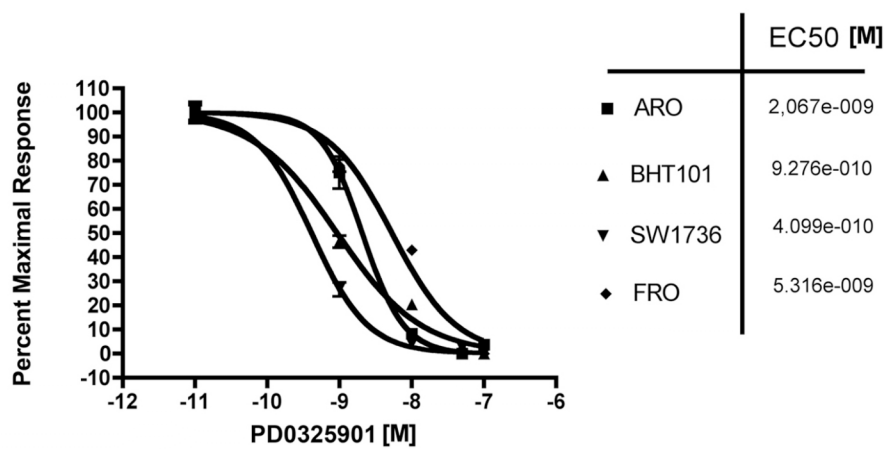


Fig. 15: EC_{50} for PD0325901-mediated growth inhibitory effects.

Flow cytometry was applied to establish the nature of PD325901 effects on thyroid cell growth. ARO and SW1736 cells underwent a marked G1 arrest upon PD0325901 (10 nM) treatment, starting at 24 hours and lasting up to 96 hours (**Figure 16** and Figure 2A of the attached manuscript #5). No significant subG1 fraction was detectable, indicating that the treatment did not kill thyroid carcinoma cells. Importantly, PD0325901 (10 nM) did not modify cell cycle profile of normal control cells.

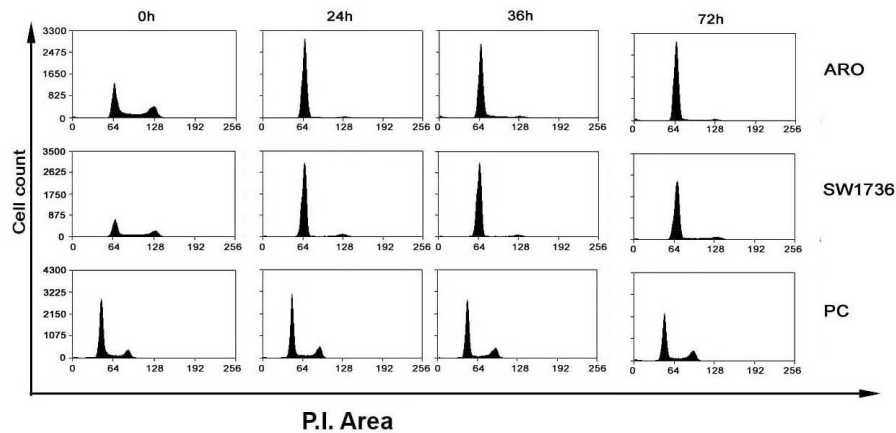


Fig. 16: FACS scan of cell cycle upon treatment with PD0325901 (modified from attached manuscript #5, see also Fig. 2A of the attached manuscript #5).

Progression through the G1/S phase of cell cycle is positively controlled by the activity of cyclin-dependent kinases (CDKs) in association with cyclins; in particular, CDK4/6 in association with D-type cyclins, and CDK2 in association with E-type cyclins phosphorylate the retinoblastoma protein (Rb). Phosphorylated Rb in turn releases E2-promoter-binding factor (E2F)-related proteins and enhances transcription of genes participating in cell cycle progression (Sherr 1996). Cell cycle, by contrast, is negatively regulated by the inhibitory activity of members of the CIP/KIP family of cyclin-dependent kinase inhibitor proteins. Thus, to study the mechanism of cell cycle arrest upon MEK inhibition, ARO and SW1736 were treated with PD0325901 and the levels of cell cycle regulator proteins were determined by immunoblot. **Figure 17** (and Fig. 2 of the attached manuscript #5) shows that upon treatment with PD0325901 a significant increase in the protein levels of both p21Cip1 and p27Kip1 was observed in ATC cells at 12 up to 48 hours of treatment. Moreover, PD0325901 treatment induced a remarkable reduction of phosphorylation of the serine 795 (a CDK2 phosphorylation site) of pRb protein. Treatment with U0126, used as control, gave similar results (Fig. 2B in

the attached manuscript #5). We did not detect significant changes in cyclin D1 and cyclin E protein levels (not shown).

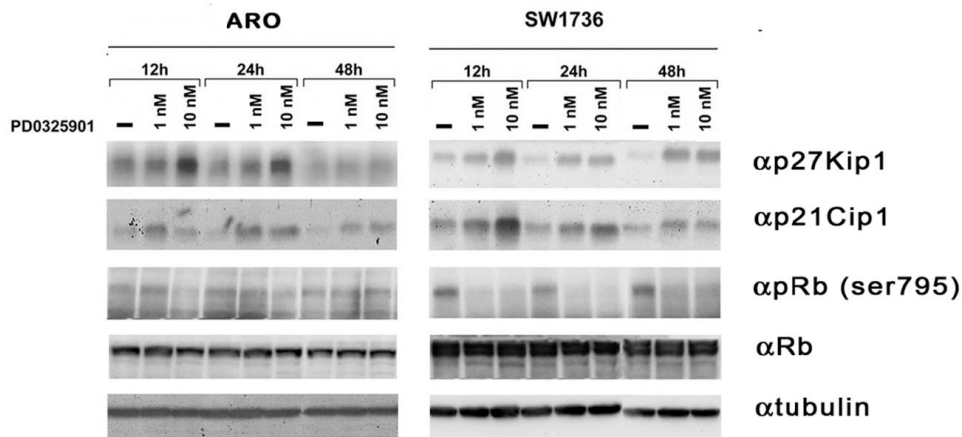


Fig. 17: Expression levels of cell cycle regulatory proteins upon treatment with PD0325901 were determined by immunoblot. Anti tubulin was used for normalization. (modified from attached manuscript #5, see also Fig. 2B of the attached manuscript).

4.4 PD0325901 inhibits the ERK pathway in BRAF mutant thyroid carcinoma cells (attached manuscript #5)

We examined the phosphorylation levels of downstream effectors of MEK, p44 and p42 ERKs, and RSK, a kinase that is phosphorylated by ERK. This was performed in the same ATC cell lines (ARO, BHT101, FRO, SW1736) used for the proliferation assays as well as in additional cell lines (Table 4). These included: FB1 (an ATC cell line which carries a heterozygous BRAF V600E mutation), NPA (a poorly-differentiated PTC cell line which carries only the BRAF V600E allele) and BCPAP (a PTC cell line, which carries a heterozygous BRAF V600E mutation). After 12 hours in low serum (2.5%), cells were treated for 2 hours with different concentrations of PD0325901 or vehicle (NT) and examined by immunoblot. Treatment with PD0325901

strongly reduced the phosphorylation of ERK at the activatory sites Thr202/Tyr204 and of RSK with an IC₅₀ of about 1 nM for NPA, FRO, BHT101, FB1, BCPAP and between 1 and 10 nM for ARO and SW1736 cells (**Figure 18**). Importantly, the compound also efficiently inhibited MAPK pathway phosphorylations in PC cells, demonstrating that its reduced growth inhibitory activity in normal thyrocytes was not due to defective effects on the target kinase but rather to the fact that normal cells are not addicted to MEK signaling.

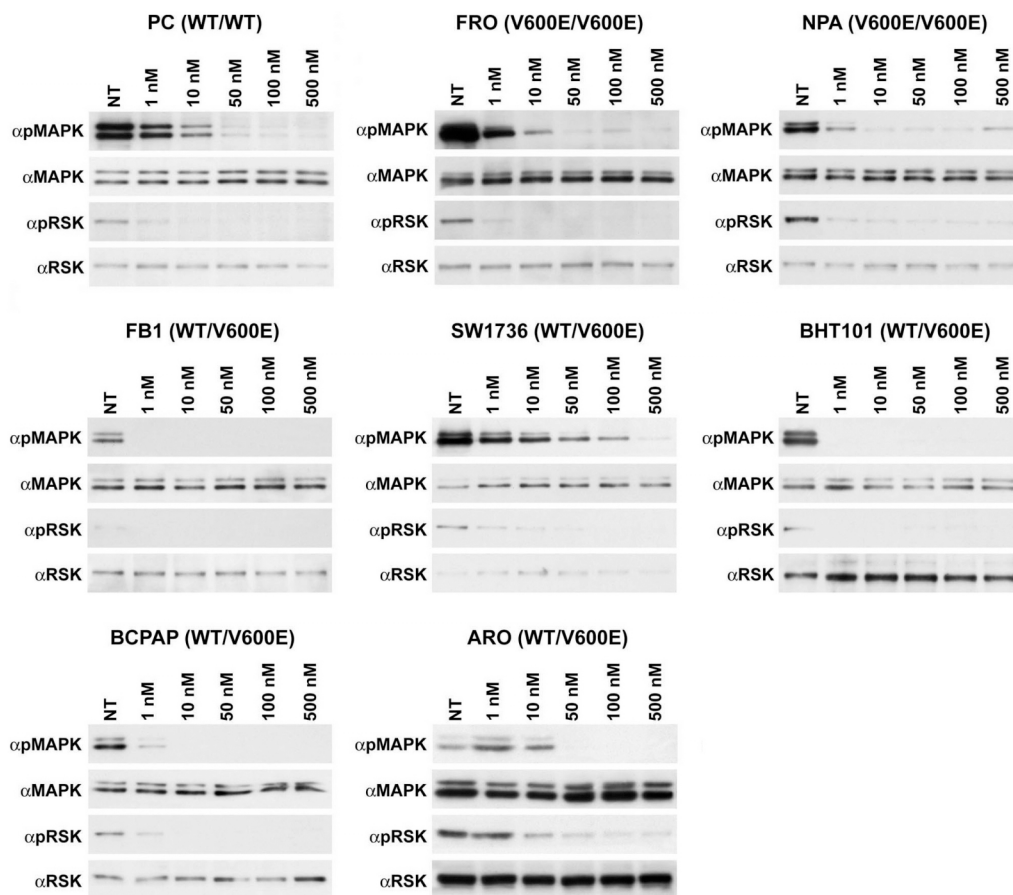


Fig. 18: Inhibition of the ERK signaling cascade in thyroid carcinoma cell lines by PD0325901 (modified form attached manuscript # 5).

4.5 Transient nature of ERK inhibition in thyroid carcinoma cells (attached manuscript #5)

We measured time-course of ERK phosphorylation upon PD0325901 treatment in ARO cells. Phosphor-imager quantitation of three independent experiments (1 and 10 nM PD0325901) at various time points is reported in **Figure 19A**, and a representative immunoblot (10 nM PD0325901), performed at early times, is reported in **Figure 19B**.

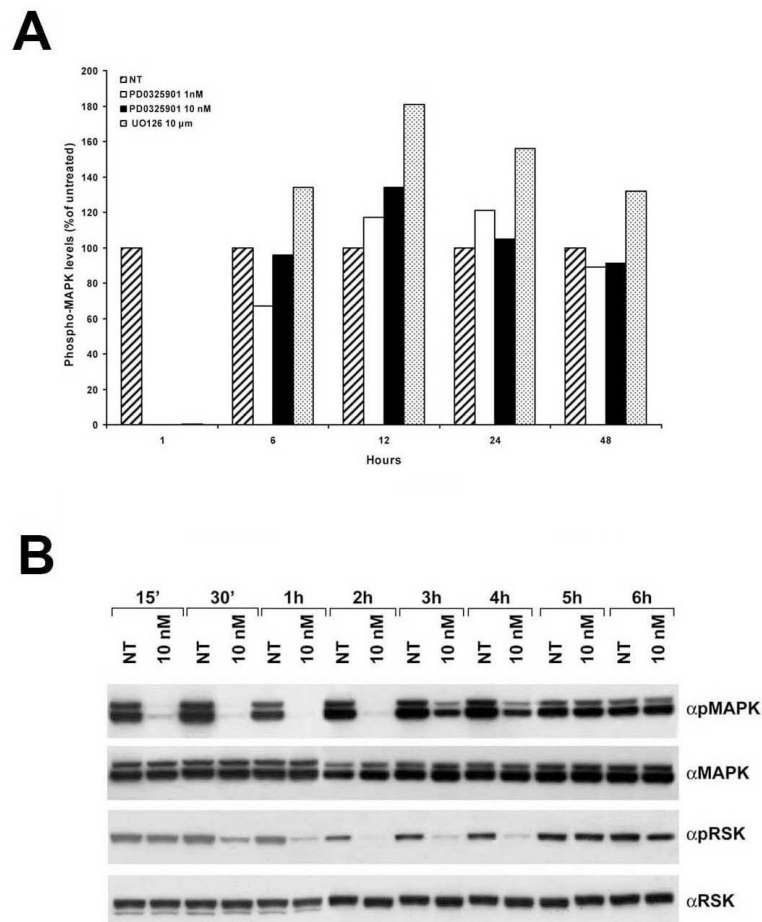


Fig. 19: Time-course of inhibition of the ERK signaling cascade in ARO cells by PD0325901 or U0126 (modified from attached manuscript # 5).

ERK inhibition was very rapid and detected as soon as after 15 min of treatment. It was almost complete, at both 1 and 10 nM PD0325901, after 1 hour of treatment. Then, ERK phosphorylation started to resume after 3 hours and returned to levels almost equivalent to untreated cells after 6 hours. RSK phosphorylation paralleled ERK activity. These transitory effects were also detected in the other BRAF mutant thyroid carcinoma cells, although they were more evident in ARO cells. **Figure 20** shows kinetics of ERK and RSK phosphorylation upon PD0325901 or U0126 treatment in ARO and SW1736 cells. Although more slowly than in ARO, also in SW1736 cells, ERK pathway resumed after a transient inhibition. The transient nature of ERK inhibition was not unique to PD0325901, because it was seen also with U0126 (**Figures 19 and 20**). Compound decay did not account for the transient nature of the effects, because PD0325901 replenishment one-hour before protein harvest did not prevent ERK phosphorylation recovery (not shown).

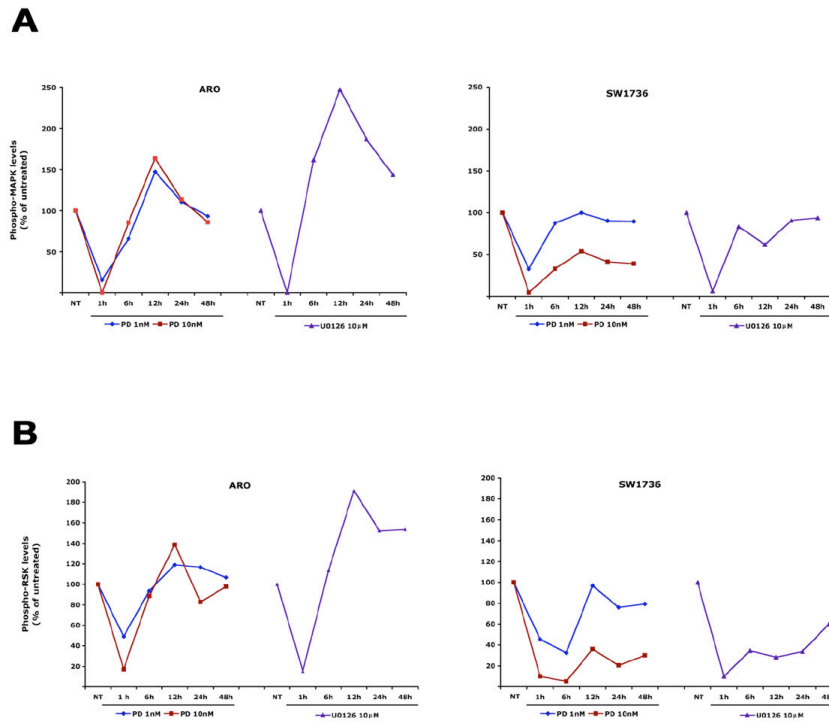


Fig. 20: Time-course of inhibition of the ERK signaling cascade (ERK in panel A and RSK in panel B) in ARO and SW1736 cells by PD0325901 or U0126.

4.6 Regulatory circuits elicited by MEK inhibition in thyroid carcinoma cells (attached manuscript #5)

In the search for the mechanism of ERK pathway restoration after MEK inhibition, we initially asked whether resumed ERK phosphorylation remained MEK-dependent. Thus, we treated ARO cells with increased doses of PD0325901 and measured ERK phosphorylation at different time points. **Figure 21** shows that at 6 hours, when in cells treated with 1 nM PD0325901 ERK phosphorylation had returned to levels comparable to untreated cells, 10 nM of compound maintained ERK phosphorylation at levels of about 50% those of untreated cells; 50 nM compound blunted almost completely ERK phosphorylation.

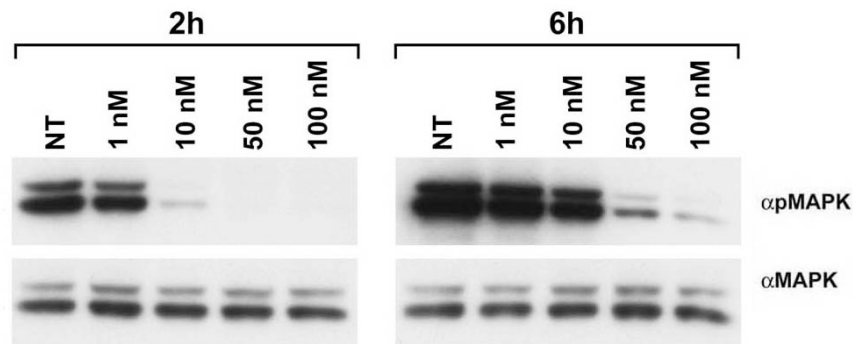


Fig. 21: Time-course of ERK phosphorylation inhibition by increasing PD0325901 doses (modified from attached manuscript #5).

ERK phosphorylation at Thr202/Tyr204 may resume either secondary to reduced response of MEK kinases to PD0325901 (which would increase the “on” rate), or to reduced levels of ERK-specific phosphatases (which would decrease the “off” rate).

We initially verified whether PD0325901 or U0126 treatment modified MEK phosphorylation levels at the activatory sites Ser217/Ser221 in the activation loop. Noteworthy, phosphorylation at these sites enhances by 7,000-fold the MEK kinase activity and it is also expected to reduce MEK inhibitor binding. **Figure 22** shows that, as soon as after 1 hour of PD0325901 treatment, MEK phosphorylation increased and remained elevated thereafter for at least 12 hours.

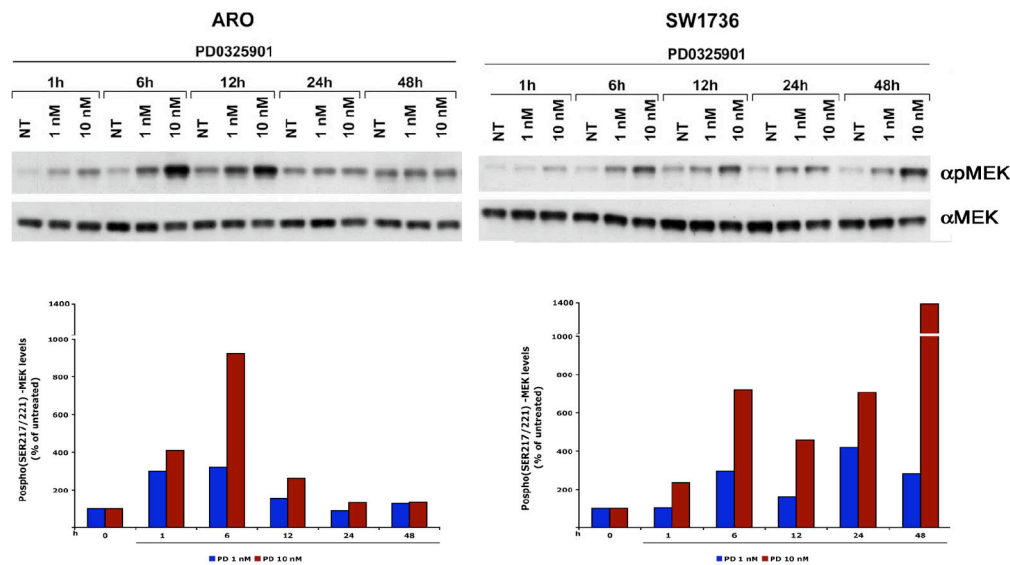


Fig. 22: PD0325901 or U0126 treatment rapidly increases stoichiometry of activatory MEK phosphorylations (modified from attached manuscript #5).

RAF proteins are the only kinases known to phosphorylate Ser217/Ser221 of MEK. Importantly, it is known that active ERKs phosphorylate CRAF on various Ser/Pro sequences (Ser29, Ser289, Ser296, Ser301, and Ser642), this resulting in the inhibition of CRAF catalytic activity, membrane localization and association to BRAF (Dougherty et al. 2005, Rushworth et al. 2006). Thus, PD0325901 treatment could result in the potentiation of CRAF secondary to the blockade of ERK-mediated inhibitory phosphorylations. Since CRAF, in turn, is involved in oncogenic BRAF-triggered phosphorylation of MEK (Garnett et al. 2005), it is possible that this mechanism has an effect on MEK phosphorylation even in BRAF mutant cells. Finally, it is important to note that also BRAF is directly phosphorylated and inhibited by ERK (Brummer et al. 2003), and therefore also BRAF de-phosphorylation upon PD0325901 may contribute to MEK hyper-phosphorylation (**Figure 23**).

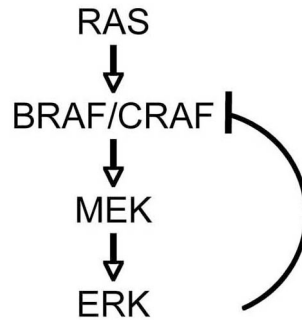


Fig. 23: Possible negative feedback on RAF kinases abrogated by MEK targeting agents

We used the available antibodies specific for CRAF phosphorylated at Ser289/296/301 to test this possibility. **Figure 24** shows that indeed the phosphorylation state of CRAF at these inhibitory sites was decreased starting at 1-6 hours after PD0325901 treatment; again these effects were also seen with the control MEK inhibitor. Accordingly, our preliminary data indicate that both CRAF and BRAF kinase activities are potentiated upon PD0325901 treatment (not shown).

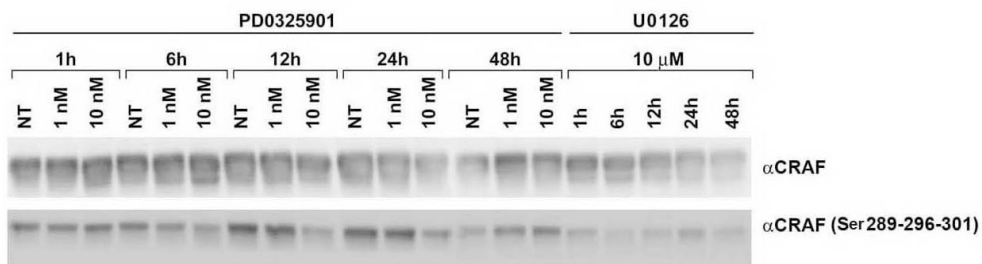


Fig. 24: Inhibitory CRAF phosphorylations are blunted by MEK targeting agents (modified from attached manuscript #5).

Dual-specificity phosphatases (DUSPs, also referred to as MAPK phosphatases -MKP), are able to dephosphorylate ERKs, and control intensity and duration of ERKs stimulation (Jeffrey et al. 2007). Importantly, DUSP/MKP are transcriptional targets of the ERK pathway, this representing a negative feedback circuit that terminates ERK signal (Jeffrey et al. 2007). Indeed, ERK activation in cells is in general transient; novel RNA transcription is required to switch-off the signal and *de novo* transcription of DUSP/MKP has been demonstrated to play a key role in signal termination (Camps et al. 2000, Keyse 2000). MKP3 (Muda et al. 1996) and DUSP5 (Mandl et al. 2005) have shown specificity for ERKs. In mammalian cells, DUSP5 expression is inducible by heat shock and growth factors (Ishibashi et al. 1994). The regulation of MKP3 expression is not clearly understood. Although MKP3 expression seems to be constitutive in some cell types (Groom et al. 1996), in others MKP3 expression is induced after exposure to growth factors (Reffas and Schlegel 2000). In thyroid PC cells, both DUSP5 and MKP3 expression is markedly induced by conditional activation of RET/PTC or BRAF V600E. Thus, changes in expression levels of DUSP/MKPs may modify the “off” rate of ERK phosphorylation and contribute to the transient nature of ERK dephosphorylation upon treatment with pathway inhibitors (**Figure 25**). Accordingly, Ouyang *et al* (2006) showed that BRAF inhibition caused reduced levels of MKP3 and DUSP5 ERK phosphatases in thyroid carcinoma cells.

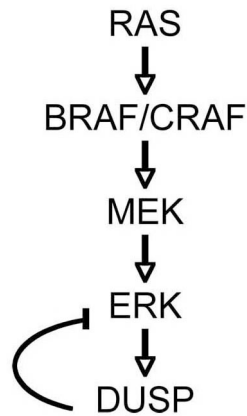


Fig. 25: Possible negative feedback based on the expression of DUSP phosphatases that may be abrogated by MEK targeting agents

To verify this possibility, we initially treated ARO cells with orthovanadate, a potent DUSP/MKP inhibitor. This treatment increased the phosphorylation levels of ERK, suggesting that, at the steady state, ERK phosphorylation is under phosphatases control in ARO cells (Fig. 5C of the attached manuscript #5). Then, we measured expression levels of DUSP5 and MKP3 in ARO and SW1736 cells treated with PD0325901, by quantitative RT-PCR. PD0325901 treatment, evoked a rapid and sustained decrease of mRNA abundance of both phosphatases starting 30 minutes upon treatment and lasting up to 12 hours (**Figure 26**).

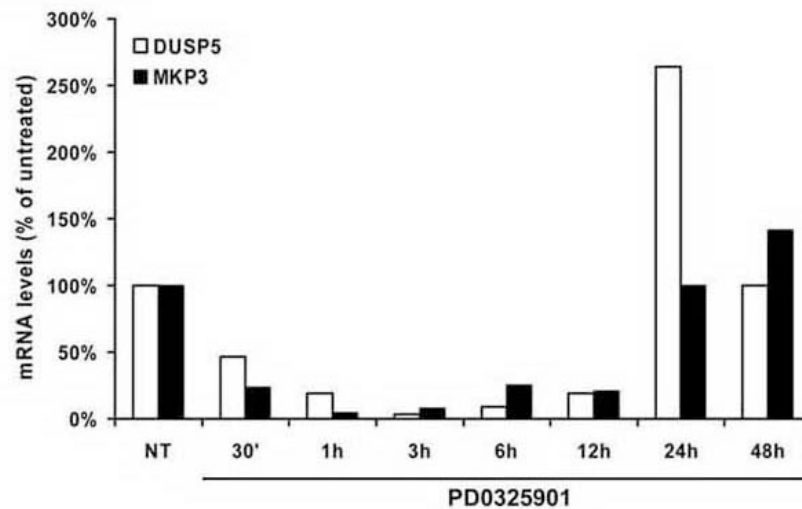


Figure 26: Quantitative RT-PCR measurement of MKP3 and DUSP5 mRNA levels in ARO cells treated with 10nM PD0325901 for the indicated times (modified from Fig 5D of the attached manuscript #5).

4.7 Cross-talk between ERK and PI3K/AKT pathways

Our data indicate that multiple levels of regulation, both at ERK upstream and downstream level, are evoked by MEK targeting agents, this blunting in turn, the efficacy of chemical ERK inhibition. We considered the possibility that similar regulatory circuits may also affect pathways other than the ERK one and focused our attention on the PI3K/AKT cascade. To this aim, we treated ARO and SW1736 cells with PD0325901 and U0126 at different time points and measured AKT phosphorylation levels by using a phosphospecific antibody recognizing Ser473-phosphorylated AKT. Intriguingly, AKT phosphorylation levels readily increased upon treatment of ATC cells with MEK inhibitory agents (**Figure 26**). This occurred with different kinetics in the

two cell lines; moreover, the effect was transient and quite rapidly it disappeared.

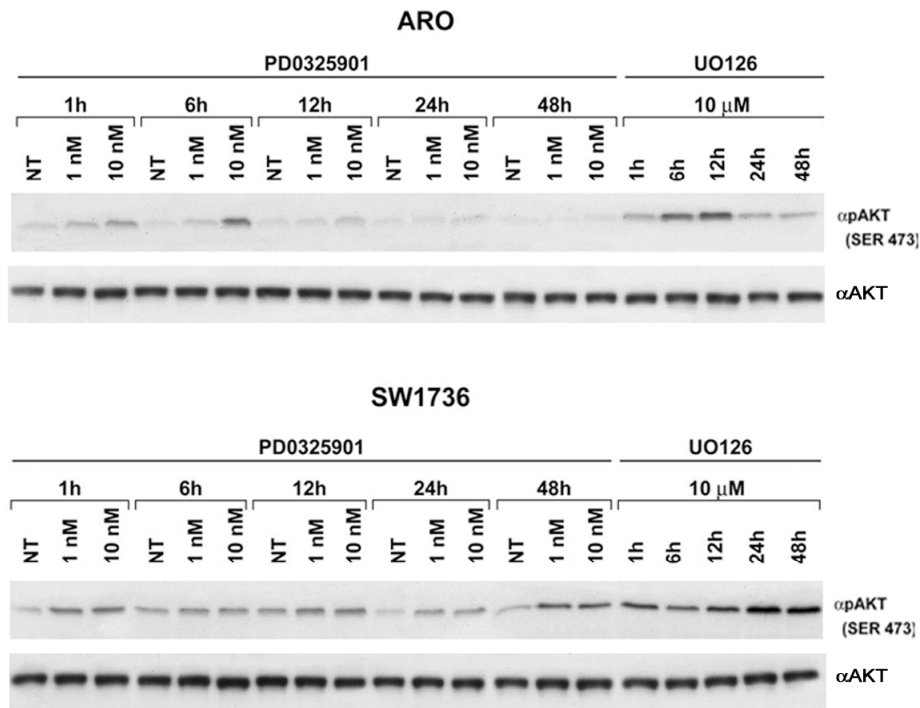


Fig. 27: Phosphorylation of AKT on serine 473 in cells treated with PD0325901 or U0126 at the indicated time points.

In principle, AKT activation could counteract cytostatic effects of MEK targeting. In turn, simultaneous inhibition of MEK and AKT could increase the efficacy of the approach. To verify this possibility, we treated ARO cells with 1 nM PD0325901 (a dose able to only partially inhibit the cellular growth) in the presence or not of two different PI3K inhibitors (LY294002 and Wortmannin). The cells were counted every day for 4 days. **Figure 28** shows

that PD0325901 cooperated with both LY294002 or Wortmannin, in the induction of ARO cells growth arrest.

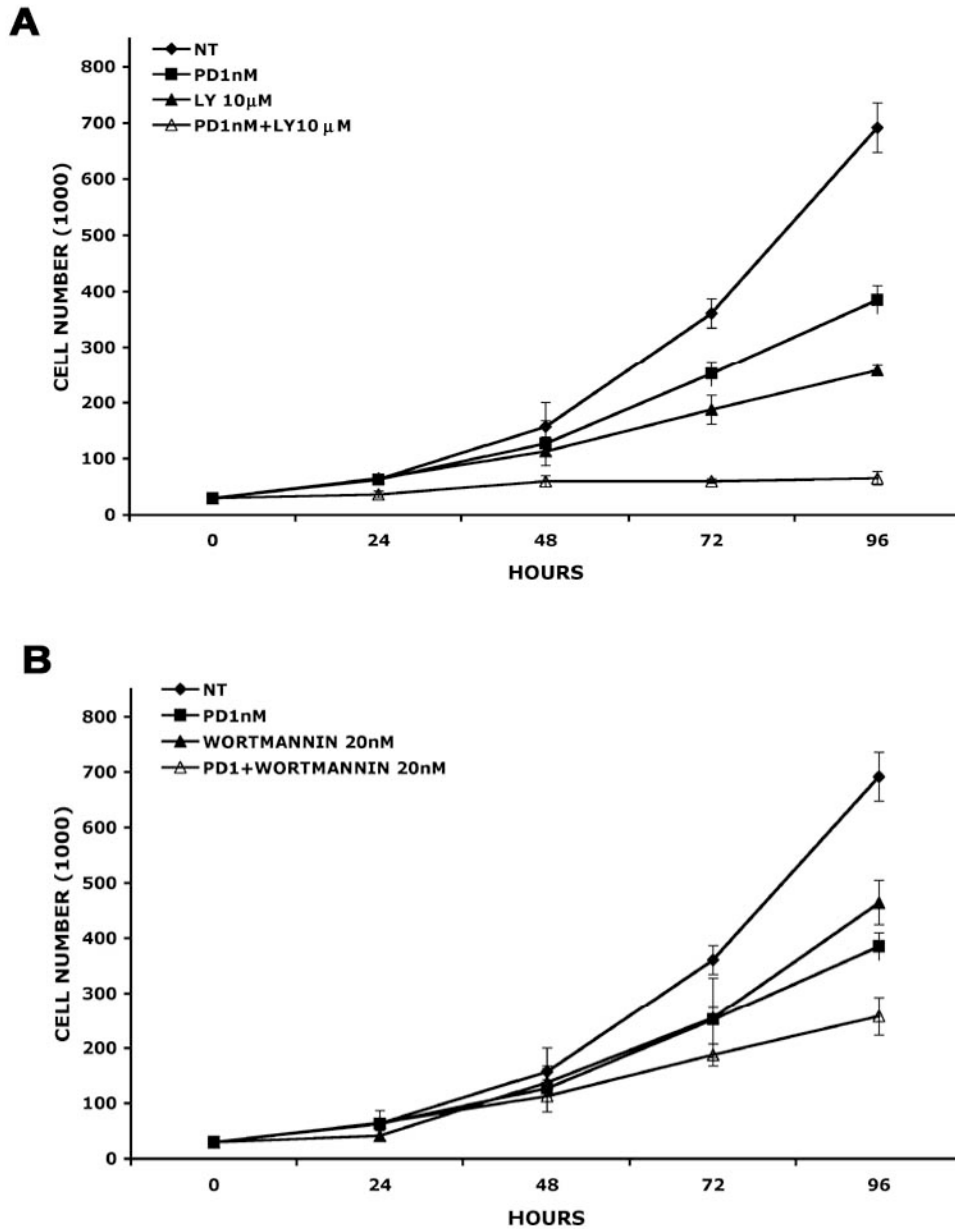


Fig 28: Additive effects of PD0325901 and LY294002 or Wortmannin in ARO cell growth inhibition.

5 DISCUSSION

Thyroid cancer has in general an indolent course and patients with WDTC are efficiently treated by surgery and adjuvant radioiodine treatment (Cooper et al. 2006, Pacini et al. 2006, Schlumberger 1998, Schlumberger et al. 2007). However, advanced WDTC (PTC and FTC) and ATC typically exhibit radioiodine resistance and poor prognosis. For these particular patients novel treatment strategies are urgently needed.

Clinical trials with different agents are in progress for aggressive thyroid cancers (www.thyroidtrials.org; www.cancer.gov/clinicaltrials) (Table 5). These agents include compounds targeting the 26S proteasome, inhibitors of molecular chaperones, inhibitors of histone deacetylases and of DNA methylases, angiogenesis inhibitors.

Table 5: Examples of ongoing clinical trials in thyroid cancer patients (informations retrieved from the American Thyroid Association and the National Institutes of Health web sites)

Trial number	Phase	Agent	Molecular target
NCT00104871	Phase II	Bortezomib (Velcade)	26S proteasome
NCT00098852	Pilot	Rosiglitazone	PPAR γ
NCT00118248	Phase II	17-AAG	HSP90
NCT00098813	Phase II	Depsipeptide	HDAC
NCT00085293	Phase II	Decitabine	DNA methylation
NCT00389441	Phase II	AG-013736 (axitinib)	VEGFR

Our studies at the preclinical level suggest that additional proteins that are highly up-regulated in ATC samples, like the chemokine receptor CXCR4 (attached manuscript #3) and the cell cycle-regulated kinase PLK1 (attached manuscript #4), deserve attention as promising targets for therapeutic intervention in ATC.

Protein kinases have emerged as prime targets for the development of novel molecularly targeted therapies for cancer patients. This concept has been applied also to thyroid cancer. For instance, different agents inhibiting

the RET kinase, involved in MTC and PTC formation, are being studied in thyroid cancer patients (Carlomagno et al. 2002, Carlomagno et al. 2006, Santoro and Carlomagno 2006). The BRAF/MEK/ERK pathway is a promising molecular therapeutic target for PTC and ATC. BRAF mutations are highly prevalent in these tumor types and, in PTC, they correlate with adverse clinical features.

Here, we studied at the molecular level the effects of BRAF and MEK targeting in BRAF mutant thyroid carcinoma cells. Our findings show the efficacy of this approach to arrest thyroid carcinoma cell proliferation. However, they also anticipate possible shortcomings of this strategy. In summary, our findings have shown that:

- BRAF mutant thyroid carcinoma cell lines are addicted to continuous BRAF expression;
- BAY 43-9006 (sorafenib) at μM concentration has cytostatic effects *in vitro* in BRAF mutant thyroid cell lines;
- BAY 43-9006 (sorafenib) has therapeutic efficacy in a xenograft model of ATC;
- MEK targeting by PD0325901 at nM concentration has cytostatic effects *in vitro* in BRAF mutant thyroid cell lines.

BAY 43-9006 (sorafenib) is a multitarget compound, able to inhibit many other kinases besides RAF, including KIT, PDGFR, RET and VEGFR (Wilhelm et al. 2006, Sebolt-Leopold and Herrera, 2004). Therefore, it remains unclear whether its clinical activity is mediated by inhibition of RAF, other kinases, or both. The compound has been approved for treatment of RCC (Baselga 2006). The disappointing clinical results obtained in melanoma can be explained by the aggressive phenotype of this tumor or by the fact that the compound in patients is not potent enough at targeting BRAF. Our data, obtained with MEK kinase inhibitors (see below), suggest that regulatory circuits elicited by ERK pathway targeting may hamper the efficacy of the inhibitors and therefore

require rational combinations rather than single agents. Other BRAF chemical inhibitors are available and some of them, like PLX4032, are in clinical development (Wang et al. 2007). We tested in ATC cell lines PLX4032 and the related compound PLX4720 and found that they potently inhibit cell proliferation (data not shown).

MEK1 and MEK2 appear to be the most critical downstream mediators of BRAF V600E signaling (Garnett and Marais 2004). Potent and selective non-ATP competitive inhibitors of MEK kinases are in clinical development (Sebolt-Leopold and Herrera 2004, Sebolt-Leopold and English 2006, Schubbert et al. 2007). Previous studies have shown that MEK blockade with U0126 inhibited proliferation of ARO and NPA thyroid carcinoma cells (Braga-Basaria et al. 2004) and partially restored thyroid differentiated phenotype (Liu et al. 2007). Recently, Ball *et al* (2007) and Liu *et al* (2007) have studied the effects of AZD6244 and CI-1040 on thyroid carcinoma cells. MEK inhibition had potent cytostatic effects in thyroid carcinoma cells harbouring the BRAF or the HRAS (Ball et al. 2007, Liu et al. 2007) mutation but not in wild type BRAF cells. The two compounds inhibited the growth of xenograft tumors in nude mice and CI-1040 restored the expression of some thyroid cell differentiation markers.

In this work, we studied the effect of PD0325901 in ATC cell lines harbouring the V600E BRAF mutation. The compound resulted extremely potent at intercepting ERK signaling and causing cell growth inhibition. Importantly, PD0325901 had effects in normal thyrocytes only at doses 5-10-fold higher than cancer cells, indicating the opportunity of a therapeutic window. Probably, normal cells as well as cancer cells bearing mutations at levels other than the BRAF one, may use redundant cell growth signaling pathway and therefore be less dependent on MEK activity. This is an important observation because MEK targeting may potentially be an extremely toxic approach. *Erk1null* mice have a twofold reduction in the number of mature

thymocytes. The involvement of the MAPK pathway in immune signalling has therefore raised important concerns about the possibility that the treatment is immunosuppressive. *Mek1null* mice undergo embryonic lethality for impaired placental development, raising further concerns about the potential deleterious clinical consequences of MEK inhibition (Sebolt-Leopold and Herrera, 2004). However, initial results of Phase I and II studies with CI-1040, ARRY-142886 and PD0325901 have demonstrated that the treatment is overall well-tolerated with rash, diarrhea, nausea, asthenia, and anemia among the most frequent side effects (Wang et al. 2007).

Besides toxicity, other possible shortcomings may limit the efficacy of kinase inhibitors in cancer treatment. Molecular resistance formation has been described as a serious concern, causing disease relapse after a initial response. Numerous mechanisms may cause resistance to protein kinase inhibitors. Among them, the expansion of clonal cells carrying mutations of the target kinase appears to be an important mechanism. In the paradigmatic example of imatinib for the treatment of CML, resistance causing mutations occur and either prevent the ABL adopting the inactive conformation to which the compounds binds, or alter the compound contact point (Sawyers 2007). It is still unknown whether BRAF or MEK kinases may be subjected to similar mutations.

Besides direct mutation in the target kinase, regulatory signaling circuits may be elicited by the treatment and dampen its efficacy. These circuits may either activate parallel pathways to complement the targeted one or may resume, at different levels, the targeted cascade. Signal transduction pathways are indeed controlled by a network of regulatory circuits. Although the major effect of these circuits is probably to prevent excessive signaling, their abrogation by molecularly targeted agents, may cause a compensatory stimulation of the pathway (Amit et al. 2007). As an example, treatment with inhibitors of mTOR, a kinase acting downstream AKT and PI3K, by removing

negative feedbacks that act upstream or at the level of AKT, exerted only transient biological effects. Importantly, this could be circumvented by combining PI3K and mTOR inhibitors (Sun et al. 2005, O'Reilly et al. 2006, Fan et al. 2006).

Our data show that treatment with MEK targeting agents is able to tune many of these controls and kinetics analysis suggests that these events contribute to rapidly attenuate ERK inhibition and perhaps biological effects of PD0325901 and U0126 treatment. We found, indeed, that these circuits affect both the ERK and the PI3K/AKT signaling cascades (**Figure 29**).

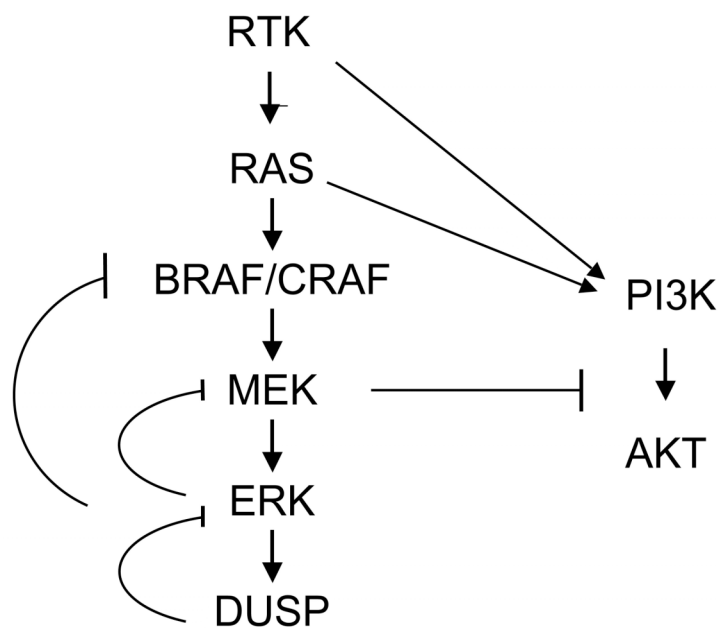


Fig. 29: Schematic representation of regulatory loops that are elicited when MEK is targeted in BRAF mutation positive thyroid cancer cells.

As far as the ERK cascade is concerned:

- at the transcriptional level, the downregulated expression of MKP3 and DUSP5, likely reduced the turn-over rate of ERK phosphorylation thereby blunting ERK inhibition upon MEK blockade;
- at the post-translational level, treatment with MEK targeting agents attenuated ERK-dependent inhibitory phosphorylations of RAF kinases, this, in turn, likely accounting for the rapid attenuation of MEK inhibition in cells treated with PD0325901.

We cannot exclude that additional regulatory mechanisms result in MEK overactivation, thus hampering the efficacy of MEK inhibitory agents. For instance, in some but not all reports, ERK-mediated phosphorylation of MEK1 on Thr292 was found to attenuate MEK activity, anticipating that ERK inhibition could potentiate it (Eblen et al. 2004, Brunet et al 1994; Gardner et al 1994). Furthermore, changes in the expression levels of MEK phosphatases, such as PP2A, may occur and affect cell response to MEK inhibition.

As far as the PI3K/AKT cascade, we noted a rapid phosphorylation of AKT secondary to MEK inhibition. The mechanism of this unexpected result is still unclear. We cannot exclude that AKT is directly modified (for instance secondary to mTOR modulation by MEK inhibitors) or that, alternatively, it is stimulated by upstream signals. The deletion of ERK-mediated inhibitory feedbacks may not only affect the RAF level of the cascade but also other upstream components, like RAS or even the growth factor receptors or their direct signaling mediators. ERK-mediated phosphorylations may inhibit receptor-coupled signaling intermediates such as the SOS exchange factor or the GAB1 docking protein. Thus, ERK inhibition secondary to MEK blockade may promote the function of these signalling molecules, thereby resulting, not only in ERK pathway, but also PI3K pathway resume. Whatever the mechanism our findings suggest that the AKT activation secondary to MEK targeting is PI3K-dependent and therefore suggest combination of MEK and PI3K inhibitors as a potential strategy to overcome the phenomenon. This

information needs to be interpreted cautiously, however, since the PI3K inhibitors we used are known to be not specific and off-target effects cannot be ruled out. Similarly, the rapid resume of the ERK cascade may be theoretically prevented by combining MEK with BRAF inhibitors. Although non-specific also Hsp90 inhibitors like 17-AAG, known to be able to promote the proteasome-mediated degradation of BRAF V600E, may also be exploited.

6 CONCLUSIONS

Here we provide evidence that BRAF and MEK targeting may be suitable approaches to arrest proliferation of thyroid cancer cells positive for the BRAF mutation. We also show that there is opportunity for a therapeutic window to be achieved with MEK kinase inhibitors. Although MEK inhibitory agents exerted significant growth inhibitory properties in thyroid carcinoma cells, they also elicited compensatory mechanisms that attenuate the duration of their effects and caused the activation of parallel signaling cascades. As with conventional chemotherapeutic agents, which are often most effective when administered as combination therapies, rationally developed combinations of molecularly targeted agents at multiple levels of the ERK cascade or at both ERK and PI3K cascades may prove to be more effective targeting strategies than single-agent therapies.

7 ACKNOWLEDGEMENTS

All my work have been conducted at the dipartimento di Biologia e Patologia Cellulare e Molecolare “L. Califano”, Università degli Studi di Napoli “Federico II”. I express gratitude to the coordinator of the international school of doctorate, Prof. Giancarlo Vecchio, who gave me the possibility to work in his department.

I want to thank all the people that help me during these years. My particular acknowledges go to my mentor, Prof. Massimo Santoro, who opened my mind to the study of oncology. My special thank go to the Prof. Giuliana Salvatore, who directly supervised my work in these years and to Prof. Alfredo Fusco for continous support and to NOGEC (Naples OncoGENomic Center) for a fellowship.

I also want to thank the colleagues that work in the Massimo Santoro’s lab, for their sustaining, friendship and instructive scientific discussions. Particularly I express gratitude to Dr. Tito Claudio Nappi who is an important member of the group I work with. I would gratefully acknowledge Bayer corporation and Pfizer Global Research and Development for providing us with the compounds.

I thank C.H. Heldin for SW1736 cells and F. Curcio for P5 cells.

I also thank S. Sequino and A. Baiano for animal care.

Finally, I wish to thank my family and my friends for the patient and support they gave me during these years.

8 REFERENCES

- Adeniran AJ, Zhu Z, Gandhi M, Steward DL, Fidler JP, Giordano TJ, Biddinger PW, Nikiforov YE. Correlation between genetic alterations and microscopic features, clinical manifestations, and prognostic characteristics of thyroid papillary carcinomas. *Am J Surg Pathol* 2006;30:216-222.
- Amit I, Citri A, Shay T, Lu Y, Katz M, Zhang F, et al. A module of negative feedback regulators defines growth factor signaling. *Nat Genet* 2007;39:503-12.
- Are C, Shaha AR. Anaplastic thyroid carcinoma: biology, pathogenesis, prognostic factors, and treatment approaches. *Ann Surg Oncol* 2006;13:453-64.
- Asklen LA, LiVolsi VA. Prognostic significance of histological grading compared with subclassification of papillary thyroid carcinoma. *Cancer* 2000;88:1902–1908.
- Bardelli A, Parsons DW, Silliman N, Ptak J, Szabo S, Saha S, Markowitz S, Willson JK, Parmigiani G, Kinzler KW, Vogelstein B, Velculescu VE. Mutational analysis of the tyrosine kinome in colorectal cancers. *Science*. 2003 May 9;300(5621):949.
- Baselga J. Targeting Tyrosine Kinases in Cancer: The Second Wave. *Science* 2006;312:1175-1178.
- Basolo F, Pisaturo F, Pollina LE, Fontanini G, Elisei R, Molinaro E, Iaconi P, Miccoli P, Pacini F. N-ras mutation in poorly differentiated thyroid carcinomas: correlation with bone metastases and inverse correlation to thyroglobulin expression. *Thyroid*. 2000;10(1):19-23.
- Bongarzone I, Butti MG, Coronelli S, Borrello MG, Santoro M, Mondellini P, Pilotti S, Fusco A, Della Porta G, Pierotti MA. Frequent activation of ret protooncogene by fusion with a new activating gene in papillary thyroid carcinomas. *Cancer Res* 1994;54:2979-2985.
- Bongarzone I, Fugazzola L, Vigneri P, Mariani L, Mondellini P, Pacini F, Basolo F, Pinchera A, Pilotti S, Pierotti MA. Age-related activation of the tyrosine kinase receptor protooncogenes RET and NTRK1 in papillary thyroid carcinoma. *J Clin Endocrinol Metab* 1996;81:2006-2009.
- Braga-Basaria M, Hardy E, Gottfried R, Burman KD, Saji M, Ringel MD. 17-Allylamino-17-demethoxygeldanamycin activity against thyroid cancer cell lines correlates with heat shock protein 90 levels. *J Clin Endocrinol Metab*. 2004; 89(6):2982-8.
- Brazil DP, Yang ZZ, Hemmings BA. Advances in protein kinase B signalling: AKTion on multiple fronts. *Trends Biochem Sci* 2004;29:233–242.
- Brown AP, Carlson TC, Loi CM, Graziano MJ. Pharmacodynamic and toxicokinetic evaluation of the novel MEK inhibitor, PD0325901, in the

rat following oral and intravenous administration. *Cancer Chemother Pharmacol* 2007; 59:671-9.

- Brummer T, Naegele H, Reth M, Misawa Y. Identification of novel ERK-mediated feedback phosphorylation sites at the C-terminus of B-Raf. *Oncogene* 2003;22:8823-34.
- Brunet A, Pagès G, Pouyssegur J. Growth factor-stimulated MAP kinase induces rapid retrophosphorylation and inhibition of MAP kinase kinase (MEK1). *FEBS Lett* 1994; 346:299-303.
- Bruni P, Boccia A, Baldassarre G, Trapasso F, Santoro M, Chiappetta G, Fusco A, Viglietto G. PTEN expression is reduced in a subset of sporadic thyroid carcinomas: evidence that PTEN-growth suppressing activity in thyroid cancer cells mediated by p27kip1. *Oncogene* 2000;19:3146–3155.
- Camps M, Nichols A, Arkinstall S. Dual specificity phosphatases: a gene family for control of MAP kinase function. *FASEB J* 2000;14:6-16.
- Cantley LC, Neel BG. New insights into tumor suppression: PTEN suppresses tumor formation by restraining the phosphoinositide 3-kinase/AKT pathway. *Proc Natl Acad Sci USA* 1999;96:4240–4245.
- Carlomagno F, Anaganti S, Guida T, Salvatore G, Troncione G, Wilhelm SM, Santoro M. BAY 43-9006 inhibition of oncogenic RET mutants. *J Natl Cancer Inst.* 2006;98(5):326-34.
- Carlomagno F, Vitagliano D, Guida T, Ciardiello F, Tortora G, Vecchio G, Ryan AJ, Fontanini G, Fusco A, Santoro M. ZD6474, an orally available inhibitor of KDR tyrosine kinase activity, efficiently blocks oncogenic RET kinases. *Cancer Res.* 2002;62(24):7284-90.
- Carta C, Moretti S, Passeri L, Barbi F, Avenia N, Cavaliere A, Monacelli M, Macchiarulo A, Santeusano F, Tartaglia M, Puxeddu E. Genotyping of an Italian papillary thyroid carcinoma cohort revealed high prevalence of BRAF mutations, absence of RAS mutations and allowed the detection of a new mutation of BRAF oncoprotein (BRAF(V599Ins)). *Clin Endocrinol (Oxf)* 2006;64:105-109.
- Castellone MD, Cirafici AM, De Vita G, De Falco V, Malorni L, Tallini G, Fagin JA, Fusco A, Melillo RM, Santoro M. Ras-mediated apoptosis of PC CL 3 rat thyroid cells induced by RET/PTC oncogenes. *Oncogene.* 2003;22(2):246-55.
- Castro P, Rebocho AP, Soares RJ, Magalhães J, Roque L, Trovisco V, Vieira de Castro I, Cardoso-de-Oliveira M, Fonseca E, Soares P, Sobrinho-Simões M. PAX8-PPARgamma rearrangement is frequently detected in the follicular variant of papillary thyroid carcinoma. *J Clin Endocrinol Metab.* 2006 ;91(1):213-20.
- Ciampi R, Knauf JA, Kerler R, Gandhi M, Zhu Z, Nikiforova MN, Rabes HM, Fagin JA, Nikiforov YE. Oncogenic AKAP9-BRAF fusion is a novel mechanism of MAPK pathway activation in thyroid cancer. *J Clin Invest* 2005;115:94-101.

- Ciampi R, Nikiforov YE. Alterations of the BRAF gene in thyroid tumors. *Endocr Pathol* 2005;16:163-172.
- Cohen Y, Xing M, Mambo E, Guo Z, Wu G, Trink B, Beller U, Westra WH, Ladenson PW, Sidransky D. BRAF mutation in papillary thyroid carcinoma. *J Natl Cancer Inst* 2003;95:625-627.
- Cooper DS, Doherty GM, Haugen BR, Kloos RT, Lee SL, Mandel SJ, Mazzaferri EL, McIver B, Sherman SI, Tuttle RM. Management guidelines for patients with thyroid nodules and differentiated thyroid cancer. *Thyroid* 2006;16:109-142.
- Cote GJ, Gagel RF. Lessons learned from the management of a rare genetic cancer. *N Engl J Med.* 2003;349(16):1566-8.
- Davies SP, Reddy H, Caivano M, Cohen P. Specificity and mechanism of action of some commonly used protein kinase inhibitors. *Biochem J.* 2000;351(Pt 1):95-105.
- De Crevoisier R, Baudin E, Bachelot A, Leboulleux S, Travagli JP, Caillou B, Schlumberger M. Combined treatment of anaplastic thyroid carcinoma with surgery, chemotherapy, and hyperfractionated accelerated external radiotherapy. *Int J Radiat Oncol Biol Phys.* 2004;60(4):1137-43.
- De Falco V, Guarino V, Malorni L, Cirafici AM, Troglio F, Erreni M, Pelicci G, Santoro M, Melillo RM. RAI(ShcC/N-Shc)-dependent recruitment of GAB 1 to RET oncoproteins potentiates PI 3-K signalling in thyroid tumors. *Oncogene* 2005;24:63036313.
- De Lellis R. Pathology and Genetics of Thyroid Carcinoma. *Journal of Surgical Oncology.* 2006;(94):662-669.
- Dhomen N, Marais R. New insight into BRAF mutations in cancer. *Curr Opin Genet Dev.* 2007;17(1):31-9.
- Di Cristofaro J, Marcy M, Vasko V, Sebag F, Fakhry N, Wynford-Thomas D, De Micco C. Molecular genetic study comparing follicular variant versus classic papillary thyroid carcinomas: association of N-ras mutation in codon 61 with follicular variant. *Hum Pathol.* 2006;37(7):824-30.
- Dougherty MK, Müller J, Ritt DA, Zhou M, Zhou XZ, Copeland TD, Conrads TP, Veenstra TD, Lu KP, Morrison DK. Regulation of Raf-1 by direct feedback phosphorylation. *Mol Cell.* 2005;17(2):215-24.
- Durante C, Haddy N, Baudin E, Leboulleux S, Hartl D, Travagli JP, Caillou B, Ricard M, Lombroso JD, De Vathaire F, Schlumberger M. Long-term outcome of 444 patients with distant metastases from papillary and follicular thyroid carcinoma: benefits and limits of radioiodine therapy. *J Clin Endocrinol Metab.* 2006 Aug;91(8):2892-9.
- Eblen ST, Slack-Davis JK, Tarcsafalvi A, Parsons JT, Weber MJ, Catling AD. Mitogen-activated protein kinase feedback phosphorylation regulates MEK1 complex formation and activation during cellular adhesion. *Mol Cell Biol* 2004; 24:2308-17.

- Eisen T, Ahmad T, Flaherty KT, Gore M, Kaye S, Marais R, Gibbens I, Hackett S, James M, Schuchter LM, Nathanson KL, Xia C, Simantov R, Schwartz B, Poulin-Costello M, O'Dwyer PJ, Ratain MJ. Sorafenib in advanced melanoma: a Phase II randomised discontinuation trial analysis. *Br J Cancer*. 2006;95(5):581-6.
- Emuss V, Garnett M, Mason C, Marais R. Mutations of C-RAF are rare in human cancer because C-RAF has a low basal kinase activity compared with B-RAF. *Cancer Res*. 2005;65(21):9719-26.
- Fan QW, Knight ZA, Goldenberg DD, Yu W, Mostov KE, Stokoe D, Shokat KM, Weiss WA. A dual PI3 kinase/mTOR inhibitor reveals emergent efficacy in glioma. *Cancer Cell* 2006; 9:341-9.
- Fenton CL, Lukes Y, Nicholson D, Dinauer CA, Francis GL, Tuttle RM. The ret/PTC mutations are common in sporadic papillary thyroid carcinoma of children and young adults. *J Clin Endocrinol Metab* 2000;85:1170-1175.
- Frêche B, Guillaumot P, Charmetant J, Pelletier L, Luquain C, Christiansen D, Billaud M, Manié SN. Inducible dimerization of RET reveals a specific AKT deregulation in oncogenic signaling. *J Biol Chem*. 2005;280(44):36584-91.
- Frisk T, Foukakis T, Dwight T, Lundberg J, Hoog A, Wallin G, Eng C, Zedenius J, Larsson C. Silencing of the PTEN tumor-suppressor gene in anaplastic thyroid cancer. *Genes Chromosomes Cancer* 2002;35:74–80
- Fusco A, Berlingieri MT, Di Fiore PP, Portella G, Grieco M, Vecchio G. One- and two-step transformations of rat thyroid epithelial cells by retroviral oncogenes. *Mol Cell Biol*. 1987;7(9):3365-70.
- Fusco A, Viglietto G, Santoro M. A new mechanism of BRAF activation in human thyroid papillary carcinomas. *J Clin Invest*. 2005;115(1):20-3.
- García-Rostán G, Costa AM, Pereira-Castro I, Salvatore G, Hernandez R, Hermsem MJ, Herrero A, Fusco A, Cameselle-Teijeiro J, Santoro M. Mutation of the PIK3CA gene in anaplastic thyroid cancer. *Cancer Res*. 2005;65(22):10199-207.
- Garcia-Rostan G, Zhao H, Camp RL, Pollan M, Herrero A, Pardo J, Wu R, Carcangiu ML, Costa J, Tallini G. ras mutations are associated with aggressive tumor phenotypes and poor prognosis in thyroid cancer. *J Clin Oncol* 2003;21:3226-35.
- Gardner AM, Vaillancourt RR, Lange-Carter CA, Johnson GL. MEK-1 phosphorylation by MEK kinase, Raf, and mitogen-activated protein kinase: analysis of phosphopeptides and regulation of activity. *Mol Biol Cell*. 1994 Feb;5(2):193-201.
- Garnett MJ, Marais R. Guilty as charged: B-RAF is a human oncogene. *Cancer Cell*. 2004;6(4):313-9.
- Garnett MJ, Rana S, Paterson H, Barford D, Marais R. Wild-type and mutant B-RAF activate C-RAF through distinct mechanisms involving heterodimerization. *Mol Cell*. 2005;20(6):963-9.

- Greenman C, Stephens P, Smith R, Dalgliesh GL, Hunter C, Bignell G, Davies H, Teague J, Butler A, Stevens C, Edkins S, O'Meara S, Vastrik I, Schmidt EE, Avis T, Barthorpe S, Bhamra G, Buck G, Choudhury B, Clements J, Cole J, Dicks E, Forbes S, Gray K, Halliday K, Harrison R, Hills K, Hinton J, Jenkinson A, Jones D, Menzies A, Mironenko T, Perry J, Raine K, Richardson D, Shepherd R, Small A, Tofts C, Varian J, Webb T, West S, Widaa S, Yates A, Cahill DP, Louis DN, Goldstraw P, Nicholson AG, Brasseur F, Looijenga L, Weber BL, Chiew YE, DeFazio A, Greaves MF, Green AR, Campbell P, Birney E, Easton DF, Chenevix-Trench G, Tan MH, Khoo SK, Teh BT, Yuen ST, Leung SY, Wooster R, Futreal PA, Stratton MR. Patterns of somatic mutation in human cancer genomes. *Nature*. 2007 Mar 8;446(7132):153-8.
- Grieco M, Santoro M, Berlingieri MT, Melillo RM, Donghi R, Bongarzone I, Pierotti MA, Della Porta G, Fusco A, Vecchio G. PTC is a novel rearranged form of the ret proto-oncogene and is frequently detected in vivo in human thyroid papillary carcinomas. *Cell* 1990;60:557-563.
- Groom LA, Sneddon AA, Alessi DR, Dowd S, Keyse SM. Differential regulation of the MAP, SAP and RK/p38 kinases by Pyst1, a novel cytosolic dual specificity phosphatase. *EMBO J* 1996;15:3621-32.
- Groussin L, Fagin JA. Significance of BRAF mutations in papillary thyroid carcinoma: prognostic and therapeutic implications. *Nat Clin Pract Endocrinol Metab*. 2006;2(4):180-1.
- Halachmi N, Halachmi S, Evron E, Cairns P, Okami K, Saji M, Westra WH, Zeiger MA, Jen J, Sidransky S. Somatic mutations of the PTEN/MMAC1 tumor suppressor gene in sporadic follicular thyroid tumors. *Genes Chromosomes Cancer* 1998;23:239-243.
- Hay N. The Akt-mTOR tango and its relevance to cancer. *Cancer Cell* 2005;8:179-183
- Hou P, Liu D, Shan Y, Hu S, Studeman K, Condouris S, Wang Y, Trink A, El-Naggar AK, Tallini G, Vasko V, Xing M. Genetic alterations and their relationship in the phosphatidylinositol 3-kinase/Akt pathway in thyroid cancer. *Clin Cancer Res*. 2007;13(4):1161-70.
- Hou P, Liu D, Xing M. Functional characterization of the T1799-1801del and A1799-1816ins BRAF mutations in papillary thyroid cancer. *Cell Cycle*. 2007 ;6(3):377-9.
- Ishibashi T, Bottaro DP, Michieli P, Kelley CA, Aaronson SA. A novel dual specificity phosphatase induced by serum stimulation and heat shock. *J Biol Chem*1994;269:29897-902.
- Jeffrey KL, Camps M, Rommel C, Mackay CR. Targeting dual-specificity phosphatases: manipulating MAP kinase signalling and immune responses. *Nat Rev Drug Discov*. 2007;6(5):391-403.

- Jhiang SM, Sagartz JE, Tong Q, Parker-Thornburg J, Capen CC, Cho JY, Xing S, Ledent C. Targeted expression of the ret/PTC1 oncogene induces papillary thyroid carcinomas. *Endocrinology* 1996;137:375-378.
- Jung HS, Kim DW, Jo YS, Chung HK, Song JH, Park JS, Park KC, Park SH, Hwang JH, Jo KW, Shong M. Regulation of protein kinase B tyrosine phosphorylation by thyroid-specific oncogenic RET/PTC kinases. *Mol Endocrinol* 2005;19:2748-2759.
- Keyse SM. Protein phosphatases and the regulation of mitogen-activated protein kinase signalling. *Curr Opin Cell Biol* 2000;12:186-92.
- Kimura ET, Nikiforova MN, Zhu Z, Knauf JA, Nikiforov YE, Fagin JA. High prevalence of BRAF mutations in thyroid cancer: genetic evidence for constitutive activation of the RET/PTC-RAS-BRAF signaling pathway in papillary thyroid carcinoma. *Cancer Res* 2003;63:1454-1457.
- Knauf JA, Kuroda H, Basu S, Fagin JA. RET/PTC-induced dedifferentiation of thyroid cells is mediated through Y1062 signaling through SHC-RAS-MAP kinase. *Oncogene* 2003;22:4406-4412.
- Knauf JA, Ma X, Smith EP, Zhang L, Mitsutake N, Liao XH, Refetoff S, Nikiforov YE, Fagin JA. Targeted expression of BRAFV600E in thyroid cells of transgenic mice results in papillary thyroid cancers that undergo dedifferentiation. *Cancer Res* 2005;65:4238-4245
- Knauf JA, Ouyang B, Knudsen ES, Fukasawa K, Babcock G, Fagin JA. Oncogenic RAS induces accelerated transition through G2/M and promotes defects in the G2 DNA damage and mitotic spindle checkpoints. *J Biol Chem.* 2006;281(7):3800-9.
- Koh CS, Ku JL, Park SY, Kim KH, Choi JS, Kim IJ, Park JH, Oh SK, Chung JK, Lee JH, Kim WH, Kim CW, Cho BY, Park JG. Establishment and characterization of cell lines from three human thyroid carcinomas: responses to all-trans-retinoic acid and mutations in the BRAF gene. *Mol Cell Endocrinol.* 2007;264(1-2):118-27.
- Kohno M, Pouyssegur. J Targeting the ERK signaling pathway in cancer therapy. *Ann Med* 2006;38:200-211.
- Kondo T, Ezzat S, Asa SL. Pathogenetic mechanisms in thyroid follicular-cell neoplasia. *Nat Rev Cancer.* 2006;6(4):292-306.
- Kumagai A, Namba H, Saenko VA, Ashizawa K, Ohtsuru A, Ito M, Ishikawa N, Sugino K, Ito K, Jeremiah S, Thomas GA, Bogdanova TI, Tronko MD, Nagayasu T, Shibata Y, Yamashita S. Low frequency of BRAFT1796A mutations in childhood thyroid carcinomas. *J Clin Endocrinol Metab* 2004;89:4280-4284.
- Leboulleux S, Baudin E, Travaglini JP, Schlumberger M. Medullary thyroid carcinoma. *Clin Endocrinol (Oxf).* 2004 Sep;61(3):299-310.
- Leboulleux S, Rubino C, Baudin E, Caillou B, Hartl DM, Bidart JM, Travaglini JP, Schlumberger M. Prognostic factors for persistent or recurrent disease of papillary thyroid carcinoma with neck lymph node

metastases and/or tumor extension beyond the thyroid capsule at initial diagnosis. *J Clin Endocrinol Metab.* 2005 Oct;90(10):5723-9.

- Lima J, Trovisco V, Soares P, Maximo V, Magalhaes J, Salvatore G, Santoro M, Bogdanova T, Tronko M, Abrosimov A, Jeremiah S, Thomas G, Williams D, Sobrinho-Simoes M. BRAF mutations are not a major event in post-Chernobyl childhood thyroid carcinomas. *J Clin Endocrinol Metab* 2004;89:4267-4271.
- Lin HY, Harris TL, Flannery MS, Aruffo A, Kaji EH, Gorn A, Kolakowski LF Jr, Lodish HF, Goldring SR. Expression cloning of an adenylate cyclase-coupled calcitonin receptor. *Science* 1991;254(5034):1022-24.
- Lin HY, Harris TL, Flannery MS, Aruffo A, Kaji EH, Gorn A, Kolakowski LF Jr, Lodish HF, Goldring SR. Expression cloning of an adenylate cyclase-coupled calcitonin receptor. *Science* 1991;254(5034):1022-24.
- Liu D, Hu S, Hou P, Jiang D, Condouris S, Xing M. Suppression of BRAF/MEK/MAP kinase pathway restores expression of iodide-metabolizing genes in thyroid cells expressing the V600E BRAF mutant. *Clin Cancer Res.* 2007 Feb 15; 13(4):1341-9.
- Lorusso PM, Adjei AA, Varterasian M, Gadgeel S, Reid J, Mitchell DY, Hanson L, DeLuca P, Bruzek L, Piens J, Asbury P, Van Becelaere K, Herrera R, Sebolt-Leopold J, Meyer MB. Phase I and pharmacodynamic study of the oral MEK inhibitor CI-1040 in patients with advanced malignancies. *J Clin Oncol.* 2005;23:5281-93.
- Lupi C, Giannini R, Ugolini C, Proietti A, Berti P, Minuto M, Materazzi G, Elisei R, Santoro M, Miccoli P, Basolo F. Association of BRAF V600E Mutation with Poor Clinicopathological Outcomes in 500 Consecutive Cases of Papillary Thyroid Carcinoma. *J Clin Endocrinol Metab.* 2007;92(11):4085-90.
- MacCorkle RA, Tan TH. Mitogen-activated protein kinases in cell-cycle control. *Cell Biochem Biophys* 2005; 43:451-461
- Mandl M, Slack DN, Keyse SM. Specific inactivation and nuclear anchoring of extracellular signal-regulated kinase 2 by the inducible dual-specificity protein phosphatase DUSP5. *Mol Cell Biol* 2005;25:1830-45.
- Manié S, Santoro M, Fusco A, Billaud M. The RET receptor: function in development and dysfunction in congenital malformation. *Trends Genet.* 2001;17(10):580-9.
- Marais R, Light Y, Paterson HF, Mason CS, Marshall CJ. Differential regulation of RAF-1, A-RAF, and B-RAF by oncogenic RAS and tyrosine kinases. *J Biol Chem* 1997;272:4378-4383.
- Marais R, Marshall CJ. Control of the ERK MAP kinase cascade by RAS and RAF. In: Parker PJ, Pawson T, editors. *Cell Signalling.* Cold

Spring Harbor, NY: Cold Spring Harbor Laboratory Press; 1996. 101-125 p.

- Mattoon, D.R., Lamothe, B., Lax, I., and Schlessinger, J.. The docking protein Gab1 is the primary mediator of EGF-stimulated activation of the PI-3K/Akt cell survival pathway. *BMC Biol* 2004;2;:24.
- McIver B, Hay ID, Giuffrida DF, Dvorak CE, Grant CS, Thompson GB, van Heerden JA, Goellner JR. Anaplastic thyroid carcinoma: a 50-year experience at a single institution. *Surgery* 2001;130(6):1028-34.
- Melillo RM, Castellone MD, Guarino V, De Falco V, CiRAFici AM, Salvatore G, Caiazzo F, Basolo F, Giannini R, Kruhoffer M, Orntoft T, Fusco A, Santoro M. The RET/PTC-RAS-BRAF linear signaling cascade mediates the motile and mitogenic phenotype of thyroid cancer cells. *J Clin Invest* 2005;115:1068-1081.
- Mercer KE, Pritchard CA. RAF proteins and cancer: B-RAF is identified as a mutational target. *Biochim Biophys Acta* 2003;1653:25-40.
- Mesa C, Jr., Mirza M, Mitsutake N, Sartor M, Medvedovic M, Tomlinson C, Knauf JA, Weber GF, Fagin JA. Conditional activation of RET/PTC3 and BRAFV600E in thyroid cells is associated with gene expression profiles that predict a preferential role of BRAF in extracellular matrix remodeling. *Cancer Res* 2006;66:6521-6529
- Messersmith WA, Hidalgo M, Carducci M, Eckhardt SG. Novel targets in solid tumors: MEK inhibitors. *Clin Adv Hematol Oncol* 2006;4:831-6.
- Mitsutake N, Knauf JA, Mitsutake S, Mesa C, Jr, Zhang L, Fagin JA. Conditional BRAFV600E expression induces DNA synthesis, apoptosis, dedifferentiation, and chromosomal instability in thyroid PCCL3 cells. *Cancer Res* 2005;65:2465-2473.
- Miyagi E, Braga-Basaria M, Hardy E, Vasko V, Burman KD, Jhiang S, Saji M, Ringel MD. Chronic expression of RET/PTC 3 enhances basal and insulin-stimulated PI3 kinase/AKT signaling and increases IRS-2 expression in FRTL-5 thyroid cells. *Mol Carcinog* 2004;41:98-107.
- Moretti S, Macchiarulo A, De Falco V, Avenia N, Barbi F, Carta C, Cavaliere A, Melillo RM, Passeri L, Santeusanio F, Tartaglia M, Santoro M, Puxeddu E. Biochemical and molecular characterization of the novel BRAF(V599Ins) mutation detected in a classic papillary thyroid carcinoma. *Oncogene*. 2006;25(30):4235-40.
- Muda M, Theodosiou A, Rodrigues N, Boschert U, Camps M, Gillieron C, Davies K, Ashworth A, Arkinstall S. The dual specificity phosphatases M3/6 and MKP-3 are highly selective for inactivation of distinct mitogen-activated protein kinases. *J Biol Chem*. 1996;271(44):27205-8.
- Niculescu-Duvaz D, Whittaker S, Springer C, Marais R. The EGF receptor Hokey-Cokey. *Cancer Cell*. 2007;11(3):209-11.

- Nikiforov YE, Erickson LA, Nikiforova MN, et al.: Solid variant of papillary thyroid carcinoma: Incidence, clinical-pathological characteristics, molecular analysis and biological behavior. *Am J Surg Pathol* 2001;25:1478–1484.
- Nikiforov YE, Rowland JM, Bove KE, Monforte-Munoz H, Fagin JA. Distinct pattern of ret oncogene rearrangements in morphological variants of radiation-induced and sporadic thyroid papillary carcinomas in children. *Cancer Res* 1997;57:1690-1694.
- Nikiforova MN, Ciampi R, Salvatore G, Santoro M, Gandhi M, Knauf JA, Thomas GA, Jeremiah S, Bogdanova TI, Tronko MD, Fagin JA, Nikiforov YE. Low prevalence of BRAF mutations in radiation-induced thyroid tumors in contrast to sporadic papillary carcinomas. *Cancer Lett* 2004;209:1-6.
- Nikiforova MN, Kimura ET, Gandhi M, Biddinger PW, Knauf JA, Basolo F, Zhu Z, Giannini R, Salvatore G, Fusco A, Santoro M, Fagin JA, Nikiforov YE. BRAF mutations in thyroid tumors are restricted to papillary carcinomas and anaplastic or poorly differentiated carcinomas arising from papillary carcinomas. *J Clin Endocrinol Metab.* 2003;88(11):5399-404.
- Ohren JF, Chen H, Pavlovsky A, Whitehead C, Zhang E, Kuffa P, Yan C, McConnell P, Spessard C, Banotai C, Mueller WT, Delaney A, Omer C, Sebolt-Leopold J, Dudley DT, Leung IK, Flamme C, Warmus J, Kaufman M, Barrett S, Teclé H, Hasemann CA. Structures of human MAP kinase kinase 1 (MEK1) and MEK2 describe novel noncompetitive kinase inhibition. *Nat Struct Mol Biol.* 2004;11(12):1192-7.
- Ong SH, Hadari YR, Gotoh N, Guy, GR, Schlessinger J and Lax I. Stimulation of phosphatidylinositol 3-kinase by fibroblast growth factor receptors is mediated by coordinated recruitment of multiple docking proteins. *Proc. Natl. Acad. Sci. USA* 2001;98,6074–6079.
- Ouyang B, Knauf JA, Smith EP, Zhang L, Ramsey T, Yusuff N, Batt D, Fagin JA. Inhibitors of Raf kinase activity block growth of thyroid cancer cells with RET/PTC or BRAF mutations in vitro and in vivo. *Clin Cancer Res.* 2006;12(6):1785-93.
- Pacini F, Schlumberger M, Dralle H, Elisei R, Smit JW, Wiersinga W; European Thyroid Cancer Taskforce. European consensus for the management of patients with differentiated thyroid carcinoma of the follicular epithelium. *Eur J Endocrinol.* 2006 Jun;154(6):787-803.
- Pasiëka JL. Anaplastic thyroid cancer. *Curr Opin Oncol* 2003;15:78-83.
- Pearse AG, Carvalheira AF. Cytochemical evidence for an ultimobranchial origin of rodent thyroid C cells. *Nature* 1967;214(91):929-30.

- Pierie JP, Muzikansky A, Gaz RD, Faquin WC, Ott MJ. The effect of surgery and radiotherapy on outcome of anaplastic thyroid carcinoma. *Ann Surg Oncol.* 2002;9(1):57-64.
- Powell DJ Jr., Russell J, Nibu K, Li G, Rhee E, Liao M, Goldstein M, Keane WM, Santoro M, Fusco A, Rothstein JL. The RET/PTC3 oncogene: metastatic solidtype papillary carcinomas in murine thyroids. *Cancer Res* 1998;58:5523-5528.
- Pulcrano M, Boukheris H, Talbot M, Caillou B, Dupuy C, Virion A, De Vathaire F, Schlumberger M. Poorly differentiated follicular thyroid carcinoma: prognostic factors and relevance of histological classification. *Thyroid.* 2007;17(7):639-46.
- Ramjaun AR, Downward J. Ras and Phosphoinositide 3-Kinase: Partners in Development and Tumorigenesis. *Cell Cycle.* 2007;6(23)
- Reffas S, Schlegel W. Compartment-specific regulation of extracellular signal-regulated kinase (ERK) and c-Jun N-terminal kinase (JNK) mitogen-activated protein kinases (MAPKs) by ERK-dependent and nonERK-dependent inductions of MAPK phosphatase (MKP)-3 and MKP-1 in differentiating P19 cells. *Biochem J* 2000;352(3):701-8.
- Reynolds L, Jones K, Winton DJ, Cranston A, Houghton C, Howard L, Ponder BA, Smith DP. C-cell and thyroid epithelial tumors and altered follicular development in transgenic mice expressing the long isoform of MEN 2A RET. *Oncogene* 2001;20(30):3986-94.
- Riesco-Eizaguirre G, Gutiérrez-Martínez P, García-Cabezas MA, Nistal M, Santisteban P. The oncogene BRAF V600E is associated with a high risk of recurrence and less differentiated papillary thyroid carcinoma due to the impairment of Na⁺/I⁻-targeting to the membrane. *Endocr Relat Cancer.* 2006;13(1):257-69.
- Rinehart J, Adjei AA, Lorusso PM, Waterhouse D, Hecht JR, Natale RB, et al. Multicenter phase II study of the oral MEK inhibitor, CI-1040, in patients with advanced non-small-cell lung, breast, colon, and pancreatic cancer. *J Clin Oncol* 2004; 22:4456-62.
- Ringel MD, Hayre N, Saito J, Saunier B, Schuppert F, Burch H, Bernet V, Burman KD, Kohn LD, Saji M. Overexpression and overactivation of Akt in thyroid carcinoma. *Cancer Res* 2001;61:6105–6111.
- Roberts PJ, Der CJ. Targeting the Raf-MEK-ERK mitogen-activated protein kinase cascade for the treatment of cancer. *Oncogene.* 2007;26(22):3291-310.
- Rodolico V, Cabibi D, Pizzolanti G, Richiusa P, Gebbia N, Martorana A, Russo A, Amato MC, Galluzzo A, Giordano C BRAF(V600E) mutation and p27(kip1) expression in papillary carcinomas of the thyroid ≤ 1 cm and their paired lymph node metastases. *Cancer* 2007;110:1218-1226.

- Rodriguez-Viciana P, Tetsu O, Oda K, Okada J, Rauen K, McCormick F. Cancer targets in the RAS pathway. *Cold Spring Harb Symp Quant Biol* 2005;70:461-467.
- Rodriguez-Viciana P, Warne PH, Dhand R, Vanhaesebroeck B, Gout I, Fry MJ, Waterfield MD and Downward J. Phosphatidylinositol-3-OH kinase as a direct target of RAS. *Nature* 1994;370:527–532.
- Rushworth LK, Hindley AD, O'Neill E, Kolch W. Regulation and role of Raf-1/B-Raf heterodimerization. *Mol Cell Biol* 2006; 26:2262-72.
- Saavedra HI, Knauf JA, Shirokawa JM, Wang J, Ouyang B, Elisei R, Stambrook PJ, Fagin JA. The RAS oncogene induces genomic instability in thyroid PCCL3 cells via the MAPK pathway. *Oncogene*. 2000;19(34):3948-54.
- Santarpia L, El-Naggar AK, Cote GJ, Myers JN, Sherman SI. PI3K/Akt and Ras/Raf-MAPK pathway mutations in anaplastic thyroid cancer. *J Clin Endocrinol Metab*. 2007 Nov 7; [Epub ahead of print]
- Santoro M, Carlomagno F. Drug insight: Small-molecule inhibitors of protein kinases in the treatment of thyroid cancer. *Nat Clin Pract Endocrinol Metab*. 2006;2(1):42-52.
- Santoro M, Chiappetta G, Cerrato A, Salvatore D, Zhang L, Manzo G, Picone A, Portella G, Santelli G, Vecchio G, Fusco A. Development of thyroid papillary carcinomas secondary to tissue-specific expression of the RET/PTC1 oncogene in transgenic mice. *Oncogene* 1996;12:1821-1826.
- Santoro M, Dathan NA, Berlingieri MT, Bongarzone I, Paulin C, Grieco M, Pierotti MA, Vecchio G, Fusco A. Molecular characterization of RET/PTC3; a novel rearranged version of the RET proto-oncogene in a human thyroid papillary carcinoma. *Oncogene* 1994;9:509-516.
- Santoro M, Melillo RM, Grieco M, Berlingieri MT, Vecchio G, Fusco A 1993 The TRK and RET tyrosine kinase oncogenes cooperate with RAS in the neoplastic transformation of a rat thyroid epithelial cell line. *Cell Growth Differ* 1994;4:77-84.
- Santoro M, Melillo RM, Carlomagno F, Vecchio G and Fusco A. RET: normal and abnormal functions. *Endocrinology*. 2004;145(12):5448-51.
- Sawyers CL. Cancer: mixing cocktails. *Nature*. 2007 Oct 25;449(7165):993-6.
- Schlumberger M, Lacroix L, Russo D, Filetti S, Bidart JM. Defects in iodide metabolism in thyroid cancer and implications for the follow-up and treatment of patients. *Nat Clin Pract Endocrinol Metab*. 2007;3(3):260-9.
- Schlumberger MJ. Papillary and follicular thyroid carcinoma. *N Engl J Med*. 1998;338(5):297-306.
- Schubert S, Shannon K, Bollag G. Hyperactive Ras in developmental disorders and cancer. *Nat Rev Cancer*. 2007;7(4):295-308.

- Sebolt-Leopold JS, English JM. Mechanisms of drug inhibition of signalling molecules. *Nature* 2006;441:457-62.
- Sebolt-Leopold JS, Herrera R. Targeting the mitogen-activated protein kinase cascade to treat cancer. *Nat Rev Cancer* 2004;4:937-947.
- Segouffin-Cariou C, Billaud M. Transforming ability of MEN2A-RET requires activation of the phosphatidylinositol 3-kinase/AKT signaling pathway. *J Biol Chem.* 2000;275(5):3568-76.
- Sherr CJ. Cancer cell cycles. *Science.* 1996;274(5293):1672-7.
- Sjöblom T, Jones S, Wood LD, Parsons DW, Lin J, Barber TD, Mandelker D, Leary RJ, Ptak J, Silliman N, Szabo S, Buckhaults P, Farrell C, Meeh P, Markowitz SD, Willis J, Dawson D, Willson JK, Gazdar AF, Hartigan J, Wu L, Liu C, Parmigiani G, Park BH, Bachman KE, Papadopoulos N, Vogelstein B, Kinzler KW, Velculescu VE. The consensus coding sequences of human breast and colorectal cancers. *Science.* 2006 Oct 13;314(5797):268-74.
- Soares P, Fonseca E, Wynford-Thomas D, Sobrinho-Simoes M. Sporadic ret-rearranged papillary carcinoma of the thyroid: a subset of slow growing, less aggressive thyroid neoplasms?. *J Pathol* 1998;185:71-78.
- Soares P, Trovisco V, Rocha AS, Lima J, Castro P, Preto A, Máximo V, Botelho T, Seruca R, Sobrinho-Simões M. BRAF mutations and RET/PTC rearrangements are alternative events in the etiopathogenesis of PTC. *Oncogene.* 2003;22(29):4578-80.
- Sobrinho-Simoes M, Asa SL, Kroll TG. Follicular carcinoma. In: DeLellis RA, Lloyd RV, Heitz PU, Eng C. editors. *Pathology and genetics of tumours of endocrine organs.* Lyon: IARC Press 2004. p. 67–72.
- Solit DB, Garraway LA, Pratilas CA, Sawai A, Getz G, Basso A, Ye Q, Lobo JM, She Y, Osman I, Golub TR, Sebolt-Leopold J, Sellers WR, Rosen N. BRAF mutation predicts sensitivity to MEK inhibition. *Nature.* 2006;19;439(7074):358-62.
- Tong Q, Xing S, Jhiang SM. Leucine zipper-mediated dimerization is essential for the PTC1 oncogenic activity. *J Biol Chem* 1997;272:9043-9047.
- Torii S, Nakayama K, Yamamoto T, Nishida E. Regulatory mechanisms and function of ERK MAP kinases. *J Biochem (Tokyo)* 2004;136:557-561
- Trovisco V, Soares P, Preto A, de Castro IV, Lima J, Castro P, Maximo V, Botelho T, Moreira S, Meireles AM, Magalhaes J, Abrosimov A, Cameselle-Teijeiro J, Sobrinho-Simoes M. Type and prevalence of BRAF mutations are closely associated with papillary thyroid carcinoma histotype and patients' age but not with tumour aggressiveness. *Virchows Arch* 2005;446:589-595.

- Trovisco V, Vieira de Castro I, Soares P, Maximo V, Silva P, Magalhaes J, Abrosimov A, Guiu XM, Sobrinho-Simoes M. BRAF mutations are associated with some histological types of papillary thyroid carcinoma. *J Pathol* 2004;202:247-251.
- Vitagliano D, Portella G, Troncone G, Francione A, Rossi C, Bruno A, Giorgini A, Coluzzi S, Nappi TC, Rothstein JL, Pasquinelli R, Chiappetta G, Terracciano D, Macchia V, Melillo RM, Fusco A, Santoro M. Thyroid targeting of the N-ras(Gln61Lys) oncogene in transgenic mice results in follicular tumors that progress to poorly differentiated carcinomas. *Oncogene*. 2006;25(39):5467-74.
- Vivanco I, Sawyers CL. The phosphatidylinositol 3-Kinase AKT pathway in human cancer. *Nat Rev Cancer*. 2002;2(7):489-501.
- Volante M, Collini P, Nikiforov YE, Sakamoto A, Kakudo K, Katoh R, Lloyd RV, LiVolsi VA, Papotti M, Sobrinho-Simoes M, Bussolati G, Rosai J. Poorly differentiated thyroid carcinoma: the Turin proposal for the use of uniform diagnostic criteria and an algorithmic diagnostic approach. *Am J Surg Pathol*. 2007;31(8):1256-64.
- Wan PT, Garnett MJ, Roe SM, Lee S, Niculescu-Duvaz D, Good VM, Jones CM, Marshall CJ, Springer CJ, Barford D, Marais R. Mechanism of activation of the RAF-ERK signaling pathway by oncogenic mutations of B-RAF. *Cell* 2004 ;116:855-867.
- Wang D, Boerner SA, Winkler JD, LoRusso PM. Clinical experience of MEK inhibitors in cancer therapy. *Biochim Biophys Acta*. 2007 ;1773:1248-55.
- Wang Y, Hou P, Yu H, Wang W, Ji M, Zhao S, Yan S, Sun X, Liu D, Shi B, Zhu G, Condouris S, Xing M. High prevalence and mutual exclusivity of genetic alterations in the phosphatidylinositol-3-kinase/akt pathway in thyroid tumors. *J Clin Endocrinol Metab*. 2007;92(6):2387-90.
- Wilhelm S, Carter C, Lynch M, Lowinger T, Dumas J, Smith RA, Schwartz B, SimantovR, Kelley S. Discovery and development of sorafenib: a multikinase inhibitor for treating cancer. *Nat Rev Drug Discov* 2006 10:835-44.
- Xing M. BRAF Mutation in Papillary Thyroid Cancer: Pathogenic Role, Molecular Bases, and Clinical Implications. *Endocr Rev*. 2007; [Epub ahead of print]
- Yeh TC, Marsh V, Bernat BA, Ballard J, Colwell H, Evans RJ et al. Biological characterization of ARRY-142886 (AZD6244), a potent, highly selective mitogen activated protein kinase kinase 1/2 inhibitor. *Clin Cancer Res* 2007;1:131576-83.
- Zhu Z, Gandhi M, Nikiforova MN, Fischer AH, Nikiforov YE. Molecular profile and clinical-pathologic features of the follicular variant of papillary thyroid carcinoma. An unusually high prevalence of ras mutations. *Am J Clin Pathol*. 2003;120(1):71-7.

Attached manuscript #1

Salvatore G, De Falco V, **Salerno P**, Nappi TC, Pepe S, Troncone G, Carlomagno F, Melillo RM, Wilhelm SM, Santoro M. BRAF is a therapeutic target in aggressive thyroid carcinoma.

Clin Cancer Res 2006;12:1623-9.

BRAF Is a Therapeutic Target in Aggressive Thyroid Carcinoma

Giuliana Salvatore,¹ Valentina De Falco,¹ Paolo Salerno,¹ Tito Claudio Nappi,¹ Stefano Pepe,² Giancarlo Troncone,³ Francesca Carlomagno,¹ Rosa Marina Melillo,¹ Scott M. Wilhelm,⁴ and Massimo Santoro¹

Abstract Purpose: Oncogenic conversion of BRAF occurs in ~44% of papillary thyroid carcinomas and 24% of anaplastic thyroid carcinomas. In papillary thyroid carcinomas, this mutation is associated with an unfavorable clinicopathologic outcome. Our aim was to exploit BRAF as a potential therapeutic target for thyroid carcinoma.

Experimental Design: We used RNA interference to evaluate the effect of BRAF knockdown in the human anaplastic thyroid carcinoma cell lines FRO and ARO carrying the BRAF V600E (^{V600E}BRAF) mutation. We also exploited the effect of BAY 43-9006 [*N*-(3-trifluoromethyl-4-chlorophenyl)-*N'*-(4-(2-methylcarbamoyl pyridin-4-yl)oxyphenyl)urea], a multikinase inhibitor able to inhibit RAF family kinases in a panel of six ^{V600E}BRAF-positive thyroid carcinoma cell lines and in nude mice bearing ARO cell xenografts. Statistical tests were two sided.

Results: Knockdown of BRAF by small inhibitory duplex RNA, but not control small inhibitory duplex RNA, inhibited the mitogen-activated protein kinase signaling cascade and the growth of ARO and FRO cells ($P < 0.0001$). These effects were mimicked by thyroid carcinoma cell treatment with BAY 43-9006 ($IC_{50} = 0.5\text{-}1 \mu\text{mol/L}$; $P < 0.0001$), whereas the compound had negligible effects in normal thyrocytes. ARO cell tumor xenografts were significantly ($P < 0.0001$) smaller in nude mice treated with BAY 43-9006 than in control mice. This inhibition was associated with suppression of phospho-mitogen-activated protein kinase levels.

Conclusions: BRAF provides signals crucial for proliferation of thyroid carcinoma cells spontaneously harboring the ^{V600E}BRAF mutation and, therefore, BRAF suppression might have therapeutic potential in ^{V600E}BRAF-positive thyroid cancer.

Thyroid tumors are the most frequent neoplasms of the endocrine system (1). Well-differentiated thyroid carcinomas account for >90% of all thyroid cancers and include papillary and follicular carcinomas. Papillary thyroid carcinoma is the most prevalent subtype. Although papillary thyroid carcinoma is usually curable with surgery and adjuvant radioiodine treatment, some patients may show an aggressive disease and lose radioiodine concentration ability. Papillary thyroid carcinoma subtypes, like the tall-cell variant, more frequently have an

aggressive behavior (2). Undifferentiated (anaplastic) thyroid carcinoma accounts for ~2% to 5% of all thyroid cancers (3). Despite its rarity, more than half of the deaths attributed to thyroid cancer result from anaplastic thyroid carcinoma (3–5). More than 25% of anaplastic thyroid carcinoma patients have coincidentally detected well-differentiated carcinoma, suggesting that, at least in some cases, anaplastic thyroid carcinoma derives from a preexisting well-differentiated carcinoma (3–5). Rapid growth and dissemination characterize the clinical course of anaplastic thyroid carcinoma. Virtually, all anaplastic thyroid carcinoma patients die from their disease in 2 to 7 months; death is attributable to upper airway obstruction and suffocation in half of the patients (3–5). Anaplastic thyroid carcinomas do not concentrate radioiodine and do not respond to conventional chemotherapy (3–5).

BRAF belongs to the RAF family of serine/threonine kinases. RAF proteins are components of the RAF-MEK [mitogen activated protein (MAP)/extracellular signal-regulated kinase (ERK) kinase]-ERK pathway, a highly conserved signaling module in eukaryotes. They are activated through binding to RAS in its GTP-bound state. Once activated, RAF kinases phosphorylate MEK, which in turn phosphorylates and activates ERK (6). Activation of BRAF has emerged as the most prevalent oncogenic mutation in thyroid carcinoma (7–14). Overall, this genetic alteration is found in ~44% of papillary thyroid carcinoma and 24% of anaplastic thyroid carcinoma (reviewed in ref. 15). In the case of anaplastic thyroid carcinoma, BRAF mutations are restricted to those cases that

Authors' Affiliations: ¹Istituto di Endocrinologia ed Oncologia Sperimentale del Consiglio Nazionale delle Ricerche, c/o Dipartimento di Biologia e Patologia Cellulare e Molecolare; ²Cattedra di Oncologia Medica; ³Dipartimento di Scienze Biomorfologiche e Funzionali, Università di Napoli Federico II, Naples, Italy; and ⁴Bayer HealthCare Pharmaceuticals, West Haven, Connecticut
Received 10/31/05; accepted 12/22/05.

Grant support: Associazione Italiana per la Ricerca sul Cancro; Progetto Strategico Oncologia of the Consiglio Nazionale delle Ricerche/Ministero per l'Istruzione, Università e Ricerca Scientifica; Italian Ministero per l'Istruzione, Università e Ricerca Scientifica; Italian Ministero della Salute; and Bayer HealthCare Pharmaceuticals.

The costs of publication of this article were defrayed in part by the payment of page charges. This article must therefore be hereby marked *advertisement* in accordance with 18 U.S.C. Section 1734 solely to indicate this fact.

Requests for reprints: Massimo Santoro, Dipartimento di Biologia e Patologia Cellulare e Molecolare, Università di Napoli Federico II, via S. Pansini 5, 80131 Naples, Italy. Phone: 39-081-7463056; Fax: 39-081-7463037; E-mail: masantor@unina.it.

© 2006 American Association for Cancer Research.
doi:10.1158/1078-0432.CCR-05-2378

arose in association with papillary thyroid carcinoma (12, 14). A transversion from thymine to adenine (T1799A), leading to a Glu for Val substitution at residue 600 (V600E), accounts for >90% of BRAF mutations in thyroid carcinomas. Other more rare mutations have been described (reviewed in ref. 15). The V600E mutation enhances BRAF activity by disrupting the autoinhibited state of the kinase (16). Another interesting mechanism for BRAF activation has been described in radiation-induced papillary thyroid carcinoma, where a paracentric inversion of chromosome 7q resulted in the in-frame fusion between the *AKAP9* gene and BRAF (17).

Consistent with a pivotal role in thyroid cancer initiation, V600E BRAF has been found in microcarcinomas (15), and it was shown to induce transformed features in thyroid follicular cells in culture (18, 19) and thyroid carcinoma formation in transgenic mice (20). Many evidences suggest that V600E BRAF plays a role in thyroid cancer progression as well: (a) Adoptive expression of V600E BRAF induces genomic instability in cultured thyrocytes (19); (b) thyroid tumors in V600E BRAF-transgenics undergo dedifferentiation and metastasis formation (20); and (c) papillary thyroid carcinoma with the V600E BRAF mutation often presents with extrathyroidal invasion, lymph node metastasis, and advanced tumor stage (14). Importantly, the V600E BRAF mutation was frequently associated to loss of I-131 avidity and papillary thyroid carcinoma recurrence (14).

In this framework, BRAF could be an appealing therapeutic target for thyroid carcinomas, especially for aggressive papillary thyroid carcinoma subtypes and anaplastic thyroid carcinoma. Here, we show that suppression of BRAF expression exerts cytostatic activity in V600E BRAF-positive thyroid carcinoma cell lines. Moreover, we show that BAY 43-9006 [*N*-(3-trifluoromethyl-4-chlorophenyl)-*N'*-(4-(2-methylcarbamoyl pyridin-4-yl)oxyphenyl)urea], a multikinase ATP-competitive inhibitor able to obstruct RAF kinases (21–24), reduces tumor growth in an anaplastic thyroid carcinoma xenograft model.

Materials and Methods

Compounds. BAY 43-9006 was provided by Bayer HealthCare Pharmaceuticals (West Haven, CT). For *in vitro* experiments, BAY 43-9006 was dissolved in DMSO. For *in vivo* experiments, BAY 43-9006 was dissolved in Cremophor EL/ethyl alcohol (50:50; Sigma Cremophor EL, 95% ethyl alcohol; Sigma Chemical Co., St. Louis, MO) at 4-fold (4×) the highest dose, foil-wrapped, and stored at room temperature. A fresh supply of the 4× stock solution was prepared every 3 days. Final dosing solutions were prepared on the day of use by dilution of the stock solution to 1× with water.

Cell cultures. We used six cancer cell lines in this study: (a) the anaplastic thyroid carcinoma cell lines ARO (25), FB1 (26), KAT4 (27), and FRO (28); (b) the 8505C cell line (29), established from an anaplastic thyroid carcinoma containing areas of papillary thyroid carcinoma; (c) the NPA cell line (28) established from a poorly differentiated thyroid carcinoma. The ARO (11), KAT4 (12), and FB1 (12) cells harbor a heterozygous BRAF V600E mutation, whereas 8505C (12), NPA, and FRO (13) express only the mutated BRAF allele. Cells were grown in DMEM supplemented with 10% fetal bovine serum (Life Technologies, Paisley, PA), 2 mmol/L L-glutamine, and 100 units/mL penicillin-streptomycin (Life Technologies). The P5 primary culture of normal human thyroid follicular cells was kindly donated by Francesco Curcio (Dipartimento Di Patologia e Medicina Sperimentale e Clinica, Udine, Italy) and was grown as described elsewhere (30). For cell proliferation assays, 5×10^4 cells were plated in 35 mm dishes in 2.5% serum. The day after plating, BAY 43-9006 or vehicle was added. Cells

were counted in triplicate every day. For flow cytometry analysis, 5×10^5 cells were plated in 100 mm dishes in 2.5% serum, and the next day they were treated with different concentrations of BAY 43-9006 or vehicle. After harvesting, cells were fixed in cold 70% ethyl alcohol in PBS. Propidium iodide (25 µg/mL) was added in the dark and samples were analyzed with a FACScan flow cytometer (Becton Dickinson, San Jose, CA) interfaced with a Hewlett-Packard computer (Palo Alto, CA).

RNA silencing. The small inhibitor duplex RNAs targeting human BRAF we used in this study (31) were chemically synthesized by PROLIGO (Boulder, CO). Sense strands for small inhibitory duplex RNA (siRNA) targeting were as follows: BRAF, 5'-AGAAUUGGAUCUG-GAUCAUUTT-3'; lamin A/C, 5'-CUGGACUCCAGAAGAACATT-3'. As a control, we used a nonspecific siRNA duplex containing the same nucleotides but in irregular sequence (scrambled). For siRNA transfection, cells were grown under standard conditions. The day before transfection, 1×10^5 cells were plated in 35 mm dishes in DMEM supplemented with 10% fetal bovine serum and without antibiotics. Transfection was done using 360 pmol siRNA and 18 µL Oligofect-AMINE reagent (Invitrogen, Groningen, the Netherlands) following the instructions of the manufacturer. Cells were kept in 2.5 serum and counted 48 and 72 hours after transfection.

Protein studies. Immunoblotting experiments were done according to standard procedures. Briefly, cells were harvested in lysis buffer [50 mmol/L HEPES (pH 7.5), 150 mmol/L NaCl, 10% glycerol, 1% Triton X-100, 1 mmol/L EGTA, 1.5 mmol/L MgCl₂, 10 mmol/L NaF, 10 mmol/L sodium PPI, 1 mmol/L Na₃VO₄, 10 µg aprotinin/mL, and 10 µg leupeptin/mL] and clarified by centrifugation at $10,000 \times g$. For protein extraction, samples of mouse xenografts were snap frozen and immediately homogenized in lysis buffer by using the Mixer Mill MM300 (Qiagen, Crawley, West Sussex, United Kingdom). Protein concentration was estimated with a modified Bradford assay (Bio-Rad, Munich, Germany). Antigens were revealed by an enhanced chemiluminescence detection kit (ECL, Amersham Pharmacia Biotech, Little Chalfont, United Kingdom). Signal intensity was evaluated with the Phosphorimager (Typhoon 8600, Amersham Pharmacia Biotech) interfaced with the ImageQuant software. Anti-phospho-p44/42 MAP kinase (MAPK), specific for MAPK (ERK1/2) phosphorylated at Thr²⁰²/Tyr²⁰⁴, anti-p44/42 MAPK, anti-phospho-p90RSK (90 kDa ribosomal S6 kinase), specific for p90RSK phosphorylated at Thr³⁵⁹/Ser³⁶³, anti-p90RSK, anti-phospho-MEK1/2 (MAPK1 and MAPK2), specific for MEK1 and MEK2 phosphorylated at Ser²¹⁷/Ser²²¹, and anti-MEK1/2 were purchased from Cell Signaling (Beverly, MA). Anti-BRAF antibody was purchased from Santa Cruz Biotechnology (Santa Cruz, CA). Monoclonal anti-α-tubulin was from Sigma Chemical. Secondary antibodies coupled to horseradish peroxidase were from Santa Cruz Biotechnology. For the BRAF kinase assay, cells were cultured for 12 hours in serum-deprived medium. Thereafter, cells were treated with BAY 43-9006 for 1 hour; BRAF kinase was immunoprecipitated with the anti-BRAF antibody and resuspended in a kinase buffer containing 25 mmol/L sodium PPI, 10 µCi [³²P]ATP, and 1 µg recombinant glutathione S-transferase-MEK (Upstate Biotechnology, Inc., Lake Placid, NY). After 30-minute incubation at 4 °C, reactions were stopped by adding 2× Laemmli buffer. Proteins were then subjected to 12% SDS gel electrophoresis. The radioactive signal was analyzed using a Phosphorimager (Molecular Dynamics, Piscataway, NJ).

Tumorigenicity in nude mice. Animals were housed in barrier facilities at the Dipartimento di Biologia e Patologia Cellulare e Molecolare (University of Naples "Federico II," Naples, Italy). They were exposed to a 12-hour light-dark cycle and received food and water *ad libitum*. All manipulations were conducted in accordance with Italian regulations for experimentation on animals. No mouse showed signs of wasting or other signs of toxicity. ARO cells (1×10^6 /mouse) were inoculated s.c. into the right flank of 4-week-old male BALB/c nu/nu mice (The Jackson Laboratory, Bar Harbor, ME). Tumors (~100 mm³) were treated with BAY 43-9006 (30 or 60 mg/kg) or vehicle alone by oral gavage for 5 consecutive days per week for 3 weeks. Tumor diameters were measured with calipers. Tumor volumes (V) were

calculated by the formula: $V = A \times B^2 / 2$ (A = axial diameter; B = rotational diameter). Another group of animals (surrogate) was treated with vehicle or 60 mg/kg of BAY 43-9006 (five animals per group) for 5 days starting when the tumors reached $\sim 300 \text{ mm}^3$. Tumors were excised 3 hours after the last dose and divided in two parts. Half of the tissue was snap-frozen in liquid nitrogen and used for protein extraction. The other half of the tissue was fixed overnight in neutral buffered formalin and processed by routine methods. Paraffin-embedded blocks were sliced into 5 μm sections and stained by H&E for histologic examination or processed for immunohistochemistry. Briefly, sections were deparaffinized, alcohol-rehydrated, subjected to heat-induced antigen retrieval, and incubated overnight with anti-Ki67/MIB-1 (1:50, 3,3'-diaminobenzidine, DAKO, Carpinteria, CA) or anti-CD31 antibodies [platelet/endothelial cell adhesion molecule 1 (M-20) goat polyclonal; Santa Cruz Biotechnology; ref. 32]. Finally, the slides were incubated with biotinylated anti-IgG and with premixed avidin-biotin complex (Vectostain ABC kits, Vector Laboratories, Burlingame, CA). The immune reaction was revealed with 0.06 mmol/L diaminobenzidine (DAKO) and 2 mmol/L hydrogen peroxide. As a negative control, tissue slides were incubated with preimmune serum. Apoptotic cell death rate was assessed in tissue slides by *in situ* labeling of DNA strand breaks as previously described (33). Briefly, dewaxed tissue sections were digested with Proteinase K (Boehringer Mannheim, Mannheim, Germany) and processed with the *in situ* cell death detection kit (Roche Diagnostics, Mannheim, Germany) used according to the instructions of the manufacturer.

Statistical analysis. Two-tailed unpaired Student's *t* test (normal distributions and equal variances) were used for statistical analysis. Differences were significant when $P < 0.05$. Statistical analysis was done using the Graph Pad InStat software program (version 3.06.3, San Diego, CA).

Results

Selective knockdown of BRAF by siRNA blocks the MAPK cascade and growth of anaplastic thyroid carcinoma cell lines. We used RNA interference (RNAi) to specifically knock down BRAF expression in two anaplastic thyroid carcinoma cell lines: FRO that express only the mutated V^{600E} BRAF allele and ARO carrying the same mutation at the heterozygous level. We used siRNAs against BRAF and, as control, a scrambled siRNA sequence or siRNA against the housekeeping lamin A/C mRNA. Transfection with BRAF siRNA, but not with the control siRNAs, diminished BRAF, but not c-RAF, protein levels in FRO and ARO cells (Fig. 1A and C). BRAF protein knockdown was significant 48 hours after transfection (Fig. 1A and C), but only very modest after 24 hours (not shown). As a positive control of transfection, lamin A/C siRNA caused a strong inhibition of lamin protein levels (Fig. 1A and C). MEK1/2 kinases, once phosphorylated by RAF kinases at serine 217 and 221, phosphorylate threonine 202 and tyrosine 204 in the activation segment of p44 and p42 MAPK (ERK1 and 2; ref. 34). Thus, we analyzed MEK1/2 and MAPK phosphorylation upon BRAF knockdown in anaplastic thyroid carcinoma cells. Consistent with a key role of BRAF in MAPK cascade, BRAF silencing in FRO and ARO cells resulted in a reduction of p44/42 MAPK (~ 5 -fold) and MEK1/2 (~ 3 -fold) phosphorylation levels 48 hours after transfection (Fig. 1A and C).

We asked whether BRAF expression was required for the growth of BRAF mutation-positive anaplastic thyroid carcinoma cells. Cell counts were obtained in triplicate after FRO and ARO cell transfection with BRAF or scrambled siRNA. The transient silencing of BRAF significantly inhibited the growth of FRO and ARO cells (in 2.5% serum), whereas the negative

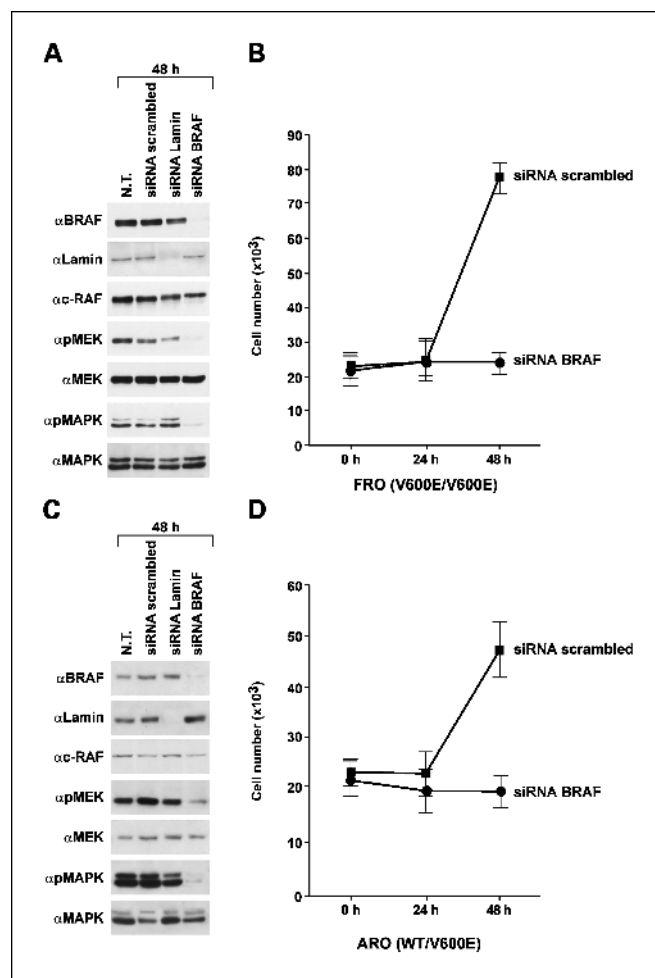


Fig. 1. Knockdown of BRAF by siRNA blocks signaling and growth of FRO and ARO cells. Cells were grown under standard conditions. The day before transfection, 1×10^5 cells were plated in 35 mm dishes in DMEM supplemented with 10% serum and without antibiotics. Transfection (day 0) was done in triplicate using 360 pmol of the indicated siRNA. Mock-transfected cells (N/T) served as a control. Cells were kept in 2.5% serum; protein lysates were harvested after 48 hours and analyzed by immunoblot with the indicated antibodies: FRO cells are shown in (A) and ARO are shown in (C). Transfected cells were counted 24 and 48 hours after transfection. Points, mean of triplicate determinations; bars, 95% confidence intervals (B and D). Statistical significance was determined by the two-tailed unpaired Student's *t* test.

control siRNA had virtually no effect (Fig. 1B and D). After 48 hours, FRO cells treated with scrambled RNAi numbered 77.3×10^3 and those treated with BRAF RNAi numbered 23.3×10^3 ($P < 0.0001$). After 48 hours, ARO cells treated with scrambled RNAi numbered 48×10^3 and those treated with BRAF RNAi numbered 18×10^3 ($P < 0.0001$). Thus, continued BRAF expression is essential for MAPK stimulation and growth of FRO and ARO cells.

Inhibition of oncogenic BRAF signaling in thyroid carcinoma cell lines by BAY 43-9006. Of the small-molecule RAF kinase inhibitors in clinical development, BAY 43-9006 is the furthest along (35). BAY 43-9006 is a multikinase inhibitor able to target not only RAF kinases but also receptor tyrosine kinases, including vascular endothelial growth factor receptor-2 (KDR) and platelet-derived growth factor receptor B. Thus, its anticancer activity is currently thought to be the result of the dual inhibition of RAF signaling and KDR-mediated and

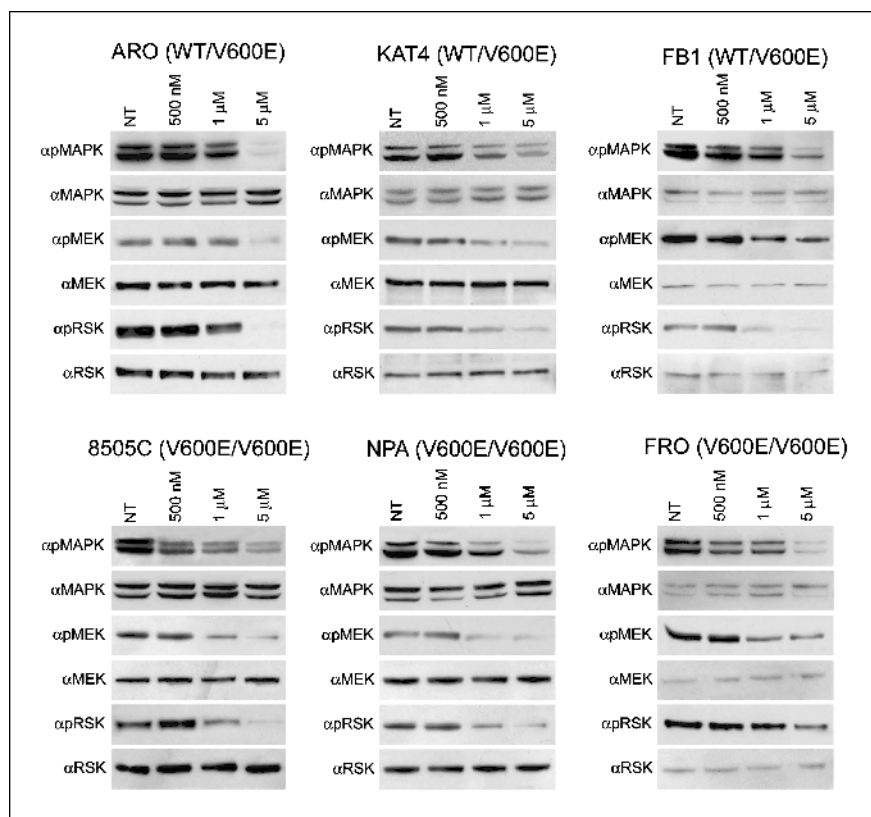


Fig. 2. *In vivo* inhibition of MAPK cascade in thyroid carcinoma cells by BAY 43-9006. The indicated thyroid carcinoma cell lines carrying homozygous or heterozygous mutations of BRAF were kept in 2.5% serum and treated with increasing concentrations of BAY 43-9006. Six hours later, cells were lysed and 50 μg of total cell lysates were analyzed by Western blotting with the indicated phosphospecific antibodies. Total amounts of MEK, MAPK, and RSK are shown for normalization. The results were quantified by the Phosphorimager. Representative of at least three different experiments.

platelet-derived growth factor receptor B-mediated tumor angiogenesis (23, 35).

Because BRAF expression was found to be essential for thyroid carcinoma cell growth, chemical BRAF blockade by BAY 43-9006 could exert cytostatic effects; thus, BAY 43-9006 could be exploited as a therapeutic tool for BRAF mutation-positive thyroid carcinoma models. To investigate this possibility, we studied the effects of BAY 43-9006 on the anaplastic thyroid carcinoma cell lines ARO, KAT4, and FB1, which carry the ^{V600E}BRAF mutation at the heterozygous level, and 8505C, FRO, and NPA, which carry only the mutated allele. After 12 hours of cultivation in low serum (2.5%), cells were treated for 6 hours with different concentrations of BAY 43-9006 or vehicle (NT) and the activity of MEK1/2, p44/p42 MAPK, and p90RSK (a p44/p42 MAPK substrate) was monitored by immunoblot with phosphospecific antibodies. Antibodies that recognize the same proteins also when nonphosphorylated were used for normalization. Immunoblots were examined with the Phosphorimager. Representative experiments are reported in Fig. 2. Consistent with the expression of an oncogenic BRAF, the MAPK cascade was constitutively active (even in low serum) in all the thyroid carcinomas tested. Treatment with BAY 43-9006 reduced the phosphorylation of MEK1/2, p44/p42 MAPK, and p90RSK with a IC₅₀ of 1 μmol/L for ARO, KAT4, and NPA cells and of 500 nmol/L for FB1, 8505C, and FRO cells. After treatment with 5 μmol/L BAY 43-9006, only residual phosphorylation levels of MEK1/2, p44/p42 MAPK, and p90RSK were detected in the carcinoma cell lines (Fig. 2).

To verify whether MAPK kinase knockdown was mediated by an inhibition of BRAF activity, we used an immunocom-

plex *in vitro* BRAF phosphorylation assay. Based on the presence of the V600E mutation, BRAF activity was high in NPA, KAT4, ARO, FRO (Fig. 3A), and FB1 and 8505C (not shown) cells, but not in normal P5 thyrocytes. We treated ARO and FRO cells with different concentrations of the compound or vehicle (NT) and examined them with the *in vitro* BRAF kinase assay. Figure 3B shows that BAY 43-9006 readily inhibited intrinsic BRAF enzymatic activity at the concentration of 1 μmol/L.

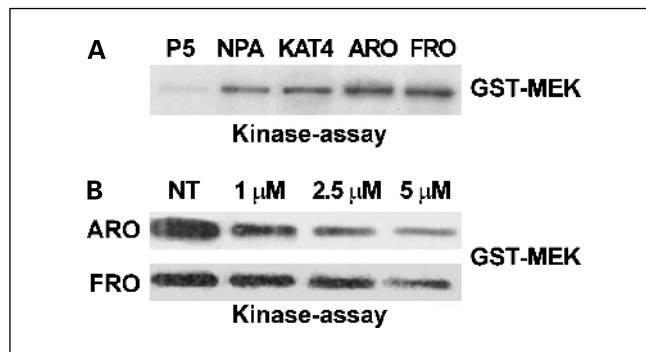


Fig. 3. ^{V600E}BRAF kinase blockade by BAY 43-9006. *A*, the indicated cell lines were cultured for 12 hours in serum-deprived medium and harvested; a BRAF kinase assay was done (see below). *B*, cells were treated for 1 hour with different doses of BAY 43-9006 and then harvested. Cell lysates (500 μg) were immunoprecipitated with an anti-BRAF-specific antibody and subjected to a kinase assay with recombinant glutathione *S*-transferase – MEK (*GST-MEK*; 1 μg) as substrate. After 30 minutes of incubation at 4°C, reactions were stopped and proteins were subjected to 12% SDS gel electrophoresis. The radioactive signal was evaluated with the Phosphorimager. Representative of at least three different experiments.

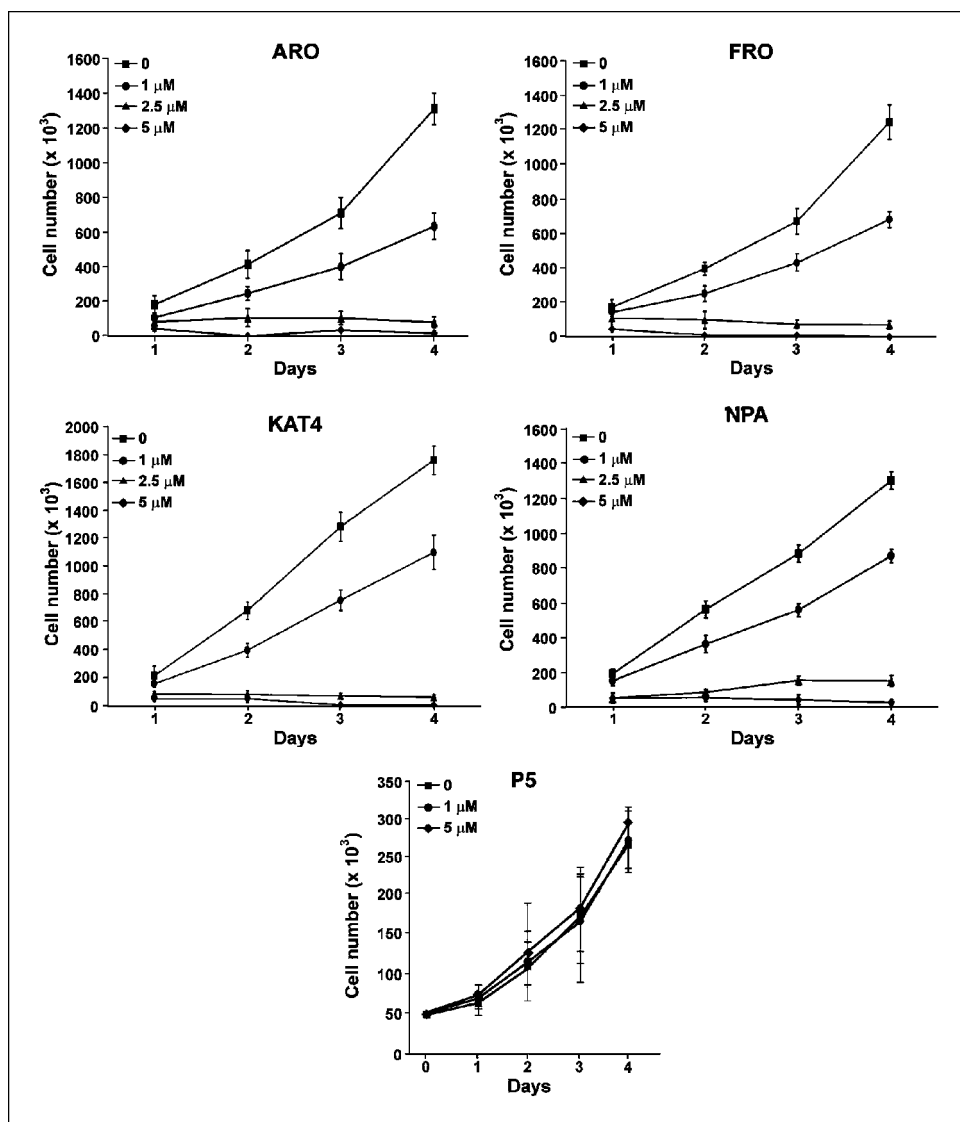


Fig. 4. BAY 43-9006 causes growth inhibition of ^{V600E}BRAF-positive thyroid carcinoma cells. The indicated cells (5×10^4) were plated in triplicate in 35 mm dishes. One day later, different concentrations of BAY 43-9006 or vehicle (0) were added (in 2.5% serum). Cells were counted at different time points. Day 0 was the treatment starting day. Points, mean value for the three dishes; bars, 95% confidence intervals. Statistical significance was determined by the two-tailed unpaired Student's *t* test.

Finally, ARO, KAT4, FRO, and NPA cells were treated (in 2.5% serum) with different concentrations of BAY 43-9006 or vehicle and counted at different time points. The average results of three independent determinations are reported in Fig. 4. BAY 43-9006 treatment readily reduced the proliferation rate of thyroid carcinoma but not of normal thyroid P5 cells. The IC_{50} for the four carcinoma cell lines was $\sim 1 \mu\text{mol/L}$; at $5 \mu\text{mol/L}$, BAY 43-9006 virtually arrested thyroid carcinoma cell growth ($P < 0.0001$; Fig. 4). Examination of the ARO cell cycle profile after BAY 43-9006 treatment (in 2.5% serum) by flow cytometry showed a marked G_1 arrest upon treatment with $2.5 \mu\text{mol/L}$ BAY 43-9006. There were a few cells in the sub- G_1 fraction, which indicates that BAY 43-9006 treatment results mainly in a cytostatic effect in these cells (not shown).

Inhibition of ARO-induced tumor formation in nude mice by BAY 43-9006. ARO cells were selected based on their high tumorigenic potential. Nude mice were injected with 1×10^6 ARO cells and after ~ 10 days, when tumors had reached $\sim 100 \text{ mm}^3$, animals (seven for each group) were randomized and treated orally 5 d/wk with BAY 43-9006 (30 or 60 mg/kg) or

with vehicle. Tumor growth was monitored with calipers. The experiment was done twice and a representative experiment is shown in Fig. 5A. After 22 days of treatment, mice treated with BAY 43-9006 at either 30 or 60 mg/kg had significantly smaller tumors than control mice ($P < 0.0001$). No significant improvement of the therapeutic effect was noted at 60 mg/kg with respect to 30 mg/kg, indicating that maximal therapeutic efficacy was already achieved at 30 mg/kg.

For mechanism of action studies, a group of mice ($n = 5$) bearing tumors of $\sim 300 \text{ mm}^3$ were treated daily with 60 mg/kg of BAY 43-9006 or with vehicle for 5 days. Three hours after the final dose, tumors were excised. Half the tissue was used for protein extraction and immunoblot analysis, and the other half was used for histologic examination. There were large areas of necrosis in tumors from treated animals at the H&E staining (Fig. 5B). Moreover, Ki67/MIB-1 immunolocalization was reduced and terminal deoxynucleotidyl transferase-mediated nick end labeling reactivity increased in treated tumors (Fig. 5B). These *in vivo* cell death effects were in contrast with the lack of apoptotic effects of the drug (see above) as well as of

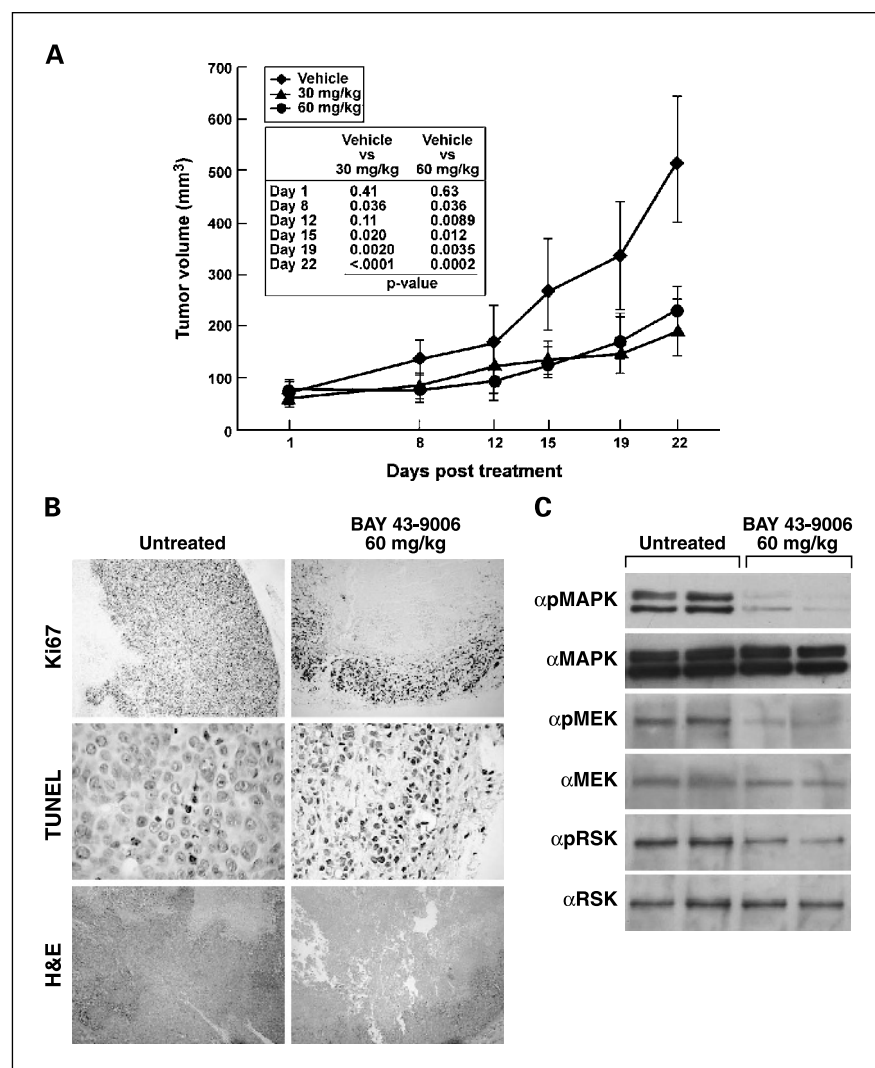


Fig. 5. Antitumor effects of BAY 43-9006 in ARO cell xenografts. **A**, ARO cells (1×10^6 per mouse) were inoculated s.c. into the right dorsal portion of BALB/c nude mice. When tumors ($\sim 100 \text{ mm}^3$) appeared, animals were randomly assigned to three groups (seven mice per group) to receive BAY 43-9006 (30 or 60 mg/kg) or vehicle by oral gavage. Treatment was administered for 5 consecutive days per week for 3 weeks (day 1 is the treatment-starting day). Tumor diameters were measured with calipers and tumor volumes were calculated. This experiment was done twice. Results are from one representative experiment. Points, tumor volume; bars, 95% confidence intervals. *P* values for the comparisons (at the different time points) between compound and vehicle are reported. Statistical significance was determined by the two-tailed unpaired Student's *t* test. **B**, animals ($n = 5$) bearing ARO tumors ($\sim 300 \text{ mm}^3$) were treated with vehicle or 60 mg/kg of BAY 43-9006 for 5 days. Tumors were excised and examined by conventional H&E and immunostaining with anti-Ki67/MIB-1. Apoptotic cell death rate was assessed by *in situ* labeling of DNA strand breaks. Representative micrographs are shown. **C**, proteins (100 μg) extracted from a representative tumor (day 5) from untreated or treated animals were immunoblotted with the indicated antibodies.

BRAF RNAi (data not shown) in cultured cells. However, by directly targeting vascular endothelial growth factor receptors in tumor endothelium (23) and by targeting RAF-regulated vascular endothelial growth factor receptor secretion (36), BAY 43-9006 might prevent the development of tumor neovascularization and therefore cause tumor cell death. Accordingly, blood vessel counting by immunoperoxidase staining with anti-CD31 revealed that BAY 43-9006 treatment reduced the number of vessels (from 20 ± 4 to 10 ± 3 per microscopic field), demonstrating that BAY 43-9006 exerted antiangiogenic effects in ARO cell xenografts. To ensure that BRAF kinase inhibition *in vivo* participated to the therapeutic effect as well, proteins were extracted from ARO tumors treated with BAY 43-9006. As shown in Fig. 5C, tumor growth inhibition was associated with a remarkable reduction of p44/42 MAPK, MEK1/2, and, at a lower extent, RSK *in vivo* phosphorylation levels.

Discussion

There is an urgent need for therapies that can slow down the progression of anaplastic thyroid carcinoma. On the other hand, although papillary thyroid carcinomas in general have an

excellent prognosis, there is no effective treatment for tumors that have lost radioiodine uptake. Based on the experimental and clinicopathologic evidences indicating that BRAF is involved in papillary thyroid carcinoma initiation and progression to anaplastic thyroid carcinoma, BRAF has emerged as a promising therapeutic target for thyroid carcinomas (15). By siRNA-mediated BRAF knockdown, here we could show that V^{600E} BRAF-expressing thyroid carcinoma cells depend on continuous BRAF activity for intracellular signaling and cell proliferation; these findings suggest that indeed BRAF can be exploited to develop novel therapies for thyroid carcinomas carrying BRAF mutations.

At a preclinical level, recent insights have shown that chemically modified siRNAs can silence endogenous genes after *i.v.* injection in mice and, therefore, be exploited for treatment of disease (37). Moreover, injection of lentiviral vectors that produce RNAi-mediated silencing of specific genes proved efficacious in animal models of disease (38). Nevertheless, in clinical setting, molecular targeting of specific protein kinases, like ABL and KIT, with small-molecule inhibitors has already proved efficacious (39). Various BRAF inhibitors have been reported and, among them, the orally available by-aryl

urea BAY 43-9006 has reached the clinical testing stage (35). BAY 43-9006 inhibits RAF kinases and the tyrosine kinases vascular endothelial growth factor receptor receptors 2/3, Flt-3, platelet-derived growth factor receptor B, FGFR1, and KIT (23). It inhibits the V600E BRAF mutant albeit with a slightly lesser potency than the wild-type kinase (23). BAY 43-9006 is undergoing advanced clinical trials (35). It is being tested in a phase II study of patients with locally advanced, metastatic, or recurrent thyroid cancer (www.cancer.gov/clinicaltrials). Thus far, phase III is achieving promising results on renal cell carcinoma, where probably BAY 43-9006 is effective for its activity on angiogenic kinases (35). Here, we show that BAY 43-9006 targets signal transduction along the MAPK cascade and tumor cell proliferation in ^{V600E}BRAF-positive thyroid carcinoma cell lines. Although *in vitro*, the compound mainly exerted cytostatic effects, it also caused tumor cell death in nude mice xenografts very likely for the concomitant angiogenesis inhibition. Tumor cells are often selected to bypass the effects of antineoplastic agents and the simultaneous assault on both neoplastic and endothelial cells may circumvent the development of resistance. This might be an advantage of drugs like BAY

43-9006 that are able to pinpoint more than one target simultaneously (40). However, BAY 43-9006 treatment did not cause a complete regression of ARO cell tumors. Similar observations have been reported upon mutant BRAF targeting in melanomas (41).

In conclusion, these findings provide the proof-of-concept that BRAF is a therapeutic target in thyroid cancer analogous to ABL and KIT in other tumors. Thus, BAY 43-9006, and perhaps other small molecules with a similar specificity profile, holds promise for molecular therapy of thyroid cancer. In a clinical setting, it will be mandatory to know the BRAF mutational status of treated patients and to show that the compound has sufficient activity to inhibit the BRAF kinase at the concentration achieved in patient tissues. Based on the preclinical data, one possibility could be to combine the drug with other synergistic therapeutics that may facilitate tumor regression.

Acknowledgments

We thank Salvatore Sequino and Antonio Baiano for animal care, Francesco Curcio for P5 cells, and Jean A. Gilder for text editing.

References

- DeLellis RA, Williams ED. Thyroid and parathyroid tumors. In: DeLellis RA, Lloyd RV, Heitz PU, Eng C, editors. Tumours of endocrine organs. World Health Organization classification of tumors. International Agency for Research on Cancer (Lyons, France): IARC Press; 2004. p. 51–6.
- Sherman SI. Thyroid carcinoma. *Lancet* 2003;361:501–11.
- Ordóñez N, Baloch Z, Matias-Guix X, et al. Undifferentiated (anaplastic) carcinoma. In: DeLellis RA, Lloyd RV, Heitz PU, Eng C, editors. Tumours of endocrine organs. World Health Organization classification of tumors. International Agency for Research on Cancer (Lyons, France): IARC Press; 2004. p. 77–80.
- Ain KB. Anaplastic thyroid carcinoma: a therapeutic challenge. *Semin Surg Oncol* 1999;16:64–9.
- Pasieka JL. Anaplastic thyroid cancer. *Curr Opin Oncol* 2003;15:78–83.
- Tuveson DA, Weber BL, Herlyn M. BRAF as a potential therapeutic target in melanoma and other malignancies. *Cancer Cell* 2003;4:95–8.
- Kimura ET, Nikiforova MN, Zhu Z, Knauf JA, Nikiforov YE, Fagin JA. High prevalence of BRAF mutations in thyroid cancer: genetic evidence for constitutive activation of the RET/PTC-RAS-BRAF signaling pathway in papillary thyroid carcinoma. *Cancer Res* 2003;63:1454–7.
- Cohen Y, Xing M, Mambo E, et al. BRAF mutation in papillary thyroid carcinoma. *J Natl Cancer Inst* 2003;95:625–7.
- Soares P, Trovisco V, Rocha AS, et al. BRAF mutations and RET/PTC rearrangements are alternative events in the etiopathogenesis of PTC. *Oncogene* 2003;22:4578–80.
- Xu X, Quiros RM, Gattuso P, Ain KB, Prinz RA. High prevalence of BRAF gene mutation in papillary thyroid carcinomas and thyroid tumor cell lines. *Cancer Res* 2003;63:4561–7.
- Xing M, Vasko V, Tallini G, et al. BRAF T1796A transversion mutation in various thyroid neoplasms. *J Clin Endocrinol Metab* 2004;88:1365–8.
- Nikiforova MN, Kimura ET, Gandhi M, et al. BRAF mutations in thyroid tumors are restricted to papillary carcinomas and anaplastic or poorly differentiated carcinomas arising from papillary carcinomas. *J Clin Endocrinol Metab* 2003;88:5399–404.
- Namba H, Nakashima M, Hayashi T, et al. Clinical implication of hot spot BRAF mutation, V599E, in papillary thyroid cancers. *J Clin Endocrinol Metab* 2003;88:4393–7.
- Xing M, Westra WH, Tufano RP, et al. BRAF mutation predicts a poorer clinical prognosis for papillary thyroid cancer. *J Clin Endocrinol Metab* 2005;90:6373–9. Epub 2005 September 20.
- Xing M. BRAF mutation in thyroid cancer. *Endocr Relat Cancer* 2005;12:245–62.
- Wan PT, Garnett MJ, Roe SM, et al. Mechanism of activation of the RAF-ERK signaling pathway by oncogenic mutations of B-RAF. *Cell* 2004;116:855–67.
- Ciampi R, Knauf JA, Kerler R, et al. Oncogenic AKAP9-BRAF fusion is a novel mechanism of MAPK pathway activation in thyroid cancer. *J Clin Invest* 2005;115:94–101.
- Melillo RM, Castellone MD, Guarino V, et al. The RET/PTC-RAS-BRAF linear signaling cascade mediates the motile and mitogenic phenotype of thyroid cancer cells. *J Clin Invest* 2005;115:1068–81.
- Mitsutake N, Knauf JA, Mitsutake S, Mesa C, Jr., Zhang L, Fagin JA. Conditional BRAFV600E expression induces DNA synthesis, apoptosis, dedifferentiation, and chromosomal instability in thyroid PCCL3 cells. *Cancer Res* 2005;65:2465–73.
- Knauf JA, Ma X, Smith EP, et al. Targeted expression of BRAFV600E in thyroid cells of transgenic mice results in papillary thyroid cancers that undergo dedifferentiation. *Cancer Res* 2005;65:4238–45.
- Lyons JF, Wilhelm S, Hibner B, Bollag G. Discovery of a novel Raf kinase inhibitor. *Endocr Relat Cancer* 2001;8:219–25.
- Lee JT, McCubrey JA. BAY-43-9006 Bayer/Onyx. *Curr Opin Investig Drugs* 2003;4:757–63.
- Wilhelm SM, Carter C, Tang L, et al. BAY 43-9006 exhibits broad spectrum oral antitumor activity and targets the RAF/MEK/ERK pathway and receptor tyrosine kinases involved in tumor progression and angiogenesis. *Cancer Res* 2004;64:7099–109.
- Strumberg D, Richly H, Hilger RA, et al. Phase I clinical and pharmacokinetic study of the novel Raf kinase and vascular endothelial growth factor receptor inhibitor BAY 43-9006 in patients with advanced refractory solid tumors. *J Clin Oncol* 2005;23:965–72.
- Pang XP, Hershman JM, Chung M, et al. Characterization of tumor necrosis factor- α receptors in human and rat thyroid cells and regulation of the receptors by thyrotropin. *Endocrinology* 1989;125:1783–8.
- Fiore L, Pollina LE, Fontanini G, et al. Cytokine production by a new undifferentiated human thyroid carcinoma cell line, FB-1. *J Clin Endocrinol Metab* 1997;82:4094–100.
- Ain KB, Tofiq S, Taylor KD. Antineoplastic activity of Taxol against human anaplastic thyroid carcinoma cell lines *in vitro* and *in vivo*. *J Clin Endocrinol Metab* 1996;81:3650–3.
- Fagin JA, Matsuo K, Karmakar A, Chen DL, Tang SH, Koeffler HP. High prevalence of mutations of the p53 gene in poorly differentiated human thyroid carcinomas. *J Clin Invest* 1993;91:179–84.
- Ito T, Seyama T, Mizuno T, et al. Unique association of p53 mutations with undifferentiated but not with differentiated carcinomas of the thyroid gland. *Cancer Res* 1992;52:1369–71.
- Curcio F, Ambesi-Impimbatto FS, Perrella G, Coon HG. Long-term culture and functional characterization of follicular cells from adult normal human thyroids. *Proc Natl Acad Sci U S A* 1994;91:9004–8.
- Hingorani SR, Jacobetz MA, Robertson GP, Herlyn M, Tuveson DA. Suppression of BRAF (V599E) in human melanoma abrogates transformation. *Cancer Res* 2003;63:5198–202.
- Cattoretti G, Becker MH, Key G, et al. Monoclonal antibodies against recombinant parts of the Ki-67 antigen (MIB 1 and MIB 3) detect proliferating cells in microwave-processed formalin-fixed paraffin sections. *J Pathol* 1992;168:357–63.
- Gavrieli Y, Sherman Y, Ben-Sasson SA. Identification of programmed cell death *in situ* via specific labeling of nuclear DNA fragmentation. *J Cell Biol* 1992;119:493–501.
- Sebolt-Leopold JS, Herrera R. Targeting the mitogen-activated protein kinase cascade to treat cancer. *Nat Rev Cancer* 2004;4:937–47.
- Beeram M, Patnaik A, Rowinsky EK. Raf: a strategic target for therapeutic development against cancer. *J Clin Oncol* 2005;23:6771–90.
- Sharma A, Trivedi NR, Zimmerman MA, Tuveson DA, Smith CD, Robertson GP. Mutant V599E B-Raf regulates growth and vascular development of malignant melanoma tumors. *Cancer Res* 2005;65:2412–21.
- Soutschek J, Akinc A, Bramlage B, et al. Therapeutic silencing of an endogenous gene by systemic administration of modified siRNAs. *Nature* 2004;432:173–8.
- Raoul C, Abbas-Terki T, Bensadoun JC, et al. Lentiviral-mediated silencing of SOD1 through RNA interference retards disease onset and progression in a mouse model of ALS. *Nat Med* 2005;11:423–8.
- Sawyers C. Targeted cancer therapy. *Nature* 2004;432:294–7.
- Frantz S. Drug discovery: playing dirty. *Nature* 2005;437:942–3.
- Karasarides M, Chilocheches A, Hayward R, et al. B-RAF is a therapeutic target in melanoma. *Oncogene* 2004;23:6292–8.

Attached manuscript #2

Salvatore G, Nappi TC, **Salerno P**, Jiang Y, Garbi C, Ugolini C, Miccoli P, Basolo F, Castellone MD, Cirafici AM, Melillo RM, Fusco A, Bittner ML, Santoro M. A cell proliferation and chromosomal instability signature in anaplastic thyroid carcinoma. *Cancer Res* 2007;67:10148-58.

A Cell Proliferation and Chromosomal Instability Signature in Anaplastic Thyroid Carcinoma

Giuliana Salvatore,¹ Tito Claudio Nappi,² Paolo Salerno,² Yuan Jiang,³ Corrado Garbi,² Clara Ugolini,⁴ Paolo Miccoli,⁴ Fulvio Basolo,⁴ Maria Domenica Castellone,² Anna Maria Cirafici,² Rosa Marina Melillo,² Alfredo Fusco,² Michael L. Bittner,⁵ and Massimo Santoro²

¹Dipartimento di Studi delle Istituzioni e dei Sistemi Territoriali, Università "Parthenope," and ²Dipartimento di Biologia e Patologia Cellulare e Molecolare "L. Califano" c/o Istituto di Endocrinologia ed Oncologia Sperimentale del Consiglio Nazionale delle Ricerche, Università "Federico II", Naples, Italy; ³National Human Genome Research Institute, Cancer Genetics Branch, Bethesda, Maryland; ⁴Dipartimento di Chirurgia, Università di Pisa, Pisa, Italy; and ⁵TGen, Phoenix, Arizona

Abstract

Here, we show that the anaplastic thyroid carcinoma (ATC) features the up-regulation of a set of genes involved in the control of cell cycle progression and chromosome segregation. This phenotype differentiates ATC from normal tissue and from well-differentiated papillary thyroid carcinoma. Transcriptional promoters of the ATC up-regulated genes are characterized by a modular organization featuring binding sites for E2F and NF- κ B transcription factors and cell cycle-dependent element (CDE)/cell cycle gene homology region (CHR) cis-regulatory elements. Two protein kinases involved in cell cycle regulation, namely, Polo-like kinase 1 (PLK1) and T cell tyrosine kinase (TTK), are part of the gene set that is up-regulated in ATC. Adoptive overexpression of p53, p21 (CIP1/WAF1), and E2F4 down-regulated transcription from the PLK1 and TTK promoters in ATC cells, suggesting that these genes might be under the negative control of tumor suppressors of the p53 and pRB families. ATC, but not normal thyroid, cells depended on PLK1 for survival. RNAi-mediated PLK1 knockdown caused cell cycle arrest associated with 4N DNA content and massive mitotic cell death. Thus, thyroid cell anaplastic transformation is accompanied by the overexpression of a cell proliferation/genetic instability-related gene cluster that includes PLK1 kinase, which is a potential molecular target for ATC treatment. [Cancer Res 2007;67(21):10148–58]

Introduction

Anaplastic thyroid carcinoma (ATC) is a highly malignant tumor that accounts for 2% to 5% of all thyroid cancers and is usually seen in the sixth to seventh decades of life. ATC ranks among the most lethal solid tumors, with a median survival of 4 to 12 months after diagnosis (1–3). ATC shares genetic alterations with well-differentiated papillary (PTC) and follicular thyroid carcinomas, namely, point mutations in *RAS* and *BRAF* (1–4) and point mutations or gene amplification of *PIK3CA* (5, 6), suggesting that it may derive from a preexisting differentiated lesion. Whereas well-differentiated thyroid carcinomas are rarely (<10%) p53-mutated, more than 70% of ATC are associated with p53 mutations (2, 4). Besides direct gene mutation, several other mechanisms can

obstruct p53 function in thyroid cancer, including the up-regulation of negative p53 regulators like HMGAI (high-mobility group A1) and Δ Np73, or proteins fostering p53 protein degradation, like HDM2 (7, 8).

ATC has a high proliferation rate and marked aneuploidy (9). Gene expression profiles correlating with mitotic rate and chromosomal instability in cancer cells have been recently defined. A gene expression signature represented by 168 cell cycle-regulated genes has been identified in *in vitro* transformed normal human fibroblasts and termed "the proliferation cluster" (10). Increased expression of many of these genes, in particular of a core set of 44 of them ("44-gene proliferation cluster"), is a surrogate measure of tumor cell proliferation and is often associated with poor outcome (11). Moreover, the up-regulation of a set of 70 genes, known as the chromosomal instability 70 ("CIN70") cluster, partially overlapping with the proliferation signature, predicted aneuploidy in several cancers (12).

Genes coding for two protein kinases, Polo-like kinase 1 (PLK1) and T cell tyrosine kinase (TTK), are included in these signatures (10–12). TTK (also called PYT or hMps1, human monopolar spindle 1 kinase) is a dual-specificity kinase involved in mitotic checkpoint control; it has been implicated in the apoptosis of p53-negative cells after DNA damage (13). PLK1 belongs to the *Polo* family of serine/threonine kinases. It is important for many cell cycle-related events, i.e., CDC2 activation, chromosome segregation, centrosome maturation, bipolar spindle formation, activation of the anaphase-promoting complex (APC), and cytokinesis and is overexpressed in many tumors (14). Adoptive overexpression of PLK1 induces NIH 3T3 cell transformation, whereas PLK1 inhibition leads to mitotic arrest and cell death (14).

Here, we show that ATC is characterized by a gene expression profile that overlaps the proliferation and CIN70 signatures, and that PLK1, which is part of these signatures, is essential for survival of ATC cells.

Materials and Methods

Tissue samples. Frozen thyroid tissue samples from 10 patients affected by PTC, 5 patients with ATC, and 4 normal thyroids (N) were used for the microarray screening (Supplementary Table S1). Independent tissue samples (19 normal thyroids, 39 PTC, and 22 ATC) were used for validation assays. All samples were retrieved from the files of the Pathology Department of the University of Pisa (Italy). The study was approved by the Institutional Ethics Committee. The samples were classified according to the diagnostic criteria required for the identification of PTC and ATC (15). The number of neoplastic cells in five areas of 0.2 mm² was calculated with a Nikon laser microdissector.

cDNA microarray screening and data analysis. The 12,000 sequence-verified human cDNA set was from the National Genome Institute

Note: Supplementary data for this article are available at Cancer Research Online (<http://cancerres.aacrjournals.org/>).

Requests for reprints: Massimo Santoro, Dipartimento di Biologia e Patologia Cellulare e Molecolare, via. S. Pansini 5, 80131 Naples, Italy. Phone: 39-81-7463056; Fax: 39-81-7463037; E-mail: masantor@unina.it.

©2007 American Association for Cancer Research.
doi:10.1158/0008-5472.CAN-07-1887

(NIH, Bethesda, MD). The cDNA clones were printed as described elsewhere (16, 17). Sample preparation and microarray hybridizations procedures are reported in detail elsewhere (17). Briefly, total RNA was labeled by direct incorporation of Cy5-dUTP or Cy3-dUTP (Amersham Pharmacia Biotech) in a reverse transcription reaction using anchored oligodeoxythymidylate primer (Genosys) and Superscript II reverse transcriptase (Life Technologies Inc.). Cy3-dUTP-tagged cDNAs were mixed with Cy5-dUTP-tagged common reference and subsequently cohybridized to the microarrays. The reference was composed of a pool of RNA from thyroid cell lines and was used throughout all hybridizations to ensure normalized measures for each gene in each individual sample. Hybridized slides were scanned using an Agilent microarray scanner (Agilent Technologies), and images were processed using a collection of IPLab (Scanalytics, Inc.) extensions developed at the Cancer Genetics Branch, National Human Genome Research Institute. The fluorescence intensities of scanned images were quantified, normalized, and corrected to yield the transcript abundance of a gene as an intensity ratio with respect to that of the signal of the references. Genes were ranked according to the weighted gene analysis. Genes with high weight (w) values create greater separation between groups and denser compaction within the groups, i.e., they have a high power to discriminate between normal thyroid, PTC, and ATC. To test the statistical significance of the discriminative weights, sample labels were randomly permuted as previously described (17). This was repeated 1,000 times to generate a w distribution that would be expected under the assumption of random gene expression, i.e., no difference between the groups. Genes that were deemed to significantly ($P < 0.001$) discriminate between the three categories were listed. The entire data set has been deposited in the National Center for Biotechnology Information's Gene Expression Omnibus (GEO)⁶ and is accessible through GEO series accession number GSE9115.

RNA extraction and quantitative reverse transcription-PCR. Total RNA was isolated with the RNeasy Kit (Qiagen). About 1 μ g of RNA from each sample was reverse-transcribed with the QuantiTect Reverse Transcription (Qiagen). To design a quantitative (Q) reverse transcription-PCR (RT-PCR) assay, we used the Human ProbeLibrary system (Exiqon). Primers pairs and PCR conditions are available upon request. PCR reactions were done in triplicate, and fold changes were calculated with the formula: $2^{-(\text{sample 1 } \Delta\text{Ct} - \text{sample 2 } \Delta\text{Ct})}$, where ΔCt is the difference between the amplification fluorescent thresholds of the mRNA of interest and the mRNA of RNA polymerase 2 used as an internal reference.

Cell cultures. The P5-3N primary culture of normal human thyroid follicular cells was grown as previously described (18). Normal human thyroid cells (S11N and S63N) were grown in RPMI (Invitrogen) containing 20% fetal bovine serum. The human ATC cell lines FB1 (19), BHT101 (20), CAL62 (20), KAT-4 (21), ARO (22), FRO (22), HTH7 (23), HTH83 (23), SW1736 (23, 24), C643 (23), and the poorly differentiated thyroid carcinoma NPA (22) were grown in DMEM (Invitrogen) containing 10% fetal bovine serum. The Fischer rat-derived differentiated thyroid follicular cell line PC Cl 3 (hereafter "PC") was grown in Coon's modified Ham F12 medium supplemented with 5% calf serum and a mixture of six hormones (6H).

Protein studies. Immunoblotting was carried out according to standard procedures. Anti-PLK1 monoclonal antibody was from Zymed Laboratories; anti-TTK polyclonal antibody was from Santa Cruz Biotechnology; monoclonal anti- α -tubulin was from Sigma-Aldrich; anti-cleaved (Asp¹⁷⁵) caspase-3 p17 and p12 fragments polyclonal (5A1) was from Cell Signaling Technology, Inc.; anti-poly(ADP-ribose) polymerase (anti-PARP) monoclonal antibody, which detects full-length PARP and the large fragment (89 kDa) produced by caspase cleavage, was from BD Biosciences. Secondary anti-mouse and anti-rabbit antibodies coupled to horseradish peroxidase were from Santa Cruz Biotechnology.

Reporter gene assay. PCR fragments of the human TTK and PLK1 promoters spanning, respectively, from -524 to +72 and from -148 to +63 relative to the transcription start were cloned into the pGL3 Basic vector (Promega Corporation), carrying the *Firefly* luciferase reporter gene.

Primer sequences are available upon request. Cells were transfected using the LipofectAMINE reagent according to manufacturer's instructions, with 500 ng of the reporter plasmid DNA, together with (when required) p53 wild-type, p21(CIP/WAF1) (25), or E2F4 (kindly donated by M. Crescenzi, Istituto Superiore di Sanita', Rome) expression vectors. A plasmid expressing the enzyme *Renilla* luciferase (pRL-null) was used as an internal control. In all cases, the total amount of transfected plasmid DNA was normalized by adding empty vector DNA. Forty-eight hours after transfection, *Firefly* and *Renilla* luciferase activities were assayed using the Dual-Luciferase Reporter System (Promega Corporation), and the Lumat LB9507 luminometer (EG Berthold). Each experiment was done in triplicate.

RNA silencing. Small inhibitor duplex RNAs targeting PLK1 and the scrambled control [nonspecific small interfering RNA (siRNA) duplex containing the same nucleotides but in irregular sequence] are described elsewhere (26). Cells were grown under standard conditions. The day before transfection, 5×10^4 cells were plated in 35-mm dishes in DMEM supplemented with 10% fetal bovine serum and without antibiotics. Transfection was done using OligofectAMINE reagent (Invitrogen) with 100 nmol/L (250 nmol/L for PC cells) siRNA. Cells were harvested and counted 24 and 48 h after transfection.

Immunofluorescence. Fixed and permeabilized cells were incubated with anti- α -tubulin antibody (Sigma) for 45 min at 37°C. Washed coverslips were incubated with rhodamine-conjugated secondary antibody (Jackson ImmunoResearch) for 30 min at 37°C. After 15 min propidium iodide (1 μ g/mL) counterstaining and coverslips mounting, stained cells were observed with a Zeiss LSM 510 META confocal microscope. The "In situ Cell Death Detection Kit, TMR red" (Roche) was used to detect terminal nucleotidyl transferase-mediated nick end labeling (TUNEL)-positive cells. At least 300 cells were counted in triplicate experiments.

Fluorescence-activated cell sorter scan analysis. Cells were harvested and fixed in 70% ethanol for 4 h. After washing with PBS, cells were treated with RNase A (100 units/mL) and stained with propidium iodide (25 μ g/mL; Sigma) for 30 min. Samples were analyzed with a CyAn ADP flow cytometer interfaced with the Summit V4.2 software (DakoCytomation). Data were analyzed with the Modfit software (Verity Software House).

Statistical analysis. The two-tailed unpaired Student's t test (normal distributions and equal variances) was used for statistical analysis. All P values were two sided, and differences were significant when $P < 0.05$. All statistical analyses were carried out using the GraphPad InStat software program (version 3.06.3).

Results

Proliferation- and chromosomal instability-associated genes are up-regulated in ATC. We used cDNA microarrays to characterize the gene expression profile of ATC compared with PTC and normal thyroid tissue samples (Supplementary Table S1). Genes were ranked according to weight values (16, 17), with the highest value indicating the most discriminative power ($P < 0.001$) between the different tissue groups. A set of 914 genes distinguished ATC from normal tissue: 371 of them were up-regulated, and 543 were down-regulated in ATC (Supplementary Table S2). Most of these genes were typical of ATC, and only 114 of them discriminated normal thyroid from both PTC and ATC (Supplementary Tables S2 and S3).

ATC featured the up-regulation of a set of 54 genes involved in the control of cell cycle progression and chromosome segregation; 7 and 13 of them were part of the 44-gene proliferation cluster (10, 11) and the CIN70 cluster (12), respectively, and 9 of both clusters (Table 1). These genes were not significantly up-regulated in PTC (Supplementary Table S3). Additional genes of the two clusters tended toward up-regulation in ATC, but the data were not statistically significant (Supplementary Table S4). Thus, ATC overexpressed genes that coded for cyclins (*CCNB2*,

⁶ <http://www.ncbi.nlm.nih.gov/geo>

Table 1. Proliferation- and chromosomal instability-related genes up-regulated in ATC

Gene	Gene description (gene ontology biological process)	Unigene number	Weight N versus ATC
ZWINT	ZW10 interactor (cell cycle)	Hs.42650	31.36
KNSL6	KIF2C kinesin family member 2C (mitosis)	Hs.69360	29.69
CENPA [¶]	Centromere protein A (17 kDa; mitosis)	Hs.1594	27.61
NEK2 [¶]	NIMA (never in mitosis gene a)-related kinase 2 (cell cycle)	Hs.153704	21.77
CEP55	Centrosomal protein (55 kDa; cell cycle)	Hs.14559	19.15
CDC20 [¶]	Cell division cycle 20 homologue (cell cycle)	Hs.82906	17.71
CENPF	Centromere protein F (350/400 kDa, mitosis; mitosis)	Hs.77204	15.24
PARP1	Poly(ADP-ribose) polymerase family 1 (adenosine diphosphate ribosyltransferase; base excision repair)	Hs.177766	14.60
SSRP1	Structure-specific recognition protein 1 (DNA replication)	Hs.523680	14.39
CCNB2 [¶]	Cyclin B2 (cell cycle)	Hs.194698	14.01
PBK	PDZ binding kinase (mitosis)	Hs.104741	13.98
TTK [¶]	TTK protein kinase (mitotic spindle checkpoint)	Hs.169840	13.52
EXOSC9	Exosome component 9 (rRNA processing)	Hs.91728	13.18
CDCA8 [¶]	Cell division cycle-associated 8 (cell cycle)	Hs.48855	12.93
CCNA2	Cyclin A2 (cell cycle)	Hs.58974	12.14
TOP2A [¶]	Topoisomerase (DNA) II α (DNA topological change)	Hs.156346	11.87
PLK1 [¶]	Polo-like kinase 1 (mitosis)	Hs.329989	11.23
GMPS	Guanine monophosphate synthetase (purine synthesis)	Hs.518345	11.17
PPM1G	Protein phosphatase 1G (cell cycle)	Hs.17883	10.81
CENPE	Centromere protein E (mitotic metaphase)	Hs.75573	10.79
PRC1 [¶]	Protein regulator of cytokinesis 1 (mitotic spindle elongation)	Hs.366401	10.71
NOL5A	Nucleolar protein 5 (rRNA processing)	Hs.376064	10.22
TPX2	Microtubule-associated, homologue (mitosis)	Hs.244580	9.92
NUSAP1	Nucleolar and spindle-associated protein 1 (mitosis)	Hs.615092	9.82
ZWILCH	Kinetochores-associated, homologue (kinetochores component)	Hs.21331	9.47
NCAPH	Non-SMC condensin I complex, subunit H (mitosis)	Hs.308045	9.39
HMMR	Hyaluronan-mediated motility receptor (cell motility)	Hs.72550	9.31
PAICS	Phosphoribosylaminoimidazole carboxylase (purine synthesis)	Hs.331420	9.30
RCC1	RCC1 regulator of chromosome condensation 1 (cell cycle)	Hs.469723	8.93
CTPS	CTP synthase (nucleotide metabolism)	Hs.473087	8.58
TYMS	Thymidylate synthetase (nucleotide metabolism)	Hs.592338	7.96
CKS1	CDC28 protein kinase regulatory subunit 1B (cell cycle)	Hs.374378	7.93
FOXM1	Forkhead box M1 (regulation of transcription)	Hs.239	7.91
HNRPF	Heterogeneous nuclear ribonucleoprotein F (RNA processing)	Hs.808	7.53
HPRT1	Hypoxanthine phosphoribosyltransferase 1 (purine synthesis)	Hs.412707	7.08
SMC4	Structural maintenance of chromosomes 4 (cell cycle)	Hs.58992	6.83
CCNE2	Cyclin E2 (cell cycle)	Hs.567387	6.79
GMNN	Geminin, DNA replication inhibitor (cell cycle)	Hs.234896	6.66
UBE2S	Ubiquitin-conjugating enzyme E2S (ubiquitin cycle)	Hs.396393	6.56
CDC2	Cell division cycle 2 (mitosis)	Hs.334562	6.55
GINS2	GINS complex subunit 2 (DNA replication)	Hs.433180	6.30
PLK4	Polo-like kinase 4 (cell cycle)	Hs.172052	6.28
DNMT1	DNA (cytosine-5-)-methyltransferase 1 (DNA methylation)	Hs.202672	5.54

(Continued on the following page)

Table 1. Proliferation- and chromosomal instability-related genes up-regulated in ATC (Cont'd)

Gene	Included in			p53 inhibited	DNA elements (binding sites)			
	Proliferation cluster*	44-gene proliferation cluster [†]	CIN70 [‡]		E2F	NF-Y	CDE	CHR
ZWINT	Yes		Yes	Yes ^{§,}	Yes*	Yes*	Yes*	
KNSL6	Yes			Yes [§]				
CENPA [¶]	Yes			Yes ^{§,}		Yes*	Yes*	Yes*
NEK2 [¶]	Yes		Yes	Yes ^{,*}				
CEP55			Yes					
CDC20 [¶]	Yes	Yes	Yes	Yes ^{§, ,*}	Yes*	Yes*		
CENPF	Yes	Yes		Yes ^{§,}	Yes*	Yes*, ^{† †}	Yes*	Yes*, ^{† †}
PARP1	Yes							
SSRP1	Yes							
CCNB2 [¶]	Yes		Yes	Yes ^{§,*}	Yes*	Yes*, ^{† †}		Yes*, ^{† †}
PBK	Yes		Yes	Yes				
TTK [¶]	Yes		Yes	Yes [§]	Yes ^{† †}	Yes*, ^{† †}		Yes*, ^{† †}
EXOSC9	Yes	Yes						
CDCA8 [¶]			Yes		Yes*	Yes*, ^{† †}	Yes	Yes*, ^{† †}
CCNA2	Yes	Yes		Yes ^{§,}	Yes*		Yes*	
TOP2A [¶]	Yes	Yes	Yes	Yes ^{§, ,*}		Yes*, ^{† †}		Yes*, ^{† †}
PLK1 [¶]	Yes	Yes		Yes ^{§,*}	Yes ^{† †}	Yes*, ^{† †}	Yes*	Yes*, ^{† †}
GMPS	Yes			Yes [§]		Yes*	Yes*	
PPM1G	Yes							
CENPE		Yes						
PRC1 [¶]	Yes		Yes	Yes	Yes*	Yes*, ^{† †}	Yes*	Yes*, ^{† †}
NOL5A	Yes					Yes*	Yes*	
TPX2			Yes	Yes ^{§,}	Yes*	Yes*		
NUSAP1	Yes			Yes	Yes*	Yes*, ^{† †}	Yes*	Yes*, ^{† †}
ZWILCH			Yes					
NCAPH			Yes					
HMMR	Yes			Yes ^{§, ,*}		Yes*, ^{† †}		Yes*, ^{† †}
PAICS	Yes			Yes				
RCC1	Yes							
CTPS		Yes	Yes					
TYMS		Yes			Yes*		Yes*	
CKS1	Yes				Yes*	Yes*	Yes*	Yes*
FOXM1			Yes	Yes ^{§,}		Yes*, ^{† †}		Yes*, ^{† †}
HNRPF	Yes			Yes ^{**}	Yes*	Yes*	Yes*	
HPRT1	Yes							
SMC4	Yes			Yes				
CCNE2	Yes			Yes				
GMNN	Yes				Yes*		Yes*	
UBE2S	Yes			Yes ^{§,*}				
CDC2	Yes		Yes	Yes	Yes*, ^{† †}	Yes*, ^{† †}	Yes*	Yes*, ^{† †}
GINS2	Yes			Yes [§]				
PLK4	Yes							
DNMT1		Yes						

(Continued on the following page)

Table 1. Proliferation- and chromosomal instability-related genes up-regulated in ATC (Cont'd)

Gene	Gene description (gene ontology biological process)	Unigene number	Weight N versus ATC
FEN1	Flap structure-specific endonuclease 1 (DNA replication)	Hs.409065	5.38
C20orf24	Chromosome 20 open reading frame 24 (RAB5-interacting protein)	Hs.584985	5.34
MCM5	Minichromosome maintenance-deficient 5 (DNA replication)	Hs.517582	5.32
UBE2C	Ubiquitin-conjugating enzyme E2C (mitosis)	Hs.93002	5.09
MCM7	Minichromosome maintenance-deficient 7 (DNA replication)	Hs.438720	5.00
ATAD2	ATPase family, AAA domain containing 2 (ATP binding)	Hs.370834	4.69
POLE	Polymerase (DNA directed), epsilon (DNA replication)	Hs.524871	4.30
CKS2	CDC28 protein kinase 2 (cell cycle)	Hs.83758	4.25
MCM6	Minichromosome maintenance-deficient 6 (DNA replication)	Hs.444118	4.25
CDC25C	Cell division cycle 25C (cell cycle)	Hs.656	4.05
RFC1	Replication factor C (activator 1) 1 (DNA replication)	Hs.507475	4.05

*Ref. 10.

†Ref. 11.

‡Ref. 12.

§Ref. 13.

||Ref. 33.

¶Genes whose up-regulation was studied also by Q-RT-PCR.

**Ref. 32.

††Ref. 28.

‡‡Ref. 38.

CCNA2, and *CCNE2*), cyclin-dependent kinases (*CDC2*), and proteins involved in nucleotide synthesis (*GMPS*, *PAICS*, *CTPS*, *TYMS*, and *HPRT1*), spindle formation, and checkpoint control (*PLK1*, *TTK*, *NEK2*, *CDCA8*, *CENPA*, *CENPF*, *CENPE*, and *KNSL6*; Table 1). According to recent reports, ATC overexpressed *UBE2C* (*UBCH10*), which encodes an E2 ubiquitin-conjugating enzyme that is required for cell cycle progression (27), and genes of the minichromosome maintenance-deficient (*MCM*) family, involved in licensing DNA for replication (25). Genes encoding other components of the DNA replication initiation complex, such as *CDC6*, *ORC1*, and *PCNA*, also tended toward up-regulation in ATC (Supplementary Table S4). ATC frequently features genetic alterations in the phosphoinositide-3-kinase (PI3K)/AKT pathway (5, 6); accordingly, the screening revealed the altered expression of some genes of this pathway in ATC samples (Supplementary Table S5).

Some cis-regulatory DNA elements, e.g., binding sites for E2F and NF-Y (CCAAT box binding) transcription factors and cell cycle-dependent element (CDE)/cell cycle gene homology region (CHR) DNA orphan binding sites, were highly represented in the promoters of the 54 genes up-regulated in ATC (refs. 10, 28–30; Table 1). The E2F family of transcription factors includes positive (E2F1–3) and negative (E2F4–6) regulators of cell cycle progression (28, 29). Activator E2Fs (in particular E2F1) are linked to the activation of genes involved in G₁-S progression, whereas repressor E2Fs (in particular E2F4) bind gene promoters featuring the NF-Y-CDE/CHR DNA module that often peak at the G₂ or G₂-M phase (10, 28–30). Many G₂-M phase genes (like *PLK1*, *TTK*, *PRC1*, *CENPE*, *CENPF*, *FOXMI*, *CCNB2*, *CDC2*, *CDCA8*, *CCNA2*, *TOP2A*, *UBE2C*, and

CDC25C) were up-regulated in ATC. Based on such a promoter architecture, it can be argued that some of the gene expression changes associated to ATC may be influenced by the loss of *p53* or *pRB* family gene function, which is able to influence the function of E2F and NF-Y proteins (10, 30–33). Accordingly, as many as 31 of the 54 genes up-regulated in ATC samples were previously reported to be under *p53* negative control (Table 1; refs. 13, 32, 33). Although the *p53* gene status of the examined ATC samples is unknown, the microarray screening (Supplementary Table S2) showed that four out of five ATC samples overexpressed *HMGAI* (weight = 4.3), a negative regulator of the *p53* function (7).

We selected an independent set of ATC samples for validation experiments. A total of 2 out of 10 of these samples harbored R248E and R280T *p53* mutations, respectively (data not shown). Moreover, five of them up-regulated *HMGAI* mRNA at a RT-PCR analysis (Supplementary Fig. S1). These samples were examined by triplicate quantitative RT-PCR for the expression of 10 of the genes reported in Table 1. The results of these experiments were in agreement with the microarray screening data. Although the expression level of single genes varied among individual ATC samples, these genes were up-regulated in practically all ATC samples examined versus normal thyroids and PTC (Fig. 1A). The difference between ATC and normal tissue was $P < 0.001$ with the Tukey-Kramer multiple comparisons procedure and $P < 0.0001$ with the one-way ANOVA test. We also measured the expression levels of the 10 genes in a panel of ATC cell lines expressing a mutated *p53* allele (34) in comparison to normal thyroid cells. All of them invariably up-regulated in cancer cells (Table 2).

Table 1. Proliferation- and chromosomal instability-related genes up-regulated in ATC (Cont'd)

Gene	Included in			p53 inhibited	DNA elements (binding sites)			
	Proliferation cluster*	44-gene proliferation cluster [†]	CIN70 [‡]		E2F	NF-Y	CDE	CHR
FEN1	Yes	Yes	Yes	Yes [§]				
C20orf24			Yes		Yes*	Yes*	Yes*	
MCM5	Yes	Yes			Yes* ^{††}	Yes*		
UBE2C	Yes		Yes	Yes [§]		Yes* ^{††}		Yes* ^{††}
MCM7			Yes	Yes ^{§ **}	Yes*	Yes*		
ATAD2			Yes					
POLE	Yes			Yes	Yes*	Yes*	Yes*	
CKS2	Yes	Yes	Yes	Yes [§]		Yes* ^{††}	Yes*	Yes* ^{††}
MCM6	Yes	Yes		Yes ^{**}	Yes* ^{††}	Yes*	Yes*	
CDC25C	Yes	Yes			Yes*	Yes*		
RFC1		Yes			Yes*		Yes*	

PLK1 and TTK transcriptional promoters are negatively controlled by p53 in ATC cells. We focused on *PLK1* and *TTK*, which encode two protein kinases involved in cell cycle progression (13, 14). As shown in Table 2, the ATC cell lines analyzed overexpressed *PLK1* and *TTK* compared with the average expression level of normal thyrocytes ($P < 0.0001$). NPA cells, which are derived from a poorly differentiated thyroid carcinoma, also up-regulated *PLK1* and *TTK* mRNAs. The up-regulation of *PLK1* and *TTK* occurred also at protein level (Fig. 1B).

We cloned the *PLK1* gene transcriptional promoter (−148 to +63; ref. 35) and a putative *TTK* promoter (−524 to +72; ref. 28) in the pGL3 vector upstream from the *Firefly* luciferase reporter (Fig. 2A). We transiently transfected the pGL3-*PLK1*-LUC and pGL3-*TTK*-LUC constructs (or the empty vector) in triplicate in a continuous line of normal thyrocytes (PC) and in ATC cells and measured luciferase activity. Transcription from the *TTK* ($P < 0.0013$) and the *PLK1* ($P < 0.0019$) promoters was strongly up-regulated in ATC with respect to normal cells (Fig. 2B).

TTK and *PLK1* feature the typical combination of E2F, NF-Y, and CHR elements (Table 1) and were reported to be negatively controlled by p53 (13, 32). To explore the mechanism of *PLK1* and *TTK* up-regulation in ATC cells, we measured the effects of wild-type p53 and the cyclin-dependent kinase inhibitor p21 (CIP1/WAF1). As shown in Fig. 2C, adoptive overexpression of both p53 and p21 decreased *TTK* (~2- and 3-fold, respectively) and *PLK1* (~2-3- and 3-5-fold, respectively) promoter activity in FRO and CAL62 cells ($P < 0.0001$). Transient expression of the negative E2F, E2F4, also reduced the activity of both promoters in ATC cells ($P < 0.0001$; Fig. 2C).

PLK1 knockdown induces mitotic death of ATC cells. *PLK1* depletion or inactivation decreased the viability of several tumor cell types (14, 26, 36, 37). We used the RNA interference method to deplete endogenous *PLK1* from ATC cells; normal PC thyrocytes served as a control. Twenty-four hours after transfection with *PLK1*-specific siRNA, *PLK1* protein was silenced in CAL62 ($\geq 75\%$) and ARO (~60%) cells, whereas a scrambled control had no effect (Fig. 3A and B). Forty-eight hours post-transfection, CAL62 cells treated with scrambled RNAi numbered 381×10^3 , whereas those

treated with *PLK1* RNAi numbered 73×10^3 ($P < 0.0001$; Fig. 3A); ARO cells treated with scrambled RNAi numbered 285×10^3 , and those treated with *PLK1* RNAi numbered 106×10^3 ($P = 0.0014$; Fig. 3B). Virtually no effect was observed in normal cells, although RNAi depleted *PLK1* in PC cells, albeit with a lower efficiency than in cancer cells (Fig. 3C).

To better characterize the effects of *PLK1* knockdown, we transfected CAL62 cells with *PLK1* siRNA or the scrambled control and analyzed them by immunoblot at different time points. Thirty-six hours post-transfection, two biochemical markers of apoptosis, i.e., cleaved products of caspase-3 and of PARP, were visible in *PLK1*-silenced cells but not in cells transfected with the scrambled control (Fig. 4A). Accordingly, *PLK1* depletion, but not control RNAi, strongly increased the rate of inter-nucleosomal DNA fragmentation in a TUNEL assay (Fig. 4B). Forty-eight hours after transfection, the percentage of apoptotic cells with a subgenomic DNA (sub-G₁) content at the fluorescence-activated cell sorter (FACS) was higher in *PLK1*-depleted cells than in control cells (14% versus 4%; data not shown). In addition, the fraction of cells with a 4N DNA complement was higher in *PLK1*-depleted cells (59% versus 14%) versus control cells, which indicates incomplete cytokinesis (data not shown).

We stained *PLK1*-silenced and control-treated CAL62 cells with anti- α -tubulin antibody and examined the mitotic spindle by confocal microscopy. Consistent with the FACS results, the number of mitotic (prometaphase-like state) cells was increased in *PLK1*-depleted cells as early as 12 h post-transfection. Forty-eight hours after transfection, $53 \pm 5\%$ of *PLK1*-depleted cells versus $3 \pm 2\%$ of control-treated cells were in the M phase (Fig. 4C). As shown in Fig. 4D, *PLK1*-depleted cells had monopolar (20% versus 0% in control cells) and disorganized (48% versus 9.8% in control cells) spindles. Moreover, in *PLK1*-depleted cells, there was an increase of bi-nucleated cells (5.4% versus 1.4% in control cells) and cells with an aberrant nuclear morphology (dumbbell-like chromatin; 12% versus 4.3% in control cells; data not shown). A dumbbell-like structure suggests the inability to separate sister chromatids at the onset of anaphase. This feature is a hallmark of so-called mitotic cell death or mitotic catastrophe, a type of apoptosis cells that are committed to when they are unable to complete cytokinesis.

Discussion

This study shows that ATC is characterized by the over-expression of genes associated with cell proliferation and chromosomal instability. This feature, not being detected in well-differentiated PTC, is typical of ATC and is consistent with the highly mitogenic and aneuploid ATC phenotype (1, 2, 9). The promoters of most of the proliferation-related genes up-regulated in ATC contain a typical combination of NF- κ B and E2F binding sites and CDE/CHR cis-elements, a feature that suggests an indirect control exerted by p53 and pRB tumor suppressors. Consistently, we could show that TTK and PLK1 promoters are negatively controlled by p53-p21(CIP/WAF1) axis in ATC cells.

Activator E2Fs-regulated promoters are repressed by pRB family members; such a repression is alleviated on by pRB phosphorylation by cyclin-associated kinases (CDK; refs. 29, 38). By stimulating increased levels of the CDK inhibitor p21(CIP/WAF1), p53 reduces pRB phosphorylation levels and, in turn, E2F transcriptional activity (29). Moreover, CDK2 activity, and therefore, p53-mediated p21(CIP/WAF1) induction, also controls NF- κ B through direct phosphorylation (28). Finally, by directly associating with NF- κ B, p53 suppresses NF- κ B binding promoters, like the *CCNB2*, *CDC25C*, and *CDC2* gene promoters (31).

The CDE/CHR DNA elements are targets of repressor E2Fs (E2F4 and 5; ref. 30). E2F4 is under the negative control of the pRB-like

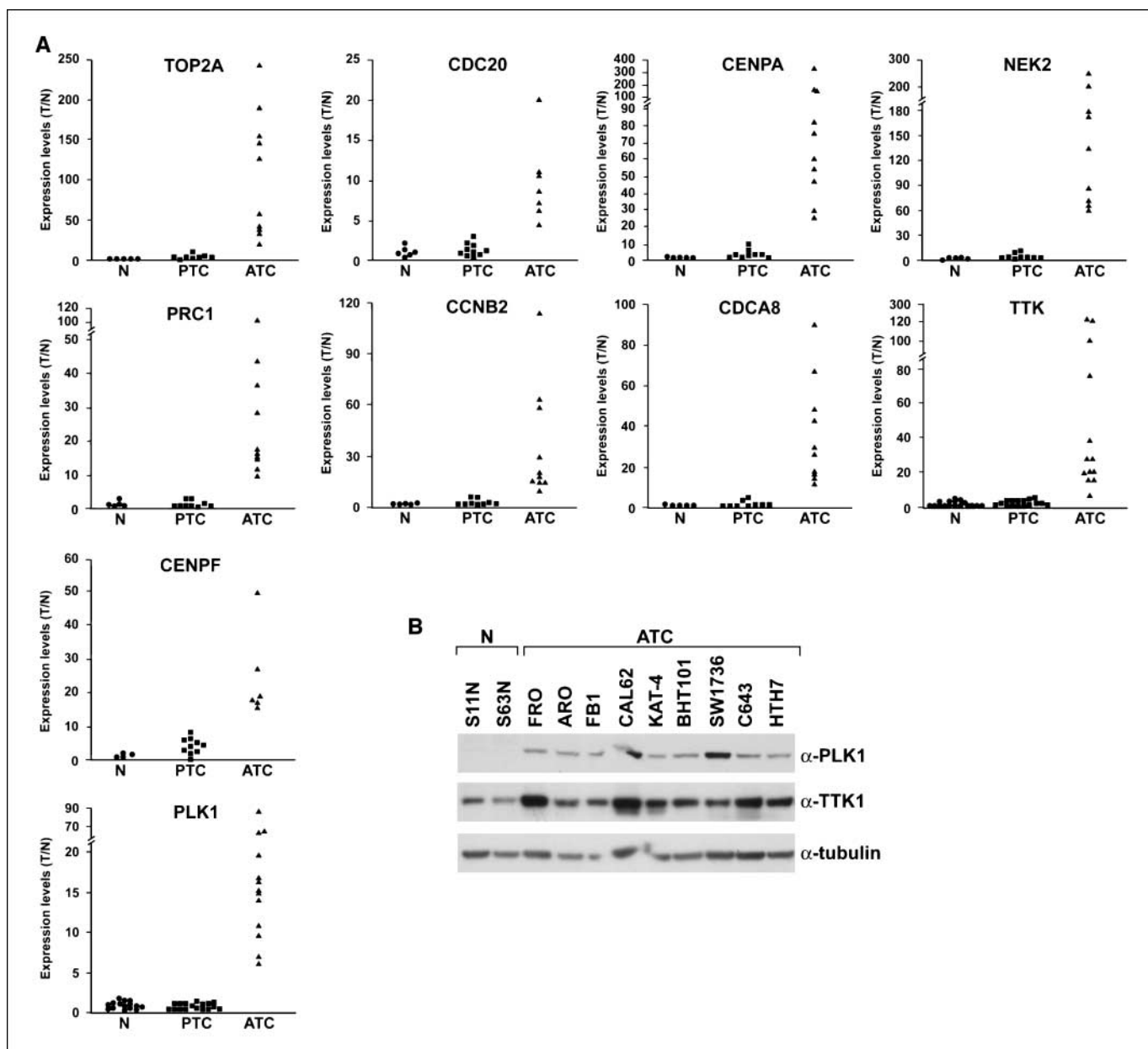


Figure 1. A, expression levels of ATC-specific genes in human thyroid samples. Quantitative RT-PCR analysis of 10 ATC-specific genes in normal thyroid (N), PTC, and ATC samples. TTK and PLK1 expression was measured in 20 N, 16 PTC, and 13 ATC samples. The other eight genes were measured in five N, nine PTC, and six ATC samples. For each gene, the expression level in a given tumor sample (T) was obtained by comparing its fluorescence threshold with the average fluorescence thresholds of normal samples (N). Values are the average results of three independent determinations. B, PLK1 and TTK protein levels in human thyroid cell lines. Fifty micrograms of protein lysate harvested from primary cultures of normal thyroid follicular (N) and ATC cells were examined by immunoblot using anti-PLK1 and anti-TTK antibodies. Equal protein loading was verified with an anti- α -tubulin antibody. Data are representative of three independent experiments.

Table 2. Expression levels of ATC-specific genes in human ATC cell lines

Expression level (fold change ATC cells versus normal thyrocytes)*

Cell line	P53 status	TOP2A	CENPA	PRC1	CCNB2	CDCA8	NEK2	TTK	PLK1	CDC20	CENPF
ARO	R273H ^{†, ‡}	1.6	2.4	6.1	3.9	4.3	6.8	8	6.5	2	4
SW1736	Null [§]	8.8	13.5	7.7	10.4	12.9	18	25	81	ND	ND
NPA	G266V ^{†, ‡}	4.8	14.4	8.1	9	6.3	11.7	16.5	46.6	8	8
BHT101	I251T [‡]	2.1	3.5	1.8	2.2	2.5	3.6	16.7	10.8	ND	ND
KAT-4	R273H ^{†, ‡}	6.7	5.9	5.5	9.7	9.2	14	13	27.1	10	8
C643	R248Q [‡]	2.7	3.9	2.5	4	6.5	5.9	25.5	8.3	ND	ND
CAL62	A161D [‡]	ND	ND	ND	ND	ND	ND	25.7	25.7	8	8
FRO	Null [†]	3.8	3.9	3.1	3.5	4.5	9.1	32.5	14.3	ND	ND

NOTE: Values are the average results of three independent determinations.

Abbreviation: ND, not done.

*Quantitative RT-PCR analysis done as indicated in the legend to Fig. 1A. For each gene, the expression level in a given ATC cell line was obtained by comparing its fluorescence threshold with the average fluorescence thresholds of two normal thyroid cell populations (P53N and S11N).

[†]Ref. 22.

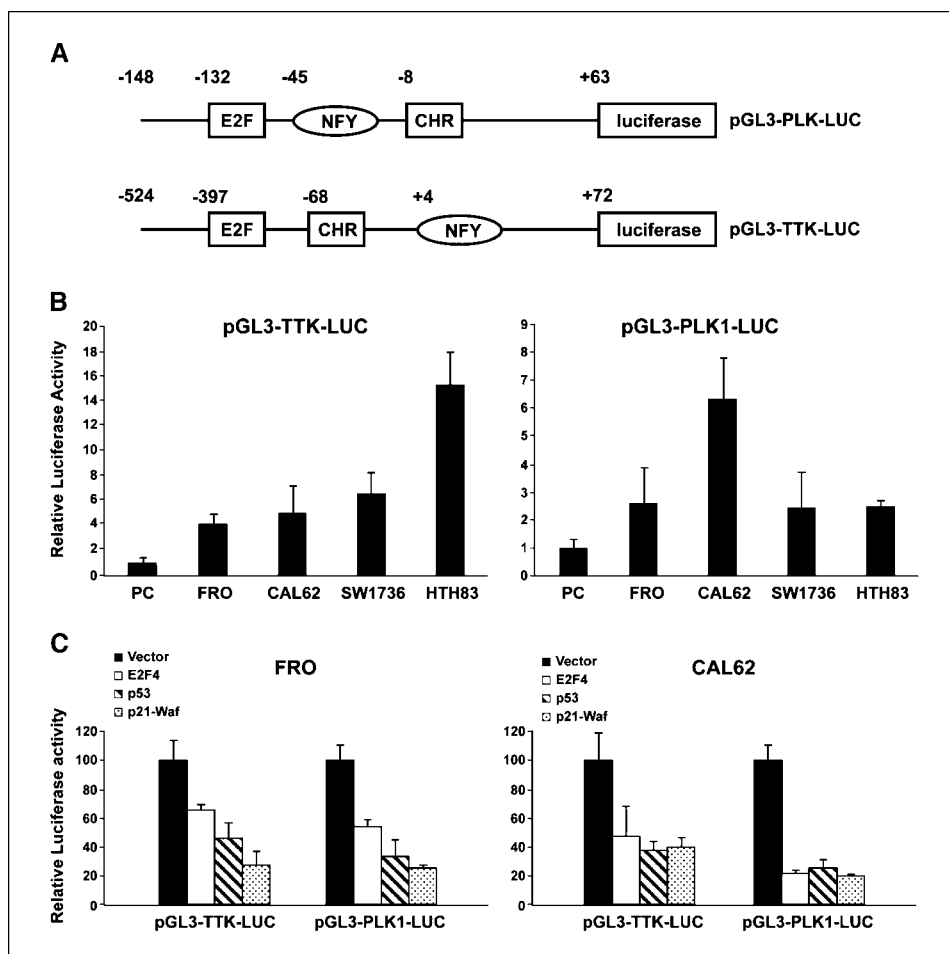
[‡]Ref. 34.

[§]Ref. 24.

p107 (RBL1) and p130 (RB2) proteins, and thus, also E2F4 and pRB-like proteins might be implicated in the regulation of proliferation-associated genes in ATC. We could indeed show that TTK and PLK1 promoters are negatively controlled by E2F4 in ATC cells.

Finally, gene promoters containing NF-Y/CDE-CHR modules often contain ELK1-binding sites (10, 28). ELK1 transcription factors are downstream targets of the mitogen-activated protein kinase pathway, and ATC often features mutation in genes (RAS or

Figure 2. PLK1 and TTK gene promoter activity in ATC cells. *A*, the two promoters are schematically represented. *B*, the indicated cell lines were transiently transfected with pGL3-TTK-LUC (*left*) or pGL3-PLK1-LUC (*right*) plasmids. The average levels of luciferase activity in three independent experiments are reported. Bars, 95% confidence intervals. *C*, FRO and CAL62 cells were co-transfected with p53, p21(CIP/WAF1), or E2F4 expression vectors (or the empty vector), together with pGL3-TTK-LUC (*left*) or pGL3-PLK1-LUC (*right*). Relative luciferase activity is reported. The average results of three independent assays are reported, and 95% confidence intervals are shown; promoter activity values in vector-transfected cells were arbitrarily set at 100.



BRAF) in this cascade (1–4). Therefore, it is likely that pathways other than the p53 and pRB ones concurrently regulate the expression of genes of the proliferation cluster.

ATC surgery is often only palliative, and there is no effective systemic treatment (2). PLK1 kinase inhibitors are currently being evaluated in clinical trials for various cancer types (14, 26, 36, 37).

Here, we show that PLK1 is required for ATC cell proliferation and survival. This requirement was restricted to ATC cells and was not detected in normal thyroid follicular cells. Although the exact mechanism of this selectivity is unknown, it has been shown that p53 depletion increases the sensitivity of various cell types to PLK1 knockdown (36, 37). Whatever the mechanism, our findings indicate

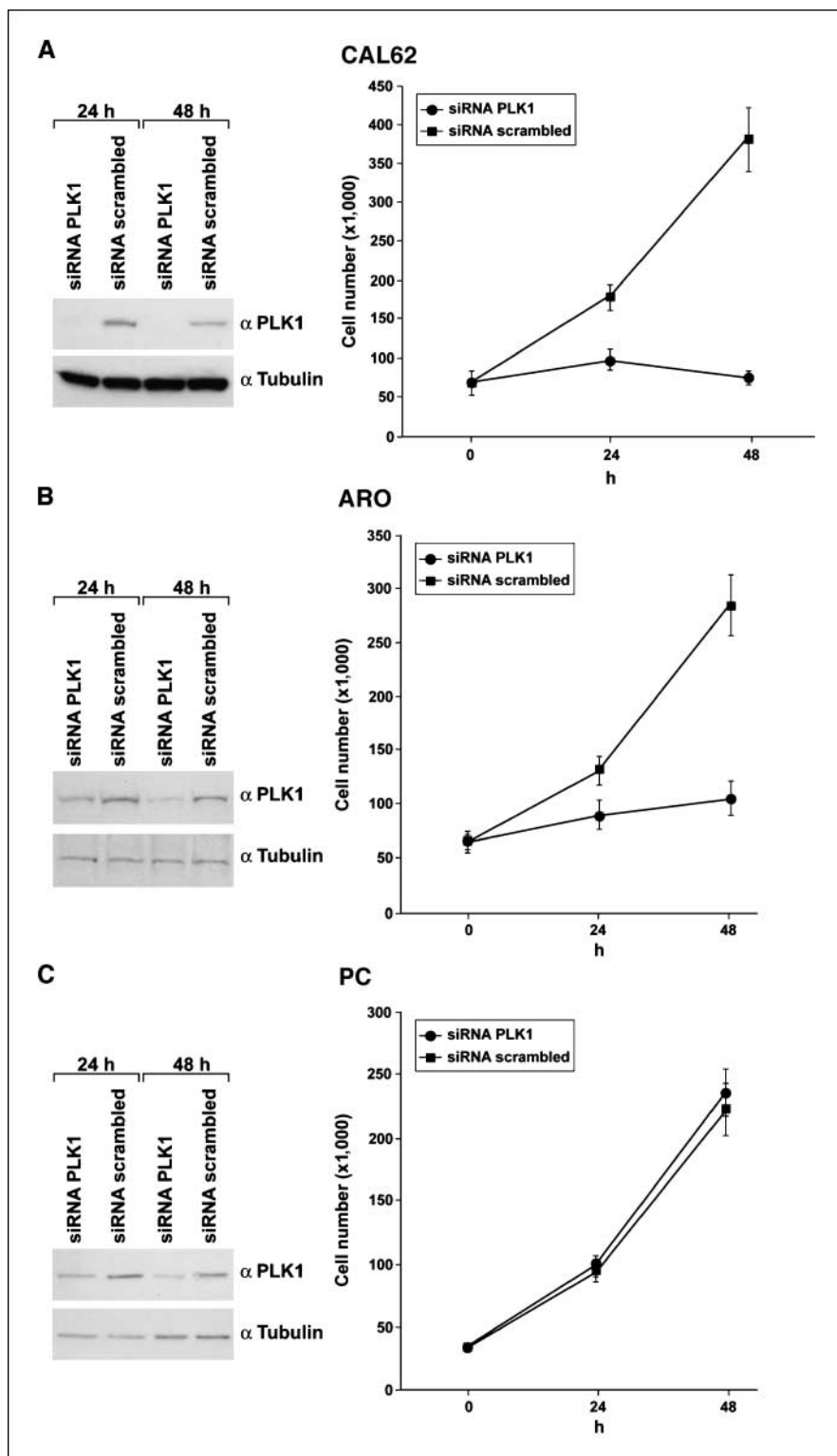
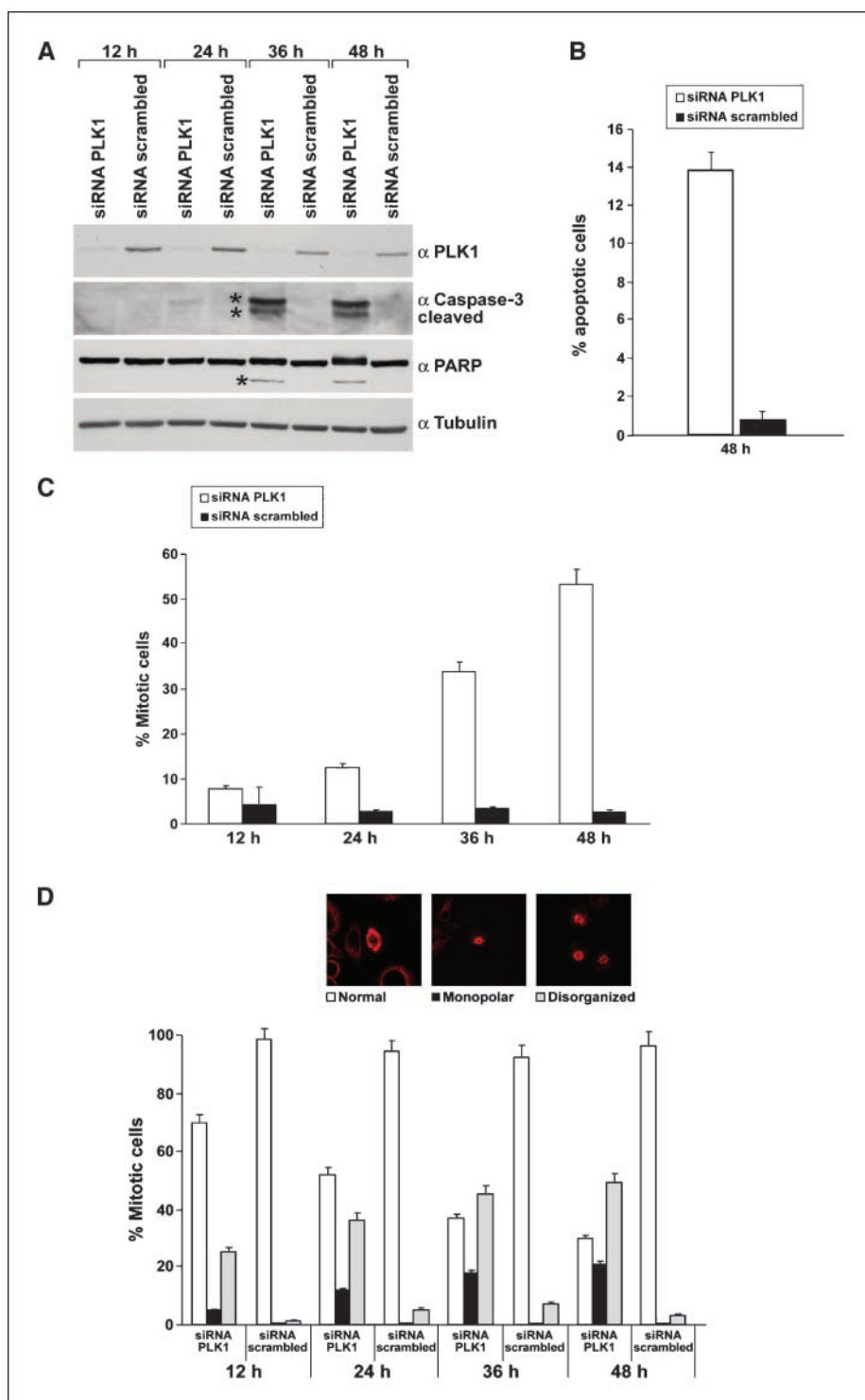


Figure 3. Effects of PLK1 knockdown on ATC cell growth. CAL62 (A), ARO (B), and normal PC (C) cells were transfected with either PLK1-siRNA or the scrambled oligonucleotide control. Cells were harvested and counted at the indicated time points. Values represent the average of triplicate determinations. Bars, 95% confidence intervals (right). Equal amounts of protein lysates were subjected to immunoblot with anti-PLK1 or α -tubulin antibodies (left).

Figure 4. Effects of PLK1 knockdown on apoptosis and cell cycle progression in ATC cells. **A**, CAL62 cells transfected with either PLK1 siRNA or its scrambled control were lysed at the indicated time points and subjected to immunoblot with anti-cleaved caspase-3 antibodies, which detect only the p17 and p12 cleaved caspase-3 fragments (*) and anti-PARP antibodies, which detect both the intact 116 kDa and its cleaved 89-kDa (*) fragment. Anti-PLK1 immunoblot was used to verify RNAi; α -tubulin levels are shown for normalization. Data are representative of at least three different experiments. **B**, TUNEL analysis of PLK1-siRNA and scrambled control-treated CAL62 cells (48 h posttransfection). The percentage of positive cells represents the average value of triplicate experiments \pm SD, in which at least 300 cells were counted. **C**, CAL62 cells, grown on glass coverslips, were transfected with PLK1-siRNA or with its scrambled control sequence. At the indicated time points, cells were fixed, stained with anti- α -tubulin, and analyzed by confocal microscopy. The percentage of mitotic cells represents the average \pm SD of three experiments in which at least 400 cells were counted. **D**, mitotic cells with normal spindles, monopolar spindles, or grossly disorganized spindles were counted. Values refer to the average \pm SD of triplicate experiments in which at least 200 mitotic cells were counted; *insets*, representative images.



that PLK1 addiction might be an Achilles' heel of ATC cells and might be exploited to develop novel treatment strategies for this cancer.

Acknowledgments

Received 5/23/2007; revised 8/1/2007; accepted 8/31/2007.

Grant support: Associazione Italiana per la Ricerca sul Cancro, Istituto Superiore di Oncologia, NOGEC (Naples OncoGenomic Center), the GEAR project from Regione Campania, Italian Ministero della Salute, Project Applicazioni Biotecnologiche

(MoMa), and E.C. Contract 03695 (GenRisk-T) to M. Santoro. P. Salerno was supported by a NOGEC fellowship.

The costs of publication of this article were defrayed in part by the payment of page charges. This article must therefore be hereby marked *advertisement* in accordance with 18 U.S.C. Section 1734 solely to indicate this fact.

We are grateful to G. Vecchio for his support. We thank F. Curcio for the P5 cells, H. Zitzelsberger for the S11N and S63N cells, C.H. Heldin for the HTH7, HTH83, C643, and SW1736 cells. We thank M. Crescenzi for expression vectors. We thank F. Merolla for help with flow cytometry studies, A. Ferraro for help with Q-RT-PCR, and J.A. Gilder for text editing.

References

1. Fagin JA. How thyroid tumors start and why it matters: kinase mutants as targets for solid cancer pharmacotherapy. *J Endocrinol* 2004;183:249–56.
2. Kondo T, Ezzat S, Asa SL. Pathogenetic mechanisms in thyroid follicular-cell neoplasia. *Nat Rev Cancer* 2006;6:292–306.
3. Espinosa AV, Porchia L, Ringel MD. Targeting BRAF in thyroid cancer. *Br J Cancer* 2007;96:1313.
4. Nikiforov YE. Genetic alterations involved in the transition from well-differentiated to poorly differentiated and anaplastic thyroid carcinomas. *Endocr Pathol* Winter 2004;15:319–27.
5. Garcia-Rostan G, Costa AM, Pereira-Castro I, et al. Mutation of the PIK3CA gene in anaplastic thyroid cancer. *Cancer Res* 2005;15:10199–207.
6. Wu G, Mambo E, Guo Z, et al. Uncommon mutation, but common amplifications, of the PIK3CA gene in thyroid tumors. *J Clin Endocrinol Metab* 2005;90:4688–93.
7. Pierantoni GM, Rinaldo C, Mottolise M, et al. High-mobility group A1 inhibits p53 by cytoplasmic relocalization of its proapoptotic activator HIPK2. *J Clin Invest* 2007;117:693–702.
8. Malaguarnera R, Vella V, Vigneri R, Frasca F. p53 family proteins in thyroid cancer. *Endocr Relat Cancer* 2007;14:43–60.
9. Wreesmann VB, Ghossein RA, Patel SG, et al. Genome-wide appraisal of thyroid cancer progression. *Am J Pathol* 2002;161:1549–56.
10. Tabach Y, Milyavsky M, Shats I, et al. The promoters of human cell cycle genes integrate signals from two tumor suppressive pathways during cellular transformation. *Mol Syst Biol* 2005;1:1–15.
11. Whitfield ML, Gorge LK, Grant GD, et al. Common markers of proliferation. *Nat Rev Cancer* 2006;6:99–106.
12. Carter SL, Eklund AC, Kohane IS, et al. A signature of chromosomal instability inferred from gene expression profiles predicts clinical outcome in multiple human cancers. *Nat Genet* 2006;38:1043–8.
13. Bionde MR, Hanski ML, Budzies J, et al. DNA damage-induced expression of p53 suppresses mitotic checkpoint kinase hMps1: the lack of this suppression in p53MUT cells contributes to apoptosis. *J Biol Chem* 2006;31:8675–85.
14. Strebhardt K, Ullrich A. Targeting polo-like kinase 1 for cancer therapy. *Nat Rev Cancer* 2006;6:321–30.
15. Hedinger C, Williams ED, Sobin LH. The WHO histological classification of thyroid tumors: a commentary on the second edition. *Cancer* 1989;63:908–11.
16. Bittner M, Meltzer P, Chen Y, et al. Molecular classification of cutaneous malignant melanoma by gene expression profiling. *Nature* 2000;406:536–40.
17. Jiang Y, Lueders J, Glatfelder A, et al. Profiling human gene expression with cDNA microarrays. New York: John Wiley & Sons, Inc.; 2001.
18. Curcio F, Ambesi-Impombato FS, Perrella G, et al. Long-term culture and functional characterization of follicular cells from adult normal human thyroids. *Proc Natl Acad Sci U S A* 1994;91:9004–8.
19. Fiore L, Pollina LE, Fontanini G, et al. Cytokine production by a new undifferentiated human thyroid carcinoma cell line, FB-1. *J Clin Endocrinol Metab* 1997;82:4094–100.
20. Gioanni J, Zanghellini E, Mazeau C, et al. Characterization of a human cell line from an anaplastic carcinoma of the thyroid gland. *Bull Cancer* 1991;78:1053–62.
21. Ain KB, Tofiq S, Taylor KD. Antineoplastic activity of taxol against human anaplastic thyroid carcinoma cell lines *in vitro* and *in vivo*. *J Clin Endocrinol Metab* 1996;81:3650–3.
22. Fagin JA, Matsuo K, Karmakar A, et al. High prevalence of mutations of the p53 gene in poorly differentiated human thyroid carcinomas. *J Clin Invest* 1993;91:179–84.
23. Heldin NE, Cvejic D, Smeds S, et al. Coexpression of functionally active receptors for thyrotropin and platelet-derived growth factor in human thyroid carcinoma cells. *Endocrinology* 1991;129:2187–93.
24. Blagosklonny MV, Giannakakou P, Wojtowicz M, et al. Effects of p53-expressing adenovirus on the chemosensitivity and differentiation of anaplastic thyroid cancer cells. *J Clin Endocrinol Metab* 1998;83:2516–22.
25. Guida T, Salvatore G, Faviana P, et al. Mitogenic effects of the up-regulation of minichromosome maintenance proteins in anaplastic thyroid carcinoma. *J Clin Endocrinol Metab* 2005;90:4703–9.
26. Nogawa M, Yuasa T, Kimura S, et al. Intravesicle administration of small interfering RNA targeting PLK-1 successfully prevents the growth of bladder cancer. *J Clin Invest* 2005;115:978–85.
27. Pallante P, Berlingieri MT, Troncone G, et al. UbcH10 overexpression may represent a marker of anaplastic thyroid carcinomas. *Br J Cancer* 2005;93:464–71.
28. Linhart C, Elkon R, Shiloh Y, et al. Deciphering transcriptional regulatory elements that encode specific cell cycle phasing by comparative genomics analysis. *Cell Cycle* 2005;4:1788–97.
29. Nevins JR. The Rb/E2F pathway and cancer. *Hum Mol Genet* 2001;10:699–703.
30. Zhu W, Giangrande PH, and Nevins JR. E2Fs link the control of G₁/S and G₂/M transcription. *EMBO J* 2004;23:4615–26.
31. Di Agostino S, Strano S, Emiliozzi V, et al. Gain of function of mutant p53: the mutant p53/NF-Y protein complex reveals an aberrant transcriptional mechanism of cell cycle regulation. *Cancer Cell* 2006;10:191–202.
32. Kho PS, Wang Z, Zhuang L, et al. p53-regulated transcriptional program associated with genotoxic stress-induced apoptosis. *J Biol Chem* 2004;279:21183–92.
33. Spurgers KB, Gold DL, Coombes KR, et al. Identification of cell cycle regulatory genes as principal targets of p53-mediated transcriptional repression. *J Biol Chem* 2006;281:25134–42.
34. Olivier M, Eeles R, Hollstein M, Khan MA, Harris CC, Hainaut P. The IARC TP53 Database: new online mutation analysis and recommendations to users. *Hum Mutat* 2002;19:607–14.
35. Uchiumi T, Longo DL, Ferris DK. Cell cycle regulation of the human polo-like kinase (PLK) promoter. *J Biol Chem* 1997;272:9166–74.
36. Gumireddy K, Reddy MV, Cosenza SC, et al. ON01910, a non-ATP-competitive small molecule inhibitor of Plk1, is a potent anticancer agent. *Cancer Cell* 2005;7:275–86.
37. Liu X, Lei M, Erikson RL. Normal cells, but not cancer cells, survive severe Plk1 depletion. *Mol Cell Biol* 2006;26:2093–108.
38. Ren B, Cam H, Takahashi Y, et al. E2F integrates cell cycle progression with DNA repair, replication, and G(2)/M checkpoints. *Genes Dev* 2002;16:245–56.

Attached manuscript #3

De Falco V, Guarino V, Avilla E, Castellone MD,
Salerno P, Salvatore G, Faviana P, Basolo F,
Santoro M, Melillo RM. Biological role and
potential therapeutic targeting of the chemokine
receptor CXCR4 in undifferentiated thyroid cancer.
Cancer Res 2007;67 (in press).

Biological Role and Potential Therapeutic Targeting of the Chemokine Receptor CXCR4 in Undifferentiated Thyroid Cancer

Valentina De Falco,¹ Valentina Guarino,¹ Elvira Avilla,¹ Maria Domenica Castellone,¹ Paolo Salerno,¹ Giuliana Salvatore,² Pinuccia Faviana,³ Fulvio Basolo,³ Massimo Santoro,¹ and Rosa Marina Melillo¹

¹Dipartimento di Biologia e Patologia Cellulare e Molecolare c/o Istituto di Endocrinologia ed Oncologia Sperimentale del CNR "G. Salvatore," Facolta' di Medicina e Facolta' di Scienze Biotechnologiche dell'Universita' "Federico II"; ²Dipartimento di Studi delle Istituzioni e dei Sistemi Territoriali, Universita' "Parthenope," Naples, Italy and ³Dipartimento di Chirurgia, Universita' di Pisa, Pisa, Italy

Abstract

Anaplastic thyroid carcinoma (ATC) is a rare thyroid cancer type with an extremely poor prognosis. Despite appropriate treatment, which includes surgery, radiotherapy, and chemotherapy, this cancer is invariably fatal. CXCR4 is the receptor for the stromal cell-derived factor-1 (SDF-1)/CXCL12 chemokine and it is expressed in a variety of solid tumors, including papillary thyroid carcinoma. Here, we show that ATC cell lines overexpress CXCR4, both at the level of mRNA and protein. Furthermore, we found that CXCR4 was overexpressed in ATC clinical samples, with respect to normal thyroid tissues by real-time PCR and immunohistochemistry. Treatment of ATC cells with SDF-1 induced proliferation and increase in phosphorylation of extracellular signal-regulated kinases and protein kinase B/AKT. These effects were blocked by the specific CXCR4 antagonist AMD3100 and by CXCR4 RNA interference. Moreover, AMD3100 effectively reduced tumor growth in nude mice inoculated with different ATC cells. Thus, we suggest that CXCR4 targeting is a novel potential strategy in the treatment of human ATC. [Cancer Res 2007;67(24):1-9]

Introduction

Thyroid cancer accounts for the majority of endocrine neoplasms worldwide (1). Malignant tumors derived from the thyroid gland include well-differentiated thyroid carcinomas (WDTC; papillary and follicular) and undifferentiated or anaplastic thyroid carcinomas (ATC). Another group of cancers falls between these two types, the so-called poorly differentiated thyroid carcinomas (PDC). WDTC represents >90% of all thyroid cancers, whereas ATC accounts for approximately 2% to 5% of them (2-4). WDTC management requires surgery and adjuvant radioactive iodine (5, 6). Whereas most of the patients with WDTC have an excellent prognosis, those that present with PDC or ATC have a poor prognosis. PDC displays intermediate biological and clinical features between WDTC and ATC. Indeed, these tumors display high propensity to recur and metastasize. Furthermore, they tend to a progressive dedifferentiation, which leads to the decrease in the levels of the sodium iodide symporter. As a consequence of this,

these tumors are unable to concentrate iodine and become resistant to radiometabolic therapy (4, 7). ATC is the most malignant thyroid tumor and one of the more fatal human malignancy with a median survival from the time of diagnosis of only 4 to 12 months (8, 9). ATC is more frequent in iodine-deficient areas and can be associated with other thyroid disorders. These tumors arise at a mean age of 55 to 65 years, are more common in women, and present usually as a rapidly growing mass, localized in the anterior neck area, which rapidly metastasizes at lungs, bone, and brain. Treatment of ATC with surgery, radiotherapy, and chemotherapy, alone or in combination, shows little or no effect on patient's survival (10). For these reasons, novel treatment strategies are urgently needed. Unlike the WDTC, the molecular mechanisms underlying the development of human ATC are largely unknown. Genetic rearrangements of the RET and TRKA tyrosine kinase receptors, point mutations of the BRAF serine-threonine kinase or, less frequently, RAS mutations, are typically found in papillary thyroid carcinoma (PTC). Rearrangements of PPAR γ or RAS point mutations are instead found in human FTC (11, 12). Among these genetic alterations, RAS or BRAF point mutations are detected at low frequency in ATC, suggesting that some ATC may arise from a preexisting WDTC, whereas others arise *de novo* (12, 13). Inactivating point mutations of the p53 tumor suppressor and activating point mutations of the β -catenin or the PIK3CA are also found in ATC (13, 14).

In the attempt to better characterize human ATC at the molecular level, we aimed to study the involvement of chemokine and chemokine receptors in these tumors. Chemokines are small secretory proteins that were initially reported to control the recruitment and the activation of immune cells in inflammation (16). These molecules exert their action through binding to a group of seven-transmembrane G protein-coupled receptors. All chemokine receptors initiate signal transduction by activating a member of the Gi family of G proteins which, on receptor activation, dissociates into α and $\beta\gamma$ subunits. The G α subunit inhibits adenylyl cyclase, whereas the G $\beta\gamma$ dimer activates the phospholipase C β and the phosphatidylinositol 3-kinase pathways, with the activation of downstream signaling. It has becoming clear recently that chemokines are also involved in cancer cell migration, survival, and growth (17). Not only chemokines regulate some important features of cancer cells but are also involved in the regulation of tumor angiogenesis and leukocyte recruitment (17). In particular, the chemokine receptor CXCR4 and its ligand stromal cell-derived factor-1 (SDF-1)/CXCL12 have been implicated in the metastatic spread of breast cancer cells (18). CXCR4 is one of the

Requests for reprints: Rosa Marina Melillo, Istituto di Endocrinologia ed Oncologia Sperimentale del CNR, via S. Pansini 5, 80131 Naples, Italy. Phone: 39-081-7463603; Fax: 39-081-7463603; E-mail: rosmelil@unina.it.

©2007 American Association for Cancer Research.
doi:10.1158/0008-5472.CAN-07-0899

most important chemokine receptors for cancer cells. Indeed, it is expressed in a great number of human solid and hematologic cancers, including breast, prostate, brain, colon, and lung cancer (19, 20). We and others previously reported the overexpression and functional activity of CXCR4 in thyroid cancer (21, 22). In this report, we show that human ATC cells express high levels of CXCR4 and that the CXCR4-SDF-1/CXCL12 axis sustains the growth of ATC cells. Finally, we provide evidences that targeting CXCR4 might be exploited as a novel anticancer therapy for human ATC.

Materials and Methods

Cell lines. Human primary cultures of normal thyroid and ATC cells were obtained from F. Curcio (P5, P5-2N, P5-3N, P5-4N, and HTU8) and H. Zitzelsberger (S11T, S77T, and S14T) and cultured as described previously (23). Primary cultures of ATC were also a kind gift of H. Zitzelsberger. Of these, only the S11T displays a BRAF(V600E) mutation in heterozygosis.⁴ Human thyroid papillary cancer cell lines TPC1, FB2, and NIM have been described previously (24–26). TPC1 and FB2 cells harbor a RET/PTC1 rearrangement. NPA87 cells derive from a PDC and harbor a BRAF(V600E) mutation in homozygosis (23). The anaplastic cells ARO, KAT4, BHT101, and FB1 cells harbor a BRAF(V600E) mutation in heterozygosis; 8505C and FRO harbor a BRAF(V600E) mutation in homozygosis (23); and CAL62 cells express wild-type BRAF but mutant NRAS allele. Continuous cell lines were maintained in DMEM supplemented with 10% fetal bovine serum, 1% penicillin-streptomycin, and 1% glutamine.

RNA extraction and reverse transcription PCR. Total RNA was isolated by the RNeasy kit (Qiagen) and subjected to on-column DNase digestion with the RNase-free DNase set (Qiagen) according to the manufacturer's instructions. The quality of RNA was verified by electrophoresis through 1% agarose gel and visualized with ethidium bromide. RNA (1 µg) from each sample was reverse transcribed with the QuantiTect Reverse Transcription (Qiagen) using an optimized blend of oligo(dT) and random primers according to the manufacturer's instructions. To design a quantitative reverse transcription-PCR (RT-PCR) assay, we used the Human ProbeLibrary system (Exiqon). Briefly, Exiqon provides 90 human prevalidated Taqman probes (8–9 nucleotides long) that recognize ~99% of human transcripts in the RefSeq database at the National Center for Biotechnology Information. The ProbeFinder assay design software (available online)⁵ was used to design primer pairs and probes. All fluorogenic probes were dual labeled with FAM at 5'-end and with a black quencher at the 3'-end. Primer pairs and PCR conditions are available on request. Quantitative RT-PCR was performed in a Chromo 4 Detector (MJ Research) in 96-well plates using a final volume of 20 µL. For each PCR, 8 µL of 2.5× RealMasterMix Probe ROX (Eppendorf AG), 200 nmol/L of each primer, 100 nmol/L probe, and cDNA generated from 50 ng of total RNA were used. PCRs were performed in triplicate and fold changes were calculated with the following formula: $2^{-(\text{sample 1 } \Delta Ct - \text{sample 2 } \Delta Ct)}$, where ΔCt is the difference between the amplification fluorescent thresholds of the mRNA of interest and the mRNA of RNA polymerase 2 used as an internal reference.

Immunohistochemistry. Retrospectively collected archival thyroid tissue samples from patients affected by ATCs were retrieved from the files of the Pathology Department of the University of Pisa on informed consent. Sections (4 µm thick) of paraffin-embedded samples were stained with H&E for histologic examination to ensure that the samples fulfilled the diagnostic criteria required for the identification of ATC. Normal thyroid tissue samples were also retrieved from the files of the Pathology Department of the University of Pisa.

For immunohistochemistry, paraffin sections (3–5 µm) were dewaxed in xylene, dehydrated through graded alcohols, and blocked with 5%

nonimmune mouse serum in PBS with 0.05% sodium azide for 5 min. Mouse monoclonal antibody against CXCR4 (clone 12G5; R&D Systems) was added at 1:1,000 dilution for 15 min. After incubation with biotinylated anti-mouse secondary antibody for 15 min followed by streptavidin-biotin complex for 15 min (Catalyzed Signal Amplification System, DAKO), sections were developed for 5 min with 0.05% 3,3'-diaminobenzidine tetrahydrochloride and 0.01% hydrogen peroxide in 0.05 mol/L Tris-HCl buffer (pH 7.6), counterstained with hematoxylin, dehydrated, and mounted.

Protein studies. Immunoblotting experiments were performed according to standard procedures. Briefly, cells were harvested in lysis buffer [50 mmol/L HEPES (pH 7.5), 150 mmol/L NaCl, 10% glycerol, 1% Triton X-100, 1 mmol/L EGTA, 1.5 mmol/L MgCl₂, 10 mmol/L NaF, 10 mmol/L sodium pyrophosphate, 1 mmol/L Na₂VO₄, 10 µg/mL aprotinin, 10 µg/mL leupeptin] and clarified by centrifugation at 10,000 × *g*. For protein extraction from human tissues, snap-frozen samples were immediately homogenized in lysis buffer by using the Mixer Mill apparatus (Qiagen). Protein concentration was estimated with a modified Bradford assay (Bio-Rad). Antigens were revealed by an enhanced chemiluminescence detection kit (Amersham). Anti-CXCR4 antibodies were from Abcam Ltd. For the evaluation of mitogen-activated protein kinase (MAPK) and AKT activity on SDF-1α triggering, BHT101 and S11T cells were serum deprived for 12 h and then stimulated with human recombinant SDF-1α (R&D Systems) for the indicated time. Anti-phosphorylated p44/42 MAPK, anti-p44/42 MAPK, anti-phosphorylated AKT, and anti-AKT antibodies were from New England Biolabs. Anti-tubulin monoclonal antibody was from Sigma Chemical. Secondary anti-mouse and anti-rabbit antibodies coupled to horseradish peroxidase were from Bio-Rad.

Flow cytometric analysis. Subconfluent cells were detached from culture dishes with a solution of 0.5 mmol/L EDTA and then washed thrice in PBS buffer. After saturation with 1 µg of human IgG/10⁵ cells, cells were incubated for 20 min on ice with phycoerythrin (PE)-labeled antibodies specific for human CXCR4 (R&D Systems) or isotype control antibody. After incubation, unreacted antibody was removed by washing cells twice in PBS buffer. Cells resuspended in PBS were analyzed on a FACSCalibur cytofluorimeter using the CellQuest software (Becton Dickinson). Analyses were performed in triplicate. In each analysis, a total of 10⁴ events were calculated.

Cell proliferation. S-phase entry was evaluated by bromodeoxyuridine (BrdUrd) incorporation and indirect immunofluorescence. Cells were grown on coverslips, kept in 2.5% serum for 24 h, and then treated with recombinant SDF-1α (100 ng/mL) for 48 h. BrdUrd was added at a concentration of 10 µmol/L for the last 1 h. Subsequently, cells were fixed in 3% paraformaldehyde and permeabilized with 0.2% Triton X-100. BrdUrd-positive cells were revealed with Texas red-conjugated secondary antibodies (Jackson ImmunoResearch Laboratories, Inc.). Cell nuclei were identified by Hoechst staining. Fluorescence was visualized with a Zeiss 140 epifluorescent microscope.

For growth curves, cells were plated at a density of 0.5 × 10⁵ in low-serum conditions (2.5%) and counted at the indicated time points.

RNA interference. Small inhibitor duplex RNAs targeting human CXCR4 have been described previously (27) and were chemically synthesized by Prologo. Sense strand for human CXCR4 small interfering RNA (siRNA) targeting was the following: 5'-GAGGGGAUCAGCAGUAUAC-3'.

Small duplex RNAs containing the same nucleotides, but in scrambled fashion (siRNA SCR), were used as a negative control. For siRNA transfection, ATC cells were grown under standard conditions. The day before transfection, cells were plated in six-well dishes at 50% to 60% confluency. Transfection was performed using 5 to 15 µg of duplex RNA and 6 µL of Oligofectamine reagent (Invitrogen). Cells were harvested at 48 and 72 h after transfection and analyzed for protein expression and biological activity.

Xenografts in nude mice. Mice were housed in barrier facilities and 12-h light-dark cycles and received food and water *ad libitum* at the Dipartimento di Biologia e Patologia Cellulare e Molecolare (University of Naples "Federico II," Naples, Italy). This study was conducted in accordance with Italian regulations for experimentation on animals. All manipulations were performed while mice were under isoflurane gas anesthesia. No mouse

⁴ G. Salvatore, unpublished observation.

⁵ <http://www.probelibrary.com>

showed signs of wasting or other signs of toxicity. BHT101, ARO, or KAT4 cells (5×10^6 per mouse) were inoculated s.c. into the right dorsal portion of 4-week-old male BALB/c *nu/nu* mice (The Jackson Laboratory). When tumors measured 40 mm³, mice were randomized to receive AMD3100 ($n = 10$; 1.25 mg/kg/twice daily) or vehicle alone ($n = 10$; PBS) by i.p. injection for 5 consecutive days per week for 3 to 4 weeks. Tumor diameters were measured at regular intervals with calipers. Tumor volumes (V) were calculated with the following formula: $V = A \times B^2 / 2$ (A = axial diameter; B = rotational diameter). Tumors were excised and fixed overnight in neutral buffered formalin and processed by routine methods.

Statistical analysis. To compare CXCR4 mRNA levels in normal thyroid tissues versus ATC samples, we used the Mann-Whitney nonparametric test and the GraphPad InStat software, v.3.0b. To compare ATC xenograft growth in AMD3100-treated versus untreated animals, we used the unpaired Student's *t* test (normal distributions and equal variances) and the GraphPad InStat software, v.3.0b. All *P* values were two sided, and differences were considered statistically significant at $P < 0.05$.

Results

CXCR4 is overexpressed in surgical samples of human ATC.

We compared CXCR4 mRNA levels in a set of ATC samples ($n = 15$)

versus different samples of normal thyroid tissue ($n = 5$). As shown in Fig. 1A, CXCR4 mRNA was found to be up-regulated in most of the tumor samples (11 of 15). When we performed statistical analysis, the differences in the expression levels of CXCR4 between tumors and normal thyroid tissues were statistically significant ($P = 0.0084$; Fig. 1A).

To verify whether CXCR4 mRNA overexpression resulted in an increase in the protein levels, we used protein extracts from a different set of ATC samples and three normal thyroid tissues in an immunoblot experiment with CXCR4-specific antibodies. As shown in Fig. 1B, CXCR4 protein levels were higher in ATC samples than in normal thyroid. As a positive control for CXCR4 expression, the ATC cell line ARO was used.

Finally, CXCR4 antibodies were used in immunohistochemical experiments. We evaluated CXCR4 expression in normal thyroid tissues and a set of ATC samples ($n = 33$). Whereas no CXCR4 expression was detected in normal thyroid tissues, 13 (39%) of the ATC samples scored positive for CXCR4. A representative CXCR4 immunostaining is shown in Fig. 1C. These data indicate that a significant fraction of human ATCs, similarly to other epithelial

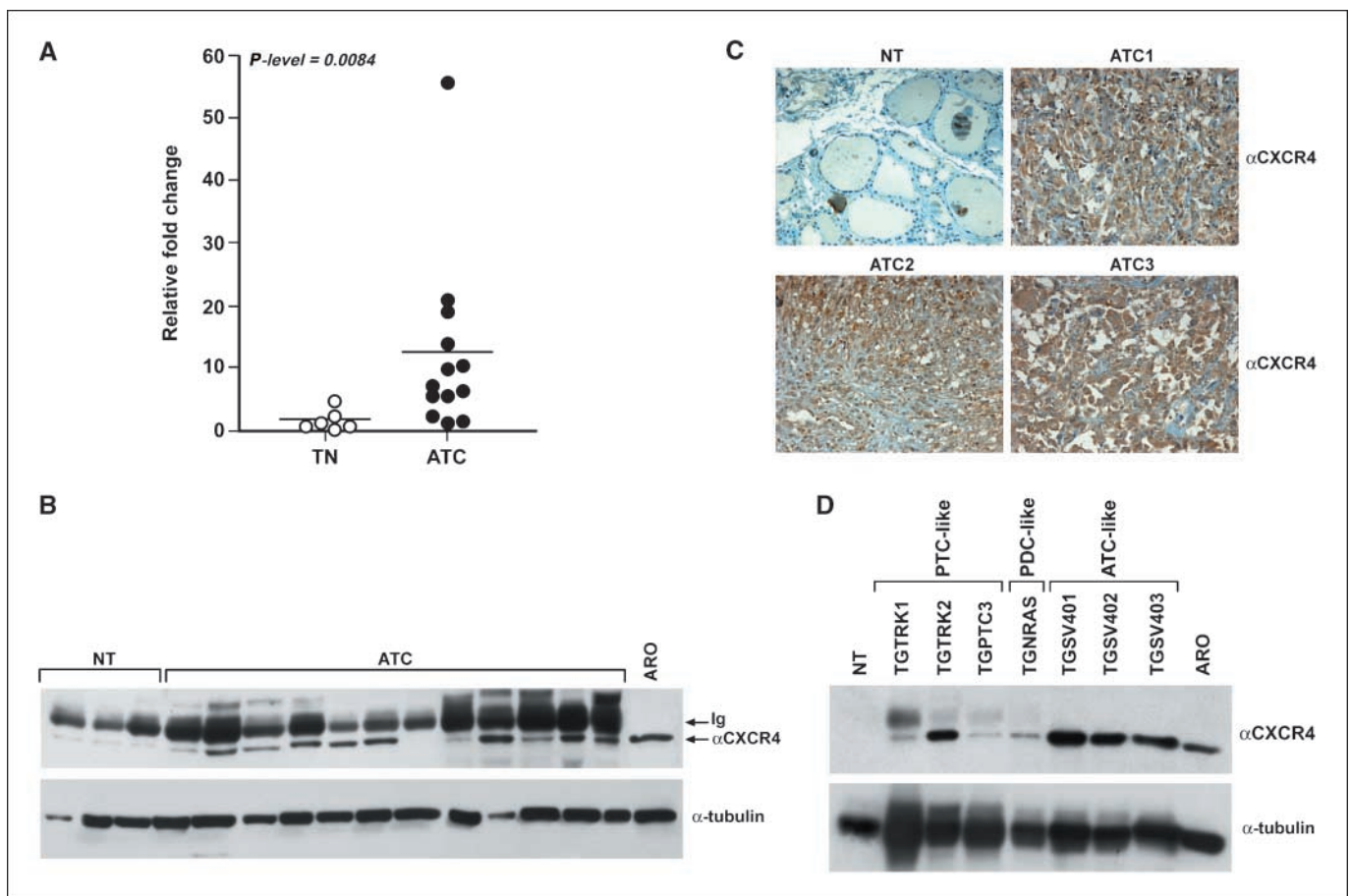


Figure 1. A, expression levels of CXCR4 in human ATC samples versus six normal thyroid tissues by real-time RT-PCR. CXCR4 expression levels of tumors (*Y* axis) are calculated relative to the mean CXCR4 level of normal human thyroid tissues (*NT*). All experiments have been performed in triplicate, and the average value of the results was plotted on the diagram. *P* value was calculated with the two-tailed, nonparametric Mann-Whitney test. B, protein lysates (100 μ g) extracted from the indicated samples underwent Western blotting with anti-CXCR4-specific antibodies. Immunocomplexes were revealed by enhanced chemiluminescence. Equal protein loading was ascertained by anti-tubulin immunoblot. C, immunohistochemical staining for CXCR4 of formalin-fixed, paraffin-embedded ATCs. Tissue samples from normal thyroid or ATC were incubated with a mouse monoclonal anti-CXCR4 antibody. ATCs show a strong immunoreactivity for CXCR4, whereas normal thyroid tissue is negative. Representative pictures of normal and pathologic positive samples are shown. Isotype control was also performed (data not shown). D, the expression levels of CXCR4 protein were analyzed in thyroid tumor samples from transgenic mice models. Tumor tissues were snap frozen and immediately homogenized by using the Mixer Mill apparatus in lysis buffer. Equal amounts of proteins were immunoblotted and stained with anti-CXCR4 polyclonal antibodies (Abcam). ATC-like samples displayed a more intense immunoreactivity for CXCR4. As a control for equal loading, the anti- α -tubulin monoclonal antibody was used.

cancers, feature high expression levels of the CXCR4 receptor. Furthermore, they suggest that the increase in CXCR4 levels occurs at the transcriptional level.

CXCR4 is highly expressed in animal models of ATC. Several transgenic mice model of thyroid cancer have been developed by using various oncogenes under the transcriptional control of the thyroid-specific thyroglobulin bovine promoter. Depending on the specific transgene, these mice develop carcinomas that resemble, for cytologic and histologic features, human PTC, FTC, or ATC. In particular, mice expressing either RET/PTC3 (TGPTC3) or TRK/T1 (TGTRK) oncogene develop PTC-like tumors (28, 29). NRAS transgene expression results in follicular tumors that progress to poorly differentiated carcinomas (TGNRS; ref. 27). Finally, animals expressing the SV40 large T antigen (TGSV) present aggressive thyroid cancer with features similar to human ATC (30). To evaluate the expression of CXCR4 in these animal models, we extracted proteins from different tumor samples of the different transgenic lines and performed Western blot analysis with CXCR4 antibodies. Histologic diagnosis of the thyroid lesion was verified before processing of the samples. As shown in Fig. 1D, CXCR4

levels were higher in ATC models than in normal mouse thyroid tissue. PTC samples displayed intermediate levels of CXCR4. These data, together with previously published data (21, 22), suggest that CXCR4 up-regulation is a frequent event in thyroid tumorigenesis and that it correlates with the malignancy of the disease.

CXCR4 is a functional receptor in human ATC cells. To study the role of CXCR4 in human ATC, we first needed to identify a suitable cell model. To this aim, various normal thyroid and ATC-derived primary cultures and continuous cell lines were tested for CXCR4 expression by Western blot analysis. As shown in Fig. 2A and B, whereas normal thyroid cultures displayed low or undetectable CXCR4 expression levels, several ATC cell lines featured high levels of the CXCR4 receptor. In particular, of 10 ATC cell lines, 7 displayed high expression levels of CXCR4. In the case of ATC cells, the increased levels of CXCR4 proteins were associated to an increase in CXCR4 mRNA levels as assessed by quantitative PCR analysis (Fig. 2C). We then asked whether this receptor was expressed on the cell surface. To this aim, we performed flow cytometry experiments using a PE-conjugated mouse monoclonal anti-CXCR4 antibody. The percentage of CXCR4-positive cells was

F2

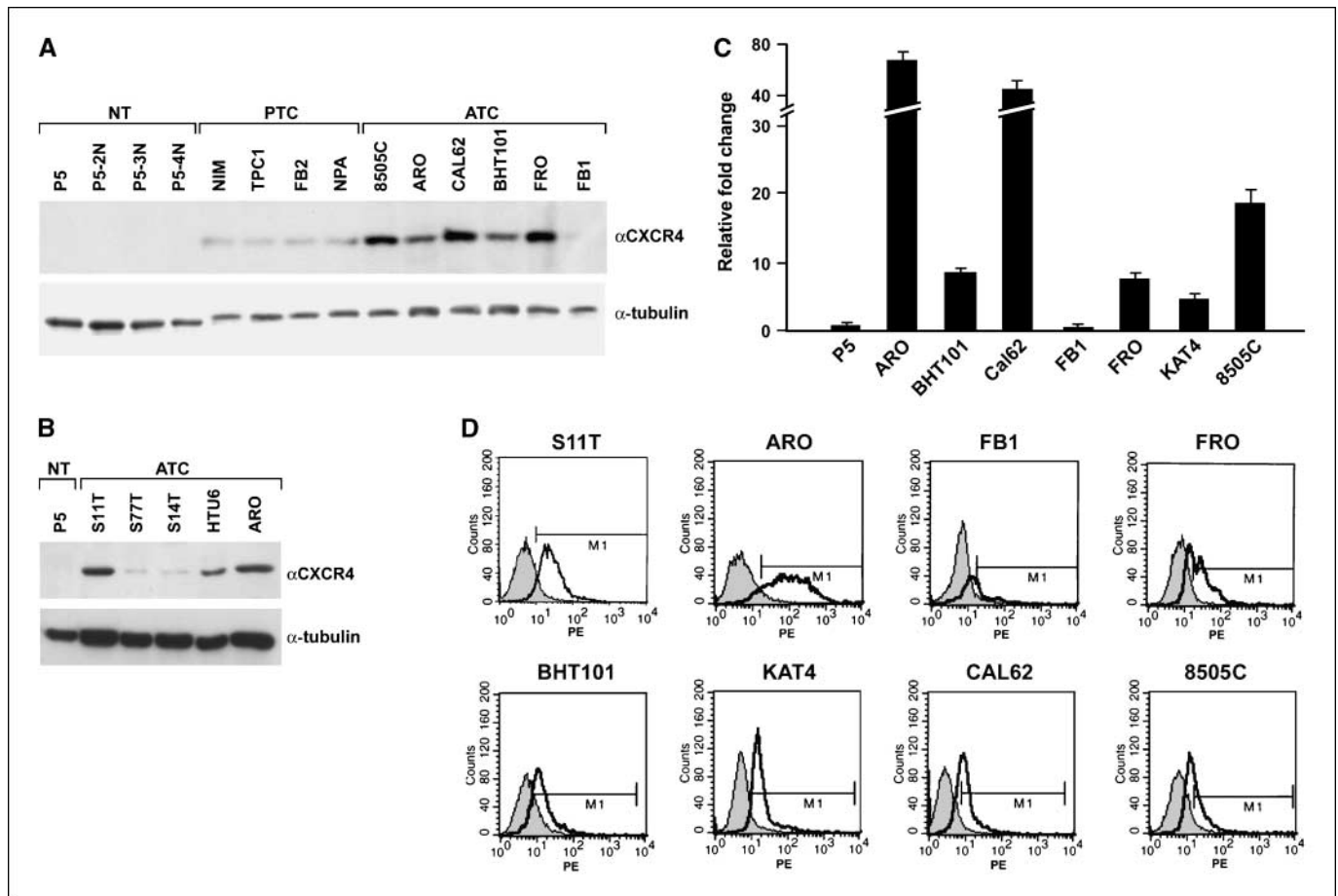
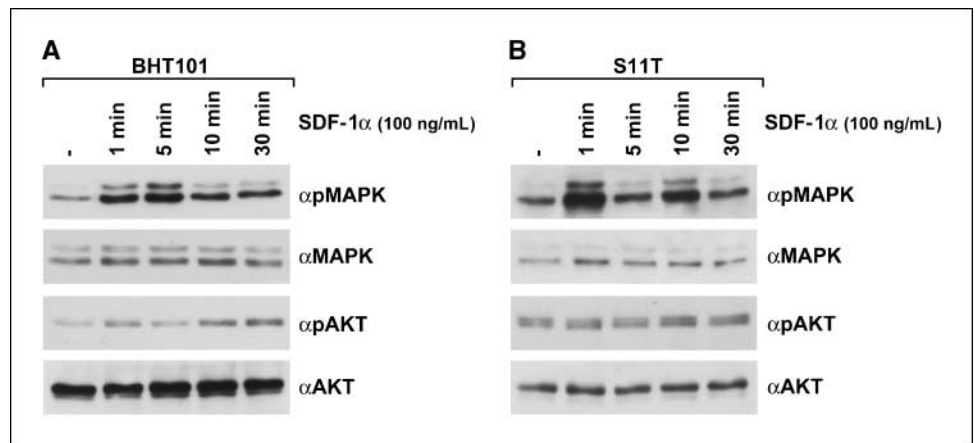


Figure 2. A, CXCR4 up-regulation in cell lines derived from human thyroid carcinomas was evaluated by immunoblot with a polyclonal anti-CXCR4 antibody. The expression levels of CXCR4 protein were analyzed in the P5 human primary thyroid cells, and in the indicated cell lines, derived from human PTCs (NIM, TPC1, FB2, and NPA) or from human ATCs (8505C, ARO, CAL62, BHT101, FRO, and FB1). B, ATC-derived (S11T, S77T, S14T, and HTU8) and normal thyroid primary culture (P5) were screened for CXCR4 expression by Western blot analysis with the polyclonal anti-CXCR4 antibody. As a control for equal loading, the anti- α -tubulin monoclonal antibody was used. C, expression levels of CXCR4 in human ATC cells versus the P5 normal thyroid culture were evaluated by real-time RT-PCR analysis. CXCR4 expression levels of ATC cell lines (Y axis) are calculated relative to the expression level in the normal human cell culture P5. All experiments were performed in triplicate, and the average value of the results was plotted on the diagram. SDs were smaller than 25% in all the cases (data not shown). D, flow cytometric analysis (fluorescence-activated cell sorting) of surface-expressed CXCR4 in ATC cells. Subconfluent cells were detached from culture dishes and incubated with PE-labeled antibodies specific for human CXCR4.

Figure 3. A and B, protein extracts from the indicated cell lines were subjected to immunoblotting with anti-phosphorylated p44/42 MAPK (α pMAPK) and with anti-phosphorylated AKT (α pAKT) antibodies. The blots were reprobed with anti-p44/42 and anti-AKT antibodies for normalization.



determined. As shown in Fig. 2D, CXCR4 was expressed in almost all the ATC cell lines tested, with the exception of the FB1 cells. The ARO cells, which in a previous report were shown to feature high CXCR4 levels (21), were included as a positive control. In contrast, normal thyroid cells did not express CXCR4 (data not shown). SDF-1, the CXCR4 ligand, was not expressed by ATC cells as assessed by quantitative PCR or ELISA assay (data not shown).

We selected two cell lines, S11T and BHT101, for further experiments. First, we tested the ability of recombinant SDF-1 α to stimulate signal transduction in ATC cells. It has been previously reported that stimulation of CXCR4 induces the activation of several kinase cascades mainly through the activation of the G β γ subunit of the Gi protein (31, 32). We therefore tested the phosphorylation of two downstream effectors, extracellular signal-regulated kinase (ERK) 1/2 and AKT, using phosphorylated-specific antibodies. To this aim, cells were serum starved for 12 h and then stimulated with SDF-1 α for different time points. As shown in Fig. 3A and B, SDF-1 α induced rapid and sustained activation of ERK1/2 in both cell lines. AKT activation was also achieved in BHT101 cells on SDF-1 α treatment, whereas it was less evident in S11T cells. Together, these data indicate that CXCR4 is functional in ATC cells. Activation of ERK1/2 and AKT was observed in virtually all the ATC cell lines expressing CXCR4, whereas normal thyroid cells, which do not express CXCR4, did not display these effects (data not shown).

Biological activity of CXCR4 in ATC cells. To further test the functional responsiveness of CXCR4 in ATC, we stimulated these cells with SDF-1 α and evaluated its ability to induce cell proliferation. To this aim, BHT101 and S11T cells were maintained in low-serum (2.5%) growth conditions for 24 h and then either left untreated or stimulated with SDF-1 α for 12 h. As a measure of DNA synthesis, we counted BrdUrd-positive cells on a 1-h BrdUrd pulse. As shown in Fig. 4, SDF-1 α consistently enhanced DNA synthesis in both BHT101 and S11T cells. We then used a specific CXCR4 inhibitor, AMD3100, to block this effect. AMD3100 is a competitive antagonist of SDF-1 α , but it also displays partial agonist activity (33). Normal thyroid cells were insensitive to SDF-1 α stimulation and to the effect of AMD3100 (data not shown). As shown in Fig. 4A, AMD3100 inhibited SDF-1 α -mediated BrdUrd incorporation in ATC cells. The positive effect of SDF-1 on cell proliferation, measured as S-phase entry, was also observed in other ATC cell lines (Fig. 5C). To evaluate whether SDF-1 α could stimulate ATC cell growth, we also performed growth curves in low-serum (2.5%) conditions. As shown in Fig. 4B, the stimulation of BHT101 with

SDF-1 α increased their proliferation rate, and AMD3100 reverted this effect. SDF-1 α was also able to increase the proliferation rate of three different ATC cell lines, KAT4, CAL62, and ARO, which express CXCR4, but was unable to do so on FB1 cells, which we previously reported to be devoid of CXCR4 (Fig. 4B). AMD3100 alone did not have any effect on ATC cells (data not shown).

To exclude off-target effects of AMD3100 and to directly determine the role of CXCR4 on ATC cell proliferation, we used small duplex RNA oligos to knock down CXCR4. CXCR4 RNA interference was verified by Western blot analysis in BHT101 cells (Fig. 5A). We then transfected CXCR4 siRNAs into BHT101, KAT4, CAL62, and 8505C cells. CXCR4 silencing substantially impaired SDF-1 α -induced S-phase entry in all the ATC cells but had no effect on BrdUrd incorporation in the absence of the chemokine, as shown in Fig. 5. When we used the control scrambled siRNA, this inhibitory effect was not observed. Furthermore, scrambled oligos had no effect on CXCR4 protein levels (Fig. 5A).

AMD3100 inhibits ATC tumor formation in nude mice. It has been previously shown that the CXCR4/SDF-1 axis plays an important role in the growth and in the metastatic ability of several epithelial cancers (20). Because we had shown that CXCR4 inhibition blocked SDF-1 α -mediated ATC cell growth in culture, and because it has been shown that this chemokine is secreted by stromal tumoral cells (34), we reasoned that SDF-1 α -CXCR4 axis blockade by AMD3100 might inhibit ATC tumor growth. To this aim, we selected BHT101, ARO, and KAT4 cells for their ability to respond to SDF-1 α and their ability to form tumors *in vivo* with high efficiency. Nude mice were injected s.c. with 5×10^6 cells. When tumors measured ~ 40 mm³, mice ($n = 20$ for each cell line) were randomized to receive AMD3100 (1.25 mg/kg/twice daily i.p.) or vehicle 5 days per week for 3 to 4 weeks. Tumor diameters were measured at regular intervals with caliper. After 21 days, the mean volume of BHT101 tumors in mice treated with AMD3100 was 48 mm³, whereas that of mice treated with vehicle was 620 mm³. Representative experiments are shown in Fig. 6A and B. Tumors induced by ARO and KAT4 reached the volume of 40 mm³ in only 1 week. In addition, in this case, AMD3100 was able to inhibit tumor growth, although to a lesser extent. In fact, ARO-induced tumor mean volume at the end of treatment with AMD3100 was 220 mm³, whereas that of mice treated with vehicle was 625 mm³. Similar results were also obtained when KAT4 cells were used. In this case, the difference between the mean volume of AMD3100-treated versus vehicle-treated tumors was not statistically significant after 3 weeks. However, when treatment

was extended for 1 additional week, AMD3100-treated tumor mean volume was 180 mm³, whereas that of mice treated with vehicle was 690 mm³, and the *P* value was 0.039 (Fig. 6A). These data, taken together, show that treatment with AMD3100 strongly inhibits ATC tumor growth.

Discussion

Despite ATC is a rare disease, it is one of the most aggressive human cancers (9). Although various therapeutic strategies have been exploited to slow down the growth of this tumor, none of

these treatments improved survival (10). The molecular pathways implicated in this disease are poorly understood, and this hampers the application of novel rational therapeutic strategies. Genetic alterations found in ATC are inactivating mutations of the p53 tumor suppressor and activating mutations of β -catenin, RAS, BRAF, and PIK3CA (11). Recently, molecular genetic alterations of FHIT have been also detected in ATC (35). Among the genes involved in ATC, BRAF serine-threonine kinase has been exploited as a potential therapeutic target (23).

Most epithelial cancers feature high levels of expression of the chemokine receptor CXCR4 (20). This receptor has been widely

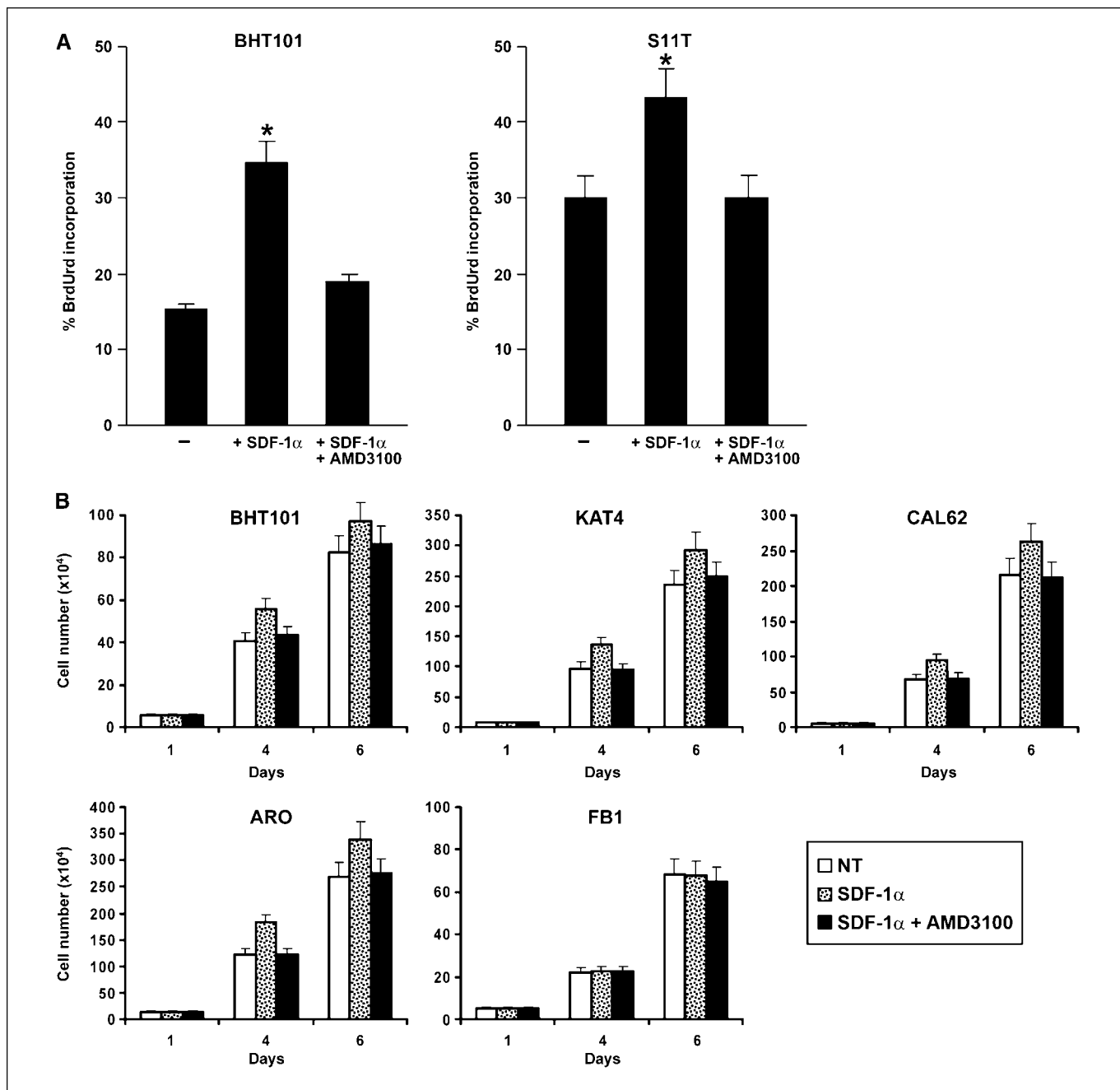


Figure 4. A, BrdUrd incorporation was measured to evaluate S-phase entry on treatment of BHT101 and S11T cells with SDF-1 α in the presence or absence of the CXCR4 inhibitor AMD3100. Columns, average results of three independent experiments; bars, SD. *P* < 0.05. B, the indicated cell lines were plated at the same density (5×10^4) in 2.5% serum, harvested, and counted at the indicated time points. Columns, average results of at least three independent determinations; bars, SD.

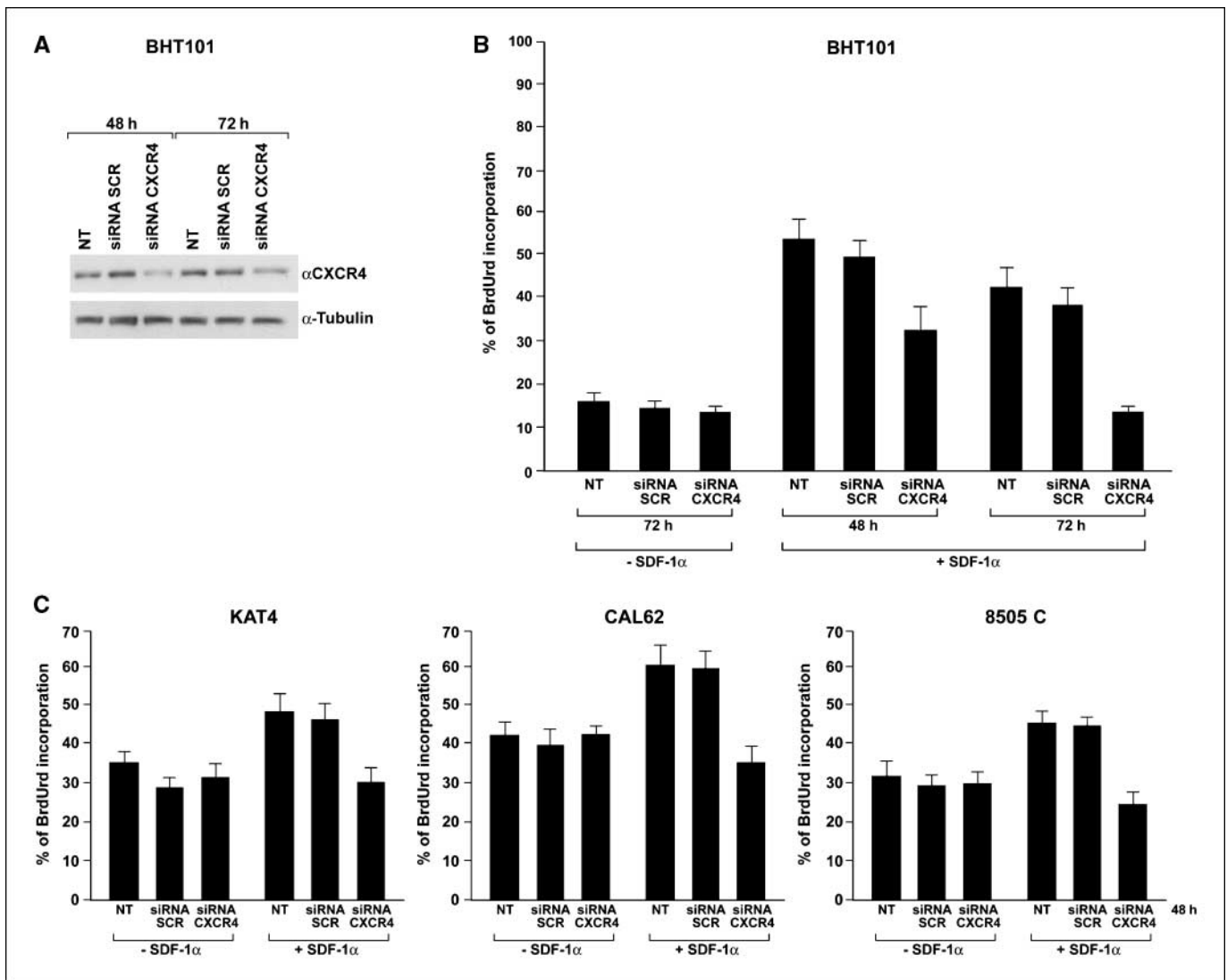


Figure 5. A, CXCR4 RNA interference was used to transiently suppress CXCR4 expression in BHT101 cells. BHT101 cells were transfected with siRNAs against CXCR4 (*siRNA CXCR4*) or control nonspecific small duplex RNA containing the same nucleotides, but in scrambled fashion (*siRNA SCR*), and harvested 48 and 72 h later. Protein lysates were subjected to immunoblotting with anti-CXCR4 and anti-tubulin antibodies. Control siRNA did not affect CXCR4 protein levels. B, CXCR4 RNA interference (*siRNA CXCR4*) in BHT101 cells inhibited SDF-1 α -stimulated S-phase entry as evaluated by BrdUrd incorporation assay. Control siRNA (*siRNA SCR*) did not inhibit DNA synthesis. Unstimulated BHT101 cells were not affected by siRNA transfection. C, CXCR4 RNA interference (*siRNA CXCR4*) inhibited S-phase entry in SDF-1 α -stimulated KAT4, CAL62, and 8505C. ATC cells were transfected with siRNAs against CXCR4 (*siRNA CXCR4*) or control siRNA (*siRNA SCR*) and harvested 48 h later. Control siRNA did not inhibit DNA synthesis. Unstimulated cells were not affected by siRNA transfection.

studied because its expression contributes to several phenotypes of cancer cells, such as the ability to grow, survive, and spread throughout the body. On the contrary, most epithelial cancers do not express SDF-1, the unique CXCR4 ligand, whereas SDF-1 is produced in high amounts in specific body districts. It has been suggested that the role of this chemokine in cancer is mainly to attract cancer cells to these districts (18). In support of this hypothesis, it has been shown that SDF-1 is produced in several metastatic sites. Recently, it has also been suggested that tumoral stroma secretes high amounts of SDF-1, supporting the concept that this chemokine is pivotal in sustaining local protumorigenic events, such as growth and survival of cancer cells (34). Furthermore, the expression of SDF-1 by stromal cancer cells directly recruits endothelial progenitors that are required for tumor angiogenesis (19). As most epithelial and hematopoietic malignancies, also thyroid cancer expresses high levels of CXCR4.

We previously reported functional expression of CXCR4 in human papillary thyroid cancer (22). Furthermore, Hwang et al. (21) showed that an anaplastic cell line, ARO, expressed high levels of functional CXCR4. In this report, we analyzed human ATC samples for CXCR4 expression. We also screened a large panel of human ATC established and primary cell cultures for CXCR4 expression. We show that, both at the mRNA and at the protein level, this receptor is overexpressed in ATC with respect to normal thyroid samples. In contrast, SDF-1 was not detected. The molecular mechanisms underlying CXCR4 up-regulation in ATC are currently unknown. Because we had previously shown that CXCR4 expression was under the control of the RET/PTC-RAS-BRAF-ERK pathway in PTCs (22), and because this pathway is also activated in ATC, we asked whether CXCR4 expression correlated with the BRAF status in ATC. The ATC cell lines that we used in this study had been previously characterized for BRAF mutations.

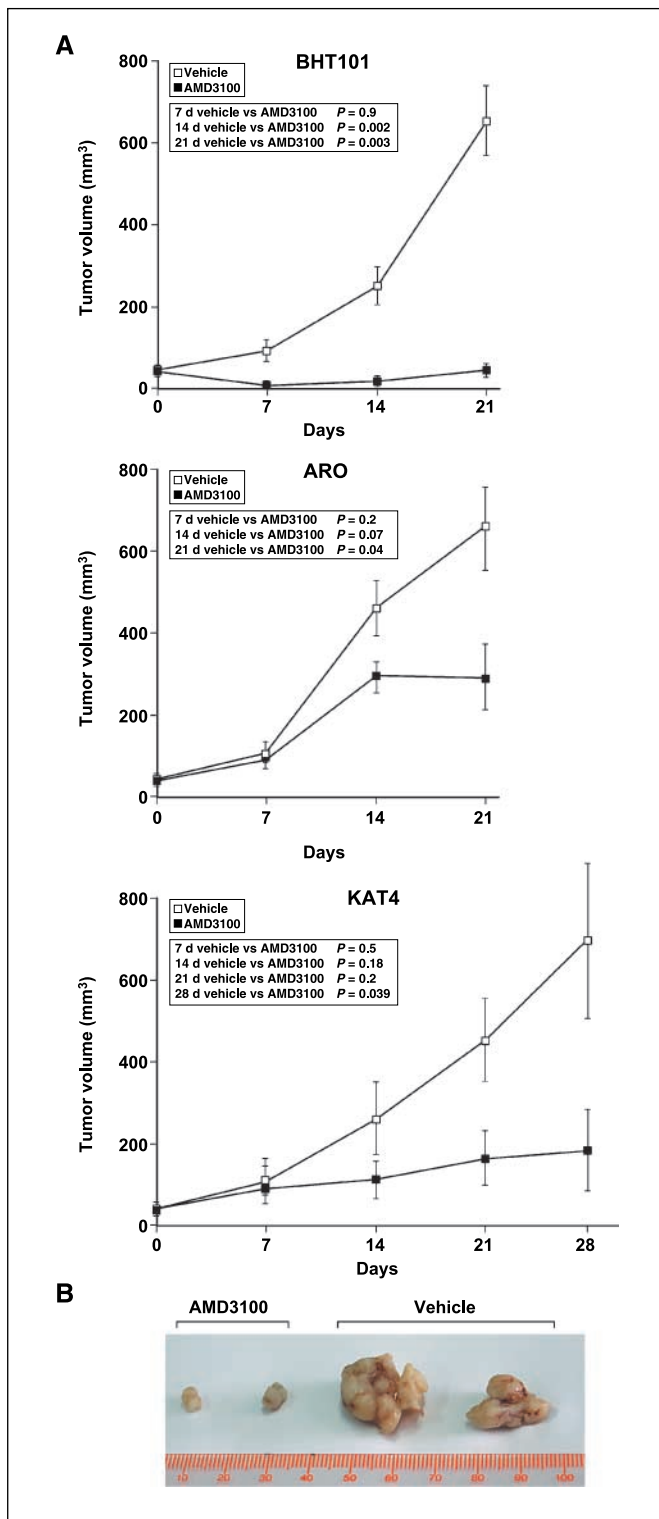


Figure 6. A, antitumor effects of AMD3100 in ATC cell xenografts. BHT101, ARO, and KAT4 cells (5×10^6 per mouse) were injected s.c. into the right dorsal portion of BALB/c athymic mice. When tumors measured 40 mm^3 , mice were randomized to two groups (10 mice per group) to receive AMD3100 or vehicle (PBS) by i.p. injection. Treatment was given for 5 consecutive days per week for 3 to 4 wks (day 1 is the treatment starting day). Tumor diameters were measured with calipers and tumor volumes were calculated. Unpaired Student's *t* test (normal distributions and equal variances) was applied. All *P* values were two sided, and differences were statistically significant at $P < 0.05$. B, tumors were excised and photographed. Two representative examples of BHT101 xenografts are shown.

Furthermore, human ATC samples were screened for the presence of BRAF mutations.⁶ We found that most of the samples expressed CXCR4, and this expression was present in both the BRAF-positive and in the BRAF-negative tumors and cell lines. These data suggest that CXCR4 up-regulation in ATC is not necessarily linked to the BRAF pathway and that it can be possibly achieved through different mechanisms. The mechanisms of CXCR4 up-regulation in cancer thus far described are various and complex. It has been shown that nuclear factor- κ B (NF- κ B) positively regulates the expression of CXCR4 (36) in breast cancer cells. Interestingly, NF- κ B is activated in human thyroid cancer cells (37, 38). Interestingly, transduction of human thyroid cancer cells with the mutant BRAF(V600E) allele induced an increase in NF- κ B DNA-binding activity (39). Thus, it is possible that CXCR4 expression in ATC is sustained by high NF- κ B activity, which can be the result either of BRAF activation or of the activation of other still undiscovered pathways.

We also show that the CXCR4 expressed on the ATC cell surface is able to transduce biochemical signals into the cell. Indeed, stimulation of ATC cells with recombinant human SDF-1 α activated ERK1/2 and, less consistently, AKT pathways in ATC cells. Moreover, we found that SDF-1 α stimulated cell growth of different ATC cell cultures, which was inhibited by the small CXCR4 inhibitor AMD3100. Given the high rate of mortality of this cancer and the lack of effective therapies, we focused our efforts in the identification of novel potential therapeutic targets in ATC. We found that the treatment with AMD3100 significantly suppressed the development of tumors in different xenograft models of ATC cells in nude mice.

The more dramatic biological effects of CXCR4 inhibition observed in the animals with respect with those observed in cell culture could be explained by the fact that SDF-1 can act, in tumor microenvironment, at multiple levels. Indeed, tumoral stromal cells, such as fibroblasts and bone marrow-derived cells, express high levels of SDF-1 (34), which can directly enhance the growth of epithelial tumoral cells and can recruit endothelial progenitors, thus favoring angiogenesis. However, when we analyzed xenograft tumors for CD31-positive tumor capillaries, we found that there were no differences in vessel density of AMD3100-treated versus untreated tumors. Preliminary data suggest that AMD3100 activity in xenografts correlates better with a proapoptotic than with an antiproliferative activity.⁷ Our findings are in accord with previous reports about the use of CXCR4 inhibitors in brain tumor models (40, 41). Although treatment of ATC xenografts with AMD3100 did not induce a complete regression of tumors, we observed a strong reduction in growth rate, which was more dramatic in the case of BHT101 xenografts. It is conceivable that the combination of conventional anticancer therapies with CXCR4 targeting would display a stronger antineoplastic effect. Given the strong antitumor activity of AMD3100, newer-generation compounds have been developed, such as AMD3465. This compound differs from the bicyclam AMD3100 in that it is a monocyclam endowed with greater solubility in water, higher affinity for CXCR4, and a potent antitumor activity (41). Although these compounds are effective in inhibiting various cancers, long-term sustained dosing of

⁶ F. Basolo and P. Faviana, unpublished observations.

⁷ V. Guarino et al., unpublished observation.

AMD3100 displayed a certain toxicity (42). For this reason, further studies, aimed at understanding the effects of long-term administration of CXCR4 inhibitors, must be pursued. Despite these considerations, our data, together with several other reports, strongly indicate that the inhibition of this pathway should be actively evaluated as a novel anticancer therapy.

In conclusion, in this report, we identify CXCR4 as another potential target of ATC anticancer therapy and suggest that AMD3100, or other specific CXCR4 inhibitors, should be developed and tested for the therapy of human ATC.

References

- De Lellis RA, Williams ED. Thyroid and parathyroid tumors. In: De Lellis RA, Lloyd RV, Heitz PU, Eng C, editors. World Health Organization classification of tumors: tumors of the endocrine organs. Lyons (France): IARC Press; 2004. p. 51–6.
- Sherman SI. Thyroid carcinoma. *Lancet* 2003;361:501–11.
- Slough CM, Randolph GW. Workup of well-differentiated thyroid carcinoma. *Cancer Control* 2006;13:99–105.
- Rosai J. Poorly differentiated thyroid carcinoma: introduction to the issue, its landmarks, and clinical impact. *Endocr Pathol* 2004;15:293–6.
- Vini L, Harmer C. Management of thyroid cancer. *Lancet Oncol* 2002;3:407–14.
- Pacini F, Schlumberger M, Dralle H, Elisei R, Smit JW, Wiersinga W; European Thyroid Cancer Taskforce. European consensus for the management of patients with differentiated thyroid carcinoma of the follicular epithelium. *Eur J Endocrinol* 2006;154:787–803.
- Patel KN, Shaha AR. Poorly differentiated and anaplastic thyroid cancer. *Cancer Control* 2006;13:119–28.
- Pasieka JL. Anaplastic thyroid cancer. *Curr Opin Oncol* 2003;15:78–83.
- Are C, Shaha AR. Anaplastic thyroid carcinoma: biology, pathogenesis, prognostic factors, and treatment approaches. *Ann Surg Oncol* 2006;13:453–64.
- Veness MJ, Porter GS, Morgan GJ. Anaplastic thyroid carcinoma: dismal outcome despite current treatment approach. *ANZ J Surg* 2004;74:559–62.
- Kondo T, Ezzat S, Asa SL. Pathogenetic mechanisms in thyroid follicular-cell neoplasia. *Nat Rev Cancer* 2006;6:292–306.
- Nikiforov YE. Genetic alterations involved in the transition from well-differentiated to poorly differentiated and anaplastic thyroid carcinomas. *Endocr Pathol* 2004;15:319–27.
- Garcia-Rostan G, Costa AM, Pereira-Castro I, et al. Mutation of the PIK3CA gene in anaplastic thyroid cancer. *Cancer Res* 2005;65:10199–207.
- Garcia-Rostan G, Tallini G, Herrero A, D'Aquila TG, Carcangiu ML, Rimm DL. Frequent mutation and nuclear localization of β -catenin in anaplastic thyroid carcinoma. *Cancer Res* 1999;59:1811–5.
- Quiros RM, Ding HG, Gattuso P, Prinz RA, Xu X. Evidence that one subset of anaplastic thyroid carcinomas are derived from papillary carcinomas due to BRAF and p53 mutations. *Cancer* 2005;103:2261–8.
- Rossi D, Zlotnik A. The biology of chemokines and their receptors. *Annu Rev Immunol* 2000;18:217–42.
- Zlotnik A. Chemokines and cancer. *Int J Cancer* 2006;119:2026–9.
- Muller A, Homey B, Soto H, et al. Involvement of chemokine receptors in breast cancer metastasis. *Nature* 2001;410:50–6.
- Burger JA, Kipps TJ. CXCR4: a key receptor in the crosstalk between tumor cells and their microenvironment. *Blood* 2006;107:1761–7.
- Balkwill F. The significance of cancer cell expression of the chemokine receptor CXCR4. *Semin Cancer Biol* 2004;14:171–9.
- Hwang JH, Hwang JH, Chung HK, et al. CXCR4 chemokine receptor 4 expression and function in human anaplastic thyroid cancer cells. *J Clin Endocrinol Metab* 2003;88:408–16.
- Castellone MD, Guarino V, De Falco V, et al. Functional expression of the CXCR4 chemokine receptor is induced by RET/PTC oncogenes and is a common event in human papillary thyroid carcinomas. *Oncogene* 2004;23:5958–67.
- Salvatore G, De Falco V, Salerno P, et al. BRAF is a therapeutic target in aggressive thyroid carcinoma. *Clin Cancer Res* 2006;12:1623–9.
- Carlomagnò F, Vitagliano D, Guida T, et al. Efficient inhibition of RET/papillary thyroid carcinoma oncogenic kinases by 4-amino-5-(4-chloro-phenyl)-7-(*t*-butyl)-pyrazolo[3,4-*d*]pyrimidine (PP2). *J Clin Endocrinol Metab* 2003;88:1897–902.
- Basolo F, Giannini R, Toniolo A, et al. Establishment of a non-tumorigenic papillary thyroid cell line (FB-2) carrying the RET/PTC1 rearrangement. *Int J Cancer* 2002;97:608–14.
- Inokuchi N, Zeki K, Morimoto I, et al. Stimulatory effect of interleukin-1 α on proliferation through a Ca²⁺/calmodulin-dependent pathway of a human thyroid carcinoma cell line, NIM 1. *Jpn J Cancer Res* 1995;86:670–6.
- Vitagliano D, Portella G, Troncone G, et al. Thyroid targeting of the N-ras(Gln61Lys) oncogene in transgenic mice results in follicular tumors that progress to poorly differentiated carcinomas. *Oncogene* 2006;25:5467–74.
- Powell DJ, Jr., Russell J, Nibu K, et al. The RET/PTC3 oncogene: metastatic solid-type papillary carcinomas in murine thyroids. *Cancer Res* 1998;58:5523–8.
- Russell JP, Powell DJ, Cunnane M, et al. The TRK-T1 fusion protein induces neoplastic transformation of thyroid epithelium. *Oncogene* 2000;19:5729–35.
- Ledent C, Dumont J, Vassart G, Parmentier M. Thyroid adenocarcinomas secondary to tissue-specific expression of simian virus-40 large T-antigen in transgenic mice. *Endocrinology* 1991;129:1391–401.
- Ganju RK, Brubaker SA, Meyer J, et al. The α -chemokine, stromal cell-derived factor-1 α , binds to the transmembrane G-protein-coupled CXCR-4 receptor and activates multiple signal transduction pathways. *J Biol Chem* 1998;273:23169–75.
- Peng SB, Peek V, Zhai Y, et al. Akt activation, but not extracellular signal-regulated kinase activation, is required for SDF-1 α /CXCR4-mediated migration of epitheloid carcinoma cells. *Mol Cancer Res* 2005;3:227–36.
- De Clercq E. Potential clinical applications of the CXCR4 antagonist bicyclam AMD3100. *Mini Rev Med Chem* 2005;5:805–24.
- Orimo A, Gupta PB, SgROI DC, et al. Stromal fibroblasts present in invasive human breast carcinomas promote tumor growth and angiogenesis through elevated SDF-1/CXCL12 secretion. *Cell* 2005;121:335–48.
- Pavelic K, Dedivitis RA, Kapitanovic S, et al. Molecular genetic alterations of FHIT and p53 genes in benign and malignant thyroid gland lesions. *Mutat Res* 2006;599:45–57.
- Helbig G, Christopherson KW II, Bhat-Nakshatri P, et al. NF- κ B promotes breast cancer cell migration and metastasis by inducing the expression of the chemokine receptor CXCR4. *J Biol Chem* 2003;278:21631–8.
- Visconti R, Cerutti J, Battista S, et al. Expression of the neoplastic phenotype by human thyroid carcinoma cell lines requires NF κ B p65 protein expression. *Oncogene* 1997;15:1987–94.
- Pacifico F, Mauro C, Barone C, et al. Oncogenic and anti-apoptotic activity of NF- κ B in human thyroid carcinomas. *J Biol Chem* 2004;279:54610–9.
- Palona I, Namba H, Mitsutake N, et al. BRAFV600E promotes invasiveness of thyroid cancer cells through nuclear factor κ B activation. *Endocrinology* 2006;147:5699–707.
- Rubin JB, Kung AL, Klein RS, et al. A small-molecule antagonist of CXCR4 inhibits intracranial growth of primary brain tumors. *Proc Natl Acad Sci U S A* 2003;100:13513–8.
- Yang L, Jackson E, Woerner BM, Perry A, Piwnicka-Worms D, Rubin JB. Blocking CXCR4-mediated cyclic AMP suppression inhibits brain tumor growth *in vivo*. *Cancer Res* 2007;67:651–8.
- Hendrix CW, Collier AC, Lederman MM, et al. AMD3100 HIV Study Group. Safety, pharmacokinetics, and antiviral activity of AMD3100, a selective CXCR4 receptor inhibitor, in HIV-1 infection. *J Acquir Immune Defic Syndr* 2004;37:1253–62.

Acknowledgments

Received 3/7/2007; revised 7/26/2007; accepted 9/28/2007.

Grant support: Associazione Italiana per la Ricerca sul Cancro and E.C. Contract 03695 (GenRisk-T). V. De Falco was a fellow of the Dipartimento di Biologia e Patologia Cellulare e Molecolare of the University of Naples. V. Guarino was a fellow of the Associazione Italiana per la Ricerca sul Cancro.

The costs of publication of this article were defrayed in part by the payment of page charges. This article must therefore be hereby marked *advertisement* in accordance with 18 U.S.C. Section 1734 solely to indicate this fact.

We thank F. Curcio for the P5 and HTU8 cells; H. Zitzelsberger for the S11T, S77T, and S147T; J. Dumont for animals expressing the SV40 transgene; and S. Sequino for excellent assistance in animal care and manipulation.

Attached manuscript #4

Nappi TC, **Salerno P**, et al. Identification of polo-like kinase 1 as a potential therapeutic target in anaplastic thyroid carcinoma.
Manuscript in preparation.

Identification of polo-like kinase 1 as a potential therapeutic target in anaplastic thyroid carcinoma

Tito Claudio Nappi, Paolo Salerno, et al.

Dipartimento di Biologia e Patologia Cellulare e Molecolare "L. Califano" c/o Istituto di Endocrinologia ed Oncologia Sperimentale del CNR, Università "Federico II", Naples, 80131, Italy; Dipartimento di Studi delle Istituzioni e dei Sistemi Territoriali, Università "Parthenope", Naples, 80133, Italy.

Running Title: PLK1 targeting in ATC

Key words: thyroid cancer, kinase, p53, PLK1, proliferation

Address correspondence to: Massimo Santoro, Dipartimento di Biologia e Patologia Cellulare e Molecolare, via. S. Pansini 5, 80131 Naples, Italy. Tel: +39 081 7463056; Fax: +39 081 7463037; e-mail: masantor@unina.it.

Abstract

Anaplastic thyroid carcinoma (ATC) is one of the most aggressive and chemoresistant type of cancer. The serine/threonine kinase Polo-like kinase 1 (PLK1), a key regulator of multiple steps during mitotic progression, is highly expressed in ATC. Here we used BI 2536, a potent small molecule PLK1 inhibitor, on a panel of ATC and normal thyroid follicular cell lines. Our data show that ATC cells are addicted to high levels of PLK1 activity for proliferation and viability. Upon treatment with nanomolar doses of BI 2536, ATC cells progressed normally through S phase but underwent massive apoptosis thereafter, directly from mitotic arrest. Immunofluorescence microscopy, immunoblot and flow cytometry analysis showed that, upon PLK1 blockade, ATC cells arrested in prometaphase with a 4N-DNA content. Treated ATC cells accumulated phosphohistone H3 and displayed characteristic mitotic (*Polo*) spindle aberrations. Normal thyroid cells were 3-13 fold less susceptible to BI 2536-induced cell cycle effects compared to ATC cells. These findings identify PLK1 as a promising target for the molecular therapy of ATC.

Introduction

Anaplastic (undifferentiated) thyroid carcinoma (ATC) is the most aggressive thyroid tumor and ranks among the most lethal human malignancies, with a median survival from diagnosis of ~ 4-12 months (1-3). Despite accounting for only 2-5% of all thyroid tumors, ATC is responsible for more than half of the deaths attributed to thyroid cancer (1-3). ATC usually presents during the 6th to 7th decade of life as a rapidly enlarging neck mass that extends locally, compresses the adjacent structures and tends to disseminate to regional nodes and distant sites (1-3). Multimodal therapy, including surgery, chemotherapy and radiotherapy, does not change the natural course of the disease; thus, treatment of ATC has often only palliative purposes (1-3). Such a dismal outcome demands for the development of novel treatment strategies.

Several genetic alterations involved in the pathogenesis of ATC are known. Some of them, namely point mutations in *RAS* and *BRAF* (4-8) and point mutations or gene amplification of *PIK3CA* (9, 10), are found not only in ATC but also in well-differentiated (papillary-PTC or follicular-FTC) carcinomas, suggesting that ATC may develop secondary to neoplastic progression of well-differentiated thyroid cancers. Conversely, *p53* mutations are rarely seen in well-differentiated lesions (<10%) whereas they occur in 67-88% of ATC (4, 5). Other mechanisms, besides gene mutation, may functionally impair *p53* in ATC (11, 12).

We have recently identified a gene expression signature associated with the high proliferative and aneuploid ATC phenotype (13). Such expression profile features up-regulation of Polo-like kinase 1 (PLK1) (13). PLK1 belongs to the *Polo* family of serine/threonine kinases, that

also includes PLK2, 3 and 4 (14). PLK1 plays a pivotal role in several G2 and M-phase related events, i.e., centrosome maturation, γ -tubulin association with centrosome and microtubule nucleation, bipolar spindle formation, CDC2 (CDK1)-cyclin B activation, anaphase-promoting complex/cyclosome (APC/C) activation by direct APC phosphorylation and by inactivation of the APC/C inhibitor Emi1, chromosome segregation and cytokinesis (14-17). Consistent with its prominent role in G2/M phase, PLK1 expression and activity is low throughout G0, G1 and S phase, and then rise in G2 and peaks during M phase (15).

PLK1 is overexpressed in several cancer types and its up-regulation often correlates with poor prognosis (14-16). Adoptive overexpression of PLK1 causes NIH 3T3 cell transformation, while its depletion/inactivation by a variety of methods (antisense oligonucleotides, small interfering RNA and dominant negative constructs) leads to mitotic arrest and cell death (18-21). Therefore, PLK1 has been envisaged as a potential target in cancer therapy, and PLK1 kinase inhibitors are currently being evaluated in preclinical and clinical studies for various cancer types (17, 22-28).

BI 2536 is a dihydropteridinone compound that inhibits PLK1 activity in a ATP-competitive manner (17, 22). BI 2536 inhibited PLK1 with high potency (half-maximal inhibitory concentration $-IC_{50}$ -of 0.83 nM); it showed a $\geq 10,000$ -fold selectivity relative to a panel of 63 other protein kinases and equipotently blocked human, rat and mouse PLK1 (22). Here, we show that BI 2536 selectively induces mitotic arrest and apoptotic death of ATC cells, suggesting that targeting PLK1 could be pursued as a novel strategy in the treatment of ATC.

Materials and Methods

Compound. BI 2536, 4-((R)-8-Cyclopentyl-7-ethyl-5-methyl-6-oxo-5,6,7,8-tetrahydro-pteridin-2-ylamino)-3-methoxy-N-(1-methyl-piperidin-4-yl)-benzamide, was provided by Boehringer Ingelheim Austria GmbH (Wien, Austria). BI 2536 was dissolved in dimethyl sulfoxide (DMSO) at a concentration of 10 mM and stored at – 80°C. Vehicle alone was used as a control.

Cell cultures. The human ATC cell lines CAL62 (29), ARO (5), SW1736 (30), and the poorly differentiated thyroid carcinoma cell line NPA (5) were grown in Dulbecco's modified Eagle's medium (DMEM) (Invitrogen, Groningen, The Netherlands) containing 10% fetal bovine serum. The Fischer rat-derived differentiated thyroid follicular cell line PC Cl 3 (hereafter "PC") was grown in Coon's modified Ham F12 medium supplemented with 5% calf serum and a mixture of six hormones (6H), including thyrotropin (10mU/ml), hydrocortisone (10nM), insulin (10µg/ml), apo-transferrin (5µg/ml), somatostatin (10ng/ml), and glycyl-histidyl-lysine (10ng/ml) (Sigma-Aldrich, St. Louis, MO, USA). For cell proliferation assays, 5×10^4 cells were plated in 35-mm dishes. The day after plating, BI2536 or vehicle was added. Cells were counted in triplicate every day. Cell counts after 72 hours treatment were used for dose-response curves and for half maximal effective concentrations (EC_{50}) calculation (Graph Pad InStat software program, version 3.06.3, San Diego, CA).

Protein studies. Immunoblotting experiments were performed according to standard procedures. Briefly, cells were harvested and lysed in a buffer containing 50 mM HEPES (pH 7.5), 1% Triton X-100, 50 mM NaCl, 5 mM EGTA, 50 mM NaF, 20 mM sodium

pyrophosphate, 1 mM sodium vanadate, 2 mM PMSF, and 1 µg/ml aprotinin. After clarification, lysates containing comparable amounts of proteins, estimated by a modified Bradford assay (Bio-Rad, Munich, Germany), were subjected to immunoblot. Immune complexes were detected with the enhanced chemiluminescence kit (Amersham Pharmacia Biotech, Piscataway, NJ).

Antibodies. Anti-PLK1 monoclonal antibody was from Zymed Laboratories (San Francisco, CA); monoclonal anti- α -tubulin was from Sigma-Aldrich; anti-cyclin B1 and anti-geminin (FL-209) polyclonals were from Santa Cruz Biotechnology (Santa Cruz, CA); anti-cleaved (Asp175) caspase-3 p17 and p19 fragments polyclonal (5A1) and monoclonal anti-phospho-histone H3 (Ser10) (6G3) were from Cell Signaling Technology, Inc. (Beverly, MA); anti-PARP [Poly (ADP-ribose) Polymerase] monoclonal antibody, which detects full-length PARP and the large fragment (89 kDa) produced by caspase cleavage, was from BD Biosciences (San Jose, CA). Secondary anti-mouse and anti-rabbit antibodies coupled to horseradish peroxidase were from Bio-Rad.

Immunofluorescence. Cells, fixed with 3% paraformaldehyde and permeabilized with 0.2% Triton X-100, were incubated with anti- α -tubulin or anti-phospho-histone H3 antibodies for 45 min at 37°C. Washed coverslips were then incubated with fluoresceine or rhodamine conjugated secondary antibodies (Jackson ImmunoResearch, West Grove, PA) for 30 min at 37°C. After 5 min DAPI counterstaining and coverslips mounting, cells were observed with a Zeiss Axioskop 2 microscope (Zeiss, Gottingen, Germany).

Cell cycle analysis. CAL62 cells were synchronized at the G1/S boundary by double thymidine block. Briefly, exponentially growing cells were treated with thymidine (4 mM) (Sigma) for 16 hours, washed thrice and incubated in normal growth medium for 6 hours and then again with thymidine for 14 hours. Released G1/S synchronized cells or unsynchronized cells were incubated with BI 2536 or vehicle. At the indicated time intervals, cells were harvested and fixed in 70% ethanol for 4 hours. After washing with PBS, cells were treated with RNase A (100 U/ml) and stained with propidium iodide (25 µg/ml) (Sigma) for 30 min. Samples were analyzed with a CyAn ADP flow cytometer interfaced with the Summit V4.2 software (DakoCytomation, Carpinteria, CO).

Statistical analysis. The two-tailed unpaired Student's t test was used for statistical analysis. All *p* value were two sided and differences were significant when $p < 0.05$. Statistical analyses were carried out using the Graph Pad InStat software program (version 3.06.3, San Diego, CA).

Results

BI 2536 reduces viability of ATC and PDC cells.

We used ATC cell lines CAL62, SW1736, ARO and the poorly-differentiated carcinoma (PDC) cell line NPA. These cells overexpress PLK1 (13) and have varied patterns of chromosome aberrations (30) and oncogene mutations: ARO, SW1736 and NPA, but not CAL62, harbour the BRAF V600E mutation; all of them have *p53* gene alterations (ARO, CAL62 and NPA are *p53* mutated while SW1736 are negative for *p53* expression) (5, 13, 30). Cells were treated with BI 2536 over a 1000-fold concentration range (starting at 0.1 nM) and counted every day. Vehicle alone was used as a control. Fig. 1 shows the average result of three independent experiments. BI 2536 treatment caused a significant ($p < .0001$) reduction of viability in the cancer cell lines. After 72 hours treatment with 5 (CAL62) or 10 (SW1736, ARO and NPA) nM BI 2536 virtually no viable cell remained in culture dishes. Half maximal effective concentrations (EC_{50}) was of 1.4 nM, 3.2 nM, 5.8 nM, 5.9 nM for CAL62, SW1736, ARO and NPA cells respectively. To analyse BI 2536 effects on non-transformed cycling thyroid cells, we used normal thyroid follicular PC cells. BI 2536 showed an EC_{50} value for PC cells (17.8 nM) that was 3-13-fold higher compared to ATC and PDC cells ($p < .0001$) (Fig. 1).

BI 2536 induces prometaphase arrest and apoptotic death in ATC cells.

To investigate the mechanisms of cell viability reduction upon BI 2536 treatment, exponentially growing CAL62 and SW1736 cells were treated with BI 2536 at the lowest effective concentration as estimated by the cell viability assays, and cell cycle profile was analyzed by flow cytometry, immunofluorescence microscopy and immunoblot. Vehicle was

used as a negative control. As shown in Fig. 2A, starting at 12 hours treatment, 5 and 10 nM BI 2536 increased the 4*N*-DNA fraction in CAL62 and SW1736 cells, respectively. This was followed at 36 and 48 hours by the appearance of a sub-G1 peak (at 48 hours, 20 % vs 0.67% in vehicle-treated cells for CAL62 and 6.15 vs 1.7 in vehicle-treated cells for SW1736), indicative of apoptosis. Cell fractions with a >4*N* DNA peak were hardly detectable, indicating that the treatment did not cause reduplication of unseparated sister chromatids after failure of cytokinesis (see also below) (Fig 2A). None of the aforementioned effects could be seen in PC cells upon incubation with 10 nM BI 2536 (Fig. 2A). In normal cells, only treatment with ≥ 50 nM concentrations of the compound gave results similar to those observed in ATC cells (data not shown).

The accumulation of cells with a 4*N* DNA content was indicative of a cell cycle block in either G2 or M phase. To distinguish between the two possibilities, BI 2536 or DMSO-treated cells were either stained with anti-phospho-histone H3 for immunofluorescence or analyzed by immunoblot for cyclin B1. Also, PLK1 protein levels were examined as surrogate G2/M phase marker. The percentage of mitotic (phospho-histone H3 positive) cells was increased in BI 2536-treated ATC, but not PC cells, as soon as 12 hours after treatment, peaking at 24 hours and decreasing thereafter (Fig. 2B). Both cyclin B1 and PLK1 protein levels underwent analogous changes upon BI 2536 treatment (Fig. 2C). These findings indicated that the compound caused M phase arrest of ATC cells. Concentrations ≥ 50 nM were required to elicit similar responses in normal PC cells (data not shown).

The reduction of phospho-histone H3 positive cells and cyclin B1 levels at the 36 hours time point could be due to the onset of apoptosis directly from mitosis; alternatively, upon the 4*N*

block cells may attempt to start a novel cycle and reduplicate their genome. As mentioned above, this second hypothesis could be ruled-out given the absence of $>4N$ DNA peaks at flow cytometry. On the other hand, two biochemical markers of apoptosis, i.e. cleaved products of caspase-3 and PARP (poly ADP-ribose polymerase), were visible by immunoblot in both ATC cell lines treated with BI 2536 (Fig. 2C). In CAL62 cells, which displayed a major reduction of cyclin B1 levels after 36 hours treatment, cleaved caspase-3 and PARP fragments were detectable as soon as 24 hours after incubation with BI 2536, and peaked at 36 and 48 hours, respectively. SW1736 cells, which showed modest reduction of cyclin B1 after 36 hours treatment, had a milder and delayed increase of the apoptotic markers compared to CAL62 cells. Taken together, these findings suggest that upon PLK1 inhibition, ATC cells rapidly undergo apoptosis directly from mitosis.

To further characterize the cell cycle effects of PLK1 inhibition, we synchronized CAL62 cells at the G1/S transition by double thymidine block; cells were released in the presence of 5 nM BI 2536 or vehicle and analyzed by flow cytometry and immunoblot at different time points. As shown in Fig. 3A, BI 2536-treated cells progressed normally through S phase and then arrested in G2/M (at 11 hours). Sub-G1 DNA fractions became detectable after 29-48 hours from release (Fig. 3A). Instead, cell released in control medium normally progressed through S and G2/M and then re-entered a new G1 phase (Fig. 3A). Western blot analysis showed consistent results: in vehicle-treated cells, cyclin B1 was downregulated after 24 hours from release as cells had exited mitosis. Instead, in cells treated with BI 2536, cyclin B1 downregulation was delayed until 35 hours because of the G2/M arrest (Fig. 3B). In treated cells, cleaved caspase-3 fragments were clearly detectable after 24 hours treatment, again suggesting apoptosis may occur directly from mitosis. Moreover, despite a reduction of cyclin

BI levels at the latest time points, BI 2536-treated cells failed to downregulate geminin (Fig. 3B), an event that is required to start a new DNA duplication cycle (31). This indicates that treated cells remained unlicensed for replication, ruling-out the possibility of reduplication of undivided cells.

BI 2536 induces characteristic mitotic-spindle aberrations in ATC cells. Depletion or inactivation of PLK1 has been reported to induce characteristic mitotic-spindle aberrations in several cancer cells (14-17, 19, 21, 22, 24). To further prove that BI 2536 effects in ATC cells were mediated by PLK1 inhibition, we asked whether treatment phenocopied PLK1 knockdown. Exponentially growing CAL62 and SW1736 cells were treated with BI 2536 (5 and 10 nM, respectively), collected at different time intervals and stained for immunofluorescence with anti- α -tubulin to visualize mitotic spindle and DAPI to visualize DNA. Consistent with the results obtained by anti-phospho-histone H3 staining, both ATC cell lines showed an accumulation of mitotic cells in a prometaphase state starting at 12 hours and peaking at 24 hours; in treated cells, anaphase and cytokinesis figures were virtually absent (Fig. 4A). No increase in the mitotic fraction could be seen in control PC cells upon treatment with 10 nM BI 2536, and all the mitotic phases were normally represented (Fig. 4A).

A characteristic phenotype in inhibitor-treated ATC cells, but not PC cells, was the presence of aberrant monopolar (*Polo*) spindles, a hallmark of PLK1 depletion/inactivation (Fig. 4B). Such *Polo* spindles are monoastral microtubule arrays nucleated from a single organizing centre and containing unseparated centrosomes circled by a ring of condensed chromosomes (15). Monopolar spindles seem to occur secondary to a defect in timely organization of

microtubule asters at prophase, followed by the instantaneous polymerization of mitotic microtubules in a monopolar aster only after nuclear envelope breakdown (17). They occurred in BI 2536-treated ATC cells along with other aberrant spindle phenotypes, like multipolar spindles and spindles without a clear spatial organization (disorganized) that accumulated with time (Fig. 4B). After 36 hours treatment, albeit only very few mitotic cells could be seen on coverslips, virtually 100% of them had an abnormal spindle. Moreover, after 36 and 48 hours treatment, in parallel with the reduction of phospho-histone H3-positive cells, cyclin B1 levels and increased levels of caspase-3 and PARP fragments, most of the remaining ATC cells either showed a nuclear apoptotic morphology or harbored decondensed/partially condensed nuclei with gross morphological aberrations (Fig. 4A). These are hallmarks of the so called mitotic catastrophe, a form of cell death taking place from within mitosis. In normal cells, a similar effect could only be obtained with compound doses ≥ 50 nM (data not shown).

Discussion

ATC displays overexpression of genes controlling multiple steps involved in mitotic progression, a signature that included the up-regulation of PLK1 (13). Targeting key components of the mitotic machinery has been envisaged as a possible strategy in cancer treatment. Among them, PLK1 has emerged as a promising candidate (15, 16). PLK1 depletion/inhibition reduces survival of several cancer cells and inhibits tumor growth *in vivo* in xenograft models (19-27). It is feasible that, based on the specific role of PLK1 in mitosis, its inhibition may avoid some of the side effects associated with current anti-mitotic agents (like taxanes and *Vinca* alkaloids derivatives) that, by targeting microtubules, affect many critical cellular processes (e.g. axonal transport) unrelated to mitosis (15, 16).

Here, we took advantage of the high potency and selectivity of BI 2536, a compound able to inhibit PLK1 activity at low nanomolar concentrations, to exploit PLK1 requirement of ATC cells. ATC cells proved to be extremely sensitive to PLK1 inactivation. Concentrations as low as 5-10 nM of BI 2536 were sufficient to cause prometaphase arrest with characteristic spindle aberrations. This likely caused mitotic entrapment, activation of the spindle assembly checkpoint and mitotic cell death (16). These effects are hallmarks of PLK1 inhibition, suggesting that the compound is exerting its effects in ATC cells by blocking PLK1 and not other targets (15-17). It is known that BI 2536 also affects the activities of PLK2 and PLK3 albeit at higher concentrations (IC_{50} of 3.5 and 9.0 nM, respectively) than PLK1 (17, 22). However, PLK2 and 3 are thought to function in G1 and S phases of the cell cycle, phases that were not significantly affected by BI 2536 treatment of ATC cells. Interestingly, polyploidy, a major concern when targeting kinases involved in mitosis/cytokinesis as it may promote

tumorigenesis (16, 32-34) was not detected, and the possibility of reduplication was ruled-out. Instead, this potentially harmful phenomenon was reported with Aurora B inhibitors that silenced the mitotic spindle checkpoint, causing precocious mitotic exit and polyploidy (16).

Importantly, in agreement with our previous observations on siRNA-induced PLK1 depletion (13), normal thyroid follicular cells proved to be less susceptible to BI 2536-induced PLK1 inactivation (with a 3-13 fold difference in potency) compared to ATC cells, suggesting the possibility of achieving a therapeutic window *in vivo*. The reason for such different PLK1 requirement remains unknown. Several reports have indicated that p53 protein is stabilized in PLK1-depleted cancer cells (20, 21), p53-depletion enhances the sensitivity of various cell types to PLK1 knock-down (21) and PLK1 expression is negatively controlled by p53 also in ATC cells (13, 15). Thus, one possibility is that p53 function may be required to survive PLK1 depletion and the frequent impairment of p53 would make ATC cells particularly susceptible to PLK1 inhibition. Importantly, all of the ATC cell lines used in this study either harbour *p53* gene mutations (ARO, CAL62 and NPA) or are negative for wild type *p53* expression (SW1736) (5, 13, 30). Another possibility is that high proliferation rate and chromosomal instability could turn mitosis and cytokinesis into critical steps in ATC cell cycle progression. Fine-tuning of the events occurring at such steps would then become vital, making ATC cells (similarly to other highly malignant cancer cells) extremely dependent on the high concentrations of functional PLK1 for faithful bipolar spindle assembly and mitosis. Consistent with this hypothesis, at low nM doses of BI 2536, ATC, but not normal, cells exert typical defects in centrosome maturation with the formation of monoastral spindles. Instead, the threshold of PLK1 activity to sustain a normal mitotic cycle was apparently lower in

normal PC cells, where the same mitotic phenotype was observed only at high doses of BI 2536.

Whatever the mechanism, our findings suggest that PLK1 might be exploited as a molecular target in ATC therapy and BI 2536, that has already progressed into phase I clinical trials in patients with advanced solid tumors (28), or other specific PLK1 inhibitors could be examined in clinical studies for the treatment of such deadly human cancer.

Acknowledgements

We thank G. Vecchio and A. Fusco for continuous support. We thank C.H. Heldin for SW1736 cells. This study was supported by the Associazione Italiana per la Ricerca sul Cancro (AIRC), the Istituto Superiore di Oncologia (ISO), the Italian Ministero della Salute, and Ministero dell'Università e della Ricerca (MiUR) and the Project Applicazioni Biotechnologiche (MoMa). PS was supported by a the NOGEC (Naples OncoGENomic Center) fellowship.

References

1. Are C, Shaha AR. Anaplastic thyroid carcinoma: biology, pathogenesis, prognostic factors, and treatment approaches. *Ann Surg Oncol* 2006;13:453-64.
2. Pasiaka JL. Anaplastic thyroid cancer. *Curr Opin Oncol* 2003;15:78-83.
3. Ordóñez N, Baloch Z, Matias-Guiu X, et al. Undifferentiated (anaplastic) carcinoma. In: *Tumours of Endocrine Organs, World Health Organization Classification of Tumors*. DeLellis RA, Lloyd RV, Heitz PU and Eng C. 2004 (eds), p. 77-80.
4. Fagin JA, Matsuo K, Karmakar A, et al. High prevalence of mutations of the p53 gene in poorly differentiated human thyroid carcinomas. *J Clin Invest* 1993; 91:179–84.
5. Kondo T, Ezzat S, Asa SL. Pathogenetic mechanisms in thyroid follicular-cell neoplasia. *Nat Rev Cancer* 2006;6:292–306.
6. Groussin L, Fagin JA. Significance of BRAF mutations in papillary thyroid carcinoma: prognostic and therapeutic implications. *Nat Clin Pract Endocrinol Metab* 2006;2:180-1.
7. Nikiforov YE. Genetic alterations involved in the transition from well-differentiated to poorly differentiated and anaplastic thyroid carcinomas. *Endocr Pathol Winter* 2004;15:319–27.
8. Xing M. BRAF Mutation in Papillary Thyroid Cancer: Pathogenic Role, Molecular Bases, and Clinical Implications. *Endocr Rev* 2007 Oct 16; [Epub ahead of print]
9. Garcia-Rostan G, Costa AM, Pereira-Castro I, et al. Mutation of the PIK3CA gene in Anaplastic Thyroid Cancer. *Cancer Res* 2005;15:10199–207.
10. Wu G, Mambo E, Guo Z, et al. Uncommon mutation, but common amplifications, of the PIK3CA gene in thyroid tumors. *J Clin Endocrinol Metab* 2005;90:4688–93.
11. Pierantoni GM, Rinaldo C, Mottolese M, et al. High-mobility group A1 inhibits p53 by cytoplasmic relocalization of its proapoptotic activator HIPK2. *J Clin Invest*

- 2007;117:693–702.
12. Malaguarnera R, Vella V, Vigneri R, Frasca F. p53 family proteins in thyroid cancer. *Endocr Relat Cancer* 2007;14:43–60.
 13. Salvatore G, Nappi TC, Salerno P, et al. A cell proliferation and chromosomal instability signature in anaplastic thyroid carcinoma. *Cancer Res* 2007;67:10148-58.
 14. Barr FA, Silljé HH, Nigg EA. Polo-like kinases and the orchestration of cell division. *Nat Rev Mol Cell Biol* 2004;5:429-40.
 15. Strebhardt K, and Ullrich A. Targeting polo-like kinase 1 for cancer therapy. *Nat Rev Cancer* 2006;6:321–30.
 16. Plyte S, Musacchio A. PLK1 inhibitors: setting the mitotic death trap. *Curr Biol* 2007;17:R280-3.
 17. Lenart P, Petronczki M, Steegmaier M, et al. The small-molecule inhibitor BI 2536 reveals novel insights into mitotic roles of Polo-like kinase 1. *Curr Biol* 2007;17:304-15.
 18. Smith MR, Wilson ML, Hamanaka R, et al. Malignant transformation of mammalian cells initiated by constitutive expression of the polo-like kinase. *Biochem Biophys Res Commun* 1997;234:397-405.
 19. Spänkuch-Schmitt B, Bereiter-Hahn J, Kaufmann M, et al. Effect of RNA silencing of polo-like kinase-1 (PLK1) on apoptosis and spindle formation in human cancer cells. *J Natl Cancer Inst* 2002; 94:1863-77.
 20. Liu X, Erikson RL. Polo-like kinase (Plk) 1 depletion induces apoptosis in cancer cells. *Proc Natl Acad Sci* 2003;100:5789-94.
 21. Liu X, Lei M, Erikson RL. Normal cells, but not cancer cells, survive severe Plk1 depletion. *Mol Cell Biol* 2006; 26:2093–108.
 22. Steegmaier M, Hoffmann M, Baum A, et al. BI 2536, a potent and selective inhibitor of

- Polo-like kinase 1, inhibits tumor growth in vivo. *Curr Biol* 2007;17:316-22.
23. Gumireddy K, Reddy MV, Cosenza SC, et al. ON01910, a non-ATP-competitive small molecule inhibitor of Plk1, is a potent anticancer agent. *Cancer Cell* 2005;7:275–86.
 24. McInnes C, Mazumdar A, Mezna M, et al. Inhibitors of Polo-like kinase reveal roles in spindle-pole maintenance. *Nat Chem Biol* 2006;2:608-17.
 25. Peters U, Cherian J, Kim JH, Kwok BH, Kapoor TM. Probing cell-division phenotype space and Polo-like kinase function using small molecules. *Nat Chem Biol*. 2006;2:618-26.
 26. Lansing TJ, McConnell RT, Duckett DR, et al. In vitro biological activity of a novel small-molecule inhibitor of polo-like kinase 1. *Mol Cancer Ther* 2007;6:450-9.
 27. Uckun FM, Dibirdik I, Qazi S, et al. Anti-breast cancer activity of LFM-A13, a potent inhibitor of Polo-like kinase (PLK). *Bioorg Med Chem* 2007;15:800-14.
 28. Munzert G, Steinbild S, Frost A, et al. A phase I study of two administration schedules of the Polo-like kinase 1 inhibitor BI 2536 in patients with advanced solid tumors. *Journal of Clinical Oncology*, 2006 ASCO Annual Meeting Proceedings Part I. Vol 24, No. 18S (June 20 Supplement), 2006: 3069
 29. Gioanni J, Zanghellini E, Mazeau C, et al. Characterization of a human cell line from an anaplastic carcinoma of the thyroid gland. *Bull Cancer* 1991;78:1053–62.
 30. Lee JJ, Foukakis T, Hashemi J, et al. Molecular cytogenetic profiles of novel and established human anaplastic thyroid carcinoma models. *Thyroid* 2007;17:289-301.
 31. Tada S. Cdt1 and geminin: role during cell cycle progression and DNA damage in higher eukaryotes. *Front Biosci* 2007;12:1629-41.
 32. Tsvetkov LM, Tsekova RT, Xu X, et al. The Plk1 Polo box domain mediates a cell cycle and DNA damage regulated interaction with Chk2. *Cell Cycle* 2005;4:609-17.

33. Sumara I, Giménez-Abián JF, Gerlich D, et al. Roles of polo-like kinase 1 in the assembly of functional mitotic spindles. *Curr Biol* 2004;14:1712-22.
34. Fujiwara T, Bandi M, Nitta M, et al. Cytokinesis failure generating tetraploids promotes tumorigenesis in p53-null cells. *Nature* 2005;437:1043-7.
35. Guan R, Tapang P, Levenson JD, et al. Small interfering RNA-mediated polo-like kinase 1 depletion preferentially reduces the survival of p53-defective, oncogenic transformed cells and inhibits tumor growth in animals. *Cancer Res* 2005;65:2698-704.

Figure legendsFigure 1: Cell viability effects of BI 2536 in thyroid cells

The indicated cell lines were treated in triplicate with different doses of BI 2536 or vehicle (NT) and counted at the indicated time points. The average results of three independent experiments are reported; error bars represent 95% confidence intervals.

Figure 2: Cell cycle effects of BI 2536 in ATC cells

A) The indicated cell lines were treated with 5 nM (CAL62) and 10 nM (SW1736 and PC) BI 2536 or vehicle (NT) and DNA content was analyzed by flow cytometry at different time points. B) CAL62 and SW1736 ATC cells or control PC cells, grown on glass coverslips, were treated with BI 2536. At the indicated time points, cells were fixed, stained with a anti-phospho-histone H3 (Ser10) and analyzed by fluorescence microscopy. The percentage of positive cells represents the average of three experiments in which at least 500 cells were counted. Representative micrographs are shown in the insets. C) CAL62 and SW1736 cells, treated with BI 2536 or vehicle (NT), were lysed at the indicated time points and subjected to immunoblot with anti-cyclin B1 and anti-PLK1, to monitor cell cycle progression, and anti-cleaved caspase-3 antibodies (which detect only the p17 and p19 cleaved caspase-3 fragments) or anti-PARP antibodies (which detect both the intact 116 kDa and its cleaved 89 kDa fragment), to monitor apoptosis. Tubulin levels are shown for normalization. Data are representative of at least three different experiments.

Figure 3: BI 2536 effects on cell cycle synchronized ATC cells

CAL62 cells were synchronized at the G1/S transition by double thymidine block, released in the presence of 5 nM BI 2536 or DMSO and analyzed, at the indicated time points, by flow cytometry (panel A) or immunoblotted with cyclin B1, geminin and cleaved caspase-3 antibodies (panel B). Tubulin levels are shown for normalization. Data are representative of at least three different experiments.

Figure 4: Mitotic spindle defects in BI 2536-treated ATC cells

Exponentially growing PC, CAL62 and SW1736 cells were treated with BI 2536 or vehicle (NT) and stained by immunofluorescence with anti- α -tubulin (red) and DAPI (cyan) at different time points. Representative micrographs are reported in panel A and percentages of mitotic cells with monopolar (*Polo*), multipolar or grossly disorganized mitotic spindles are reported in panel B. Values refer to the average of triplicate experiments in which at least 300 mitotic cells were counted. Of note is the nuclear apoptotic morphology showed by ATC cells after 36-48 hours treatment (panel A).

Fig. 1

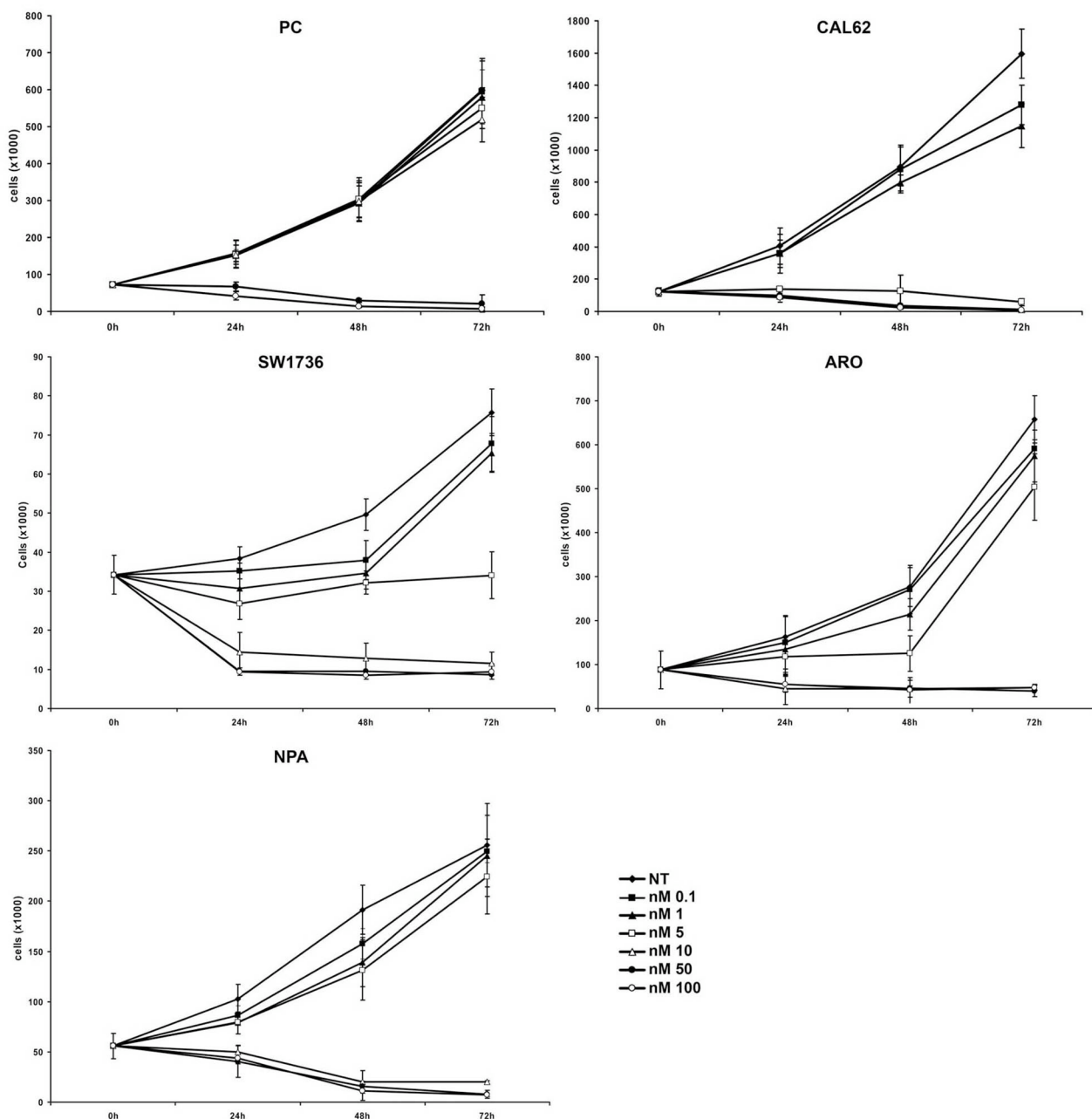


Fig. 2

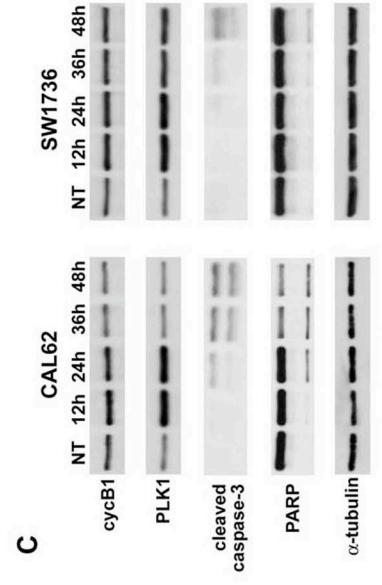
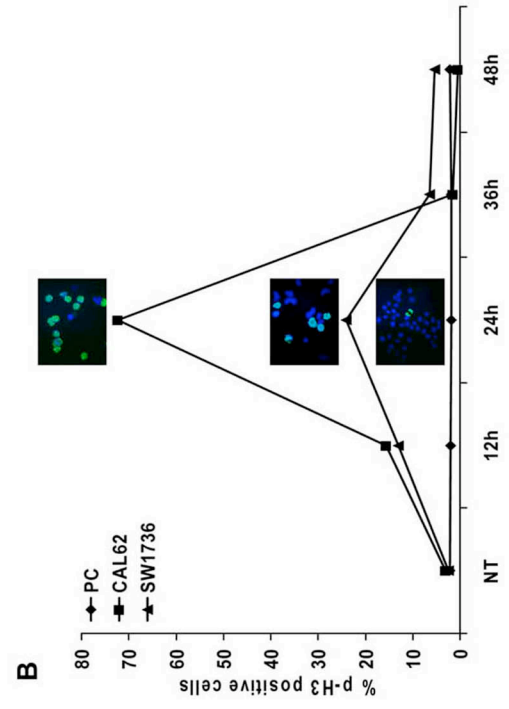
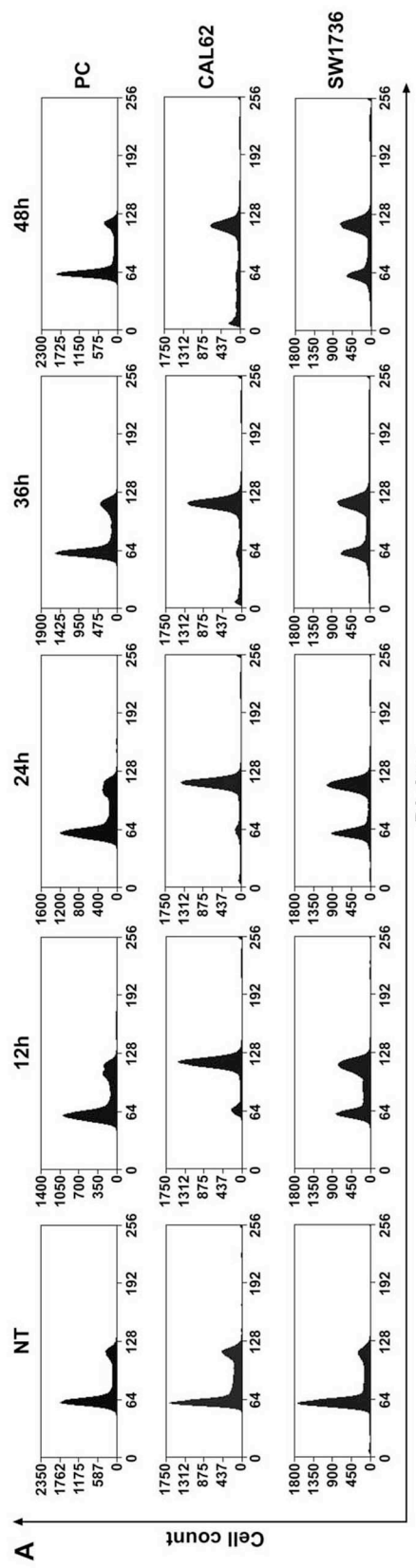


Fig. 3

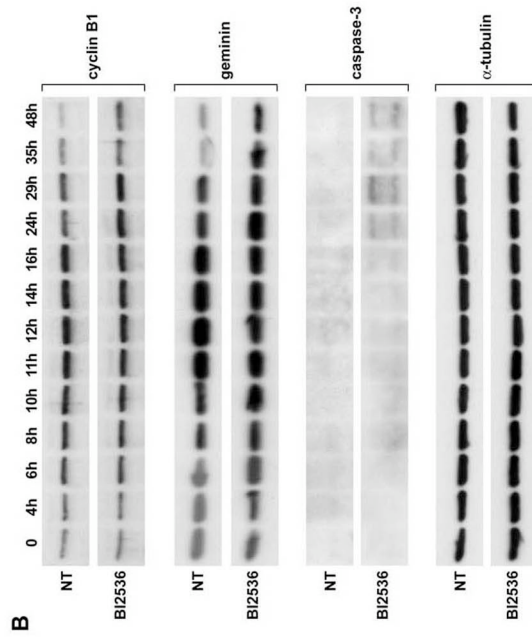
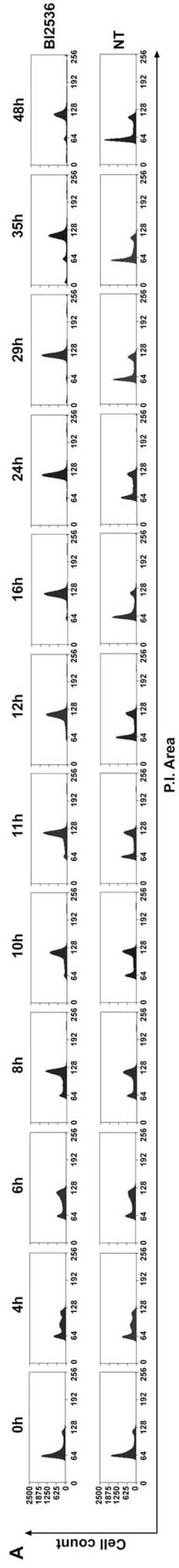
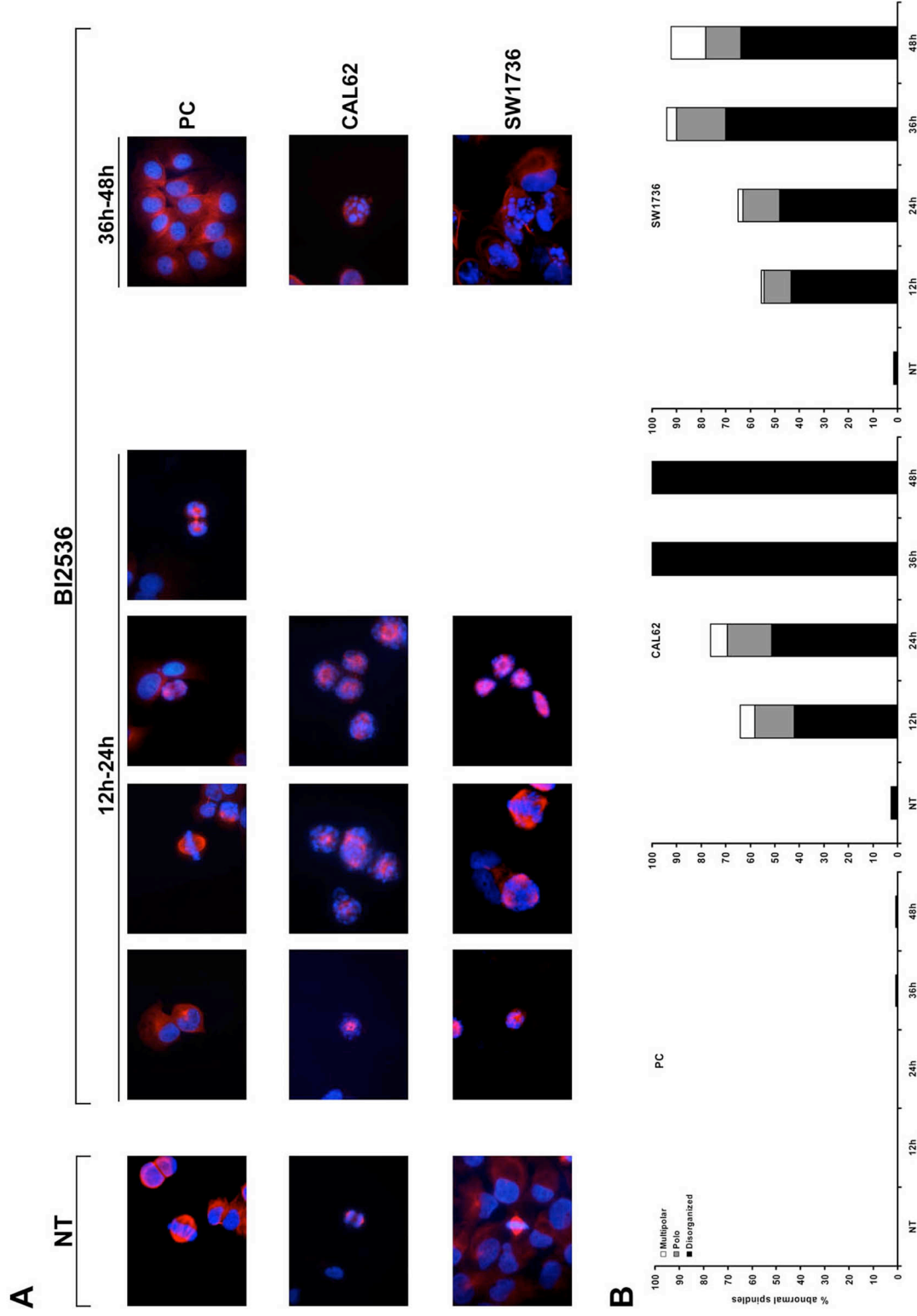


Fig. 4



Attached manuscript #5

Salerno P, Nappi TC, et al. Multiple regulatory circuits affect ERK inhibition upon MEK targeting in thyroid carcinoma cells. Manuscript in preparation.

Multiple regulatory circuits affect ERK inhibition upon MEK targeting in thyroid carcinoma cells

Paolo Salerno, Tito Claudio Nappi, et al.

Dipartimento di Biologia e Patologia Cellulare e Molecolare "L. Califano" c/o Istituto di Endocrinologia ed Oncologia Sperimentale del CNR, Università "Federico II", Naples, 80131, Italy ; Dipartimento di Studi delle Istituzioni e dei Sistemi Territoriali, Università "Parthenope", Naples, 80133, Italy .

Running Title: MEK inhibition in thyroid carcinoma

Keywords: PD0325901, thyroid cancer, negative feedback, MAPK pathway, MEK.

Address correspondence to: Massimo Santoro, Dipartimento di Biologia e Patologia Cellulare e Molecolare, via. S. Pansini 5, 80131 Naples, Italy. Tel: +39 081 7463056; Fax: +39 081 7463037; e-mail: masantor@unina.it.

ABSTRACT

Purpose: Here we have studied the consequences of MEK inhibition with the potent and selective PD0325901 compound in thyroid carcinoma cells. **Experimental design:** We used thyroid carcinoma cell lines carrying the BRAF V600E mutation to examine cell proliferation and phosphorylation levels of ERK cascade components. **Results:** PD0325901 exerted potent cytostatic effects on carcinoma cell lines, but not normal thyroid follicular cells, confirming recent published data with other MEK inhibitors. These effects were accompanied by increased p27Kip1 and p21Cip1 and decreased phosphorylated Rb levels. While inhibiting MEK-mediated phosphorylation of ERKs, PD0325901 rapidly caused increased MEK phosphorylation in the activation loop. Moreover, at compound doses close to its IC₅₀ for MEK, ERK inhibition was not durable and resumed after few hours treatment. Reduced levels of ERK-mediated inhibitory phosphorylation of CRAF and ERK-specific phosphatases (DUSP5 and MKP3) may account for the transient nature of ERK inhibition. **Conclusions:** MEK inhibition is a promising approach to reduce proliferation of BRAF mutation-positive thyroid carcinoma cells. Strategies to counteract the regulatory circuits that are elicited by the treatment need to be envisaged to further increase its efficacy.

.

INTRODUCTION

The RAS-RAF-ERK (extracellular signal regulated kinase) cascade is a highly conserved signaling module in eukaryotes, that is often targeted by oncogenic mutations. The RAS small GTPase is activated upon growth factor stimulation, and, in turn, activates RAF family (CRAF, BRAF, ARAF) serine/threonine kinases. RAFs activate MEK1/2 dual-specificity kinases through phosphorylation on Ser217/Ser221 in their activation loop. MEK1/2, in turn, activate the ERK (p44 and p42 ERKs) subgroup of MAPKs (mitogen activated protein kinases) by dual-phosphorylation on Thr202/Tyr204 within the Thr-Glu-Tyr motif in the activation loop (1, 2). MEK and ERK activation is transient and is followed by the initiation of negative feedback mechanisms that terminate the signal (1, 2). Dual-specificity phosphatases (DUSPs, also referred to as MAPK phosphatases - MKP), which are able to dephosphorylate ERKs, control intensity and duration of ERKs stimulation (3).

Thyroid carcinomas are often associated to oncogenic conversion of proteins acting in the ERK cascade (4, 5). In particular, activation of BRAF occurs in about 44% of papillary (PTC) and 25% of undifferentiated (anaplastic) (ATC) thyroid carcinomas (4-8). BRAF mutations are associated with such adverse PTC clinical features as extracapsular invasion, lymph node and distant metastases, and clinical recurrence (5-8). ATC is one of the most aggressive and chemoresistant type of cancer; multimodal therapy approaches failed so far to improve the survival of ATC patients (9, 10).

The T1799A BRAF mutation, which causes a V600E amino acid change, accounts for the vast majority of BRAF mutations in PTC and ATC. By targeting the activation loop of the

kinase, the V600E mutation strongly potentiates BRAF catalytic activity (11). Moreover, mutated BRAF is able to activate MEK also indirectly by allosterically activating CRAF through heterodimerization (11).

Solit and colleagues have shown that cancer cells bearing an activating BRAF mutation are extremely sensitive to MEK kinase inhibitors (12). Available MEK targeting agents are allosteric inhibitors, rather than competitive with ATP, a feature that may contribute to their high specificity (2, 13-15). PD98059 and U0126 were initially developed as MEK inhibitors for *in vitro* studies (2). CI-1040 was the first MEK inhibitor ($IC_{50} = 17$ nM) evaluated in clinical trials (2, 15). A structurally related molecule, AZD6244 (ARRY-142886), is a potent MEK inhibitor ($IC_{50} = 12$ nM) and entered clinical trials for various tumors (2, 15, 16). Finally, PD0325901 was recently developed as another potent MEK inhibitor ($IC_{50} = 1$ nM); phase II trials with this agent are underway (17).

MEK inhibition with U0126 inhibited proliferation of ARO and NPA thyroid carcinoma cells (18) and partially restored thyroid differentiated phenotype (19). Recently, Ball *et al* (20) and Liu *et al* (21) have studied the effects of AZD6244 and CI-1040 on thyroid carcinoma cells. MEK inhibition had potent cytostatic effects in thyroid carcinoma cells harbouring the BRAF (20, 21) or the HRAS (21) mutation but not in wild type BRAF cells. The two compounds inhibited the growth of xenograft tumors in nude mice (20, 21) and CI-1040 restored the expression of some thyroid cell differentiation markers (21).

Here we have studied the effects of PD0325901 on cell proliferation and the mechanism of PD0325901-mediated downregulation of ERK signaling in BRAF mutant thyroid carcinoma cells.

MATERIALS AND METHODS

Compounds

PD0325901 was synthesized by Pfizer Global Research and Development, Ann Arbor, MI, USA. PD0325901 was dissolved in dimethyl sulfoxide (DMSO) at a concentration of 10 mM and stored at -80°C . U0126, was purchased from Cell Signaling (Beverly, MA, USA), dissolved in DMSO at a concentration of 10 mM and stored at -20°C . Orthovanadate was purchased from Sigma-Aldrich (St. Louis, MO, USA) and used at a concentration of 100 μM .

Cell cultures

The human thyroid carcinoma cell lines ARO, FRO, NPA, BHT101, FB1, BCPAP, and SW1736 were grown in Dulbecco's modified Eagle's medium (DMEM) (Invitrogen, Groningen, The Netherlands) containing 10% fetal bovine serum. The Fischer rat-derived differentiated thyroid follicular cell lines PC Cl 3 (hereafter "PC") and FRTL5 were grown in Coon's modified Ham F12 medium supplemented with 5% calf serum and a mixture of six hormones (6H) (Sigma-Aldrich), as previously reported (22).

Cell proliferation and Flow Cytometry assays

For cell proliferation assay, 5×10^4 cells were plated in 35-mm dishes in low serum (2.5% for carcinoma cell lines and 1.25% for normal cell lines). The day after plating, PD0325901 or vehicle was added. The media was changed every 2 days and cells were counted in triplicate every day.

For flow cytometry analysis, 5×10^5 cells were treated with vehicle or PD0325901 (10 nM) in low serum and collected every 12 hours. Cells were fixed in ice-cold 70% ethanol in phosphate-buffered saline. Propidium iodide (25 $\mu\text{g}/\text{ml}$) was added in the dark, and samples were analyzed with a FACScan flow cytometer (Becton Dickinson, San Jose, CA) interfaced with a Hewlett Packard computer (Palo Alto, CA).

Protein studies

Immunoblotting experiments were performed according to standard procedures. Briefly, cells were harvested in lysis buffer (50 mM Hepes, pH 7.5, 150 mM NaCl, 10% glycerol, 1% Triton X-100, 1 mM EGTA, 1.5 mM MgCl_2 , 10 mM NaF, 10 mM sodium pyrophosphate, 1 mM Na_3VO_4 , 10 μg of aprotinin/ml, 10 μg of leupeptin/ml) and clarified by centrifugation at 10,000 g. Protein concentration was estimated with a modified Bradford assay (Bio-Rad, Munich, Germany). Antigens were revealed by an enhanced chemiluminescence detection kit (ECL, Amersham Pharmacia Biotech, Little Chalfort, UK). Signal intensity was evaluated with the Phosphor-imager (Typhoon 8600, Amersham Pharmacia Biotech) interfaced with the ImageQuant software.

Antibodies

Anti-phospho p44/42 (#9101), specific for MAPK (ERK1/2) phosphorylated at Thr202/Tyr204, anti-p44/42 (#9102), anti-phospho p90RSK (90 kDa ribosomal S6 kinase) (#9344), specific for p90RSK phosphorylated at Thr359/Ser363, anti-p90RSK (#9347), anti-phospho MEK1/2 (#9121), specific for MEK1/2 phosphorylated at Ser217/Ser221, anti-MEK1/2 (#9122), anti phospho-CRAF (#9431) specific for CRAF phosphorylated at Ser289/296/301, anti phospho Rb (#9301) specific for Rb phosphorylated at Ser795 and

anti p27Kip1 antibodies were from Cell Signaling (Beverly, MA). Anti p21Cip1 (F5) and secondary antibodies coupled to horseradish peroxidase were from Santa Cruz Biotechnology (Santa Cruz, CA).

RNA extraction and RT-PCR

Total RNA was isolated with the RNeasy Kit (Qiagen, Crawley, West Sussex, UK). One μg of RNA from each sample was reverse-transcribed with the QuantiTect[®] Reverse Transcription (Qiagen) according to manufacturer's instructions. Expression levels of ERK phosphatases DUSP-5 and MKP-3 were measured by quantitative RT-PCR, using the Human ProbeLibray[™] system (Exiqon, Denmark). PCR reactions were performed in triplicate and fold changes were calculated with the formula: $2^{-(\text{sample 1 } \Delta\text{Ct} - \text{sample 2 } \Delta\text{Ct})}$, where ΔCt is the difference between the amplification fluorescent thresholds of the mRNA of interest and the mRNA of RNA polymerase 2 used as an internal reference. Primers sequences are available upon request.

Statistical analysis

Two-tailed unpaired Student's t test (normal distributions and equal variances) were used for statistical analysis. Differences were significant when $P < 0.05$. Statistical analysis was performed using the GraphPad Prism software program (version 4, San Diego, CA, USA).

RESULTS

PD0325901 inhibits the proliferation of BRAF mutant thyroid carcinoma cells

We initially tested the effects of PD0325901 on the proliferation rate of ARO, BHT101, FRO and SW1736 ATC cell lines carrying homozygous or heterozygous BRAF V600E alleles (Fig. 1). Normal PC and FRTL5 thyrocytes were used as control. Cells were treated with different concentrations of PD0325901 or vehicle (NT) and counted every day for four days. The average results of three independent determinations are reported in Fig. 1. Treatment with PD0325901 caused a dose-dependent growth inhibition of all carcinoma cell lines with a half maximal efficacy concentration (EC_{50}) ranging from 0.4 to 5 nM; doses of 10 nM or higher had to be used to suppress ATC cell proliferation by 90%. Importantly, 50% growth inhibition was observed in normal thyrocytes only at concentrations \geq 50 nM (Fig. 1).

ARO and SW1736 cells underwent a marked G1 arrest upon PD0325901 (10 nM) treatment, starting at 24 hours and lasting up to 96 hours (Fig. 2A). No significant sub G1 fraction was detectable, indicating that the treatment did not kill thyroid carcinoma cells (Fig. 2A). PD0325901 (10 nM) did not modify cell cycle profile of normal control cells (Fig. 2A). ARO cells were treated with 1 and 10 nM PD0325901 and expression levels of p27Kip1, p21Cip1, and phospho Rb (Ser795) were determined by immunoblot at different time points. A remarkable increase in the expression levels of p27Kip1 and p21Cip1 was observed starting at 6 hours and lasting up to 24 (p27Kip1) or 48 (p21Cip1) hours upon treatment (Fig. 2B). Consistently, the phosphorylation of Rb was inhibited compared to untreated cells (Fig. 2B). Treatment with U0126, used as control, gave similar results (Fig. 2B).

Effects of PD0325901 on ERK phosphorylation in thyroid carcinoma cells

We examined the phosphorylation levels of downstream effectors of MEK, p44 and p42 ERKs, and RSK, a kinase that is phosphorylated by ERK. This was performed in the same ATC cell lines (ARO, BHT101, FRO, SW1736) used for the proliferation assays as well as in additional cell lines. These included: FB1 (an ATC cell line which carries a heterozygous BRAF V600E mutation), NPA (a poorly-differentiated PTC cell line which carries only the BRAF V600E allele) and BCPAP (a PTC cell line, which carries a heterozygous BRAF V600E mutation). After 12 hours in low serum (2.5%), cells were treated for 2 hours with different concentrations of PD0325901 or vehicle (NT) and examined by immunoblot. Treatment with PD0325901 strongly reduced the phosphorylation of ERK at the activatory sites Thr202/Tyr204 and of RSK (IC₅₀ of about 1 nM for NPA, FRO, BHT101, FB1, BCPAP and between 1 and 10 nM for ARO and SW1736) (Fig. 3). The compound also efficiently inhibited MAPK pathway phosphorylations in PC cells (Fig. 3), demonstrating that its reduced growth inhibitory activity in normal thyrocytes was not due to defective effects on the target kinase but rather to the fact that normal cells are not addicted to MEK signaling.

Transient nature of ERK inhibition in thyroid carcinoma cells

We measured time-course of ERK phosphorylation upon PD0325901 treatment in ARO cells. Phosphor-imager quantitation of three independent experiments (1 and 10 nM PD0325901) at various time points is reported in Fig. 4A, a representative immunoblot (10 nM PD0325901), performed at early times, is reported in Fig. 4B. ERK inhibition was very rapid and detected as soon as after 15 min of treatment (Fig. 4B). It was almost

complete, at both 1 and 10 nM PD0325901, after 1 hour of treatment (Fig. 4A, B). Then, ERK phosphorylation started to resume after 3 hours (Fig. 4B) and returned to levels almost equivalent to untreated cells after 6 hours (Fig. 4A, B). RSK phosphorylation paralleled ERK activity (Fig. 4A, B). These transitory effects were also detected in the other BRAF mutant thyroid carcinoma cells, although they were more evident in ARO cells (not shown). The transient nature of ERK inhibition was not unique to PD0325901, because it was seen also with U0126 (Fig. 4A). Compound decay did not account for the transient nature of the effects, because PD0325901 replenishment one-hour before protein harvest did not prevent ERK phosphorylation recovery (not shown). Moreover, recovered ERK phosphorylation remained MEK-sensitive because it could be abrogated by increasing the doses of PD0325901 or U0126 (Fig. 4C).

Regulatory circuits elicited by MEK inhibition in thyroid carcinoma cells

ERK phosphorylation at Thr202/Tyr204 may resume either secondary to reduced response of MEK kinases to PD0325901 (which would increase the “on” rate), or to reduced levels of ERK-specific phosphatases (which would decrease the “off” rate). We explored both possibilities. Fig. 5A shows that, as soon as after 1 hour of PD0325901 treatment, MEK phosphorylation levels at the activatory sites Ser217/Ser221 increased and remained elevated thereafter for at least 12 hours. Noteworthy, phosphorylation at these sites enhances by 7,000-fold the MEK kinase activity and it is expected to reduce MEK inhibitor binding (23, 24).

RAF proteins are the only kinases known to phosphorylate Ser217/Ser221 of MEK (1, 2). Importantly, active ERKs phosphorylate CRAF on various Ser/Pro sequences (Ser29,

Ser289, Ser296, Ser301, and Ser642), this resulting in the inhibition of CRAF catalytic activity, membrane localization and association to BRAF (25, 26). CRAF, in turn, is involved in oncogenic BRAF-triggered phosphorylation of MEK (11). Thus, PD0325901 treatment could result in the potentiation of CRAF secondary to the blockade of ERK-mediated inhibitory phosphorylations. We used the available phospho-antibodies specific for CRAF phosphorylated at Ser289/296/301 to test this possibility. Fig. 5B shows that indeed the phosphorylation state of CRAF at these inhibitory sites was decreased starting at 1-6 hours after PD0325901 treatment; again these effects were also seen with the control MEK inhibitor. It is important to note that also BRAF is directly phosphorylated and inhibited by ERK (27), and therefore also BRAF de-phosphorylation upon PD0325901 may contribute to MEK hyper-phosphorylation. Accordingly, our preliminary data indicate that both CRAF and BRAF kinase activities are potentiated upon PD0325901 treatment (not shown).

DUSP/MKP are transcriptional targets of the ERK pathway, this representing a negative feedback circuit that is able to terminate ERK signal (3). Changes in expression levels of DUSP/MKPs may modify the “off” rate of ERK phosphorylation and contribute to the transient nature of ERK de-phosphorylation upon treatment with pathway inhibitors.

Accordingly, Ouyang *et al* showed that BRAF inhibition caused reduced levels of MKP3 and DUSP5 ERK phosphatases in thyroid carcinoma cells (28). We treated ARO cells with orthovanadate, a potent DUSP/MKP inhibitor. This treatment increased the phosphorylation levels of ERK, suggesting that, at the steady state, ERK phosphorylation is under phosphatases control in ARO cells (Fig. 5C). Then, we measured expression levels of DUSP5 and MKP3 in ARO cells treated with PD0325901, by quantitative RT-

PCR. PD0325901 treatment, evoked a rapid and sustained decrease of mRNA abundance of both phosphatases starting 30 minutes upon treatment and lasting up to 12 hours (Fig. 5D).

DISCUSSION

Advanced PTC typically exhibits radioiodine resistance and there is currently modest therapeutic option for these patients (29, 30). ATC is a very rare but almost invariably fatal tumor (9, 10). Thus, novel therapeutic strategies are urgently needed for these particular patients.

The BRAF/MEK/ERK pathway seems a promising molecular therapeutic target for PTC and ATC (18-21, 28, 31). Here we studied at the molecular level the effects of MEK targeting in BRAF mutant thyroid carcinoma cells. Our findings confirm the efficacy of this approach to arrest thyroid carcinoma cell proliferation (18-21). However, they also anticipate possible shortcomings of this strategy.

Signal transduction pathways are controlled by a network of regulatory circuits (32).

Although the major effect of these circuits is probably to prevent excessive signaling, their abrogation by molecularly targeted agents, may cause a compensatory stimulation of the pathway and therefore limit treatment efficacy. As an example, treatment with inhibitors of mTOR, a kinase acting downstream AKT and PI3K, by removing negative feedbacks that act upstream or at the level of AKT, exerted only transient biological effects (33, 34). Importantly, this could be circumvented by combining PI3K and mTOR inhibitors (35).

Multiple levels of control exist in the ERK cascade (1, 2). Our data show that treatment with MEK targeting agents is able to tune many of these controls (Fig. 5E) and kinetics analysis suggests that these events contribute to rapidly attenuate ERK inhibition upon PD0325901 and U0126 treatment. Our findings show that, at the transcriptional level, the

downregulated expression of MKP3 and DUSP5, likely reduces the turn-over of ERK phosphorylation thereby blunting ERK inhibition upon MEK blockade. We also show that at the post-translational level, treatment with MEK targeting agents attenuated ERK-dependent inhibitory phosphorylations of RAF kinases; it is feasible that this accounts for the rapid attenuation of MEK inhibition in cells treated with PD0325901.

We cannot exclude that additional regulatory mechanisms result in MEK overactivation, thus hampering the efficacy of MEK inhibitory agents. For instance, in some (36, 37) but not all (38) reports, ERK-mediated phosphorylation of MEK1 on Thr292 was found to attenuate MEK activity, anticipating that ERK inhibition could potentiate it. Furthermore, changes in the expression levels of MEK phosphatases such as PP2A (39) may occur and affect cell response to MEK inhibition. Whatever the mechanism, our findings suggest that the resumed ERK pathway remains MEK-dependent and, accordingly, we could keep it knocked-down by using higher doses of PD0325901.

In conclusion, although MEK inhibitory agents exert significant growth inhibitory properties for thyroid carcinoma cells, they also elicit compensatory mechanisms that attenuate the duration of their effects. Increasing the dose of one inhibitor, as our data suggest, or combining inhibitors that act at different levels of the ERK cascade, like compounds targeting MEK and RAF (RAF kinase inhibitors or Hsp90 inhibitors, ref. 18) may counteract these regulatory circuits and prove to be an effective targeting strategy. It is feasible, however, that compensatory mechanism adjunctive to those described here may occur under MEK inhibition and affect other components of the cascade, even upstream from MEK and RAF kinases (like RAS or membrane receptors). This may result

in the activation of pathways other than the ERK one, and therefore require a rationally-designed multi-pathway targeting approach.

ACKNOWLEDGEMENTS

We thank Pfizer Global Research and Development for providing us with PD0325901. We are grateful to G. Vecchio and A. Fusco for continuous support and to C.H. Heldin for SW1736 cells. This study was supported by the Associazione Italiana per la Ricerca sul Cancro (AIRC), the Istituto Superiore di Oncologia (ISO), the NOGEC (Naples OncoGENomic Center), the Italian Ministero della Salute, and the Italian Ministero dell'Università e della Ricerca (MiUR). PS was recipient of a NOGEC fellowship.

REFERENCES

1. Dhanasekaran DN, Johnson GL. MAPKs: function, regulation, role in cancer and therapeutic targeting. *Oncogene* 2007; 26:3097-9.
2. Sebolt-Leopold JS, Herrera R. Targeting the mitogen-activated protein kinase cascade to treat cancer. *Nat Rev Cancer* 2004; 4:937-47.
3. Jeffrey KL, Camps M, Rommel C, Mackay CR. Targeting dual-specificity phosphatases: manipulating MAP kinase signalling and immune responses. *Nat Rev Drug Discov.* 2007 May;6(5):391-403.
4. DeLellis RA, Williams ED. Thyroid and parathyroid tumors. In *Tumours of Endocrine Organs, World Health Organization Classification of Tumors*. In DeLellis RA, Lloyd RV, Heitz PU and Eng C. 2004 (eds), p. 51-56.
5. Kondo T, Ezzat S, Asa SL. Pathogenetic mechanisms in thyroid follicular-cell neoplasia. *Nat Rev Cancer* 2006; 6:292-306.
6. Groussin L, Fagin JA. Significance of BRAF mutations in papillary thyroid carcinoma: prognostic and therapeutic implications. *Nat Clin Pract Endocrinol Metab* 2006; 2:180-1.
7. Nikiforov YE. Genetic alterations involved in the transition from well-differentiated to poorly differentiated and anaplastic thyroid carcinomas. *Endocr Pathol* Winter 2004; 15:319-27.
8. Xing M. BRAF Mutation in Papillary Thyroid Cancer: Pathogenic Role, Molecular Bases, and Clinical Implications. *Endocr Rev* 2007 Oct 16; [Epub ahead of print]
9. Ain KB. Anaplastic thyroid carcinoma: a therapeutic challenge. *Semin Surg Oncol* 1999; 16:64-69.

10. De Crevoisier R, Baudin E, Bachelot A, Leboulleux S, Travagli JP, Caillou B, Schlumberger M. Combined treatment of anaplastic thyroid carcinoma with surgery, chemotherapy, and hyperfractionated accelerated external radiotherapy. *Int J Radiat Oncol Biol Phys.* 2004;60(4):1137-43.
11. Garnett MJ, Rana S, Paterson H, Barford D, Marais R. Wild-type and mutant B-RAF activate C-RAF through distinct mechanisms involving heterodimerization. *Mol Cell* 2005; 20:963-9.
12. Solit DB, Garraway LA, Pratilas CA, Sawai A, Getz G, Basso A, et al. BRAF mutation predicts sensitivity to MEK inhibition. *Nature* 2006; 439:358-62.
13. Thompson N, Lyons J. Recent progress in targeting the Raf/MEK/ERK pathway with inhibitors in cancer drug discovery. *Curr Opin Pharmacol* 2005; 5:350.
14. Messersmith WA, Hidalgo M, Carducci M, Eckhardt SG. Novel targets in solid tumors: MEK inhibitors. *Clin Adv Hematol Oncol* 2006; 4:831-6.
15. Wang D, Boerner SA, Winkler JD, LoRusso PM. Clinical experience of MEK inhibitors in cancer therapy. *Biochim Biophys Acta.* 2007 Aug; 1773(8):1248-55.
16. Yeh TC, Marsh V, Bernat BA, Ballard J, Colwell H, Evans RJ et al. Biological characterization of ARRY-142886 (AZD6244), a potent, highly selective mitogen-activated protein kinase kinase 1/2 inhibitor. *Clin Cancer Res* 2007 1; 13:1576-83.
17. Brown AP, Carlson TC, Loi CM, Graziano MJ. Pharmacodynamic and toxicokinetic evaluation of the novel MEK inhibitor, PD0325901, in the rat following oral and intravenous administration. *Cancer Chemother Pharmacol* 2007; 59:671-9.
18. Braga-Basaria M, Hardy E, Gottfried R, Burman KD, Saji M, Ringel MD. 17-Allylamino-17-demethoxygeldanamycin activity against thyroid cancer cell lines

- correlates with heat shock protein 90 levels. *J Clin Endocrinol Metab.* 2004 Jun; 89(6):2982-8.
19. Liu D, Hu S, Hou P, Jiang D, Condouris S, Xing M. Suppression of BRAF/MEK/MAP kinase pathway restores expression of iodide-metabolizing genes in thyroid cells expressing the V600E BRAF mutant. *Clin Cancer Res.* 2007 Feb 15; 13(4):1341-9.
 20. Ball DW, Jin N, Rosen DM, Dackiw A, Sidransky D, Xing M, et al. Selective Growth Inhibition in BRAF Mutant Thyroid Cancer by the MEK $\frac{1}{2}$ Inhibitor AZD6244 (ARRY-142886). *J Clin Endocrinol Metab* 2007; Sep 18 [Epub ahead of print].
 21. Liu D, Liu Z, Jiang D, Dackiw AP, Xing M. Inhibitory Effects of the MEK Inhibitor CI-1040 on the Proliferation and Tumor Growth of Thyroid Cancer Cells with BRAF or RAS Mutations. *J Clin Endocrinol Metab* 2007; Oct 2 [Epub ahead of print].
 22. Fusco A, Berlingieri MT, Di Fiore PP, Portella G, Grieco M, Vecchio G. One- and two-step transformations of rat thyroid epithelial cells by retroviral oncogenes. *Mol Cell Biol.* 1987 Sep; 7(9):3365-70.
 23. Alessi DR, Cuenda A, Cohen P, Dudley DT, Saltiel AR. PD 098059 is a specific inhibitor of the activation of mitogen-activated protein kinase kinase in vitro and in vivo. *J Biol Chem.* 1995 Nov 17; 270(46):27489-94.
 24. Bain J, McLauchlan H, Elliott M, Cohen P. The specificities of protein kinase inhibitors: an update. *Biochem J.* 2003 Apr 1; 371(Pt 1):199-204.
 25. Dougherty MK, Müller J, Ritt DA, Zhou M, Zhou XZ, Copeland TD, et al. Regulation of Raf-1 by direct feedback phosphorylation. *Mol Cell* 2005; 17:215-24.

26. Rushworth LK, Hindley AD, O'Neill E, Kolch W. Regulation and role of Raf-1/B-Raf heterodimerization. *Mol Cell Biol* 2006; 26:2262-72.
27. Brummer T, Naegele H, Reth M, Misawa Y. Identification of novel ERK-mediated feedback phosphorylation sites at the C-terminus of B-Raf. *Oncogene* 2003; 22:8823-34.
28. Ouyang B, Knauf JA, Smith EP, Zhang L, Ramsey T, Yusuff N, et al. Inhibitors of Raf kinase activity block growth of thyroid cancer cells with RET/PTC or BRAF mutations in vitro and in vivo. *Clin Cancer Res* 2006; 12:1785-93.
29. Cooper DS, Doherty GM, Haugen BR, Kloos RT, Lee SL, Mandel SJ, Mazzaferri EL, McIver B, Sherman SI, Tuttle RM; The American Thyroid Association Guidelines Taskforce. Management guidelines for patients with thyroid nodules and differentiated thyroid cancer. *Thyroid*. 2006 Feb; 16(2):109-42.
30. Pacini F, Schlumberger M, Dralle H, Elisei R, Smit JW, Wiersinga W; European Thyroid Cancer Taskforce. European consensus for the management of patients with differentiated thyroid carcinoma of the follicular epithelium. *Eur J Endocrinol*. 2006 Jun; 154(6):787-803.
31. Salvatore G, De Falco V, Salerno P, Nappi TC, Pepe S, Troncone G, Carlomagno F, Melillo RM, Wilhelm SM, Santoro M. BRAF is a therapeutic target in aggressive thyroid carcinoma. *Clin Cancer Res*. 2006 Mar 1; 12(5):1623-9.
32. Amit I, Citri A, Shay T, Lu Y, Katz M, Zhang F, et al. A module of negative feedback regulators defines growth factor signaling. *Nat Genet* 2007; 39:503-12.
33. Sun SY, Rosenberg LM, Wang X, Zhou Z, Yue P, Fu H, et al. Activation of Akt and eIF4E survival pathways by rapamycin-mediated mammalian target of rapamycin inhibition. *Cancer Res* 2005; 65:7052-8.

34. O'Reilly KE, Rojo F, She QB, Solit D, Mills GB, Smith D, et al. mTOR inhibition induces upstream receptor tyrosine kinase signaling and activates Akt. *Cancer Res* 2006; 66:1500-8.
35. Fan QW, Knight ZA, Goldenberg DD, Yu W, Mostov KE, Stokoe D, Shokat KM, Weiss WA. A dual PI3 kinase/mTOR inhibitor reveals emergent efficacy in glioma. *Cancer Cell* 2006; 9:341-9.
36. Eblen ST, Slack-Davis JK, Tarcsafalvi A, Parsons JT, Weber MJ, Catling AD. Mitogen-activated protein kinase feedback phosphorylation regulates MEK1 complex formation and activation during cellular adhesion. *Mol Cell Biol* 2004; 24:2308-17.
37. Brunet A, Pagès G, Pouyssegur J. Growth factor-stimulated MAP kinase induces rapid retrophosphorylation and inhibition of MAP kinase kinase (MEK1). *FEBS Lett* 1994; 346:299-303.
38. Gardner AM, Vaillancourt RR, Lange-Carter CA, Johnson GL. MEK-1 phosphorylation by MEK kinase, Raf, and mitogen-activated protein kinase: analysis of phosphopeptides and regulation of activity. *Mol Biol Cell*. 1994 Feb;5(2):193-201.
39. Alessi DR, Gomez N, Moorhead G, Lewis T, Keyse SM, Cohen P. Inactivation of p42 MAP kinase by protein phosphatase 2A and a protein tyrosine phosphatase, but not CL100, in various cell lines. *Curr Biol*. 1995 Mar 1;5(3):283-95.

FIGURE LEGENDSFigure 1. Growth inhibition by PD0325901 of BRAF mutant thyroid carcinoma cells.

The indicated cell lines (5×10^4) were plated in triplicate in 35-mm dishes (in 2.5% serum). The BRAF status of the different cell lines is reported. One day later, different concentrations of PD0325901 or vehicle (NT) were added. Cells were counted at different time points. Day 0 was the treatment-starting day. Each point represents the mean value and error bars represent 95% confidence intervals. Statistical significance was determined by the two-tailed unpaired Student's *t* test.

Figure 2. Mechanisms of PD0325901 growth inhibition in thyroid cancer cell lines.

A) Cells were incubated with 10 nM PD0325901 at the indicated time points and cell cycle distribution was determined by flow cytometry. B) ARO cells were treated with PD0325901, U0126 or vehicle (NT) at different time points and expression levels of cell cycle regulatory proteins were determined by immunoblot. Anti tubulin was used for normalization.

Figure 3. Inhibition of ERK cascade in thyroid carcinoma cells by PD0325901.

The indicated cell lines (their BRAF status is indicated) were kept in 2.5% serum and treated with increasing concentrations of PD0325901 or vehicle (NT) for 2 hours. Cell lysates were immunoblotted with the indicated antibodies. Total amounts of proteins are shown for normalization. Data are representative of at least three different experiments.

Figure 4. Transient ERK inhibition by PD0325901 in ARO cells.

A) ARO cells were incubated with different doses of PD0325901 or U0126 for the indicated time points. Protein extracts were immunoblotted with phosphoERK antibodies and the results were measured by phosphor-imaging; the average pERK/total ERK results of three independent experiments are reported in the bar graphs. B) Cells were treated with PD0325901 or vehicle (NT) and ERK and RSK phosphorylations were measured by immunoblot at early time points. C) Cells were treated with PD0325901 for 2 or 6 hours and kinetics of ERK phosphorylation was measured by immunoblot.

Figure 5. Altered regulatory phosphorylations and DUSPs levels upon treatment with MEK targeting agents.

A, B) ARO cells were treated with PD0325901 or U0126 at the indicated time points. Total cell lysates were analyzed by western blotting with phosphospecific antibodies detecting activatory MEK phosphorylations on Ser217/Ser221 (A) or inhibitory CRAF phosphorylations on Ser289/Ser296/301 (B). C) Cells were treated with orthovanadate at the indicated time points and cell extracts were immunoblotted with the indicated antibodies. D) Cells were incubated with PD0325901 (10 nM), RNA was extracted and MKP-3 and DUSP5 mRNA levels were measured by quantitative RT-PCR and reported as % change with respect to vehicle treated cells. E) A scheme of the activatory (\downarrow) and inhibitory (\perp) regulatory circuits that are affected by MEK targeting in thyroid carcinoma cells.

Fig. 1

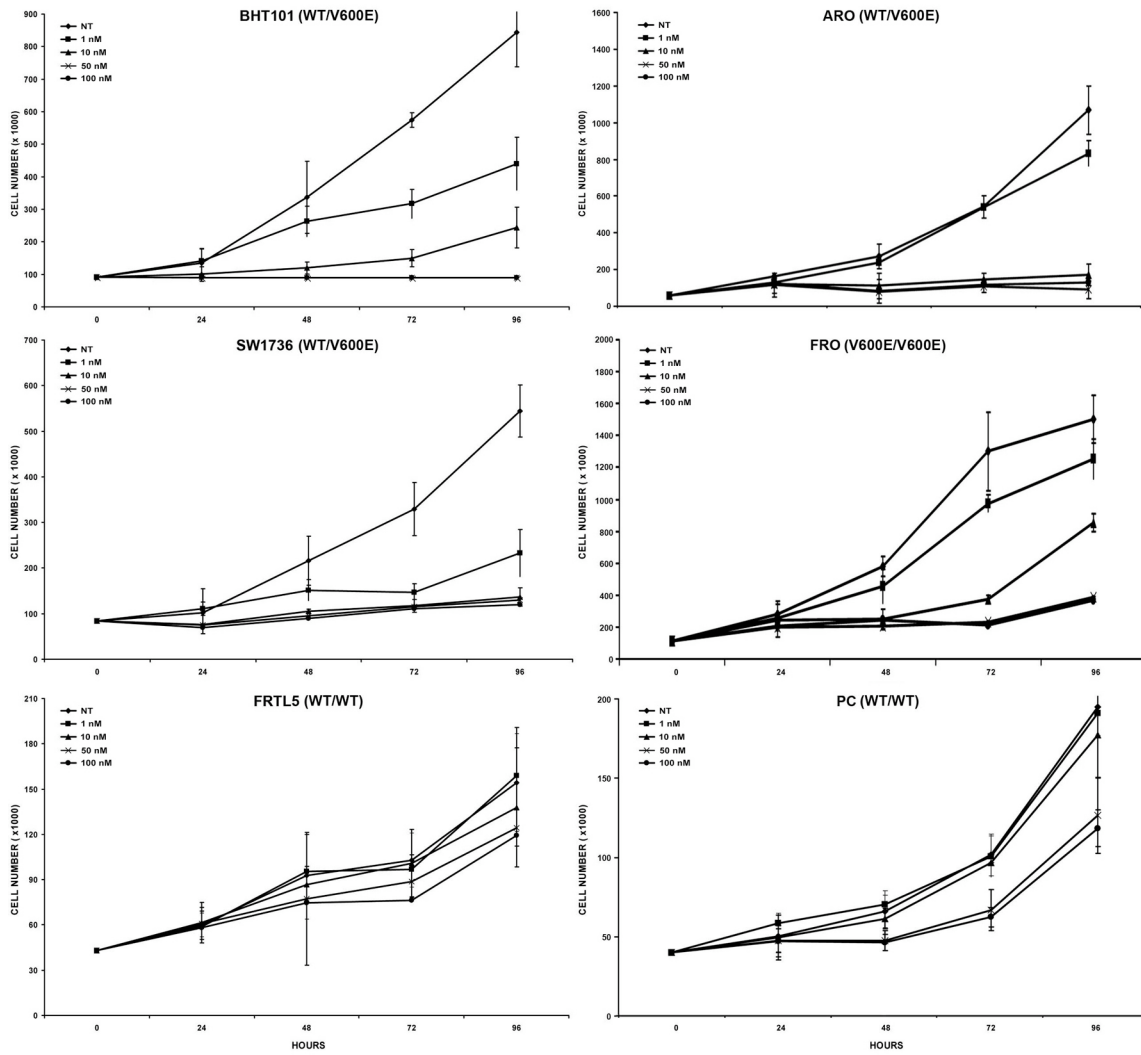


Fig. 2

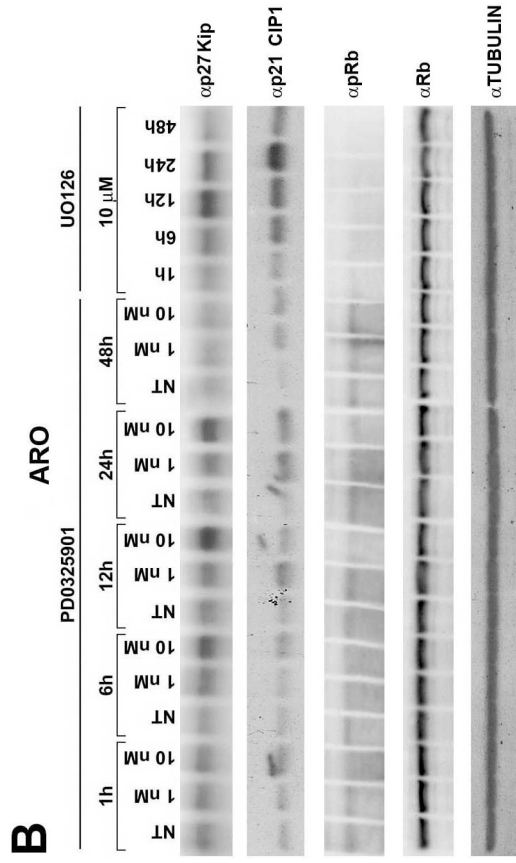
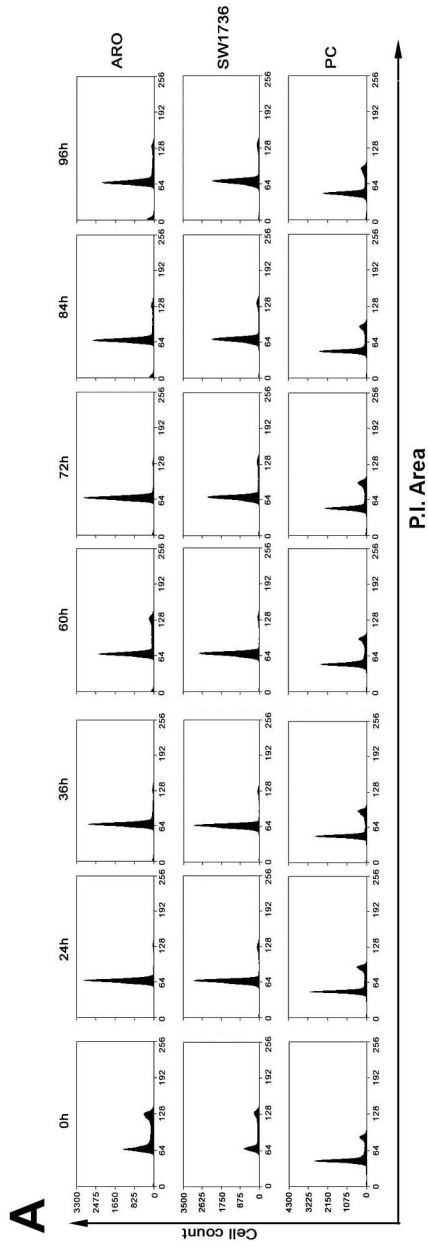


Fig. 3

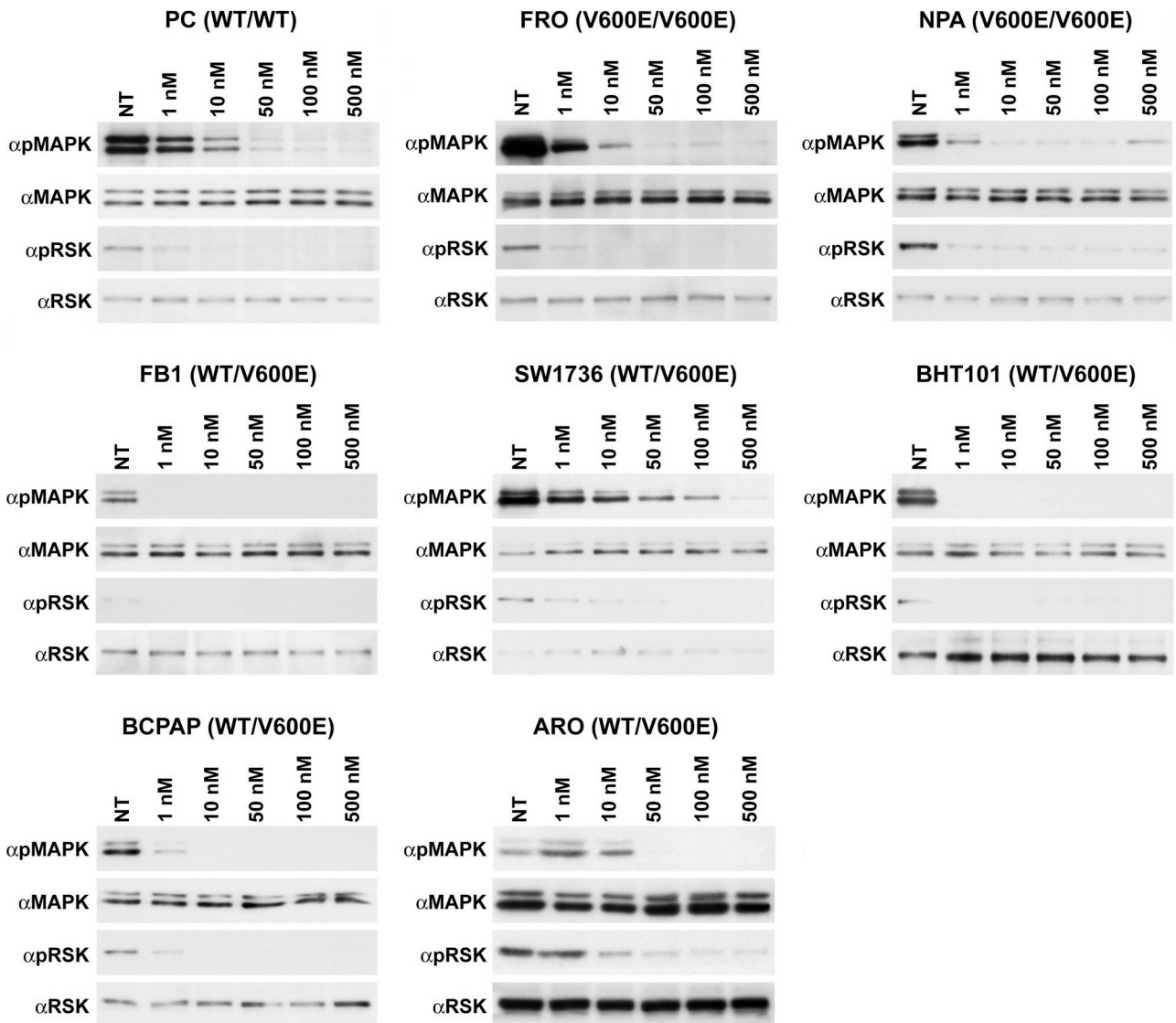
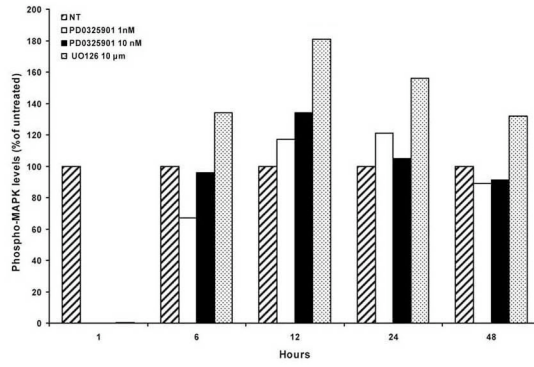
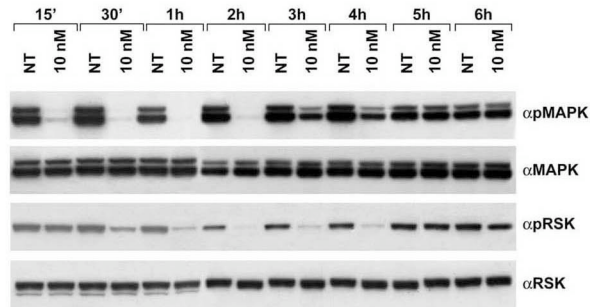


Fig. 4

A



B



C

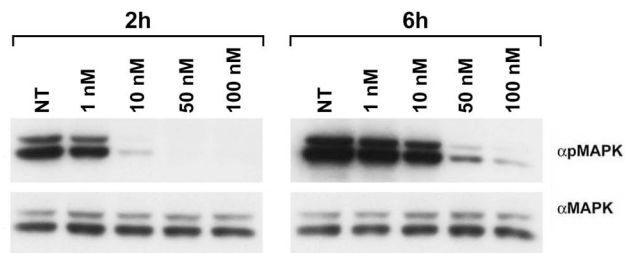
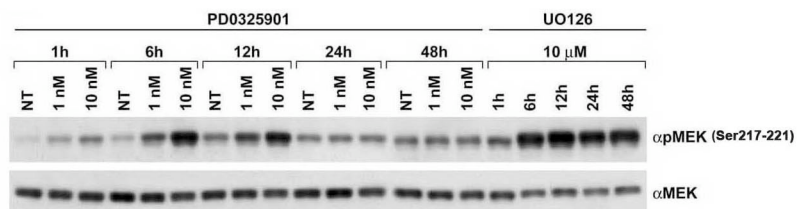
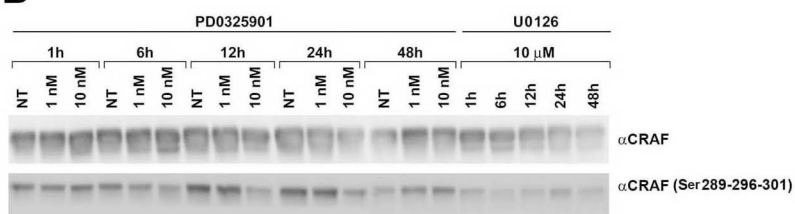


Fig. 5

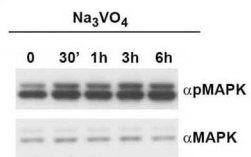
A



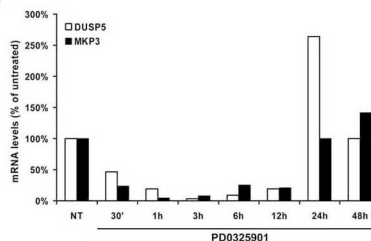
B



C



D



E

